YILDIZ TECHNICAL UNIVERSITY'S TECHNOPARK COMPANY OF

PROMECH TEKNOLOJİ VE BİLİŞİM SİSTEMLERİ SANAYİ LTD. ŞTİ.

PROCEEDINGS BOOK OF

1th INTERNATIONAL CONFERENCE ON ADVANCES IN SCIENCE AND ARTS

SUPPORTED BY

JOURNAL OF THERMAL ENGINEERING

INTERNATIONAL JOURNAL OF ADVANCES ON AUTOMOTIVE AND TECHNOLOGY

ISBN 978-605-9546-03-4

ICASA 2017

MARCH 29-31,2017

ISTANBUL, TURKEY

POSTER PRESENTATIONS

OPENING SPEECH

Dear our audience,

It gives me great pleasure to extend to you all a very warm welcome on behalf of the organizing committee. It is an opportune time to have collaboration with other researchers and discuss problems of mutual interest with participants from the world now.

First of all, we need to thank our rector again for his support to this organization. There were over 255 accepted abstracts and 4 invited speakers as they can be seen from our conference website. Unfortunately, we have got 90 submitted full papers and posters in our conference proceedings. Finally, we would like to reveal that our aim is to gather over 1000 participants from all over the world in the near future. Make sure that we will do our best to reach this aim as we have been doing for all our involved social and scientific works.

We would like emphasize the importance of the use of energy sources efficiently again here. We are in a new period where we should surpass traditional power generating systems, owing to critical energetic, environmental and sustainability subjects.

The existing energy situation of the world has presented some difficulties to be solved such as the integration of clean energy generation and the usage of efficient high-power and energy storage systems. The energy industry has to struggle against difficulties brought by the integration of renewable energy systems regarding with reliability and stability of the power grid. In any case, it becomes extremely significant to benefit from energy storage systems in order to stabilize and improve the efficiency of the power systems using ultimate generation batteries, ultra-capacitors, hydrogen based systems and mechanical systems, among others. Recently, the power electronics suggests effective way outs to be applied to the new spread energy grid idea.

A micro power generation with diesel systems and renewable energy is considerably depending on instabilities directly attributed to the fluctuations and the range ability of the resources. It seems extremely suggested to use storage units in order to confirm the accessibility of energy, endurance and efficiency of the system. Consistent with the formulation of the problem of energy storage, time or regularity properties tied to the existing technologies should be connected to the problem of multi-objective management of energy. The related offered proposals deal with strategies for managing energy in a power system including wind, diesel engine, flywheel, battery and super capacitor as hybridization nominees.

In concluding, I wish you every success in your deliberations and a very pleasant stay in Istanbul.

Regards,

Ahmet Selim Dalkilic

CONFERENCE CHAIRMAN

Ahmet Selim Dalkılıç, Yildiz Technical University, TR

ORGANISING COMMITTEE

1. Ahmet Selim Dalkılıç, Yildiz Technical University, TR (ConferenceChair)

2. Övün IŞIN, Yildiz Technical University, TR

3. Tarkan SANDALCI, Yildiz Technical University, TR

4. Levent YÜKSEK, Yildiz Technical University, TR

5. Orkun ÖZENER, Yildiz Technical University, TR

6. Yasin KARAGÖZ, Yildiz Technical University, TR

7. Emre ORAK, Yildiz Technical University, TR

SCIENTIFIC COMMITTEE

1. Hakan KALELİ, Yildiz Technical University, TR

2. Ümit KÖYLÜ, Missouri University of Science and Technology, USA

3. Balaram Kundu, Jadavpur University, India

4. Dongsheng Wen, University of Leeds, United Kingdom

5. Godson Asirvatham Lazarus, Karunya University, India

6. Enrico Scıubba, Roma University, Italy

7. Ehsan Ebrahimnia-Bajestan, Graduate University of Advanced Technology, Iran

8. Tzvetelin Georgiev, University of Ruse, Bulgaria

9. Ioan Pop, Emanuel University Oradea Oradea, Romania

10. Moh'd A. Al-Nımr, Jordan University of Science and Technology, Jordan

11. Mohamed Awad, Mansoura University, Egypt

12. Patrice Estelle, Université Rennes 1, France

13. Somchai Wongwises, King Mongkut's University of Technology Thonburi, Thailand

14. Ahmed Kadhim Hussein, University of Babylon, Iraq

15. Ahmet Selim Dalkılıç, Yildiz Technical University, TR

16. Tarkan SANDALCI, Yildiz Technical University, TR

17. Övün IŞIN, Yildiz Technical University, TR

18. Orkun ÖZENER, Yildiz Technical University, TR

19. Levent YÜKSEK, Yildiz Technical University, TR

20. Tolga TANER, University of Aksaray, TR

ADVISORY COMMITTEE

1. Hakan KALELİ, Yildiz Technical University, TR

2. Brian AGNEW, Northumbria University, UK

3. Dongsheng WEN, University of Leeds, United Kingdom

4. Ümit KÖYLÜ, Missouri University of Science and Technology, USA

INTERNATIONAL CONFERENCE ON ADVANCES IN SCIENCE AND ARTS ISTANBUL 2017
29 – 31 MARCH 2017, Istanbul, Turkey

A 3D ANALYSIS FOR A SIMPLY SUPPORTED, RECTANGULAR, FUNCTIONALLY GRADED MATERIAL SANDWICH PLATE

***Hamidi Ahmed**
Tahri Mohamed University
Department of Civil Engineering
Béchar, Algeria

Zidour Mohamed
Ibn khaldoun University
Department of Civil Engineering
Tiaret, Algeria

Tounsi Abdelouahed
University of Sidi Bel Abbes,
Department of Civil Engineering
Sidi Bel Abbes, Algeria

Bedia El Abbas ADDA
University of Sidi Bel Abbes,
Department of Civil Engineering
Sidi Bel Abbes, Algeria

Keywords: Sandwich plate, thermomechanical, analytical modeling, functionally graded material, stretching effect
** Corresponding author:, Phone:, Fax: +213670135727*
E-mail address: hamidiahmed82@yahoo.fr

ABSTRACT

In this research, a simple but accurate sinusoidal plate theory for the thermomechanical bending analysis of functionally graded sandwich plates is presented. The main advantage of this approach is that, in addition to incorporating the thickness stretching effect, it deals with only 5 unknowns as the first order shear deformation theory (FSDT), instead of 6 as in the well-known conventional sinusoidal plate theory (SPT). The material properties of the sandwich plate faces are assumed to vary according to a power law distribution in terms of the volume fractions of the constituents. The core layer is made of an isotropic ceramic material. Comparison studies are performed to check the validity of the present results from which it can be concluded that the proposed theory is accurate and efficient in predicting the thermomechanical behavior of functionally graded sandwich plates. The effect of side-to-thickness ratio, aspect ratio, the volume fraction exponent, and the loading conditions on the thermomechanical response of functionally graded sandwich plates is also investigated and discussed.

INTRODUCTION

Sandwich structures are employed in a variety of engineering industries including aircraft, construction and transportation where strong, stiff and light structures are required. The advantages of these structures are that it provides high specific stiffness and strength for a low-weight consideration. Due to the mismatch of stiffness properties between the face sheets and the core, sandwich plates are susceptible to face sheet/core debonding, which is a major problem in sandwich construction, especially under impact loading. To increase the resistance of sandwich plates to this type of failure, the concept of a Functionally Graded Material (FGM) is being actively explored in sandwich structure design. FGMs are achieved by gradually changing the composition of the constituent materials along one (or more) direction(s), usually in the thickness direction, to obtain smooth variation of material properties and optimum response to externally applied loading. Increased use of FGMs in various structural applications necessitates the development of accurate theoretical models to predict their response.

Most of these above-mentioned theories neglect the thickness stretching effect (i.e., $\varepsilon_z = 0$) by assuming a constant transverse displacement through the thickness of the plate. This assumption is appropriate for thin or moderately thick FGM plates, but is inadequate for thick FGM plates (Carrera et al. [12]; Bessaim et al. [08]; Houari et al. [16]; Hebali et al. [15]; Fekrar et al. [13]; Belabed et al. [06]. The effect of the thickness stretching in FG plates was studied by Carrera et al.

[12] and Bessaim et al. [08], and it becomes significant in thick plates. Thus, it should be taken into consideration.

This research work aims to present a simple quasi-3D theory with only five unknowns for thermomechanical bending analysis of FGM sandwich plates. The beauty of the present formulation is that, in addition to including the thickness stretching effect ($\varepsilon_z \neq 0$), the displacement field is modeled with only 5 unknowns as the FSDT, instead of 6 as in the well-known conventional sinusoidal plate theory (SPT). The sandwich plate faces are assumed to have isotropic, two-constituent (metal-ceramic) material distribution through the thickness, and the modulus of elasticity, Poisson's ratio, and thermal expansion coefficient of the faces are assumed to vary according to a power law distribution in terms of the volume fractions of the constituents. The core layer is still homogeneous and made of an isotropic ceramic material. The plate's governing equations are obtained by using the principle of virtual work. Numerical results for deflections and stresses are investigated. The effects of temperature field on the dimensionless axial and transverse shear stresses of the FGM sandwich plate are studied.

THEORETICAL FORMULATION

Consider a sandwich plate composed of three layers as shown in Fig. 1. Two FG face sheets are made from a mixture of a metal and a ceramic, while a core is made of an isotropic homogeneous material. The material properties of FG face sheets are assumed to vary continuously through the plate thickness by a power law distribution as

$$P^{(n)}(z) = P_2 + (P_1 - P_2)V^{(n)} \tag{1}$$

where $P^{(n)}$ is the effective material property of FGM of layer n like Young's modulus E, Poisson's ratio ν, and thermal expansion coefficient α. P_1 and P_2 are the properties of the top and bottom faces of layer 1, respectively, and vice versa for layer 3 depending on the volume fraction $V^{(n)}$, ($n = 1,2,3$) defined by

$$\begin{cases} V^{(1)} = \left(\dfrac{z - h_0}{h_1 - h_0}\right)^p & \text{for } z \in [h_0, h_1] \\ V^{(2)} = 1 & \text{for } z \in [h_1, h_2] \\ V^{(3)} = \left(\dfrac{z - h_3}{h_2 - h_3}\right)^p & \text{for } z \in [h_2, h_3] \end{cases} \tag{2}$$

where p is the power law index ($0 \le p \le +\infty$), which dictates the material variation profile through the thickness.

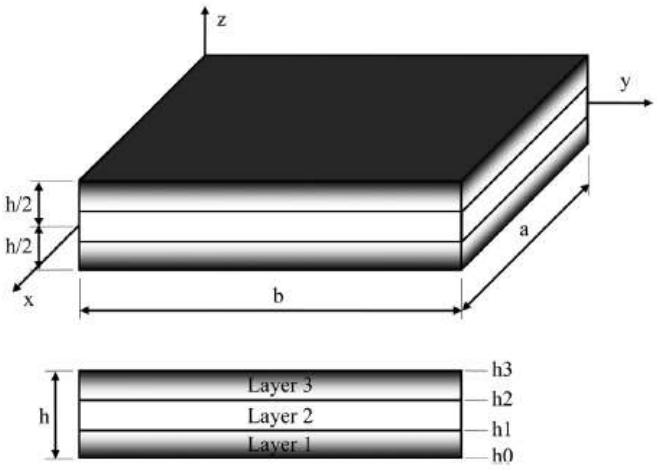

Figure 1. Geometry and coordinates of rectangular FGM sandwich plate.

KINEMATICS

The displacement field of the present formulation is considered based on the following assumptions: (1) The transverse displacement is superposed into three parts, namely: bending, shear and stretching components; (2) the axial displacement is divided into extension, bending and shear components; (3) the bending parts of the axial displacements are similar to those given by CPT; and (4) the shear parts of the axial displacements give rise to the sinusoidal variations of shear strains and hence to shear stresses through the thickness of the plate in such a way that the shear stresses vanish on the top and bottom surfaces of the plate. Based on these assumptions, the following displacement field relations can be obtained: (1)

$$\begin{aligned} u(x,y,z,t) &= u_0(x,y,t) - z\frac{\partial w_b}{\partial x} - f(z)\frac{\partial w_s}{\partial x} \\ v(x,y,z,t) &= v_0(x,y,t) - z\frac{\partial w_b}{\partial y} - f(z)\frac{\partial w_s}{\partial y} \\ w(x,y,z,t) &= w_b(x,y,t) + w_s(x,y,t) + g(z)\,\varphi(x,y,t) \end{aligned} \tag{3}$$

where u_0 and v_0 denote the displacements along the x and y coordinate directions of a point on the mid-plane of the plate; w_b and w_s are the bending and shear components of the transverse displacement, respectively; and the additional displacement φ accounts for the effect of normal stress (stretching effect). The shape functions $f(z)$ and $g(z)$ are given as follows

$$f(z) = z - \frac{h}{\pi}\sin\left(\frac{\pi z}{h}\right) \tag{4}$$

and

$$g(z) = 1 - f'(z) \tag{5}$$

The non-zero strains associated with the displacement field in Eq. (3) are:

$$\begin{Bmatrix} \varepsilon_x \\ \varepsilon_y \\ \gamma_{xy} \end{Bmatrix} = \begin{Bmatrix} \varepsilon_x^0 \\ \varepsilon_y^0 \\ \gamma_{xy}^0 \end{Bmatrix} + z \begin{Bmatrix} k_x^b \\ k_y^b \\ k_{xy}^b \end{Bmatrix} + f(z) \begin{Bmatrix} k_x^s \\ k_y^s \\ k_{xy}^s \end{Bmatrix},$$
$$\begin{Bmatrix} \gamma_{yz} \\ \gamma_{xz} \end{Bmatrix} = g(z) \begin{Bmatrix} \gamma_{yz}^0 \\ \gamma_{xz}^0 \end{Bmatrix}, \quad \varepsilon_z = g'(z)\, \varepsilon_z^0 \tag{6}$$

where

$$\begin{Bmatrix} \varepsilon_x^0 \\ \varepsilon_y^0 \\ \gamma_{xy}^0 \end{Bmatrix} = \begin{Bmatrix} \dfrac{\partial u_0}{\partial x} \\ \dfrac{\partial v_0}{\partial x} \\ \dfrac{\partial u_0}{\partial y} + \dfrac{\partial v_0}{\partial x} \end{Bmatrix}, \quad \begin{Bmatrix} k_x^b \\ k_y^b \\ k_{xy}^b \end{Bmatrix} = \begin{Bmatrix} -\dfrac{\partial^2 w_b}{\partial x^2} \\ -\dfrac{\partial^2 w_b}{\partial y^2} \\ -2\dfrac{\partial^2 w_b}{\partial x \partial y} \end{Bmatrix},$$
$$\begin{Bmatrix} k_x^s \\ k_y^s \\ k_{xy}^s \end{Bmatrix} = \begin{Bmatrix} -\dfrac{\partial^2 w_s}{\partial x^2} \\ -\dfrac{\partial^2 w_s}{\partial y^2} \\ -2\dfrac{\partial^2 w_s}{\partial x \partial y} \end{Bmatrix}, \quad \begin{Bmatrix} \gamma_{yz}^0 \\ \gamma_{xz}^0 \end{Bmatrix} = \begin{Bmatrix} \dfrac{\partial w_s}{\partial y} + \dfrac{\partial \varphi}{\partial y} \\ \dfrac{\partial w_s}{\partial x} + \dfrac{\partial \varphi}{\partial x} \end{Bmatrix}, \quad \varepsilon_z^0 = \varphi \tag{7}$$

and

$$g'(z) = \frac{dg(z)}{dz} \tag{8}$$

CONSTITUTIVE RELATIONS

The linear constitutive relations are given as:

$$\begin{Bmatrix} \sigma_x \\ \sigma_y \\ \sigma_z \\ \tau_{yz} \\ \tau_{xz} \\ \tau_{xy} \end{Bmatrix} = \begin{bmatrix} Q_{11} & Q_{12} & Q_{13} & 0 & 0 & 0 \\ Q_{12} & Q_{22} & Q_{23} & 0 & 0 & 0 \\ Q_{13} & Q_{23} & Q_{33} & 0 & 0 & 0 \\ 0 & 0 & 0 & Q_{44} & 0 & 0 \\ 0 & 0 & 0 & 0 & Q_{55} & 0 \\ 0 & 0 & 0 & 0 & 0 & Q_{66} \end{bmatrix} \begin{Bmatrix} \varepsilon_x - \alpha\Delta T \\ \varepsilon_y - \alpha\Delta T \\ \varepsilon_z - \alpha\Delta T \\ \gamma_{yz} \\ \gamma_{xz} \\ \gamma_{xy} \end{Bmatrix} \tag{8}$$

where (σ_x, σ_y, σ_z, τ_{yz}, τ_{xz}, τ_{xy}) and (ε_x, ε_y, ε_z, γ_{yz}, γ_{xz}, γ_{xy}) are the stress and strain components, respectively.

where $\Delta T = T - T_0$ in which T_0 is the reference temperature.

The applied temperature distribution $T(x, y, z)$ through the thickness are assumed to be

$$T(x, y, z) = T_1(x, y) + \frac{z}{h} T_2(x, y) + \frac{1}{\pi} \sin\left(\frac{\pi z}{h}\right) T_3(x, y) \tag{8}$$

Using the material properties defined in Eq. (1), stiffness coefficients, Q_{ij}, can be expressed as

$$Q_{11} = Q_{22} = Q_{33} = \frac{E(z)}{1-\nu^2}, \tag{11a}$$

$$Q_{12} = Q_{13} = Q_{23} = \frac{\nu\, E(z)}{1-\nu^2}, \tag{11b}$$

$$Q_{44} = Q_{55} = Q_{66} = \frac{E(z)}{2(1+\nu)}, \tag{11c}$$

GOVERNING EQUATIONS

The governing equations of the present theory are derived using the principle of virtual work; the following expressions can be obtained:

$$\int_{-h/2}^{h/2} \int_{\Omega} \begin{bmatrix} \sigma_x \delta\varepsilon_x + \sigma_y \delta\varepsilon_y + \sigma_z \delta\varepsilon_z + \tau_{xy} \delta\gamma_{xy} \\ + \tau_{yz} \delta\gamma_{yz} + \tau_{xz} \delta\gamma_{xz} \end{bmatrix} d\Omega\, dz$$
$$- \int_{\Omega} q \delta w\, d\Omega = 0 \tag{12}$$

where Ω is the top surface and q is the distributed transverse load.

Substituting Eqs. (3), (6) and (9) into Eq. (12) and integrating through the thickness of the plate, Eq (12) can be rewritten as

$$\delta U = \int_{\Omega} \begin{bmatrix} N_x \delta\varepsilon_x^0 + N_y \delta\varepsilon_y^0 + N_z \delta\varepsilon_z^0 + N_{xy} \delta\gamma_{xy}^0 \\ + M_x^b \delta k_x^b + M_y^b \delta k_y^b + M_{xy}^b \delta k_{xy}^b \\ + M_x^s \delta k_x^s + M_y^s \delta k_y^s + M_{xy}^s \delta k_{xy}^s \\ + S_{yz}^s \delta\gamma_{yz}^0 + S_{xz}^s \delta\gamma_{xz}^0 - q\delta w \end{bmatrix} d\Omega = 0 \tag{13}$$

where the stress resultants (N, M^b, M^s, S^s and N_z) are as follows:

$$\left(N_i, M_i^b, S_i^b\right) = \sum_{n=1}^{3} \int_{h_{n-1}}^{h_n} (1, z, f)\, \sigma_i\, dz, \quad (i = x, y, xy),$$

$$S_i^s = \sum_{n=1}^{3} \int_{h_{n-1}}^{h_n} \tau_i\, g(z) dz, \ (i = xz, yz) \text{ and} \tag{14}$$

$$N_z = \sum_{n=1}^{3} \int_{h_{n-1}}^{h_n} \sigma_z\, g'(z) dz$$

The governing equations of equilibrium can be derived from Eq. (13) by integrating the displacement gradients by parts and setting the coefficients δu_0, δv_0, δw_b, δw_s and $\delta\varphi$ to zero separately. Thus one can obtain the equilibrium equations associated with the present simple quasi-3D theory,

$$\begin{aligned}
&\delta u_0: \ \frac{\partial N_x}{\partial x}+\frac{\partial N_{xy}}{\partial y}=0\\
&\delta v_0: \ \frac{\partial N_{xy}}{\partial x}+\frac{\partial N_y}{\partial y}=0\\
&\delta w_b: \ \frac{\partial^2 M_x^b}{\partial x^2}+2\frac{\partial^2 M_{xy}^b}{\partial x\partial y}+\frac{\partial^2 M_y^b}{\partial y^2}+q=0\\
&\delta w_s: \ \frac{\partial^2 M_x^s}{\partial x^2}+2\frac{\partial^2 M_{xy}^s}{\partial x\partial y}+\frac{\partial^2 M_y^s}{\partial y^2}+\frac{\partial S_{xz}^s}{\partial x}+\frac{\partial S_{yz}^s}{\partial y}+q=0\\
&\delta\varphi: \ \frac{\partial S_{xz}^s}{\partial x}+\frac{\partial S_{yz}^s}{\partial y}-N_z=0
\end{aligned} \tag{15}$$

By substituting Eq. (6) into Eq. (9) and the subsequent results into Eq. (14), the stress resultants are readily obtained as:

$$\begin{Bmatrix} N\\ M^b\\ M^s\end{Bmatrix}=\begin{bmatrix} A & B & B^s\\ B & D & D^s\\ B^s & D^s & H^s\end{bmatrix}\begin{Bmatrix}\varepsilon\\ k^b\\ k^s\end{Bmatrix}+\begin{bmatrix} L\\ L^a\\ R\end{bmatrix}\varepsilon_z^0-\begin{Bmatrix} N^T\\ M^{bT}\\ M^{sT}\end{Bmatrix},\quad S=A^s\gamma, \tag{16 a}$$

$$\begin{aligned} N_z=&R^a\varphi+L\left(\varepsilon_x^0+\varepsilon_y^0\right)+L^a\left(k_x^b+k_y^b\right)\\ &+R\left(k_x^s+k_y^s\right)-N_z^T,\end{aligned} \tag{16 b}$$

where

$$\begin{aligned} N=\left\{N_x,N_y,N_{xy}\right\},&\quad M^b=\left\{M_x^b,M_y^b,M_{xy}^b\right\},\\ M^s=\left\{M_x^s,M_y^s,M_{xy}^s\right\},&\end{aligned} \tag{17 a}$$

$$\begin{aligned} N^T=\left\{N_x^T,N_y^T,0\right\},&\quad M^{bT}=\left\{M_x^{bT},M_y^{bT},0\right\},\\ M^{sT}=\left\{M_x^{sT},M_y^{sT},0\right\},&\end{aligned} \tag{17 b}$$

$$\begin{aligned} \varepsilon=\left\{\varepsilon_x^0,\varepsilon_y^0,\gamma_{xy}^0\right\},&\quad k^b=\left\{k_x^b,k_y^b,k_{xy}^b\right\},\\ k^s=\left\{k_x^s,k_y^s,k_{xy}^s\right\},&\end{aligned} \tag{17 c}$$

$$A=\begin{bmatrix} A_{11} & A_{12} & 0\\ A_{12} & A_{22} & 0\\ 0 & 0 & A_{66}\end{bmatrix},\ B=\begin{bmatrix} B_{11} & B_{12} & 0\\ B_{12} & B_{22} & 0\\ 0 & 0 & B_{66}\end{bmatrix},\ D=\begin{bmatrix} D_{11} & D_{12} & 0\\ D_{12} & D_{22} & 0\\ 0 & 0 & D_{66}\end{bmatrix}, \tag{17 d}$$

$$B^s=\begin{bmatrix} B_{11}^s & B_{12}^s & 0\\ B_{12}^s & B_{22}^s & 0\\ 0 & 0 & B_{66}^s\end{bmatrix},\ D^s=\begin{bmatrix} D_{11}^s & D_{12}^s & 0\\ D_{12}^s & D_{22}^s & 0\\ 0 & 0 & D_{66}^s\end{bmatrix},\ H^s=\begin{bmatrix} H_{11}^s & H_{12}^s & 0\\ H_{12}^s & H_{22}^s & 0\\ 0 & 0 & H_{66}^s\end{bmatrix}, \tag{17e}$$

$$S=\left\{S_{xz}^s,S_{yz}^s\right\},\ \ \gamma=\left\{\gamma_{xz},\gamma_{yz}\right\},\ \ A^s=\begin{bmatrix} A_{44}^s & 0\\ 0 & A_{55}^s\end{bmatrix}, \tag{17f}$$

$$\begin{Bmatrix} L\\ L^a\\ R\\ R^a\end{Bmatrix}=\sum_{n=1}^{3}\int_{h_{n-1}}^{h_n}Q_{11}^{(n)}\begin{Bmatrix}\nu^{(n)}\\ \nu^{(n)}z\\ \nu^{(n)}f(z)\\ g'(z)\end{Bmatrix}g'(z)dz$$

Here the stiffness coefficients are defined as:

$$\begin{Bmatrix} A_{11} & B_{11} & D_{11} & B_{11}^s & D_{11}^s & H_{11}^s\\ A_{12} & B_{12} & D_{12} & B_{12}^s & D_{12}^s & H_{12}^s\\ A_{66} & B_{66} & D_{66} & B_{66}^s & D_{66}^s & H_{66}^s\end{Bmatrix} \tag{18a}$$

$$=\sum_{n=1}^{3}\int_{h_{n-1}}^{h_n}Q_{11}^{(n)}\left(1,z,z^2,f(z),z\,f(z),f^2(z)\right)\begin{Bmatrix}1\\ \nu^{(n)}\\ \dfrac{1-\nu^{(n)}}{2}\end{Bmatrix}dz$$

and

$$\begin{aligned}&\left(A_{22},B_{22},D_{22},B_{22}^s,D_{22}^s,H_{22}^s\right)\\ &=\left(A_{11},B_{11},D_{11},B_{11}^s,D_{11}^s,H_{11}^s\right),\\ &Q_{11}^{(n)}=\frac{E(z)}{1-\nu^2}\end{aligned} \tag{18b}$$

$$A_{44}^s=A_{55}^s=\sum_{n=1}^{3}\int_{h_{n-1}}^{h_n}\frac{E(z)}{2(1+\nu)}\left[g(z)\right]^2dz, \tag{18c}$$

The resultant efforts, $N_x^T=N_y^T$, $M_x^{bT}=M_y^{bT}$, $M_x^{sT}=M_y^{sT}$ and N_z^T induced by the thermal effect are expressed by

$$\begin{Bmatrix} N_x^T \\ M_x^{bT} \\ M_x^{sT} \\ N_z^T \end{Bmatrix} = \sum_{n=1}^{3} \int_{h_{n-1}}^{h_n} \frac{E^{(n)}(z)}{1-(\nu^{(n)})^2}\left(1+2\nu^{(n)}\right)\alpha^{(n)} T \begin{Bmatrix} 1 \\ z \\ f(z) \\ g'(z) \end{Bmatrix} dz \quad (19)$$

GOVERNING EQUATIONS IN TERMS OF DISPLACEMENTS

Introducing Eq. (15) into Eq. (13), the governing equations can be expressed in terms of displacements (δu_0 , δv_0 , δw_b , δw_s , $\delta \varphi$) and the appropriate equations take the form:

$$\begin{aligned} &A_{11}d_{11}u_0 + A_{66}d_{22}u_0 + (A_{12}+A_{66})d_{12}v_0 \\ &- B_{11}d_{111}w_b - (B_{12}+2B_{66})d_{122}w_b \\ &-\left(B_{12}^s+2B_{66}^s\right)d_{122}w_s - B_{11}^s d_{111}w_s + Ld_1\varphi = p_1, \end{aligned} \quad (20a)$$

$$\begin{aligned} &A_{22}d_{22}v_0 + A_{66}d_{11}v_0 + (A_{12}+A_{66})d_{12}u_0 \\ &- B_{22}d_{222}w_b - (B_{12}+2B_{66})d_{112}w_b \\ &-\left(B_{12}^s+2B_{66}^s\right)d_{112}w_s - B_{22}^s d_{222}w_s + Ld_2\varphi = p_2, \end{aligned} \quad (20b)$$

$$\begin{aligned} &B_{11}d_{111}u_0 + (B_{12}+2B_{66})d_{122}u_0 + (B_{12}+2B_{66})d_{112}v_0 \\ &+ B_{22}d_{222}v_0 - D_{11}d_{1111}w_b - 2(D_{12}+2D_{66})d_{1122}w_b \\ &- D_{22}d_{2222}w_b - D_{11}^s d_{1111}w_s - 2\left(D_{12}^s+2D_{66}^s\right)d_{1122}w_s \\ &- D_{22}^s d_{2222}w_s + L^a(d_{11}\varphi + d_{22}\varphi) = p_3, \end{aligned} \quad (20c)$$

$$\begin{aligned} &B_{11}^s d_{111}u_0 + \left(B_{12}^s+2B_{66}^s\right)d_{122}u_0 + \left(B_{12}^s+2B_{66}^s\right)d_{112}v_0 \\ &+ B_{22}^s d_{222}v_0 - D_{11}^s d_{1111}w_b - 2\left(D_{12}^s+2D_{66}^s\right)d_{1122}w_b \\ &- D_{22}^s d_{2222}w_b - H_{11}^s d_{1111}w_s - 2\left(H_{12}^s+2H_{66}^s\right)d_{1122}w_s \\ &- H_{22}^s d_{2222}w_s + A_{44}^s d_{11}w_s + A_{55}^s d_{22}w_s + R(d_{11}\varphi + d_{22}\varphi) \\ &+ A_{44}^s d_{11}\varphi + A_{55}^s d_{22}\varphi = p_4, \end{aligned} \quad (20d)$$

$$\begin{aligned} &L(d_1u_0 + d_2v_0) - L^a(d_{11}w_b + d_{22}w_b) + \left(R - A_{44}^s\right)d_{11}w_s \\ &+ \left(R - A_{55}^s\right)d_{22}w_s + R^a\varphi - A_{44}^s d_{11}\varphi - A_{55}^s d_{22}\varphi = p_5, \end{aligned} \quad (20e)$$

where d_{ij} , d_{ijl} and d_{ijlm} are the following differential operators:

$$d_{ij} = \frac{\partial^2}{\partial x_i \partial x_j}, \quad d_{ijl} = \frac{\partial^3}{\partial x_i \partial x_j \partial x_l}, \quad (21)$$

$$d_{ijlm} = \frac{\partial^4}{\partial x_i \partial x_j \partial x_l \partial x_m}, \quad d_i = \frac{\partial}{\partial x_i}, \ (i, j, l, m = 1,2).$$

The components of the generalized force vector $\{p\}$ are given by

$$\begin{aligned} p_1 &= \frac{\partial N_x^T}{\partial x}, \quad p_2 = \frac{\partial N_y^T}{\partial y}, \\ p_3 &= q - \frac{\partial^2 M_x^{bT}}{\partial x^2} - \frac{\partial^2 M_y^{bT}}{\partial y^2}, \\ p_4 &= q - \frac{\partial^2 M_x^{sT}}{\partial x^2} - \frac{\partial^2 M_y^{sT}}{\partial y^2}, \quad p_5 = N_z^T \end{aligned} \quad (22)$$

ANALYTICAL SOLUTIONS

Consider a simply supported rectangular plate with length a and width b under transverse load q . To solve this problem, Navier presented the transverse mechanical and temperature loads q , T_1 , T_2 , and T_3 in the form of a double trigonometric series as

$$\begin{Bmatrix} q \\ T_1 \\ T_2 \\ T_3 \end{Bmatrix} = \begin{Bmatrix} q_0 \\ t_1 \\ t_2 \\ t_3 \end{Bmatrix} \sin(\lambda x)\sin(\mu y) \quad (23)$$

where q_0 , t_1 , t_2 and t_3 are constants, $\lambda = \pi / a$, $\mu = \pi / b$. Based on Navier solution method, we assume the following solutions form for displacements (u_0 , v_0 , w_b , w_s , φ):

$$\begin{Bmatrix} u_0 \\ v_0 \\ w_b \\ w_s \\ \varphi \end{Bmatrix} = \begin{Bmatrix} U\cos(\lambda x)\sin(\mu y) \\ V\sin(\lambda x)\cos(\mu y) \\ W_b\sin(\lambda x)\sin(\mu y) \\ W_s\sin(\lambda x)\sin(\mu y) \\ \Phi\sin(\lambda x)\sin(\mu y) \end{Bmatrix} \quad (24)$$

where U , V , W_b , W_s and Φ unknown parameters must be determined. By considered equations (20) and (24), the following equation is obtained

$$[C]\{\Delta\} = \{P\} \quad (25)$$

where $\{\Delta\} = \{U, V, W_b, W_s, \Phi\}^t$ and $[C]$ is the symmetric matrix expressed by

$$[C]=\begin{bmatrix} a_{11} & a_{12} & a_{13} & a_{14} & a_{15} \\ a_{12} & a_{22} & a_{23} & a_{24} & a_{25} \\ a_{13} & a_{23} & a_{33} & a_{34} & a_{35} \\ a_{14} & a_{24} & a_{34} & a_{44} & a_{45} \\ a_{15} & a_{25} & a_{35} & a_{45} & a_{55} \end{bmatrix} \tag{26}$$

in which:

$$\begin{aligned}
a_{11} &= -\left(A_{11}\lambda^2 + A_{66}\mu^2\right) \\
a_{12} &= -\lambda\,\mu\left(A_{12} + A_{66}\right) \\
a_{13} &= \lambda[B_{11}\lambda^2 + (B_{12} + 2B_{66})\,\mu^2] \\
a_{14} &= \lambda[B^s_{11}\lambda^2 + (B^s_{12} + 2B^s_{66})\,\mu^2] \\
a_{15} &= L\lambda \\
a_{22} &= -\left(A_{66}\lambda^2 + A_{22}\mu^2\right) \\
a_{23} &= \mu[(B_{12} + 2B_{66})\,\lambda^2 + B_{22}\mu^2] \\
a_{24} &= \mu[(B^s_{12} + 2B^s_{66})\,\lambda^2 + B^s_{22}\mu^2] \\
a_{25} &= L\mu \\
a_{33} &= -\left(D_{11}\lambda^4 + 2(D_{12} + 2D_{66})\lambda^2\mu^2 + D_{22}\mu^4\right) \\
a_{34} &= -\left(D^s_{11}\lambda^4 + 2(D^s_{12} + 2D^s_{66})\lambda^2\mu^2 + D^s_{22}\,\mu^4\right) \\
a_{35} &= -L^a\left(\lambda^2 + \mu^2\right) \\
a_{44} &= -\begin{pmatrix} H^s_{11}\lambda^4 + 2(H^s_{11} + 2H^s_{66})\lambda^2\mu^2 \\ + H^s_{22}\mu^4 + A^s_{55}\lambda^2 + A^s_{44}\mu^2 \end{pmatrix} \\
a_{45} &= -\left(A^s_{44}\lambda^2 + A^s_{55}\mu^2 + R\left(\lambda^2 + \mu^2\right)\right) \\
a_{55} &= -\left(A^s_{44}\lambda^2 + A^s_{55}\mu^2 + R^a\right)
\end{aligned} \tag{27}$$

and the components of the generalized force vector $\{P\} = \{P_1, P_2, P_3, P_4, P_5\}^t$ are expressed by

$$\begin{aligned}
P_1 &= \lambda\left(A^T t_1 + B^T t_2 + {}^aB^T t_3\right), \\
P_2 &= \mu\left(A^T t_1 + B^T t_2 + {}^aB^T t_3\right), \\
P_3 &= -q_0 - h\left(\lambda^2 + \mu^2\right)\left(B^T t_1 + D^T t_2 + {}^aD^T t_3\right), \\
P_4 &= -q_0 - h\left(\lambda^2 + \mu^2\right)\left({}^sB^T t_1 + {}^sD^T t_2 + {}^sF^T t_3\right), \\
P_5 &= -h\left(L^T t_1 + {}^aL^T t_2 + R^T t_3\right),
\end{aligned} \tag{28}$$

where

$$\begin{aligned}
&\left(A^T, B^T, D^T\right) \\
&= \sum_{n=1}^{3} \int_{h_{n-1}}^{h_n} \frac{E^{(n)}(z)}{1-(\nu^{(n)})^2}\left(1 + 2\nu^{(n)}\right)\alpha^{(n)}\left(1, \bar{z}, \bar{z}^2\right)dz
\end{aligned} \tag{29a}$$

$$\begin{aligned}
&\left({}^aB^T, {}^aD^T\right) \\
&= \sum_{n=1}^{3} \int_{h_{n-1}}^{h_n} \frac{E^{(n)}(z)}{1-(\nu^{(n)})^2}\left(1 + 2\nu^{(n)}\right)\alpha^{(n)}\,\overline{\Psi}(z)\left(1, \bar{z}\right)dz
\end{aligned} \tag{29b}$$

$$\begin{aligned}
&\left({}^sB^T, {}^sD^T, {}^sF^T\right) \\
&= \sum_{n=1}^{3} \int_{h_{n-1}}^{h_n} \frac{E^{(n)}(z)}{1-(\nu^{(n)})^2}\left(1 + 2\nu^{(n)}\right)\alpha^{(n)}\,\overline{f}(z)\left(1, \bar{z}, \overline{\Psi}(z)\right)dz
\end{aligned} \tag{29c}$$

$$\begin{aligned}
&\left(L^T, L^T_a, R^T\right) \\
&= \sum_{n=1}^{3} \int_{h_{n-1}}^{h_n} \frac{E^{(n)}(z)}{1-(\nu^{(n)})^2}\left(1 + 2\nu^{(n)}\right)\alpha^{(n)}\,\overline{g}'(z)\left(1, \bar{z}, \overline{\Psi}(z)\right)dz,
\end{aligned} \tag{29d}$$

with $\bar{z} = z/h$, $\overline{f}(z) = f(z)/h$ and $\overline{\Psi}(z) = \frac{1}{\pi}\sin\left(\frac{\pi z}{h}\right)$.

NUMERICAL RESULTS AND DISCUSSION

To assess the performance of present theory under mechanical and thermal loads, simply supported functionally graded sandwich plates are considered with following material properties:

- Metal (Titanium, Ti-6Al-4V): $P_2 = 66.2$ GPa; $\nu_2 = 1/3$; $\alpha_2 = 10.3\ (10^{-6}/K)$.
- Ceramic (Zirconia, ZrO_2): $P_1 = 117.0$ GPa; $\nu_1 = 1/3$; $\alpha_1 = 7.11\ (10^{-6}/K)$.

The results are presented in the following normalized forms for displacements and stresses according to Saidi et al (2013) for the purpose of presentation in this article.

- center deflection
$$\bar{w} = \frac{10^3}{q_0 a^4/(E_0 h^3) + 10^3 \alpha_0 t_2\, a^2/h}\, w\left(\frac{a}{2}, \frac{b}{2}\right),$$
- axial stress
$$\bar{\sigma}_x = \frac{10}{q_0 a^2/h^2 + 10 E_0 \alpha_0 t_2\, a^2/h^2}\, \sigma_x\left(\frac{a}{2}, \frac{b}{2}, \frac{h}{2}\right),$$
- shear stress
$$\bar{\tau}_{xz} = \frac{1}{q_0 a/h + E_0 \alpha_0 t_2 a/(10h)}\, \tau_{xz}\left(0, \frac{b}{2}, 0\right).$$

where the reference values are taken as $E_0 = 1$ GPa and $\alpha_0 = 10^{-6}$/K.

It is assumed, unless otherwise stated, that $a/h=10$, $a/b=1$, $t_1=0$, and $q_0=t_2=t_3=100$. The shear correction factor of FSDT is fixed to be $K=5/6$.

Fig. 2 shows the effect of the aspect ratio a/b on the dimensionless center deflection $\bar{w}$ for FG sandwich plate. The effect of the mechanical and thermal loads is taken into consideration. It is found that the aspect ratio effect is more pronounced on the thermomechanical bending deflection $\bar{w}$

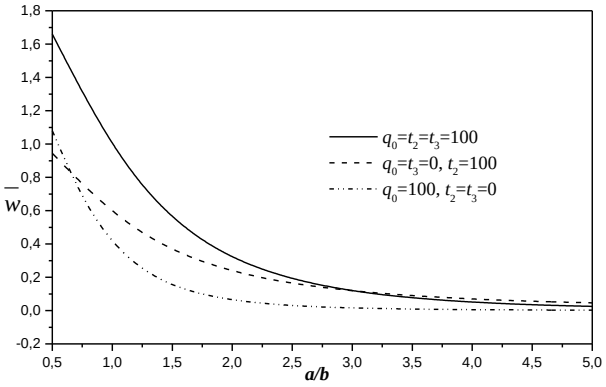

Figure 2. Effect of mechanical and temperature loads on the dimensionless center deflection of FG sandwich plate versus a/b ($t_{FGM}=0.6h$, $p=2$).

In Fig. 3 and 4, we have plotted the through-the-thickness distributions of the dimensionless axial stress $\bar{\sigma}_x$ and the transverse shear stress $\bar{\tau}_{xz}$ of the FG sandwich plate for $p=2$ and $t_{FGM}=0.6h$, respectively. These figures show the great influence played by the different thermal and bending loads on the axial and transverse shear stresses.

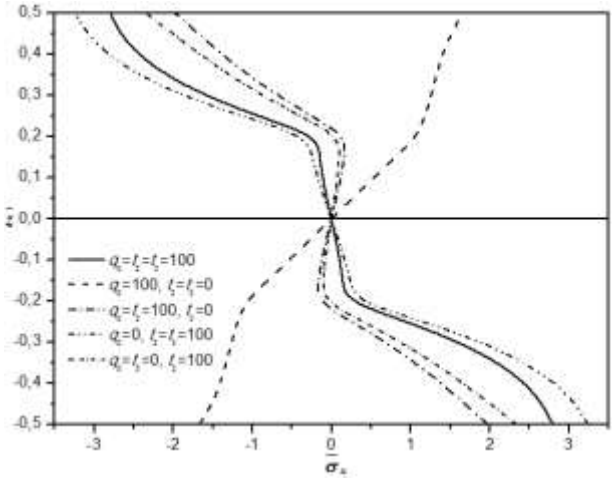

Figure 3. Effect of mechanical and temperature loads on the dimensionless axial stress of FG sandwich plate ($t_{FGM}=0.6h$, $p=2$).

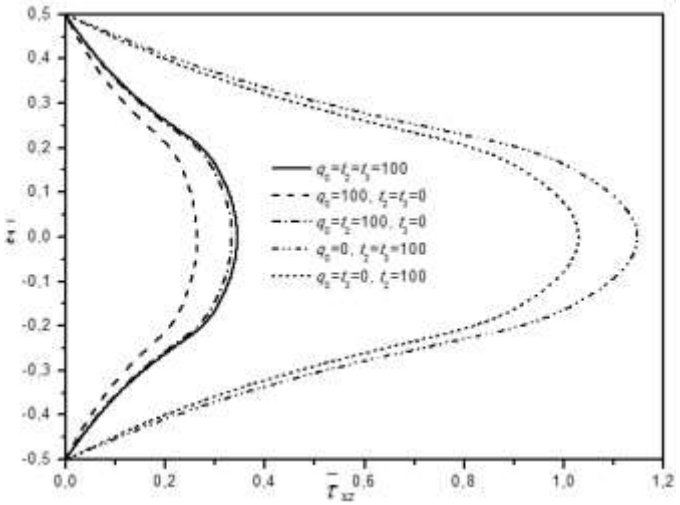

Figure 4. Effect of mechanical and temperature loads on the dimensionless transverse shear stress of FG sandwich plate ($t_{FGM}=0.6h$, $p=2$).

CONCLUSION

A new 5-unknowns quasi-3D sinusoidal plate theory with stretching effect for the thermomechanical bending of FG sandwich plates is presented in this work. The main assumption of this formulation is the decomposition of the transverse displacement into bending and shears components. This theory is free of the zero in-plane resultant forces assumption used in developing the other four variables shear deformation theories and hence have the potential to be used for modeling of the nonlinear FG plate problems. Results demonstrate that the proposed theory is able to provide very accurate results compared with the CPT, FSDT and other HSDTs with higher number of unknowns and so deserve special attention and offer potential for future research. The main point that can be outlined from the present study is that the thickness stretching effect is more pronounced for thick plates and it needs to be taken in consideration in the modeling.

REFERENCES

[1] M. Ait Amar, H. Abdelaziz, and A. Tounsi, "An efficient and simple refined theory for buckling and free vibration of exponentially graded sandwich plates under various boundary conditions," *Sandwich Structures Materials*, (Accepted), 2014.

[2] T.A. Anderson, "A 3-D elasticity solution for a sandwich composite with functionally graded core subjected to transverse loading by a rigid sphere," *Compos Struct*, vol. 60, pp. 265–274, 2013.

[3] M. Bachir Bouiadjra, E.A. Adda Bedia, and A. Tounsi, "Nonlinear thermal buckling behavior of functionally

graded plates using an efficient sinusoidal shear deformation theory," *Structural Engineering and Mechanics*, vol. 48, pp. 547 – 567, 2013.

[4] M. Bachir Bouiadjra, M.S.A. Houari, and A. Tounsi, "Thermal buckling of functionally graded plates according to a four-variable refined plate theory," *Journal of Thermal Stresses*, vol. 35, pp. 677 – 694, 2012.

[5] K. Bakhti, A. Kaci, A.A. Bousahla, M.S.A. Houari, A.Tounsi, E.A. Adda Bedia, "Large deformation analysis for functionally graded carbon nanotube-reinforced composite plates using an efficient and simple refined theory," *Steel and Composite Structures*, vol. 14(4), pp. 335 – 347, 2013.

[6] Z. Belabed, M.S.A. Houari, A. Tounsi, S.R. Mahmoud, and O. Anwar Bég, "An efficient and simple higher order shear and normal deformation theory for functionally graded material (FGM) plates," *Composites: Part B*, vol. 60, pp. 274–283, 2014.

[7] A. Benachour, H. Daouadji Tahar, H. Ait Atmane, A.Tounsi, and S.A. Meftah, "A four variable refined plate theory for free vibrations of functionally graded plates with arbitrary gradient," *Composites Part B: Engineering*, vol. 42, pp. 1386-1394, 2011.

[8] A. Bessaim, M.S.A. Houari, A.Tounsi, S.R. Mahmoud, and E.A. Adda Bedia, "A new higher-order shear and normal deformation theory for the static and free vibration analysis of sandwich plates with functionally graded isotropic face sheets," *Sandwich Structures Materials*, vol. 15(6), pp. 671–703,2013.

[9] R.K. Bhangale, and N. Ganesan, "Thermoelastic buckling and vibration behavior of functionally graded sandwich beam with constrained viscoelastic core," *Sound Vib*, vol. 295, pp. 294–316, 2006.

[10] M. Bourada, A. Tounsi, M.S.A. Houari, and E.A. Adda Bedia, "A new four-variable refined plate theory for thermal buckling analysis of functionally graded sandwich plates," *Sandwich Structures Materials*, vol. 14,pp. 5 – 33, 2012.

[11] B. Bouderba, M.S.A. Houari, and A. Tounsi, "Thermomechanical bending response of FGM thick plates resting on Winkler–Pasternak elastic foundations," *Steel and Composite Structures*, vol. 14(1), pp. 85 – 104, 2013.

[12] E. Carrera, S. Brischetto, M. Cinefra, and M. Soave, "Effects of thickness stretching in functionally graded plates and shells," *Compos Part B: Eng*, vol. 42(2), pp. 123–133, 2011.

[13] A. Fekrar, M.S.A. Houari, A. Tounsi , and S.R. Mahmoud, "A new five-unknown refined theory based on neutral surface position for bending analysis of exponential graded plates," *Meccanica*, vol. 49, pp. 795 – 810, 2014.

[14] M.E. Golmakani, and M. Kadkhodayan, "Nonlinear bending analysis of annular FGM plates using higher order shear deformation plate theories," *Composite struct*, vol. 93, pp. 973-982, 2011.

[15] H. Hebali, A. Tounsi, M.S.A. Houari, A. Bessaim, and E.A. Adda Bedia, "New quasi-3D hyperbolic shear deformation theory for the static and free vibration analysis of functionally graded plates," *Journal of Engineering Mechanics (ASCE)*, vol. 140, pp. 374 – 383.

[16] Houari, M.S.A., Tounsi, A., Anwar Bég, O. (2013), "Thermoelastic bending analysis of functionally graded sandwich plates using a new higher order shear and normal deformation theory", *International Journal of Mechanical Sciences*, 76, 467 – 479.

[17] F.Z. Kettaf, M.S.A. Houari, M. Benguediab, and A. Tounsi, "Thermal buckling of functionally graded sandwich plates using a new hyperbolic shear displacement model," *Steel and Composite Structures*, vol. 15(4), pp. 399-423, 2013.

[18] I. Klouche Djedid, A. Benachour, M.S.A. Houari, and A. Tounsi, "A *n*-order four variable refined theory for bending and free vibration of functionally graded plates," *Steel and Composite Structures*, (Accepted), 2014.

[19] H. Matsunaga, "Free vibration and stability of functionally graded plates according to a 2-D higher-order deformation theory," *Composite struct*, vol. 82, pp. 499-512, 2008.

[20] H. Matsunaga, "Stress analysis of functionally graded plates subjected to thermal and mechanical loadings," *Composite struct*, vol. 87, pp. 344-357, 2009.

[21] R. Menaa, A. Tounsi, F. Mouaici, M. Zidi, and E.A. Adda Bedia, "Analytical solutions for static shear correction factor of functionally graded rectangular beams," *Mechanics of Advanced Materials and Structures*, vol. 19, pp. 641–652, 2012.

[22] R.D. Mindlin, "Influence of rotary inertia and shear on flexural motions of isotropic, elastic plates," *ASME Journal of Applied Mechanics*, vol. 18, pp. 31–38.

INVESTIGATING THE PAKISTAN'S OFFSHORE SOFTWARE INDUSTRY INFRASTRUCTURE

Zia ur Rahman
Department of Computer Science
Bacha Khan University
Charsadda, Khyber Pakhtunkhwa, Pakistan
zia.cs@bkuc.edu.pk

Izaz Ahmad Khan
Department of Computer Science
Bacha Khan University
Charsadda, Khyber Pakhtunkhwa, Pakistan
azazhmd2005@gmail.com

***Abstract*— Offshore software production is a legally binding business of great programming creation at seaward destinations with critical cost-sparing. Main purpose of this research paper is to evaluate the offshore software industry infrastructure. We conduct a questionnaire surveys with 50 experts of 20 different software houses of Pakistan. We asked from the software houses to rank each important factor on a five point scale to determine show the perceived value of each success factor. Our survey consist of valuable factors identified in the previous findings of our literature review. We have recognized Components for example, cost-saving, infrastructure. We have also identified cost-saving as being common in three types of organizations (i.e. small, medium and large). Cost-saving and appropriate infrastructure should be addressed by vendor organizations in order to compete in the offshore outsourcing business.**

Keywords*— Cost reduction. Outsourcing, project management, Pakistan Software Export Board

I. INTRODUCTION

The world is entering into information age which has brought about significant change in the manner the world use to run due to which a notable change is occurring in societies, associations, agencies, corporations and industries. The software industry is also in a state of transition under the impact of globalization. The software industry started in mid-1964's but its impact on the world was almost invisible till 1970 with annual turnover of $0.5 billion as shown in figure 1. The Software industry has stated development in 1970 when the IBM has started to decide investing in software. In 1979 the annual sales of US software companies was about $20 billion, in 1982 it was $10 billion and in 1985 it was came up to $25 billion [1]. The US department of commerce produced a report with the name of A Competitive Assessment of the United States Software Industry (1984) to give suggestions for keeping US at leading position in software industry after a committee of OECD conducted during 1983-84[2]. The suggestions were about achieving intellectual property legislation, dealing with piracy and reduction of tariffs to US software exports. The balance of payment in Britain became worse in 1980 due to which a study was conducted Advisory Council for Applied Research and Development (ACARD) known as A Vital Key To UK Competitiveness (1986).

A.T. Kearney report highlights, automation combined with business process as a service (BPaaS) has the potential to be an even more powerful of disruptive change, also identify the strongest underlying fundamentals to potentially deliver information technology (IT), business process outsourcing and voice services [3]. There are 1,500 registered software firms with US $1.4 billion of exports. The major attracting factors of Pakistan as an offshore destination for software development includes highly skilled man-power with 20,000 IT graduates produced each year, English as medium of education, friendly tax policies and easy starting of business [4].

The size of industry and exports are US $ 2.8 billion and US $ 1.4 billion respectively based on the WTO-prescribed formula with 61% exports over last year. The figure 6 also records that there are approximately 20,000 produced by 110 educational institutes offering IT related programs; there are more than 15,000 professionals employed in export oriented activities while approximately 110,000 are total number of IT professionals. The figure 6 also shows the export targets for year 2007-08 that is US$ 162 million and a total spending for the fiscal year 2005-06 is US$ 1.4 billion. The number of IT parks is eleven with an area of 750,000 sq ft. The total software exports for fiscal year 2005 are US$ 1.050 billion. The major attractions for the offshore clients are high quality software developments, speedy and painless establishment of business, low cost basis, and emerging and state of the art telecommunication and IT infrastructure. The estimated growth is considered to be 33% annually with an estimated US$ 10 billion in the next five year [5].

The software firms are divided into software contractors, packaged software and PC software industry. The software contractors were developing software's for computer users and manufacturers and were the starter of the industry in the mid 1950's. The packaged software firms started in the 1960's to develop the software for public and private sector organizations with the competition among them. The PC industry developed in late 1970's for personal computers. The IBM was the largest producers of the software with few Fujitsu and Microsoft as second and third respectively in 1992. The

figure 1 shows software revenues from 1964 to 1985 in which an exponential growth is recorded after 1979. The term software was coined in 1959. The employment in the software industry was small in the beginning which later on increased with the time. The famous software companies of late 1950's were TRW, THE MITRE Corporation, and Hughes dynamics. Later on other companies emerged in the industry which includes computer usage company (CUC), Computer Science Corporation (CSC), The Planning Research Corporation (PRC), Informatics, and Applied Data Research (ADR) in early in 1960's [6].

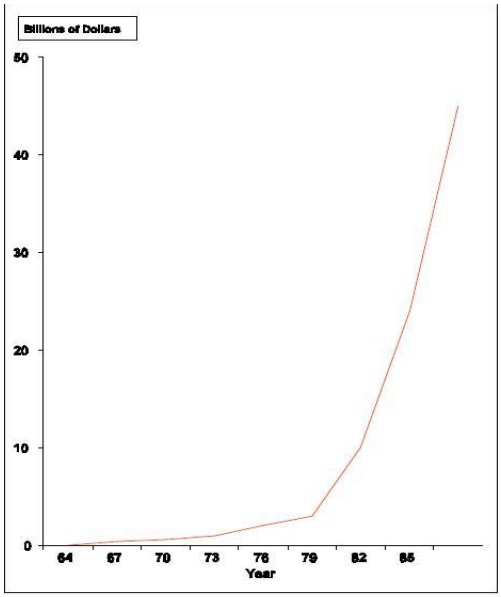

Figure 1. Growth Curve of World Wide Software Revenues 1964-1986

The figure 2 shows the major global software industries. The industries of India, Israel and Ireland are export oriented while that of Brazil and china is domestic. The figure 2 also shows that in 2002 Indian and Chinese industries were of almost similar sizes $12.5 and $13.3 billion while that of Brazil and Israel were $7.7 and $4.1 billion respectively in 2001. The Irish industry was $13.9 billion in total sales in 2002 of which $12.3 billion was the multinational companies and $1.6 billion domestic. The US is the largest producer of software $200 billion in sales while Japan and Germany are second and third with $85 billion $40 billion in sales. The Chinese and Brazilian industries are domestic but the growth is substantial e.g. the Chinese industry growth was 5% in 1999-2000 to 11% in 2002. The Indian software industry started with the on sight model in which Indian firms hired software programmers to work on the client side and under the client's management and same was done by the US firms. The Indian firms have a major cost advantage over there US partners in the lower end of the software services but they could not run directly with big producers as the likes of EADS, Computer Science Corporation, Anderson consulting (now Accenture) and IBM. The Indian software houses have shown competiveness by doing large projects like Y2K which has improved their image as global producers [7].

Countries	Sales ($ billion)	Empl (000)	Sales/ Empl (000)	Software Sales/GDP (%)	Software Development Index
Brazil *	7.7	160 **	45.5 **	1.5	0.22
China	13.3	190 **	37.6 **	1.1	0.23
India	12.5	250	50.0	2.5	0.96
Ireland (MNE)	12.3	15.3	803.9	10.1	0.34
Ireland (Domestic)	1.6	12.6	127.0	1.3	0.04
Israel *	4.1	15	273.3	3.7	0.17
US	200	1024	195.3	2.0	0.05
Japan **	85	534	159.2	2.0	0.08
Germany *	39.8	300	132.7	2.2	0.09

Various sources. * = 2001; ** = 2000;

Figure 2. The Software industry in Brazil, China and the 3Is and by comparison in the US, Japan and Germany

II. Major Software Developing Countries

The globalization of production of the software industry is often associated with major multinational companies (MNCs). The MNCs has a sizeable presence all around the world where development of the software is going on. The MNCs came to Israel for doing R&D to develop new technologies and techniques for developing software. The Indian software industry is service oriented where MNCs went for inexpensive skilled workers because the Indian developers are highly efficient and skilled and at the same time the cost is many time less than those in developed countries. The Irish provided them with the tax and incentives due to which MNCs started investing in Ireland by developing software products at low cost and the Irish developers provided them with European standard of skills with low cost. These MNCs includes oracle, Microsoft, Sun Microsystems, IBM etc. Other software producing companies are North Korea, Hungary, Philippines, Czech Republic and Taiwan but there size of production is comparatively small. The current global spending on the IT services, software and BPO with US $1.045 trillion [9].

III. Offshoring

The research studies by NASSCOM, Gartner and Forester suggests that there is an estimated US $ 1.045 trillion of current spending on the IT services, software and BPO out of which US $280 billion is potentially offshorable [10] but the actual revenue from offshoring is US $ 40 billion[9].

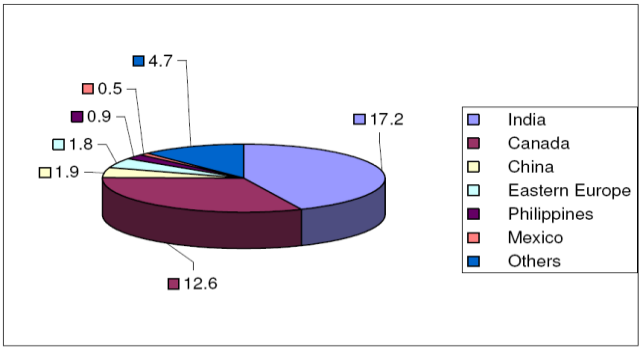

Figure 3: Major offshore outsourcing countries

(Bacha Khan University, Charsadda)

The figure 3 shows that the major offshore outsourcing countries. India is the leading country responsible for 17.2% of global offshoring followed by Canada with 12.6%, china is third with 1.9% and Eastern Europe with 1.8%, Philippines 0.9% and Mexico 0.5%, while other countries have 4.7%[9].

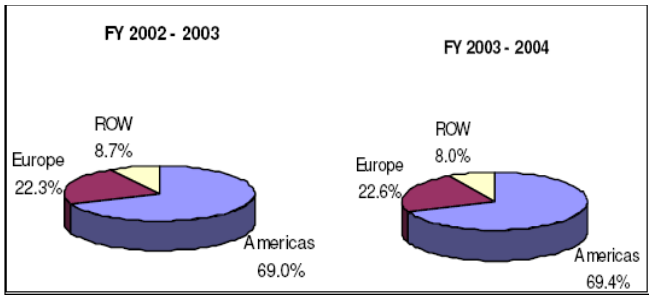

Figure 4: Major Offshore outsourcing importers

The figure 4 shows the major global importers for fiscal year of 2002-2003 and fiscal year 2003-2004. Americas are the largest importers with 69.0% and 69.4%, Europe has 22.3% and 22.6% while rest of the world has 8.7% and 8.0% for both the respective years [9]. The term off shoring is highly related to outsourcing. Outsourcing is the phenomenon by which an organization selects and buy items that was made within the organization or service which were also performed within the organization [11]. The term offshoring has different meaning to different people due to which it has been confused. He further suggests that offshoring is much more than outsourcing and sometime do not even include outsourcing, an organization can offshore by opening its production or services in overseas as well it can to a foreign long term contractor [12]. A phenomenon when outsourcing is outside the principal company's country [13].

The off shoring is current research has been taken as both outsourcing as well as the establishment of business of a company outside its country of origin. The offshore outsourcing involves Information Technology Outsourcing (ITO) and business process outsourcing (BPO). In ITO the contracted company provides a specific application for example all related servers, networks and software upgrades while in BPO the contracted company managers all the business processes for example accounting, procurement or HR [11]. Other types of Offshoring are staff augmentation, bundled maintenance, application support services, turnkey projects, net sourcing, enterprise partnership and joint venture [14].

In case of staff augmentation the clients manage and supplement in house teams with supplier staff while in bundled maintenance supplier is responsible for small maintenance items and minor requests, in turn key projects the supplier manage and provide final project while in net sourcing supplier hosts application and services are provided through a network. While in enterprise partnerships shared services are created to fulfil the demands of the client which ends when transformation is complete, in the case of joint venture the client and supplier commercialize the clients back office services. The ITO consists of both application support services and application outsourcing. The evolution of off shoring started when manufacturing work in 1980's shifted to the area with low labor costs. The reason behind the migration of manufacturing work between Urban and rural areas were cheap lands, tax incentives, holidays and skilled labor at lower costs. This trend is followed by global corporations by achieving higher cost arbitrage through moving internal manufacturing, operations and service functions for example call centers and back-office work to lower cost countries [13]. With further motivation of remaining close and gaining improved access to foreign markets. These organizations have started to outsource the non-principal activities to local or regional suppliers to gain access to the specialized expertise as well as low costs.

The latest trend of off shoring among the global corporation is motivated by two factors to countries mainly like India and China, while other locations are Philippines, Brazil, Ireland and Czech Republic [11].The offshore outsourcing or sometime Global outsourcing has a market of Euro 185 Billion in 2005, which will increase considerably in near future [15]. The Offshoring process is getting acceleration but apparently it is still modest because it cannot be applied to all sectors. The automobile has seen high level of Offshoring with 30% in UK and 15% in USA while the average across manufacturing is 25 % in UK and 12% in USA [12]. According to software engineering institute 40% high level of the companies are Indian in origin [16]. Forrester Research reveals that 14% of 3.30 million offshore white collar jobs will end up in low cost countries. There are many advantages of off shoring, some of the advantages are [17]

A. Cost saving

It is the most important factor in information system (IS) outsourcing [18][19] and off shoring as well [20]. The reason for the low cost is the difference of salaries between in the customer firm and the staff working in the firm which provides the outsourced services [20].

B. Technical fesability

The second advantage is the technical feasibility in measurement of security and storage which leaves off shoring much easier [21].

C. Flexibility and speed

Most of the customers firm of off shoring are located in USA and Western Europe while the suppliers are in Asian countries. Due to the time difference 24 hour's work is possible on a project. Thus off shoring give us the feasibility of working 24 hours on a project this is increasing flexibility and speed [20].

D. High Standards and Entering to potential new market.

Customer also wants quality, [20] suggests that many US firms thinks that off shoring enhances quality as of the high staff turnover rate that they experience is not as common as with the firms providing these services [22]. All the big Indian firms have maximum level of CMM certificate [20].

Offshoring is a way of entering into new markets with high potential [23]. For example in case of china and Russia both are new markets with low labour costs but also with high economic growth as well as large population size [20].

IV. Numerical Results

According to Aberdeen group" If you are an offshore provider and you are not CMM certified, companies do not even consider you", which shows that quality initiative is highly important for the industry in Pakistan. The majority of surveyed firms recognize the importance of certification. The research results point out that 63.6% of the firms are ISO/SEI certified. The figure 5 shows that all of the firms i.e. 100.0% consider the ISO/SEI certification. The results shows that 100.0% have a high level of certification which is a positive sign and can easily attract the potential customers.

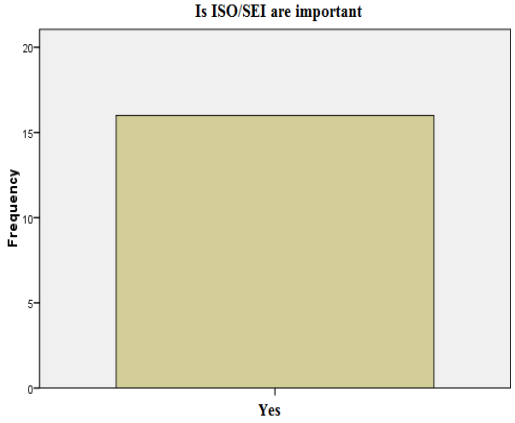

Figure 5. Quality initiative and industry infrastructure - Is ISO/SEI important?

The figure 6 shows that almost all the firms involved in the research are the members of the PSEB (Pakistan Software Export Board). The PSEB is established by the government of Pakistan to promote the export of software products and development of industry. The figure 6 shows that the 100.0% of the firms are the members of the PSEB. The results show that there is a high level of awareness about the organization because the firms see a purpose in joining it. The PSEB also provides link to the firms registered on its website.

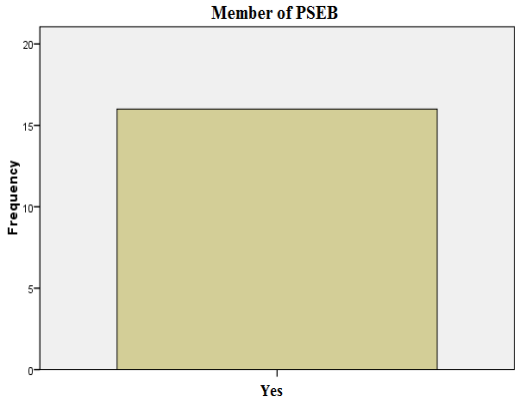

Figure 6. Quality initiative and industry infrastructure - member of the PSEB (Pakistan Software Export Board)

V. Conclusion

The research shows that most of the firms are aware of the internal standards i.e. ISO/SEI, and a majority of them have certification which is an important factor for attracting potential clients. The study has also revealed the fact that association support in Pakistan is high because all most all of the firms are the members of the PSEB. The PSEB provides an important facility to all software firms to be registered with it incredibly easy from where it can accessed by the potential clients much more easily. The PSEB provides an increasingly important facility of membership but now it needs to think beyond by developing the resources.

References

[1] M. Phister, Data processing technology and economics, 2nd ed. Bedford, VA: Digital Press, 1979

[2] "A competitive assessment of the U.S. Software industry," 1984. [Online]. Available: http://www.worldcat.org/title/competitive-assessment-of-the-us-software-industry/oclc/11615871. Accessed: Oct. 10, 2016.

[3] A.T. Kearney, "On the eve of disruption" [Available at] http://www.atkearney.com/, 2016.

[4] PSEB, "Overview: Pakistan software export board (PSEB)," [Available at] http://pseb.org.pk/about-us/overview.html, 2016.

[5] PSEB, "IT Industry overview," [Available at] 2016.

[6] M. C Kelly, "Development and Structure of the International Software Industry, 1950-1990," Business History Conference, vol. Volume 24, no 2, Winter 1995, ISSN 0849-6825, pp. 73–110, 1995

[7] F.T Tschang and L. Xue, "Underdogs to Tigers: The Rise and Growth of the Software Industry in Brazil, China, India, Ireland, and Israel. Research Collection Lee Kong Chian School Of Business," in The Chines Software Industry. 2005

[8] A. Arora and A. Gambardella, "The globalization of the software industry: Perspectives and opportunities for developed and developing countries," Innovation Policy and the Economy, vol. 5, pp. 1–32, Jan. 2005.

[9] Bearing Point, "Strategy for increasing export of BPO (Business Process Outsourcing)," Document Number: PSEB_VOL_9, Document Version: 0. 9, Disposition: Final Report. pp 8-10, 2005

[10] Young, Allie, Dane S. Anderson, Kenneth F. Brant, Robert H. Brown, Linda R. Cohen, Susan Cournoyer, et al. "Gartner on outsourcing, 2008–2009." Gartner. http://www. gartner. com/DisplayDocument, 2008

[11] C. Research, A. T. Kearney, and I. A. T. Kearney, Outsourcing strategically for sustainable competitive advantage. Tempe, AZ: CAPS Research, 2005

[12] Off shoring, "Off shoring - Process, pain or profit: Report on the Workshop held under the auspices of the Adecco Professorship of Business and Society at London Business School, Monday February 28th 2005," 2005.

[13] B. Ghodeswar and J. Vaidyanathan, "Business process outsourcing: An approach to gain access to world - class capabilities," Business Process Management Journal, vol. 14, no. 1, pp. 23-38, Feb. 2008

[14] Lacity, M.C. and Willcocks, L.P, "Relationships in IT outsourcing: a stakeholder perspective," in Zmud, R.W. (Ed.), Framing the Domains of IT Management: Projecting the Future through the Past, Pinnaflex Educational Resources, Cincinnati, OH, 2008.

[15] IDATE Foundation, "Digiworld 2005. Los retos del mundo digital," IDATE-ENTER, Montpellier, Francia, available at http://enter.es/enter/file/espanol/texto/digiworld.2005. pdf , 2005

[16] W. R. King, "Outsourcing becomes more complex," Information Systems Management, vol. 22, no. 2, pp. 89–90, Mar. 2005

[17] S. Palvia, "Global Outsourcing of IT and IT enabled services: Impact on US and global economy," Journal of Information Technology Case and Application Research, vol. 5, no. 3, pp. 1–11, Jul. 2003

[18] P. Gottschalk and Solli‐SætherHans, "Critical success factors from IT outsourcing theories: An empirical study," Industrial Management & Data Systems, vol. 105, no. 6, pp. 685‐702, Aug. 2005.

[19] G. G. Udo, "Using analytic hierarchy process to analyze the information technology outsourcing decision," Industrial Management & Data Systems, vol. 100, no. 9, pp. 421–429, Dec. 2000.

[20] R. Gonzalez, J. Gasco, and J. Llopis, "Information systems offshore outsourcing," Industrial Management & Data Systems, vol. 106, no. 9, pp. 1233–1248, Dec. 2006

[21] R. B. Misra, "Global IT Outsourcing: Metrics for success of all parties," Journal of Information Technology Case and Application Research, vol. 6, no. 3, pp. 21–34, Jul. 2004

[22] R. Ravichandran and N. U. Ahmed, "Offshore systems development," Information & Management, vol. 24, no. 1, pp. 33–40, Jan. 1993

[23] M. G. Sobol and U. Apte, "Domestic and global outsourcing practices of America's most effective IS users," Journal of Information Technology, vol. 10, no. S4, pp. 269–280, Dec. 1995

INTERNATIONAL CONFERENCE ON ADVANCES IN SCIENCE AND ARTS ISTANBUL 2017

29 – 31 MARCH 2017, Istanbul, Turkey

EFFECT ON LEVEL OF PLASMA MALONDIALDEHIDE OF BELLIS IN *CYPRINUS CARPIO*

AkramMudherKareem ALJBORI[1], Haci Ahmet DEVECİ[2], Gökhan NUR[2],

Hussein Mudheher Kareem ALGBURI[3] , Canan CAN[1]

[1] Gaziantep Üniversitesi, Biokimya Bilimi ve Tekno Bölümü, Gaziantep
[2] Gaziantep Üniversitesi, Islahiye Meslek Yüksekokulu, Veterinerlik Bölümü, Gaziantep
[3] Tikrit Üniversitesi , Mühendislik Fakültesi

INTRODUCTION

Environmental pollution is the most important one of the reasons used against agriculture in the widely used pestisitlerdir.tarımsal activity in major causative fungal agent material losses Bellis, pistachio in Gaziantep region, pomegranate is an effective, being used widely fungicides in crops such as cherries and apples. Bellis carp made in this study Malondialdehide(MDA) aimed to investigate the effect on the activity.

MATERIALS AND METHODS

In this study, 24 fish (200-300 g*) Cyprinuscarpio* (L. 1758) from ıslahiyetahtaköpr's dam were used. The fish were transported to the laboratory in polyethylene tanks for a period of 5 days (22-25 ° C and normal photoperiod). The new environment has provided adaptation for them . Then they were divided into 3 groups of 8 fish: A control group , group of 0.025 mg / L Bellis and a group of 0.050 mg / L Bellis . After the end of 14 days of application, blood samples were taken from the fish and the serums were separated. The obtained serum samples of Malondialdehide (MDA) were analyzed .

RESULTS

Life environment to 0.025 and 0.050 mg / L Bellis added fish with untreated control group of fish of 14 days is received when a blood sample biochemical parameters are in Bellisgrup compared to assess when the control group (0.025 and 0.050 mg / L) was found to decrease in Malondialdehide(MDA) levels**.**

PARAMETERS	**GROUPS**			
	Control (n = 8)	**Bellis I (0.025 mg/L) (n = 8)**	**Bellis II (0.050 mg/L) (n = 8)**	**p <**
MDA (µmol/l)	1.47± 0.13[a]	1.74± 0.25[b]	1.83± 0.24[b]	**

[a, b] There are significant differences between the averages with different letters in the same row (**: p< 0.05). There is not significant difference between the avarages with same letters in the same row (p>0.05)

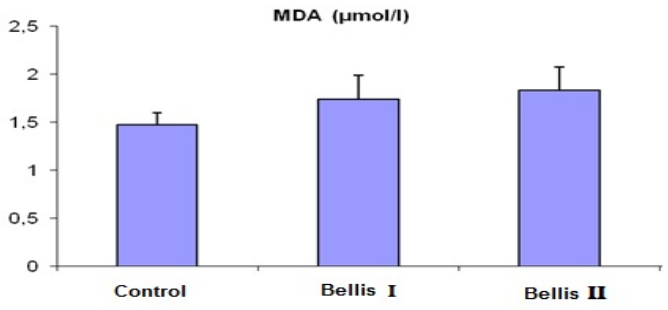

Statistically significant difference was found between control and Bellis I groups in terms of MDA amount ($p<0.05$). In addition significant difference was found between control and Bellis II groups ($p<0.05$). As a result of the statistical analysis it was determined that the difference between Bellis I and Bellis II was not significant ($p>0.05$)

Conclusion: The results of studies that have recently begun to be used in an effective fungicide, which Bellis carp due fish involved in the detoxification of pesticides Malondialdehide(MDA) .

INTERNATIONAL CONFERENCE ON ADVANCES IN SCIENCE AND ARTS ISTANBUL 2017
29 – 31 MARCH 2017, Istanbul, Turkey

GEOMETRIC SCALE EFFECT ON PERFORMANCE OF PEM FUEL CELLS

***Sertaç GÜNEY**
Süleyman Demirel University, Department of Textile Engineering
Çünür, 32260, Isparta, Turkey

Filiz GÜNEY
Süleyman Demirel University, Department of Textile Engineering
Çünür, 32260, Isparta, Turkey

İbrahim ÜÇGÜL
Süleyman Demirel University,
Department of Textile Engineering
Çünür, 32260, Isparta, Turkey

Keywords: scale, dimensions, fuel cell, PEM, fluent
** Corresponding author:, +90 246 2111576, +90 246 2111180*
E-mail address: sertacguney@sdu.edu.tr

ABSTRACT

In this paper, the effect of geometric scaling on fuel cell performance has been investigated. The geometry of a fuel cell flow structure involves several dimensional parameters, e.g., flow channel and rib shapes, catalyst and diffusion layer thickness. Practically, it is impossible to research the effects from all combinations of these parameters simultaneously. We investigated a single turn serpentine pattern with rectangle-shaped channels and ribs. A model based on three-dimensional computational flow dynamics (Ansys Inc. Fluent) has been developed which predicts that scale changing of cross section effect on performance. The operating condition of the fuel cell associates several parameters as well, such as the gas stoichiometric number, cell temperature, and gas humidity. These parameters had remained constant for a fair comparison of performance at each feature size in this study. We have presented observations on cross sectional scaling effects in fuel cells. This study can provide a good opportunity for designing PEM fell cell in respect of size scaling.

INTRODUCTION

Fuel cell technology has been drawing increasing attention as renewable energy source for stationary and portable power systems. Proton exchange membrane (PEM) fuel cell is the most common type of low-temperature fuel cell. The researchers have focused on improving performance of PEM fuel cells in recent years. Design and manufacturing process parameters influencing performance of PEM fuel cells are electrolyte thickness, diffusion layer structure and electrode and flow channel geometry.

Fuel cell components are made of relatively square components so creating accurate curved surfaces is not necessary. However the accuracy of the geometry can greatly affect the results of the simulation, particularly in the flow field [1].

A variety of studies have been done on the effect of the flow channels' different geometric variables on different operating aspects of the PEMFC [2-4]. Cha et all (2004), have experimentally investigated the scaling effect of flow channels on fuel cell performance. In addition, computational flow dynamics (CFD) modeling has been employed for comparison with experiment. They present a description of the flow channel scaling investigation and results from the model prediction. In their paper, parallel flow patterns with square-shaped channels and ribs are studied by observing the performance of flow channels [5].

RESULTS AND DISCUSSION

In the present investigation, a single turn serpentine pattern with rectangle-shaped channels and ribs was simulated in a model based on three-dimensional computational flow dynamics (Fig.1).

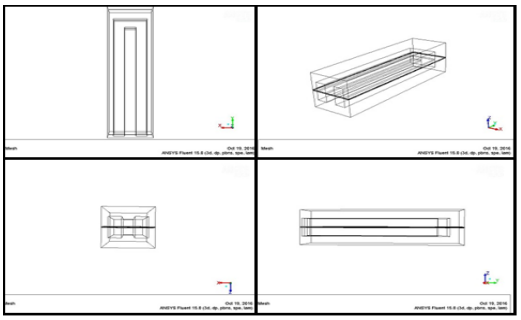

Figure 1. A single turn serpentine PEM fuel cell

We used the fuel cell geometrical dimensions given in Table 1.

Table 1. Fuel Cell Geometrical Dimensions

Part	Length (mm)	Width (mm)	Height (mm)
GDL	120	32	0.3
Catalyst Layer	120	32	0.06
Membrane	120	32	0.15
Channels	110	8	6
Collector	120	32	12

To observe the scaling behavior of flow channels by simply varying the scaling factors (x and y coordinates) in scaling mesh. The dimension of channel length was held constant. Five samples were created for comparison with scaling factors varying as 0.9, 0.8, 0.7, 0.6 and 0.5 for each x and y coordinates respectively. So we obtained ten different cross-section surfaces of fuel cell on xy coordinate plane.

The flow channel scaling effect for x coordinate is shown in Fig.1. The model shows that the performance of fuel cell decreases as dimension along x coordinate (x scaling factor) decreases. Because of the contact area decreasing along the channel length.

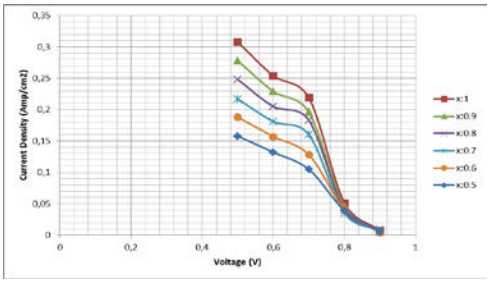

Figure 1. Polarization curves under different x scaling factors.

In the other hand, the flow channel scaling effect for y coordinate is shown in Fig.2. Unlike x scaling factors, performance of fuel cell increases as dimension along y coordinate (y scaling factor) decreases.

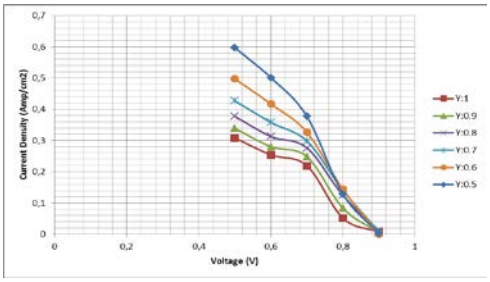

Figure 2. Figure 1. Polarization curves under different y scaling factors.

Gas velocity increases in smaller channels. Accordingly, smaller channels can take out the water more efficiently by enhanced convection. The contours of velocity magnitude are shown in Fig.3.

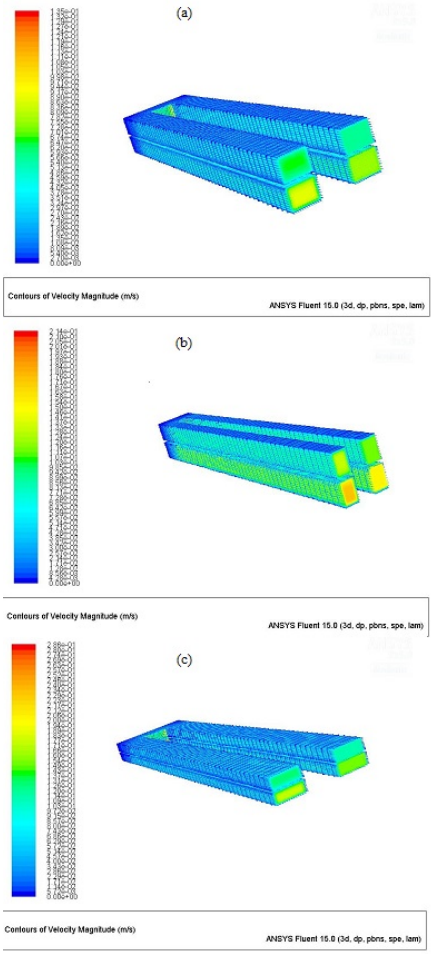

Figure 3. Contours of Velocity Magnitude (a) x:1 ,y:1 ,z:1 (b) x:0.5, y:1, z:1 (c) x:1, y:0.5, z:1

Velocity magnitude can be ranked as c>b>a according to the scaling factors. As mentioned before, in scaling factor (x:1,

y:0.5, z:1) it has the same contact area but smaller channels so it showed mcuh more velocity magnitude

The same temperature must be maintained throughout the cell in order to prevent destruction of cell. The contours of total temperature are shown in Fig.4. The temperature for all samples is 353 K.

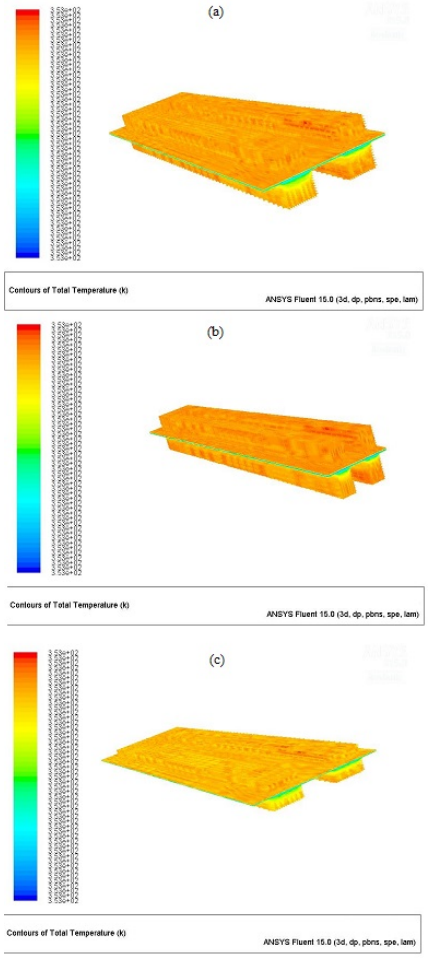

Figure 4. Contours of Total Temperature (a) x:1 ,y:1 ,z:1 (b) x:0.5, y:1, z:1 (c) x:1, y:0.5, z:1

CONCLUSION

In this study, we investigated the influence of the flow channel's cross section geometry under varying scaling factors on how a fuel cell works. We analysed the distributions of velocity and temperature for models created in Ansys Inc. Fluent. While Scaling factor on y coordinate decreases, the current density increases and it gives better performance. The results can be used to discuss important aspects affecting the design of fuel cell and improving this design and opmising its performance.

REFERENCES

[1] Arvay, A., (2011), Proton Exchange Membrane Fuel Cell Modeling and Simuation using Ansys Fluent, Arizona State University.

[2] Yoon Young Gi, Lee Won Yong, Park Gu Gon, Yang Tae Hyun, Kim Chang Soo. Effects of channel and rib widths of flow field plates on the performance of a PEMFC. International Journal of Hydrogen Energy 2005;30:1363e6.

[3] Shimpalee S, Van Zee JW. Numerical studies on rib & channel dimension of flow-field on PEMFC performance. International Journal of Hydrogen Energy 2007;32:842e56.

[4] Jeon DH, Greenway S, Shimpalee S, Van Zee JW. The effect of serpentine flow-field designs on PEM fuel cell performance. International Journal of Hydrogen Energy 2008;33:1052e66.

[5] Cha, S.W., O'Hayre, R. and Prinz, F.B., (2004), The Influence of size scale on the performance of fuel cells, Solid State Ionics, (175), p.789-795.

INTERNATIONAL CONFERENCE ON ADVANCES IN SCIENCE AND ARTS ISTANBUL 2017
29 – 31 MARCH 2017, Istanbul, Turkey

FEYNMAN PATH INTEGRAL METHOD APPLIED TO THE FROST-MUSULIN POTENTIAL

***Diaf Ahmed**
Laboratoire de l'énergie et des systèmes intelligents, Khe
mis Miliana University, Algeria

Amrouche Assia
Médéa University, Algeria

Bakhti Hadjer
Médéa University, Algeria

Keywords: Path integral, the Frost-Musulin potential, l-states
** Corresponding author:Diaf Ahmed:*
E-mail address: s_ahmed_diaf@yahoo.fr

ABSTRACT

We present the l-states solutions of the Feynman kernel for the Frost- Musulin potential within the framework of the Duru-Kleinert transformation method. We show that the bound state energy eigen-values can be obtained for any n and l values without using an approximation of the centrifugal term required by other methods. Our results are in good agreement with those obtained with other methods.

INTRODUCTION

The search for exact solutions of the radial Schrödinger equation constitutes a very useful research area and is of general interest. There are only a few potentials that can be solved explicitly for all n and ℓ but can not be generalized to exponential type potentials. In this case, the radial Schrödinger equation as well as relativistic Dirac and Klein-Gordon equations are solved either numerically [1], or by approximation methods [2].
In this work, we study an exponential-type potential, namely a Frost-Musulin potential [3-4] of the form:

$$U(r) = D_e\left[1 - \frac{\left(r+\delta r_e r-\delta r_e^2\right)e^{-\delta(r-r_e)}}{r}\right], \qquad (1)$$

Where r ∈ (0, ∞), and the three positive parameters D_e, r_e and δ denote the dissociation energy, the equilibrium bound length and the range of the potential well, respectively. Jia et al. [4] found that this potential has a minimum value at

$$r_e = \frac{1}{2}\frac{\delta p_1+\sqrt{\delta^2 p_1^2+4\delta p_1 p_2}}{\delta p_2}, \qquad (2)$$

with $p_1 = \frac{\delta D_e r_e^2}{e^{-\delta r_e}}$ and $p_2 = \frac{D_e(1+\delta r_e)}{e^{-\delta r_e}}$. This potential is often used in molecular physics [5, 6]. This paper is organized as follows. In Sec. 2, we derive arbitrary ℓ-states solutions of the Frost-Musulin potential within the Feynman path integrals formalism by approximate method. In Sec.3, the numerical calculations are given to compare with those obtained by other method. The concluding remarks are given in Sec. 4.

PATH INTEGRAL METHOD

The propagator for a particle of mass μ in the spherically symmetric potential can be developed into a sum of partial waves of the form [7]:

$$K(r'',t'';r',t') = \sum_{\ell=0}^{\infty}(2\ell+1)K_\ell(r'',t'';r',t')P_\ell(cos\theta) \qquad (2)$$

$P_\ell(cos(\theta))$ is the Legendre polynomial and

$$K(r'',t'';r',t')\lim_{n\to\infty}\left(\frac{\mu}{2\pi i\hbar\varepsilon}\right)^{\frac{1}{2}}\int\dots\int exp\left\{\frac{i}{\hbar}\sum_{j=1}^{n}S_j\right\}\prod_{j=1}^{n-1}dx_j \quad (3)$$

Here

$$S_j = \frac{\mu}{2\varepsilon}(r_j - r_{j-1})^2 - \varepsilon U_{eff}(r_j,\ell) \qquad (4)$$

With

$$\Delta r_j = r_j - r_{j-1}, \qquad \varepsilon = \Delta t_j = t_j - t_{j-1}, t' = t_0 \text{ and } t'' = t_n.$$

Where

$$U_{eff}(r_j,\ell) = U(r_j) + \frac{\ell(\ell+1)\hbar^2}{2\mu r^2}. \quad (5)$$

To calculate the propagator K_ℓ given by equation (3) for ℓ-States, we apply the following approximate scheme to the centrifugal term:

$$\frac{1}{r^2} \approx \delta^2\left[\frac{e^{-\delta r}}{(1-e^{-\delta r})} + \frac{e^{-\delta r}}{(1-e^{-\delta r})^2}\right]. \quad (6)$$

In addition, the term $\frac{1}{r}$ in the potential is replaced by

$$\frac{1}{r} \approx \frac{\delta e^{-\delta r}}{(1-e^{-\delta r})}, \quad (7)$$

The potential (5), becomes

$$U_{eff}(r_j,\ell) = \left(\frac{V_0}{(1-e^{-\delta r})} + \frac{\gamma}{(1-e^{-\delta r})^2} + V_1, \quad (8)$$

with

$$\begin{cases} V_0 = \delta p_1 \\ \gamma = \frac{\ell(\ell+1)\delta^2\hbar^2}{2\mu} \\ V_1 = -\delta p_1\left(1+e^{-\delta r}\right) - p_2 e^{-\delta r} + D_e + \gamma C_0 \end{cases} \quad (9)$$

Putting $t = \frac{e^{-\delta r}}{(1-e^{-\delta r})}$, $\delta \to 2\delta$,

this gives

$$U_{eff}(r_j,\ell) = -A\coth(\delta r) + \frac{B}{\sinh^2(\delta r)} + C \quad (10)$$

With

$$\begin{cases} A = \frac{\gamma - V_2}{2} \\ B = \frac{\gamma}{4} \\ C = \frac{\gamma - V_2}{2} + V_3 \end{cases}, \quad (11)$$

and

$V_2 = (V_0 + 2\gamma), V_3 = V_0 + V_1 + \gamma.$

In the following, we study the potential (10) with the Duru-Kleinert method [8]. The path integral for the potential (7) is

$$K_\ell(r'',t'';r',t') = \int Dr(t) exp\int_{t'}^{t''}\left(\frac{\mu}{2}\dot{r}^2 - U_{eff}(r_j,\ell)\right)dt \quad (12)$$

By achieving the space-time transformations

$$\begin{cases} r = f(q) \\ dt = f'^2(q)\,ds \end{cases} \quad (13)$$

In our case, we choose

$$r = \frac{1}{\delta} arcoth\,(2coth^2 q - 1) \quad (14)$$

This transformation allows us to reformulate the problem of the potential to the modified Pöschl–Teller potential, which is a known solved problem.

ENERGY SPECTRUM

Calculating allows us to obtain the Green function *G*. Then, the whole energy spectrum is derived from the poles, and the corresponding wave functions from the residues at the poles. The energy spectrum is given by

$$E_{n,\ell} = -\left[\frac{\hbar^2(s+2n+1)^2\delta^2}{32\mu} + \frac{8\mu A}{\hbar^2\delta^2(s+2n+1)^2}\right] + C, \quad (15)$$

With

$$s = \sqrt{1 + \frac{32\mu B}{\delta^2\hbar^2}}.$$

RESULTS AND DISCUSSION

To show the accuracy of energy levels obtained in this work with the path integral method, we calculate the energy levels (15) for different quantum numbers n and ℓ with two different values of parameter r_e. These results are compared to those exact results obtained by using the finite difference method in MATLAB. as shown in Tables 1 and 2. In addition, a comparison is made with the calculations of A. G Adepoju and E. J. Eweh[9], who solved analytically the Schrödinger equation, but using the same approach for the centrifugal barrier. We remark that our results are almost indistinguishable from the numerical ones. Nevertheless, except in a few cases, we get results closer to the numerical estimates compared to the method (Exact). This is due to our choice of the centrifugal barrier.

Table 1: Eigen values $E_{n,\ell}$ for the Frost-Musulin potential in atomic units: $\hbar$=μ= 1, δ=0.1 and D_e=15.

		r_e=0.4		
n	ℓ	Present	E(Approximate)	E(Exact)
0	0	-1.306565925	-1.306565933	-1.306565952
1	0	-1.286916924	-1.286916932	-1.286916962
1	1	-1.297164827	-1.297164835	-1.297164845
2	0	-1.288833776	-1.288833784	-1.288833784
2	1	-1.302940890	-1.302940898	-1.302940898
2	2	-1.326412739	-1.326412747	1.326412747
3	0	-1.296067174	-1.296067182	-1.296067198
3	1	-1.312814382	-1.312814390	-1.312814392
3	2	-1.338315508	-1.338315516	-1.338315526
3	3	-1.372736143	-1.372736151	-1.372736168
4	0	-1.306615204	-1.306615212	-1.306615243
4	1	-1.325816649	-1.325816658	-1.325816634
4	2	-1.353451686	-1.353451695	-1.353451667
4	3	-1.389759060	-1.389759069	-1.389759087
4	4	-1.435009149	-1.435009157	-1.435009168
5	0	-1.319983887	-1.319983895	-1.319983888
5	1	-1.341615790	-1.341615798	-1.341615746
5	2	-1.371478773	-1.371478782	-1.371478726
5	3	-1.409824978	-1.409824986	-1.409824946
5	4	-1.456927190	-1.456927198	-1.456927199

5	5	-1.513019245	-1.513019253	-1.513019287

Table 2: Eigen values E n, ℓ for the Frost-Musulin potential in atomic units: $\hbar$ =μ= 1, δ=0.1 and D_e=15.

		r_e=0.8		
n	ℓ	Present	E[9]	Exact
0	0	-3.247247646	-3.247247643	-3.247247667
1	0	-2.845432289	-2.845432286	-2.845432299
1	1	-2.793688211	-2.793688208	-2.793688256
2	0	-2.776577594	-2.776577591	-2.776577585
2	1	-2.770853172	-2.770853170	-2.770853185
2	2	-2.787403456	-2.787403453	-2.787403464
3	0	-2.759040950	-2.759040947	-2.759040987
3	1	-2.767483812	-2.767483809	-2.767483897
3	2	-2.790181073	-2.790181070	-2.790181089
3	3	-2.823937248	-2.823937246	-2.823937288
4	0	-2.758123989	-2.758123986	-2.758123999
4	1	-2.773292431	-2.773292428	-2.773292487
4	2	-2.799815071	-2.799815068	-2.799815098
4	3	-2.836255199	-2.836255196	-2.836255189
4	4	-2.882181607	-2.882181604	-2.882181656
5	0	-2.765264776	-2.765264773	-2.765264756
5	1	-2.784754028	-2.784754025	-2.784754034
5	2	-2.814271032	-2.814271029	-2.814271078
5	3	-2.853095407	-2.853095404	-2.853095443
5	4	-2.901050931	-2.901050928	-2.901050943
5	5	-2.958152409	-2.958152406	-2.958152414

CONCLUSION

In this paper, we have presented a path integral treatment for the Frost-Musulin potential. By using an approximation scheme for the centrifugal term and a nonlinear space-time transformation in the radial path integral, we were able to derive explicit expression of the energy eigenvalues in function of the potential parameters.

The barrier approximation being fixed, we note that the Feynman integral method gives results closer to numerical one than solving the Schrödinger equation.

To conclude, our method is efficient in solving this type of potentials. We intend in a near future, to expand the path integral method to a more general form of potentials and relativistic cases.

REFERENCE

[1] W. Lucha and F.F. Schöberl, Int. J. Mod. Phys. C 10, 607(199).

[2] A Diaf Chin. phys. V24, N02 (2015) 020302.

[3] A.A. Frost and B. Musulin. J. Chem. Phys. 22, 1017 (1954). doi:10.1063/1. 1740254.

[4] C.S. Jia, Y.F. Diao, X.J. Liu, P.Q. Wang, J.Y. Liu, and G.D. Zhang.J. Chem. Phys. 137, 014101 (2012). doi:10.1063/1.4731340. PMID: 22779631.

[5] E. Maghsoodi, H. Hassanabadi and O. Aydodu, Phys. Scripta 86 (2012)015005.

[6] E. Z. Livert, E. G. Drukarev, R. Krivec and Mandelzweig, Few-Body Syst. 44 (2008) 367.

[7] D.C. Khandekar, S.V. Lawande, Path Integral Methods and their Applications, World Scientific, Singapore, 1986.

[8] Duru I H and Kleinert H , Phys. Lett. B 84 (1979) 185.

[9] A.G. Adepoju and E.J. Eweh, Can. J. Phys. **92**: 18–21 (2014) dx.doi.org/10.1139/cjp-2013-0299

INTERNATIONAL CONFERENCE ON ADVANCES IN SCIENCE AND ARTS ISTANBUL 2017
29 – 31 MARCH 2017, Istanbul, Turkey

DAIRY INDUSTRY EFFLUENTS: CHARACTERIZATION AND IMPACT ON THE RECEIVING NATURAL ENVIRONMENT

***Khedidja Benouis**
University of Djillali Liabes
Sidi Bel Abbes, Algeria

Amina Amar
University of Djillali Liabes
Sidi Bel Abbes, Algeria

Mokhtar Bouhafes
University of Djillali Liabes
Sidi Bel Abbes, Algeria

Keywords: Dairy effluent, Characterization, Impact, Pollution, Environment.

** Corresponding author:*
E-mail address: benouiskhadidja@yahoo.fr

ABSTRACT

Like any human activity, agro-industry generates waste and effluent, pollutants that should be eliminated or at least minimized before being released into the environment.

Unfortunately, some industrial production units release its effluent into the natural environment without prior treatment; which can cause severe environmental pollution.

This study concerns itself with the characterization and impact of effluents discharged into the natural environment by some dairy production units in Algeria to give an example of the type and the degree of the environmental pollution generated by this industrial sector.

INTRODUCTION

All industrial sectors leave an environmental footprint because they use energy or raw materials and produce waste or effluent which is found after rejected in nature.

Generally, Agri-food industries, in particular dairies industries are among the most demanding industries in terms of quantity and quality of water used. They are considered from the most environmentally polluting activities because they consume not only big volumes of water for the milk and its derivatives fabrication and for cleaning and disinfection, but also reject them in form of Wastewater rich in micro-organisms and organic matter.

Before being discharged into nature, this wastewater must be treated by an efficient sanitation system, maintained and adapted to his characteristics. Unfortunately, some industrial production units reject their raw effluents into the natural environment without prior treatment, which can lead to serious environmental pollution.

This study investigates the characterization and the impact of effluent discharged into the natural environment by some dairy production units in Algeria to give an example of environmental pollution's type and degree generated by this industrial sector.

MATERIALS AND METHODS

The three production units which were the object of our study are: The BAHDJA and SIDI KHALED, two dairy units located in the region of Tiaret; and the SOURCE, which is located in the region of Saida.

All measurements necessary to quantify pollution parameters are standardized according to Algerian standards for industrial liquid discharges [1].

The analyses were carried out on samples taken from the end of the discharge during a normal period of operation of all the workshops of the units. The sampling took place during the morning, where the discharge of the evacuated waste water is very high.

The samples were taken from polyethylene bottles and preserved in a cooler and transported to the laboratory for analysis where they were stored in the freezer at 4 °C in order to avoid any change in the characteristics of the wastewater.

Physico-chemical analyses have focused on the following parameters: Temperature (° C), pH, Total Suspended Solids (TSS), Chemical Oxygen Demand (COD), Biological Oxygen Demand (BOD5), Oils and Fats.
Temperature in °C and pH were measured in situ using a Multi-parameter analyzer.
The other parameters were determined in the laboratory according to International Standards:

• Total Suspended Solids (TSS): according to the International Standard ISO 11923-1997 [2],

• Chemical Oxygen Demand (COD): according to the International Standard ISO 6060-1989 [3],

• Biological Oxygen Demand (BOD5): according to the International Standards ISO 5819-1989 [4],

• Oils and Fats: according to the International Standard method JIS 0102.24.2 [5].

RESULTS AND DISCUSSION

The results of physic-chemical analysis are presented in Table I.

Table I. The Physico-Chemical Characteristics Of The Dairy Effluents

Parameter	Unit	BAHDJA	SIDI KHALED	SOURCE	Algerian Standards [1]
T	°C	14.40	16.90	26.20	30
pH	-	8.14	8.10	8.15	6.5 - 8.5
TSS	mg/L	280	460	200	35
COD	mg O_2/L	790	430	878	120
BOD5	mg O_2/L	77	100	380	35
Oils -Fats	mg/L	170	11	07	20

Temperature (T °C)

Temperature is one of the most important ecological factors affecting all aquatic organisms. Regardless of the receiving medium type, the temperature of the discharge must be less than 30 ° C [1]. A value greater than 30 °C may have for effect to kill some Species, but also to foster the development of other species resulting in Ecological imbalance.
The obtained results show that the temperature of the samples analyzed does not exceed the limit set by Algerian legislation for liquid discharges in a receiving environment.

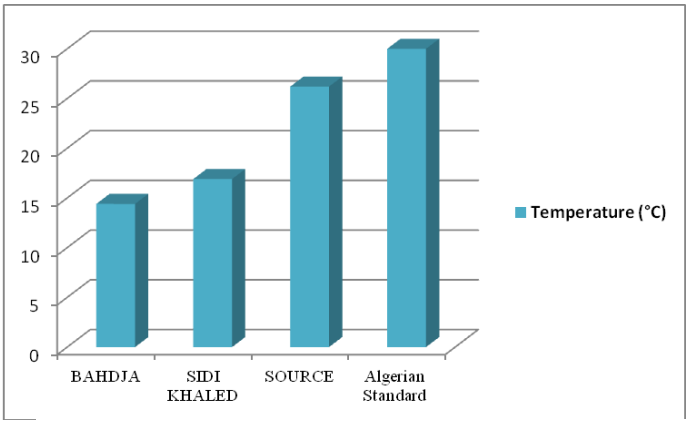

Figure 1. Temperature Of Dairy Effluents Ph

The pH of the three effluents is close to the maximum value Authorized by the said standard and which is 8.5. The analysis showed pH values of the order of 8.1, 8.14 and 8.15 (figure 2). These discharges are slightly alkaline, due to the use of the sodium hydroxide (NaOH) in the washing of the apparatus.

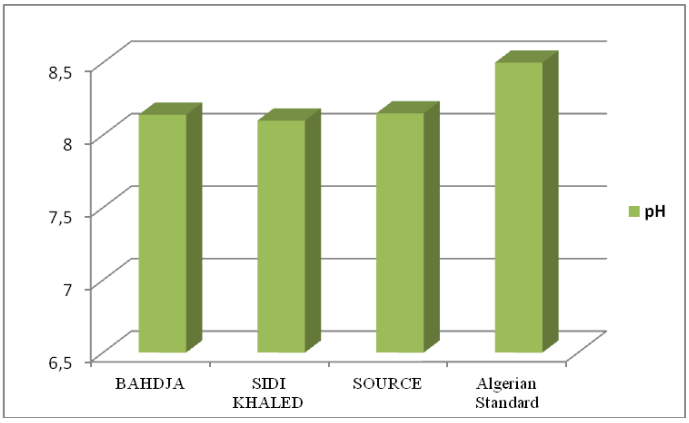

Figure 2. Ph Of Dairy Effluents

Total Suspended Solids (TSS)

Significant levels of total suspended solids have been detected in the analyzed rejects: 200 mg/L, 280 mg/L and 460 mg/L (figure 3). These high values are compared to the 30 mg/L value fixed by Algerian legislation as limit value for direct liquid reject in the natural environment.
TSS can be effectively eliminated by a simple liquid-solid separation technique, either by gravity or flotation. Despite that the dairy of SIDI KHALED is equipped with a purification plant, its effluent is characterized by high contents of TSS (460 mg /L), it is 15 times more than the standard value. This indicates that the technique of elimination of TSS at the station level is not really effective.
This abundance of TSS in the discharge can reduce the luminosity which lowers the productivity of a watercourse and causes a decrease in dissolved O_2 by slowing down the photosynthetic phenomena that contribute to the aeration of the

water. They may also be responsible for the physical clogging soil, which leads to a decrease in its permeability and in consequent the destruction of its quality during irrigation [6].
The abundance of suspended solids can also be the cause of many problems, such as those related to the deposition of materials, their physico-chemical adsorption capacity or the phenomena of deterioration of the material (clogging, abrasion, etc.). It can seriously compromise the operation of the sewer system.

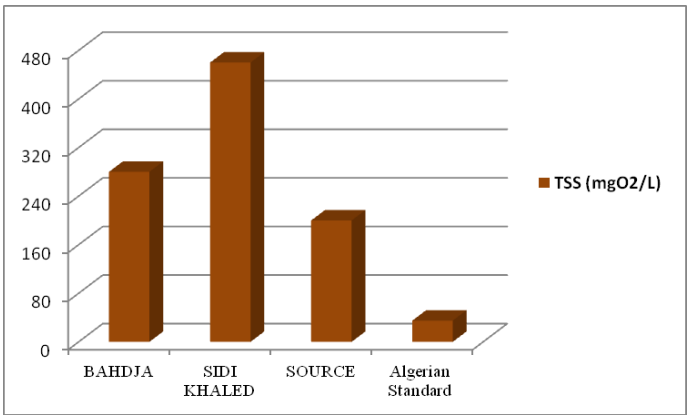

Figure 3. Tss Of Dairy Effluents

Chemical Oxygen Demand (COD)

Very high values of COD were detected in the two effluents discharged by the two dairies: 790 mg O_2/L, 430 mg O_2/L and 878 mg O_2/L (figure 4), well above the value authorized by the said standard which is of the order of 120 mg O_2/L (6 times the standard), reflecting the large amount of oxidizable matter contained in the final discharge.
Pollution by organic matter (protein, amino acids, lipids and other reserves), which is degradable or not, discharged into watercourses, leads to a consumption of the oxygen dissolved in the water, which is to the detriment of living organisms [7, 8].

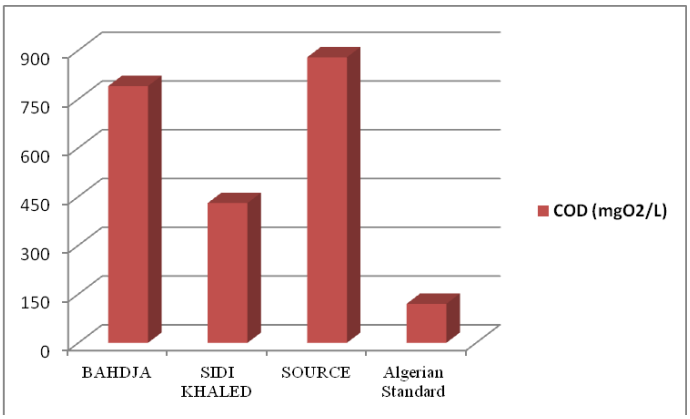

Figure 4. Cod Of Dairy Effluents

Biochemical Oxygen Demand (BOD5)

For BOD5, the values recorded were 77 and 100 mg O_2/L and 380 mg O_2/L for the effluents of the three dairies BAHDJA, SIDI KHALED and SOURCE respectively (figure 5). It is 2, 3 and 10 times higher than the value of 35 mg O_2/L authorized by the Algerian standard for direct discharges in a receiving environment, which confirm the absence of microorganisms that promote the oxidation of organic matter.
Any biodegradable organic matter released will result in oxygen consumption during self-purification processes [9, 10].
The COD / BOD5 ratio of the effluent discharged by the three dairies and which is indicative of the biodegradability of an effluent is higher than 4 for the BAHDJA and SIDI KHALED units, it is in order of 10 and 4.3 respectively. This indicates that effluents are hardly biodegradable.
These results are explained by the fact that the collectors drain effluent containing the residues of multi-products used in the various cleaning operations (production rooms, water treatment room, milk preparation room and its derivatives) using various detergents and adjuvant as well as disinfection with sodium hypochlorite.

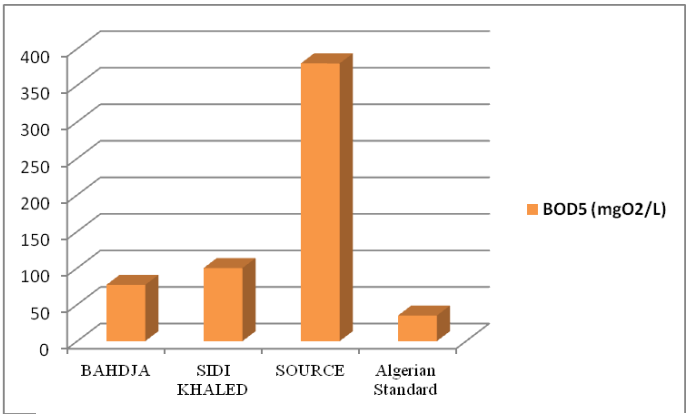

Figure 5. Bod5 Of Dairy Effluents

Oils and Fats

The presence of fats in the effluent is due to the raw material used in the dairy industry. Their content in the effluent of the SIDI KHALED unit and the SOURCE unit is 11 and 7 mg/L respectively (figure 6), which respects the Algerian standard set at 20 mg/L, this value is largely exceeded in the rejection of the BAHDJA unit, the concentration reached 170 mg/L.
Oils and fats are substances of animal or vegetable origins; they are hardly biodegradable [11] and can pose various problems such as greasy sludge [12], and the appearance of filamentous bacteria.
They are also very damaging for equipment and especially for pumps.

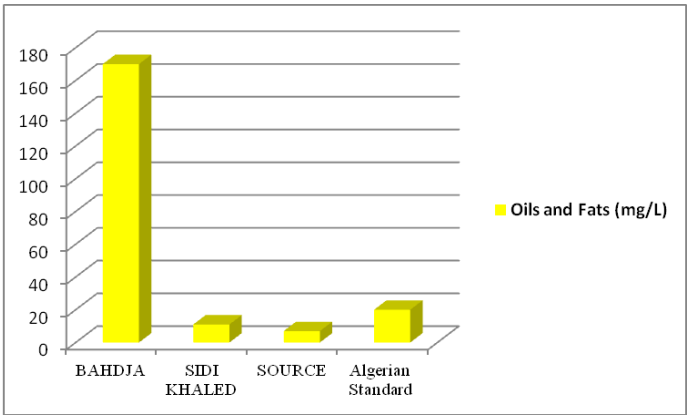

Figure 6. Oils And Fats Of Dairy Effluents

CONCLUSION

The physicochemical characterization of the global effluents discharged by the two dairies revealed their richness in organic matter expressed in terms of COD and BOD5, in TSS, and in oils and fats.

The detected levels exceeded for the majority of the parameters, the norm values of rejection fixed by the Algerian legislation.

Treatment must take place before releasing these effluents into the natural environment. The Coagulation-Flocculation process can serve as a pretreatment step to reduce COD and BOD5 mainly because they are associated with the TSS which can be removed by a liquid-solid separation technique, either by gravity or flotation. A complementary biological treatment is necessary to remove the organic matter.

The treatment will generate a sludge which constitutes the waste of the treatment, waste whose composition it is important to know and to ensure a correct elimination to protect the natural environment.

REFERENCES

[1] Official Journal of the Algerian Republic N ° 2624 Rabi al-awwal-23 April 2006, ANNEX I, 5.

[2] ISO International Organization for Standardization. Water quality -- Determination of suspended solids by filtration through glass-fibre filters ISO 11923:1997.

[3] ISO International Organization for Standardization. Qualité de l'eau -- Détermination de la demande chimique en oxygène ISO 6060:1989.

[4] ISO International Organization for Standardization. Water quality. Determination of biochemical oxygen demand after 5 days (BOD5). Dilution and seeding method ISO :5815 - 1989(F).

[5] JIS Japanese Industrial Standard. International Standard method JIS 0102.24.2.

[6] Landreau A., La réutilisation des eaux usées épurées par le sol et le sous-sol : adéquation entre la qualité de l'eau, l'usage et la protection du milieu naturel, Séminaire sur les eaux usées et le milieu récepteur, Casablanca 9-11 avril 1987, 1-13.

[7] Cary Institute of Ecosystem Studies, Changing Hudson Project, Dissolved Oxygen, 1-3.

[8] Geneviève M. Carr,James P. Neary , Water Quality for Ecosystem and Human Health 2Nd Edition, UNEP, UNESCO, Chapter 2, measuring water quality,2008, 7-31.

[9] G. Friedrich, D. Chapman, A. Beim. Water Quality Assessments - A Guide to Use of Biota, Sediments and Water in Environmental Monitoring – 2Nd Edition. Deborah Chapman Edition, UNESCO/WHO/UNEP, Chapter 5* - The use of biological material, 1996, 1-64.

[10] P.G. Whitehead , T . Lack, Dispersion and self-purification of pollutants in surface water systems. Technical paper in hydrology 23,A contribution to the International hydrological programme, UNESCO, 1982.

[11] Colin R, Peter SSD, James R. Biotechnology for the Oils and Fats Industry. American Oil Chemist's Society, 1984, 64.

[12] Proceedings of the ... National Conference on Hazardous Wastes and Hazardous Materials,
Hazardous Materials Control Research Institute, Volume 5,1988.

INTERNATIONAL CONFERENCE ON ADVANCES IN SCIENCE AND ARTS ISTANBUL 2017
29 – 31 MARCH 2017, Istanbul, Turkey

LIQUID-LIQUID PHASE EQUILIBRIA OF (WATER + 2-ACITIC ACID n-ALKANES) TERNARY SYSTEMS

*** Nadjet Boulkroune**
Laboratoire de l'Ingénierie des Procédés
d'Environnement, Faculté du Génie des Procédés
Université Constantine 3
Algeria 25000

Samah Zermane
Laboratoire de l'Ingénierie des Procédés
d'Environnement, Faculté du Génie des Procédés
Université Constantine 3
Algeria 25000

Keywords: Equilibrium data, Distribution coefficient, Separation factor
** Corresponding author:, Phone: 0021331786126, Fax: 0021331786126*
E-mail address: boulkrounenadjet@yahoo.fr

ABSTRACT

Liquid-liquid equilibrium (LLE) data for the ternary systems: (water/Acetic acid/ Alkanes at room temperature are reported. The phase equilibirium diagrams for all studied systems: distribution curves, selectivity curves, distribution coefficients and separation factors are presented.

The Othmer-Tobias and Hand equations used to verify the quality of the experimental data, gave similar results. The experimental ternary liquid-liquid equilibrium data were correlated with the NRTL model. The values of distribution coefficients, separation factors and selectivity for solvent separation efficiency, derived from the tie line data, were used to guide the choice of solvent.

INTRODUCTION

Liquid-liquid equilibrium (LLE) data from ternary systems are required for the design and improvement of many chemical processes to optimize separation processes. The equilibrium data also provide valuable information on molecular and macroscopic interactions. In recent years LLE's investigations of ternary systems have been a subject of great interest.

The high purity of chemical products are difficult to separate using the ordinary distillation process. Since they have boiling points in a narrow range. This is why we are interested in liquid-liquid extraction as a separation technique which is interesting in comparison with distillation. The study of the liquid-liquid equilibria in these systems is not very difficult, but the major problems are the analysis of the phase equilibrium, in particular with low solubility. The latter is also useful for mixtures of three liquid components when heterogeneous regions are needed to be avoided. The main factors influencing equilibrium characteristic of the separation process are the type of solvent, the nature and concentration of the solute and the appearance of three phases.

The aim of this study is to present liquid-liquid equilibrium data measured for ternary systems water + Acetic acid + n-hexane, water + Acetic acid + n-heptane, at room temperature and atmospheric pressure. The liquid-liquid equilibria were studied by the cloud-point method [1].

The tie line compositions were correlated by the methods of Othmer-Tobias and Hand [2].

EXPERIMENTAL

1. MATERIAL AND METHODS

All the materials used were of laboratory reagent grade, are shown in table 1.

Data for the solubility of curves of the ternary systems were determined by the cloud-point method where the known mixture of two components with the third one to the point of first appearance of permanent turbidity and refractive index of mixture at this point is measured by Euromex RD654 precision 10^{-4}. To add tie-line data, various mixtures of known compositions within the heterogeneous region were prepared, brought to equilibrium and compositions of the conjugate phases were determined by measurement of refractive index, in conjunction with the calibration curves prepared with the systems of known compositions on the solubility curves [2]

Table 1: Pure component physical properties

Materials	Materials Molecular weight [g/mol]	Refractive index n20
Acetic Acid	60.05	1.3727
n- Hexane	86.18	1.3779
n- Heptane	100.21	1.4001

RESULTS AND DISCUSSION

THE SOLUBILITY CURVE

The solubility curve data and the experimental tie lines for 1-water + Acetic acid + n-heptane, water + Acetic acid + n-heptane ternary systems are presented in Tables 1 and in Figs. 1-2. The Wi are the mass fraction of the components in the mixtures for the solubility curves data; the Wi2 and Wi3 are the mass fraction of the ith component in aqueous phase and in organic respectively, for the tie lines data. The Figs. 3-4 present the binodal curves. All ternary systems exhibit the type-1 behavior of LLE, the most frequent encountered situation of the measured ternary systems.

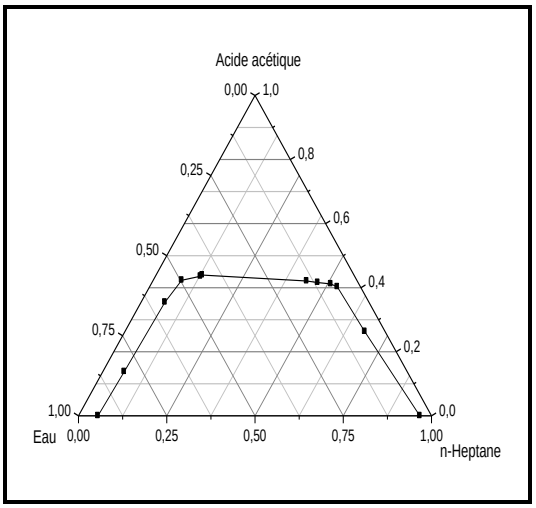

FIG.1: Solubility Curve Data for Water/ Acetic Acid /n-Heptane system

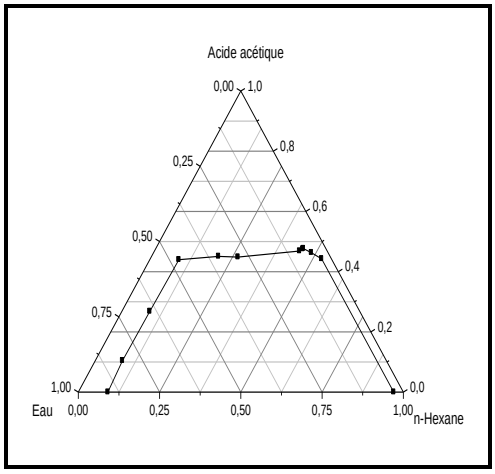

Fig 2: Solubility Curve Data for Water/ Acetic Acid /n-Hexane system

Table 2: liquid-liquid equilibrium for water/acetic acid/alkanes

Water(1)/Acetic acid(2)/n-Heptane(3)			
W_1	W_2	W_3	IR
0,96693	0	0,03307	1,3332
0,67932	0,26302	0,05766	1,3566
0,53181	0,40259	0,06560	1,3628
0,50865	0,41182	0,07953	1,3642
0,46961	0,41619	0,11421	1,3680
0,43595	0,42092	0,14313	1,3723
0,13086	0,43949	0,42965	1,3846
0,12770	0,43557	0,43673	1,3852
0,08062	0,42307	0,49631	1,3888
0,06758	0,35462	0,57780	1,3916
0,06091	0,13768	0,80142	1,3958
0,05525	0	0,94475	1,3999
Water(1)/Acetic acid(2)/n-Hexane(3)			
W_1	W_2	W_3	IR
0.97062	0	0.02938	1.3330
0.52724	0.44267	0.03010	1.3641
0.48543	0.46314	0.05143	1.3655
0.45419	0.47667	0.06914	1.3662
0.45288	0.47530	0.07181	1.3664
0.44647	0.46857	0.08496	1.3668
0.26704	0.44841	0.28455	1.3765
0.20612	0.45068	0.34320	1.3768
0.08960	0.43978	0.47062	1.3775
0.08598	0.26801	0.64600	1.3780
0.08375	0.10435	0.81190	1.3785
0.09099	0	0.09091	1.3773

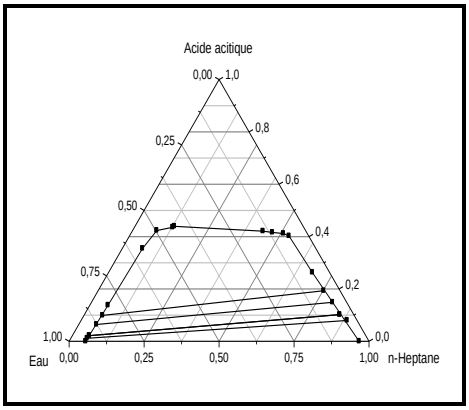

Fig 3 : Experimental Tie Lines Data For Water/ Acetic Acid/N-Heptane System

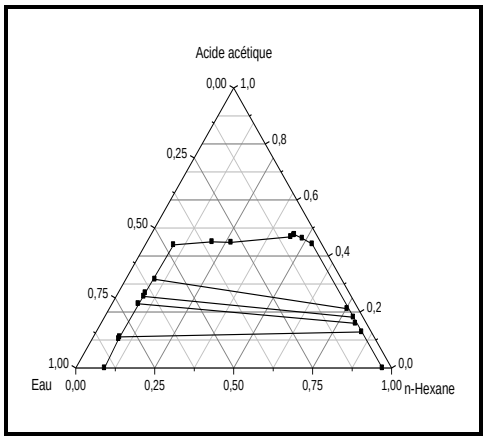

Fig 4: Experimental tie lines data for Water/ Acetic acid /n-Hexane

DETERMINATION OF SEPARATION FACTOR AND SELECTIVITY DIAGRAM

The separation factor and the distribution coefficient of acetic acid between water and alkanes were determined numerically [3] from the tie line data, shown in the Table 3. The ration of weight fraction of acetic acid in solvent phase to the weight fraction of acetic acid in diluents phase for each tie line gives the distribution coefficient of acetic acid. Separation factor is a ratio of distribution coefficient of solute (acetic acid) to the distribution coefficient of diluents (water). Hence the factor, $S=D_s/D_d$ .the distribution coefficient of diluents D_d is the ratio of the weight fraction of diluents in solvent phase to that in diluents phase. Selectivity diagram were constructed by plotting weight percent of acetic acid in the solvent phase against that in the diluent phase both on solvent free basis. Selectivity diagrams of all the systems are shown in fig 5.

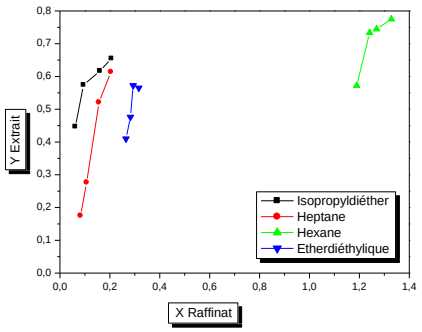

Fig 5: Selectivity diagram for Wataer/ acetic acid /Alkanes systems

Table 3: Separation factor data for water/ acetic acid / alkanes

D_s	D_d	$S= D_s / D_d$
Water/Acetic acid/Heptane		
0,01294586	0,06089516	0,21259259
0,02538858	0,06639097	0,38241019
0,07982435	0,07344288	1,08689024
0,13153802	0,08268978	1,59074104
Water/Acetic acid/Hexane		
0,13220408	0,09899247	1,33549627
0,28469291	0,10329676	2,75606825
0,32435004	0,11113649	2,91848385
0,42082061	0,1221219	3,44590627

CONSISTENCY OF EXPERIMENTAL TIE-LINE DATA

The reliability of experimentally measured tie line data is ascertained by applying Othmer-Tobias (Eq. 1) and Hand (Eq. 2) equations. [4]

The correlation coefficients (a, b) and correlation factors (r^2) were determined by the least-squares method and are given in Table 4. The correlations are shown in Figs. 5 and 6. The Othmer-Tobias and Hand equations show a good correlations and straight lines for each ternary system. The linearity of the plot indicates the good degree of consistency of related data.

$$\ln\frac{1-w_{33}}{w_{33}} = a_1 + b_1 \ln\frac{1-w_{22}}{w_{22}} \qquad (1)$$

$$\ln\frac{w_{13}}{w_{33}} = a_2 + b_2 \ln\frac{w_{12}}{w_{22}} \qquad (2)$$

Table 4: The correlation coefficients and correlation factors for the Othmer-Tobias and Hand equations for all systems studies

Coefficients Othmer-Tobias			**Coefficients Hand**		
a_1	**b_1**	**R^2**	**a_2**	**b_2**	**R^2**
Eau/Acide acétique/Heptane					
-0.4235	1.1139	0.9766	2.2181	0.9752	0.9897
Eau/Acide acétique/Hexane					
1.8356	1.9169	0.9652	2.2546	2.19110	0.93582

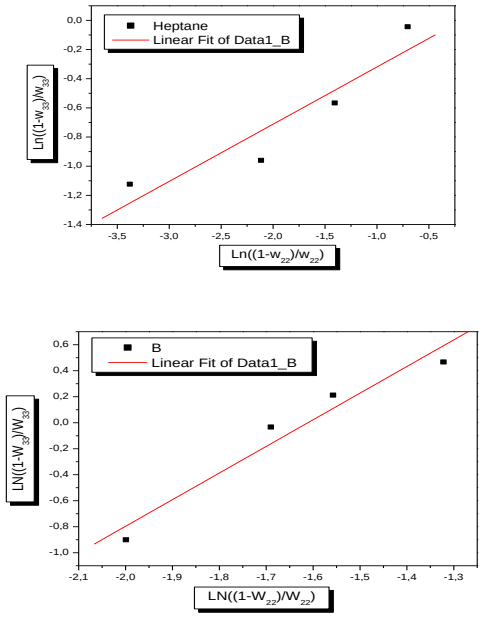

Fig 6 Othmer-Tobias Plot for : Water/Acetic acid/n-Heptane, Water/Acetic acid/n-Hexane,

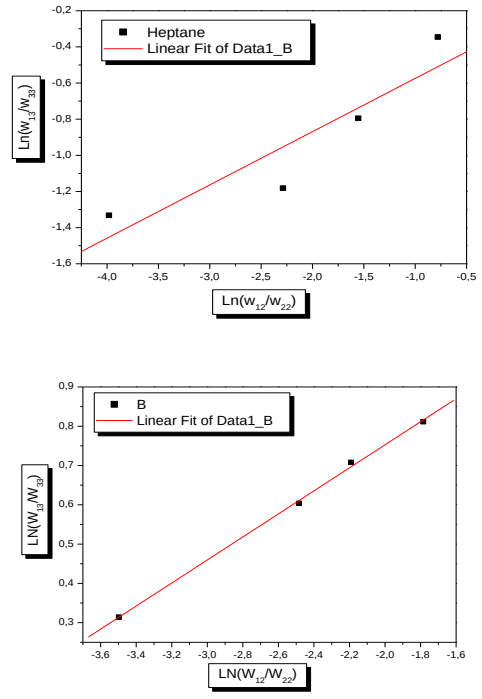

Fig 7 **:** Hand Plot for : Water/Acetic acid/n-Heptane, Water/Acetic acid/n-Hexane,

CONCLUSION

Liquid-liquid equilibria were measured at room temperature for water / Acetic acid/ n-hexane, water/ acetic acid/ n-heptane ternary systems. The solubility curves and the tie lines were obtained. For the separation of the acetic acid from its aqueous solutions by using solvents (hexane, heptane) the distribution coefficients, separation factor data and selectivity diagram of these systems were performed and thus it is to be said that hexane is is most selective for the separation of acetic acid from its aqueous studies.

All these ternary systems exhibit the type-1 behavior of LLE, the most frequently encountered situation of the measured ternary systems. The Othmer-Tobias and Hand correlations indicate a good degree of consistency of the related data.

NOMENCLATURE

w_{12} : Fraction massique du soluté dans le raffinat.

w_{13} : Fraction massique du soluté dans l'extrait.

w_{22} : Fraction massique de diluant dans le raffinat.

w_{33} : Fraction massique de solvant dans l'extrait.

a_1, b_1 : Constantes d'Othmer-Tobias.

a_2, b_2 : Constantes de Hand.

REFERENCES

[1] J. P. Novák, J. Matouš and J. Pick, "Liquid-liquid equilibria", Elsevier, (1987), Amsterdam, New York.

[2] Othmer D.F, White R.E and Trueger E, Liquid liquid extraction data. *Ind, Eng. Chem (1941) 33:1240.*

[3] Rahman M. A, Rahman M.S and Roy B. C. Ternary phase equilibrium data for glycerol-water –alchol systems and extraction of glycerol from spent soep lye using alcohols as solvent. *The Rajshahi University studies (part B)19:7*

[4] Cristina S, Olga I and Raluca I, *liquid-liquid phase equilibria of (1-propanol + water + n-alcohol) ternary systems at 294.15 k. 1-propanol + water + 1-butanol or 1-pentanol or 1-hexanol, Rev. Roum. Chim., (2011), 56(5), 553-560*

chartering that during the years in maritime trade associations and special transactions and commodities exchanges have been expanded as well.

In this study, while explaining ship chartering contracts, we try to find problems between ship owners and charterers on piracy and its impact on the contractual terms of charter parties.

Also, by analyzing the issues raised in the courts, standard forms of ship chartering, have challenged the contradictions in contractual terms of ship chartering and insurance law, and it is hoped to contribute to solving this global problem.

RESEARCH QUESTIONS

1. In the event of the phenomenon of piracy, is charterers' liability to pay rent during the term of imprisonment of ship removed?
2. In case of change in ferry route from the main and conventional route, to prevent a collision with the pirates, is charterer responsible to pay the costs of extra time to change direction?
3. Is piracy a factor for the cancellation of the ship chartering contract?

Hypothesis

1. It seems that in the phenomenon of piracy in the detention of the ship, liability for the charterer to pay the rent remains.
2. It seems that the cost of additional time to redirect the ship to avoid a collision with the pirates is in charge of charterer.
3. In case of logical disappointment of returning the vessel and cargo, piracy can lead to the revocation of the ship chartering contract.

CHAPTER ONE: CONCEPTS AND OVERVIEW

Legal history

Piracy has a long history and it is as old as the history of human mastery over the seas, and besides the slave trade is as the first example of international crime which is subject to universal jurisdiction. Law governing piracy has been evolving over historical periods. In ancient Roman laws, which was formulated by the parliament of Rome, the piracy is mentioned as a crime against individuals and society in general. (Yekdelehpour, 2011: 62).

The law to date form the basis for international criminal law and confirm the concept of universal jurisdiction to deal with piracy. After a period of stagnation in the fight against piracy, in the seventeenth century with the end of the Spanish war, anti-piracy laws were revived briefly, despite the fact that pirates in the era enjoyed a set of rules of conduct for the organization of pirate vessels and their integration. (Journal of sea and port, 2012: 70).

Gradually, more and more state laws were led towards defining piracy as a crime against humanity. In 1856 Declaration of Paris, which was almost signed by all the major powers, all forms of piracy was declared as abolished and emphasized that the pirates must be arrested and prosecuted. Paris Declaration and its subsequent decisions for the first time considered a legal entity separate from the individuals and governments for pirates. Therefore, piracy was considered as a political tool lacking the government support and the support of nationals. (Yekdelehpour, 2011: 63).

Since its establishment, the international community, as one of the first crimes has criminalized piracy. Committee of Experts of the international community, for the gradual development of international law in the field of piracy in 1926, published the regulations for the repression of piracy on the eight articles. These regulations limited piracy to committing acts with personal intentions and on the high seas and allowed countries to take certain decisions about the status of rebels (Wilson, 2008: 320)

1-2 Pirate

Pirate attacks caused many deaths and injuries of personnel and imposed many damages to commercial ships, which was strongly condemned by the international community, especially from the early nineteenth century. Piracy is the oldest international crime and it can be aligned with crimes such as war crimes and crimes against humanity. (Journal of message of sea, 2011: 48).

"Under international law, pirate is the enemy of humanity and the enemy of humanity is sentenced on behalf of all mankind." (Michel, 2008: 115).

The purpose of traditional piracy is to seize any personal or state vessels or persons and goods in it on the high seas. Usually, their aim was seizing and looting cargo vessel that in these cases, pirates abandoned crew and passengers after the seizure of cargo, or seized the ship and murdered the crew. (Beygzadeh, 2009: 25)

In the latest way of piracy, kidnapping for ransom was extended from Somalia and in the Gulf of Aden since early 2001, the target of pirates was kidnapping crew and passengers, and then negotiating to obtain huge bribes in exchange for their freedom. In this case, the pirates don't need much precious cargo and property in the vessel which is attacked but after the kidnapping operation they receive exorbitant bribes in exchange for the return of the vessel, the crew and passengers. (Beygzadeh, 2009: 25)

PROPOSED DEFINITION OF PIRACY

Legally, there are different views in relation to piracy and definitions related to it. By different definitions, we mean that depending on the type of legislation that deals with piracy and prosecuting this crime, a separate definition of piracy is provided by it. For example, international law, criminal law and domestic laws, that each have different definitions of piracy. (Todd, 2010: 52).

The simplest definition of piracy is an act that the pirate or pirates will be at the way of maritime trade and goods that are transported by ships at sea with trick or using guns, and by plunder of the goods and sometimes is also accompanied with killing the crew and sinking them, and thus they steal the wealth and power of ships.[1]

In providing various definitions of the crime of piracy in international documents and treaties, we should not forget that the involvement of international channels and the performance of state legislature lead to develop the concept of piracy in the definitions. On the other hand, given that the definition of piracy is caused changes in the final statistical calculation. So, these definitions are influenced by specific benefits and incentives of reference providing the definition. For example, according to the International Maritime Bureau definition, piracy is to attack any ship with the intention of committing any theft or any other crime and with the aim or the possibility of using force to advance the action. Obviously, the purpose of this definition is nothing but increasing the inclusion of the enumerated acts of piracy to use a tool to justify the insurance rate structure and insurance revenues in areas under the control of pirates. (Report Group, 2010: 106).

In 1958 the common law in relation to piracy was codified by "the Geneva Convention on the High Seas" in law. Then, in 1982, "United Nations Convention on the Law of the Sea" was adopted. The Convention entered into force in 1994 with the approval of the sixtieth signatory state. According to Article 101 of the Convention, such as Article 15 of the Geneva Convention offered a similar definition of piracy on the high seas, piracy is defined as:

A. Any illegal acts of violence or detention, or any loot that is committed by crew or passengers of a private ship or a private aircraft for the private purposes.
B. Any illegal acts of violence or detention or any loot against a private ship or a private aircraft, or against persons or property on board of ships and aircraft on the high seas.
C. Any illegal acts of violence or detention or any loot against a ship, aircraft, persons or property in a place that is not within the jurisdiction of any country.
D. Any voluntary cooperation in the operation of a ship or an aircraft knowing that it is an aircraft or a pirate ship.
E. Any action that leads to the stimulation for preparation to do actions referred to in paragraphs (A) and B (Taghizadeh, 2012: 82)

Definitions and legal status of the high seas

The definition of the high seas in Article 1 of the Convention of the High Seas 1958 is as follows:

"All regions of sea, except the internal waters and waters that are part of the territory of a country are called the high sea» (Convention on the high sea, 1958: 1). In the meantime, despite the exclusive economic zones and the waters of the

archipelago, this definition is modified by Article 86 of the United Nations Convention on the Law of the Sea 1982 as "all sea regions except exclusive economic zones and inland waters and waters that are part of the territory of a the country and also except the waters of the archipelago of a country are called high sea ». (UNCLOS, 1982: 86)

Convention on the High Seas, which, along with the 1958 Geneva Conventions, codified customary international law has several provisions that one of the main principles is identifying crime of piracy in modern times. Many of the provisions relating to the jurisdiction of the state and freedom of the seas and piracy. But other things are allocated to some specific issues that after 1958 has attracted a lot of attention (Bigdeli, 2005: 321).

Article 2 of the Geneva Convention of 1958 preserved the right for sailing, fishing, piping and cabling and their repair in the high seas as well as the right to fly over the seas for all countries. According to this Convention, the freedoms mentioned above are reserved for all countries given the rational considerations and so that the right of other countries is not misused. According to Article 87 of the United Nations Convention on the Law of the Sea 1982, construction of artificial islands and other installations and scientific research have been added to the list of freedoms (Bigdeli, 2005: 322)

Chapter Two: types of ship chartering contract and the impact of piracy on its provisions

Definition of ship chartering and its existence

Some of the authors consider the ship chartering contract as a contract whereby the owner should offer all or part of his ship in exchange for a certain fee to the charterer. Conditions and the effects of chartering contract are determined by parties to the lease agreement. From the perspective of some legal dictionaries, ship chartering is a written contract between the owner or master of the ship on one hand and the product owner (charterer) on the other hand and includes the rights and obligations of the parties, details of the ships and goods and many mutually acceptable cases. (Najafi Asfad, 2008: 152)

Parties to the ship chartering contract

Ship chartering contract is a written document between the ship owner or his authorized representative on the one hand and the tenant on the other hand. As can be seen, the principal parties to the lease agreement whose names should be mentioned in the preamble of the agreement, are the ship`s owner and tenant, in fact, contract results from negotiations, bargaining and agreements. But since the principle parties often are not technically, commercially and legally prepared for presence in negotiation meetings or for any other reasons are not willing to do so, in the international market of ship chartering, responsibility for such acts and conclusion of charter parties will be assigned to professional speculators. These individuals as "representative" undertake the responsibility on behalf of owners and tenants that are not dissimilar to advocacy and negotiate and bargain on their behalf professionally and finally, the chartering contract is signed with the terms of interest of both parties. (Najafi Asfad, 2008: 153)

Types of ship chartering contracts

According to international maritime law, all or part of the ship can be rented for a specified period for one or more travels and thus, ship owners and ship users are allowed to conclude charter parties with diverse and different contents. (Najafi Asfad, 2008)

Ship chartering contract is divided into three main types as:

1. Voyage Charter Party
2. Time Charter Party
3. Bare Boat Charter Party

TIME CHARTER PARTY

According to Article 7 of the Law of 18 June 1966 France further noted, in the long or long-term lease, the lessor undertakes to provide fully equipped ship to the tenant. As shown in this article, two points are missed by the legislator, first the payment of wage or rent fee that logically should be determined in the contract and second specifying ship that is one of the pillars of the lease agreement. But by referring to the article 1 and 2 of this law it can be seen that the French

lawmaker has generally obliged the tenant to pay for all the money equating for the action of giving ship to the tenant as a right of the owner for all types of shipbuilding contracts by inserting the words "acquisition fee" and has made the tenant to pay rent, and thereby removed shortcomings related to the rent from this article of law. But the silence of the legislator in specifying the ship, which may be interpreted as an objection has remained. The definition in article 7 of the Law of 18 June 1966 in France is more fully discussed in paragraph 1 of article 170 of the maritime trade law of Lebanon, and includes all important points. Based on this definition, the shipbuilding contract makes the owner to give a certain, well-equipped ship to the tenant for a specific time period and while getting the rent. Based on this contract, the renter has the right to use the ship legally, rationally, and freely for the time specified in the charter party when the ship in his hands. It is obvious that in case any damage is done on the ship during this production time, the tenant is responsible to pay for fixing the damage (Seddigh, 2014:279)

Moreover, as the ship is in hands of the renter for a certain time period based on the nature of lease time contract, so the commercial management of the ship has to inevitably pass to the renter regarding the commercial shipping circumstances. Therefore, the commander of the hired ship not only is in touch with the ship owner as the main employer, but also has to obey the rules and opinions of the renter of the ship for a better management of the ship to serve the rights of tenant and with the purpose of protecting his employer`s rights. According to these explanations, the commander can be considered as the representative of the ship renter as long as the lease contract is valid (Najafi Asfad, 2013:158).

One of the purposes of the renter of taking the ship could be supervising in the area of maritime transport. In fact, the renter could aim to do shipping services as a supervisor by signing the lease time contract. Then the renter is allowed by the contract to load the whole ship or a part of it with any legal cargo and send it to any desired safe port. That`s why some lawyers consider the lease time contract a maritime transport contract (Najafi Asfad, 2013:158).

In a form which is used in accordance with the terms of the lease trip, the renter can calculate his costs more easily. Because the act independently and freely with time in their lease trip. The calculated and payable fees according to the time is on the renter or anyone who accepted the risk and danger of all delays (Najafi Asfad, 2013:159).

The ship commander can change the direction of the ship and choose a longer route in order to prevent piracy. If the ship is hijacked by the pirates, it won`t be useable for the renter any longer. The effect of piracy on lease time contracts of the ships will be discussed in the next sections.

In freight contract as lease time, the payment for rent for the ship and its personnel is calculated according to time, where the renter has accepted the risk and danger of delay in delivering the goods, which is one of its differences with lease trip contract. This issue does not affects directly the long ferry route or the amount of cargo that must be carried. So it is obvious that lease trip motivates the renter to consider the fastest and best way to load and unload the cargo on-time payment of the costs in ship delays (Safazadeh et. al., 2006:240).

In lease time contracts, there`s usually one term or one clause for not paying the rent by the renter in case the ship is out of service. For example when the ship is out of service for maintenance, the ship commander must typically act based on the renter`s instruction. Although the commander and crew are chosen and hired by the ship owner, sometimes the ship owner cannot take the full control and supervision of the ship, and as it was mentioned earlier, the renter`s instructions must be obeyed (Sadeghi Moghaddam, 2000:98).

TERMS OF SHIPBUILDING CONTRACT

Changing the original direction of the ship

Changing the original direction of the ships in order to prevent the risks might cause some extra costs for the renter in a lease time contract. In lease time contracts, the renter gives the necessary instructions to the ship and the ship which is under the control of the renter, has to follow these instructions, though the ship commander was responsible for the safety of the

ship and its sailing up to now, and eventually it's the captain or ship commander who takes the final decision foe changing the direction of ship, and so the renter has to pay for the extra costs caused by longer route (Mashhadchi, 1982:115).

When there is not enough reasons for changing the original direction of the ship, the ship commander has to direct the ship in its original route with the utmost safety in the shortest selected route according to the legal specified path. According to the sentence in paragraph 4 of article 55 of the Law of the Sea of Iran, "any change in the direction of the ship in the sea for surviving and saving human life and property, or any rational deviation of the ship is not against the maritime transport regulations, and the charter supervisor won`t responsible for loss or damages arising from it". A little attention and focus on this legal statement allows us to conclude and deduce the followings:

First, the general legal principle is that the direction of the ship must be in the route specified in advance in a sea journey.

Second, deviation from this route is not permitted except in exceptional cases determined by law, and will result in responsibility lawsuit against the supervisor maritime transport. Third, deviation from the specified route is considered legal in case it aims to survive and save human life and property or it is done rationally and logically (Najafi Asfad, 2013:168).

Although this law is the exact translation of article 4 of the convention 1924 in Brussels, it shouldn`t be denied that using the complicated and ambiguous expression of "any rational deviation" has made access to the intention of the legislator largely difficult, and inevitably one should speculate for better understanding.

Some empirical examples of "any rational deviation" based on speculation in this regard are as the following:

Situation where deviation of the ship from the normal path takes place with the purpose of overcoming the inability of sailing and serious and inevitable maintenance.

Situation where deviation of the ship from the normal path takes place to prevent the ship from facing natural hazards such as hurricane and smog.

Situation where the commander changes the ship direction unintentional because of sickness or sudden incurable illness at sea, so that he can be treated in the nearest possible port (Najafi Asfad, 2013169).

Commitment to safety of port

The question arises regarding the topic of this paper that can the ports with pirates in their nearby be considered to be unsafe? Piracy can in fact be called a marine occupation, but there is a classic definition for safe port in the report of 1985 by Lloyds which states:

"… No port can be considered safe unless a specific ship can access to that during the certain time period in charter party, and also be able to exit it without any raucous event, and with no risk or threat which is essentially not avoidable that relying on good navigation and efficient marine personnel …" (maclachlan, 2004: 376)

This definition informs us about a safe port to a large extent, and so a safe port can be distinguished from an unsafe and dangerous port by referring to that. Based on this definition, a port can be considered safe when treating climate or situations in port, such as political unrest, revolution, blockade etc. cannot be avoided by appropriate and desired sailing and efficient naval personnel and seafarers.

But in some cases, the situation in the port is determined to make different situation and conditions compared to the previous situation, i.e. in the lease time contract, the tenant committed to direct the ship by his command to a port where was considered to be safe at the time of commanding. But the en route ship finds out this port has lost its safety due to occurrence of new events and has become an unsafe port. In this situation, the tenant has a second commitment to cancel his previous command and moves the ship with his new command to a port where is safe at the time of recent command (Seddigh, 2014:282).

But another situation can also be imagined in which the ship moves to a safe port specified in advance in charter party by the tenant command and reaches it and a new danger threatens the port after berthing at it, thereby makes it unsafe. In this circumstance, the only solution for the

tenant is to leave the port as soon as possible and keeps the ship away from danger. But if the tenant doesn`t have time for that and it is not possible for him to avoid danger and a damage is done on the ship, the tenant won`t have any responsibility in this regard (Seddigh, 2014:284).

Air and sea blockade of Lebanon which started from 12 January, 2006 at war with Israel and continued to a couple of days after issuing the statement No. 1701 in 11 August, 2006 by UN Security Council, is a suitable and illustrative example for this hypothesis. In this armed conflict which may be considered as a War and/or War-Like situation, a number of ports in Lebanon became unsafe, and many ships which had moved to the ports of these countries because of safety of coasts of this region were in dangerous situation due to unsafety of these ports. However, it has to be referred to the context of charter parties signed among ship owners and renters and the approach to set the terms of the contract in order to achieve precise legal ruling in this regard. Therefore, it seems that there`s no second commitment, and the tenants of the ships traveled to these ports were not able to leave the unsafe ports due to the escalation of war, so they have no responsibility in this regard (Najafi Asfad, 2008:173).

Article 155 of our country`s marine law has appointed in this regard that:

"If due to port blockade or any other coercive powers, it wouldn`t be possible to enter the target port, the commander has to unload the goods efficiently in the nearest port according to the interests of the sender, or return them to the origin port, in case of not receiving instructions or receiving unenforceable orders".

As it can be seen, the implicit terms of this legal statement are mostly in accordance with the first situation mentioned above, i.e. the situation where the en route ship becomes aware of unsafety of the anticipated safe ports in the lease contract. According to this article, the commander`s duty is subjected to the fulfillment of two conditions: first, entrance of the ship to the target port becomes impossible due to unsafety resulted from different coercive reasons or naval blockade and, second, no order is issued by the tenant or his representative in this regard, or if it is issued, it is unaffordable (Sadeghi Moghaddam, 2000:105).

Anyway, if no physical harm threatens the port is not a sufficient reason for its safety. According to lease time contracts, the ship owner has to direct the hired ship according to his commitments to the port specified by the renter. On the other hand, most of forms of shipbuilding contracts include an article related to the fact that the renter is committed to make sure the ports where the hired ship is supposed to commute are completely safe (Wilson, 2008: 349). Some judicial precedents and judicial procedures occurred in these cases determine a port is not safe, unless the goods ship has its own floating during unloading the goods, and can leave the port safely after unloading (halburys Laws of Singapore (carriers), 1989: 215).

So, a port where it is not possible to enter without any risk is not a safe port, and therefore when a piracy is near a port and is a barrier to access the port, that port will be called unsafe.

There is no doubt that the ship owner does not guarantee for the renter not to direct the ship towards a port where there are pirates, and also it has to be considered that a renter who orders the ship to go an unsafe port, has violated the law regarding the shipbuilding and freight contract. So the ship owner can cancel the contract and considers the renter responsible for all damages to the ship. The question that arises in this situation is that was the ports of interest a safe port at the time of signing the contract or did the renter know about its unsafety while moving towards it? If a port which was safe at the time of signing the contract becomes unsafe after signing the contract, the ship owner has to inform the renter the mentioned port is unsafe from now on, and the renter had to avoid moving there based on the information he gets about the unsafe port. If the renter doesn`t obey these rules, the ship owner can direct the ship to the nearest safe port and act according to the terms and rules of fright contract about the ongoing event. Here, the dispute among charter parties` terms is that whether the route where ships commute in the Indian Ocean and Gulf of Aden and there is no need to go to ports (unsafe ports) where pirates are and they only to pass through this route to commute is unsafe or not? No jurisdiction and legislation has ever answered to this question up to now, and this has resulted in some disputes between the ship owners and

renters in paying additional expenses (Mirmohammadi, 2010:73).

Making a ship out of service or off hiring a ship

The general principle of lease time contracts is that the ship is completely in hands of the renter for a certain time specified in the contract, and the total rent of the ship is paid to its owner, unless a provision of this contract becomes infringed during the lease time. In this case, a provision or clause will act that excludes the commitments of the renter related to making the ship out of service. Most of the charter parties include a term called "making the ship out of service" or more technically "off hiring" that frees the renter from paying the rent to the ship owner when the ship is out of service . For example, in the form NYPE93 (New York produce Exchange) which is usually used, in its 17th article, it is stated about the events included in off hires that:

"losing time because of negligence or failure of ship officers or crew, shortcomings in storage and spare parts for ships, fire in the ship, damage or engine failure or damage to the hull and rigging, ship aground, arrest and detention of the ship (unless the renter himself, his renting officers, or his representative are the reason of this arrest), or to seizure the ship due to legal incidents occurred for the cargo or the ship, change in the quality and nature of the cargo or damage to the cargo, the ship`s pool deck to repair or to paint, or its inspection, or any other similar reason that prevents servicing and full performance of the ship" (Sadeghi Moghaddam, 2000:113).

In interpreting the sentence "or any other similar reason that prevents servicing and full performance of the ship", it is a quite general sentence and includes different states of off hires. However, this question arises that is hijacking the ship by pirates sufficient for off hiring the ship or making it out of service?

The answer to this question might be that off hires doesn`t involve piracy. Words like "similar reason" stated in the definition of off hire are probably related to physical states and problems of the ship or its personnel and doesn`t involve piracy (Sadeghi Moghaddam, 2000:113).

In the ship Saldanha, the form NYPE93 was used and the piracy was not considered as a "sea damage" or "any similar reason". G. Grass suggested that the word "any" has to be added to the above provision so that it could be possible to consider piracy as one of the events included in off hires (EWHC, 2010: 532).

The ship in the below situations is off hired or out of service and cannot be used.

Dismantled or cannot be used.

Missing Vessel.

Dry-docking for maintenance.

The actions related to preserving the sailing ability of the ship and its equipping is being done.

Lack of crew or deficit in requirements in observed in the ship.

Events and accidents other than exceptional risks and damages caused by them that lead to the loss of more than 24 hours.

In the lease time contract of Baltaym 1939 related to making the ship out of service, it is stated in its clause A, article 11 that "if a ship has stopped more than 24 hours due to ship maintenance, or necessary plans for preserving the efficiency of the ship, or inefficiency of ship personnel or the fuels in ship`s storage, or technical defects or damage to the body, or other accidents, no rent is payable during stop, so any prepaid money has to be adjusted". (Sadeghi Moghaddam, 2000:114).

LEASE TRIP CONTRACT

In a lease trip contract, the ship owner is committed to give the specified ship with full equipment to the tenant for one or more voyage in exchange for a specified rent. The amount of rent can paid as a lump sum by mutual agreement of the contract correspondents, but the amount paid depends on the value of the goods, and its main specification related to lease time contract is that it doesn`t depend on the time duration of the trip (Najafi Asfad, 2008:175).

So it is the ship owner who takes the cost of any delay. If the trip becomes longer than the expected time, it’s the ship owner who has lost in terms of time, and cannot ask for any excess payment from the renter to compensate the

occurred delay. He also cannot use the ship to earn money from other places to compensate the lost time. On the other hand, if the trip becomes shorter than the expected time, it is the owner`s profit as he can rent the ship to somewhere else to earn more money. So the main and fundamental difference in lease time and lease trip contract is specified here; in lease time, the renter takes the risk of any delay, while in lease trip, it is the ship owner who takes the risk of delay, and usually no certain speed is specified for the ship, and the common speed is considered (Todd, 1988: 65).

According to these contracts, the ship owner not only takes sailing management, but also the commercial management is on him. In other words, the main commitments of the ship owner includes three parts:

Giving his owned ship.

Providing the staff and commander who are led by him.

Carrying the loaded goods on the ship.

In fact, the main commitment of the ship owner is to carry the cargo belonged to the renter according to the agreements, using two other elements, i.e. ship and staff, to the desired destination(s) and deliver them to the interested parties (Najafi Asfad, 2008:178).

The ship owner and tenant can set the lease contract based on the principle of free will, so that it would meet the demands of each of the parties. Usually, each of the parties states their own opinions that are representative of their own interests in the proposed talks, negotiations and bargaining. In the meantime, do not forget the profound and direct effects of international forms of charter parties, which always pervade the negotiation process and overshadows the final adjustment to the lease agreement between owner and tenant. In most of the cases, the lease contract which both parties eventually agree on it is either the complete form of international sample charter party or a modified form of it (Seddigh, 2014:303).

In 19 August, 2008, tanker ship carrying chemical called Bvngamlaty medicine moving from Malaysia to Rotterdam was hijacked by Somali pirates in the Gulf of Aden. The ship, its crew, and its cargo were directed by the pirates to the internal waters of Somalia, and the pirates asked for ransom money from the ship owner after a short while to release the ship (EWCA, 2011: 321).

Argument between owners of the goods and their insurers began and led them to attend the court and ask the judge Steel J. that based on marine insurance law in 1906, whether the piracy can take the control of ship and its cargo based on the clause "actual total loss" or "assumed total loss", so this way the owners of the cargo can access to their rights (EWCA, 2011: 321).

According to its rules, the court states that this case is neither actual total loss nor assumed total loss. It was mentioned in its proof and transparency that the key point is whether the ship owner is fully disappointed from getting his ship and its cargo back, and there is no way to take it back, and the ship is totally destroyed. In relation to the ship Bvngamlaty medicine, discussion and negotiation started between pirates and ship owner hoping to release the ship. During negotiation which continued around one month, and the ship was in hand of the pirates, the ship owner warned his ship insurer for assignment of ship and cargo, and turn away from property, and this issue was refused by the insurer, but the pirates and ship owner reached an agreement, and the ship owner paid the ransom money to the pirates, and eventually the ship, its personnel, and its cargo were freed in 29 September, 2008, and reached Rotterdam in 26 October, 2008, and its cargo was unloaded without any damage (EWCA, 2011: 322).

From cargo owner`s view, hijacking the ship by the pirates and moving it to the coast of Somalia means his goods are included in the clause of actual total loss, and the ship and its cargo cannot be returned to their owners, and based on the insurance contract, this state is included in actual total loss, and the cargo owner asked for compensating the loss of his goods from the insurance, and eventually, the ship owner set free the ship and its cargo along with the personnel against general policies to combat piracy by paying tribute to the pirates (EWCA, 2011: 322).

About the expression of being impossible to take the ship and its cargo back when the warning for

leaving the ship and turning away from the property was announced from the owners of ship and goods, the appeal court considered factors that had an important role in this regard, such as being interested parties where they were fully aware of the compensation for their loss. Moreover, there were signs of agreement between the ship owner and pirated in paying the ransom money. But the court still insisted on its previous decision, and eventually the ship, its personnel and cargo were set free after 6 weeks (EWCA, 2011: 323).

The moment when ship was ordered to be evacuated, there was no sign of the possibility of getting the ship and its cargo back. Because in professional goods` insurer`s view, within a year before the ship Bvngamlaty medicine was seized by pirates, the had the experience of hijacking and releasing 9 other ships, and the Somali pirates` approach is so that no damage is imported on the ship and its cargo when the ship becomes released (EWCA, 2011: 323).

Steel J. says about his policies in this case about general policies and arguments and debates about piracy that paying ransom money to pirates motivates them to do the same in future. He also stated that military interventions cannot prevent this action as well. So practically, there is one way left, which is paying the ransom money to the pirates and it can be said that it is the only effective ways that prevents any harm to the personnel, ship, and cargo. Finally, he mentioned the money which is paid to pirates in exchange of setting free the ship can be compensated as public loss (EWCA, 2011: 324).

So the appeal by the owner of the goods was settled for two reasons cited below.

First, owners of goods claimed that seizing the ship is immediately included in actual total loss clause, even if there is the possibility of getting back the original property. Steel J. concluded in his statements that the insurer doesn`t fully disappoint from his ship and cargo unless it is physically impossible to get them back, even if this getting back results in inappropriate costs for its owner. Then the owners of goods stated the theory that hijacking and seizing the ship by the pirates immediately includes in actual total loss clause unless returning the ship to its owner happens prior to warning to leave the ship by the personnel and disappointment of the owner from the ship. The appeal court refused this justification after the analysis (EWCA, 2011: 324).

Second, owners of the goods justify that the law doesn`t want to or cannot consider paying ransom money as a legal way for getting back the ship, while the owners of the goods know that paying ransom to pirates to set the ship free in illegal in England, Somalia, Malaysia, and even international law, and they claim that such ransom payment to the pirates is not pleasant from the standpoint of public interest, public morals and universal principles. In the other words, paying ransom to the pirates cannot be considered as a part of insurance duties for saving the ship, its personnel, and its cargo. Because the ship is irretrievably lost by its owner physically as well as legally, and the only of getting the property back has to be done by the insurance, and is not logically acceptable (EWCA, 2011: 324).

However, as there is no legal barrier for paying the ransom money for setting the ship and its cargo free, and this expense will actually be compensated by the insurance through public loss, the appeal court concluded that they cannot resist general policies in this regard, and eventually, by further investigation and acquiring sufficient proof related to shipping and marine insurance about piracy, the court insisted on negotiation with the pirates in order to prevent any harm to the personnel, ship, and cargo, and refused the issue of actual total loss (EWCA, 2011: 324).

As it can be seen from the particular case of piracy above, there is no certain law in courts to refer directly, and the legislator can judge based on it, and this has causes some disputes between the court and owners of the goods regarding the sentence issued by the court. According to the topic of this research, piracy not only affects the shipbuilding contracts, but also has some effects on marine insurances and other related parts.

Saldanha ship and Royal Creek ship

Saldanda was a Panamax-size bulk carrier ship which was time leased on 5th of July, 2008, for 50 months according to the form of New York produce Exchange, or NYPE form. On 30th of

January, 2009, the renter ordered to load coal in Indonesia for transportation to the port of Koper in Slovenia. The ship owner assumed the route to be through passing the Cape of Good Hope, while the renter had considered it through Suez Canal. When the renter says to the ship owner that the route is through crossing the Suez Canal, the ship owner reserves the right to cancel the contract due to the path where there is the risk of piracy, unless the renter commits to pay the extra costs the ship owner that the ship owner has to pay it to the insurer. These extra costs include paying war insurance because of entrance of the ship to such regions, and in this particular case, the renter commits to pay it based on the lease contract (EWCH, 2010: 638).

On 22 February, 2009, while the ship was moving through the water corridor route determined to pass through the Gulf of Aden, it was hijacked by Somali pirates. The pirates made the ship commander to move towards the waters off the Somali coast, and the ship was in hands of the pirates up to 25 April, 2009. The ship was moved back to its previous place at the time of hijacking and was able to continue its path after freedom on 2 May, 2009 (EWCH, 2010: 638).

The renter refused to pay the rent during this time, from 22 February, 2009, to 2 May, 2009. On the other hand, the ship owner claimed for damages related to not paying the rent and cost of fuel in this duration by the renter and other excess costs for war insurance and reward of crew for the war zone. The renter also claimed for damage because of unpreparedness of the ship and its crew members to counter a pirate attack (EWCH, 2010: 639).

According to the sentence issued by the jury in the first court on 8 December, 2009, hijacking the ship by the pirates doesn`t allow the renter to consider the ship out of service or off hired relying on the article 17 of the form NYPE and refusing to pay rent to the owner (EWCH, 2010: 639).

The court investigated other terms of the contract in this particular case as well, and in short, the court issued a ruling as follows: according to the article 39 of shipbuilding contracts, the ship was not out of service or so-called off hired, and the article related to the war zones and premium related to it in charter party doesn`t make the ship owner to neglect his right about ship rent during the time when the ship was in hands on pirates (EWCH, 2010: 640). With this sentence issued by the court, there would be no objection to this ruling and there is no need to discuss this issue any further. So we can focus just of the article 17 related to making the ship out of service or off hiring it. The article 17 of shipbuilding contract states that:

In case of losing time due to negligence or failure of staff in doing their responsibilities, such as striking of the officers and crew, fire, breaking or damage to the hull, machinery, or equipment, grounding, seizing due to regular accidents of the ship or goods, drydocking for maintenance or painting, or any other reason resulting in the lower efficiency of the ship and its inability to full service, the rent payment is not on the renter anymore during the lost times.

As can be inferred from the above statement, there are three reasons for making the ship out of service by the renter:

Seizing the ship for reasons other than "particular accidents" happened for ship or cargo.

Negligence of the staff in their duties.

Any other reason (EWCH, 2010: 641).

The rule of paying rent in a lease time contract is based in the agreements in the contract. The rent of the ship is payable during the time it is in hands of the tenant. However, the renters can have some exceptions; the burden of proving these claims is on the renters themselves.

Here, the issue of negligence of the crew is discussed.

If the ship commander failed to perform operations against piracy before attack of the pirates, and the pirates seize the ship, this problem might be due to reasons other than negligence of the crew.

A special case related to this issue bringing up the article 17 of the form NYPE in the court to prove their claim is about "Royal Greek". The renter orders the ship to move in this case, but the crew say the ship movement is conditional to be caravan in the specified route. As the debate on this issue, the renter considers his orders to be refused and therefore off hires the ship, or makes it out of service.

As it was mentioned earlier, the court doesn`t give the right to the renter to make the ship out of service and refusing to pay the rent relying on one single expression (negligence of the crew in their duties). In fact, the meaning of the expression which results in making the ship out of service in this case is that "lack in the number of crew, including officers and sailors in the ship that cause negligence in duties are included in making the ship out of service". In this case, however, the ship was fulfilled in terms of the number of crew, and in fact, these words doesn`t help in paying rent (EWCH, 2010: 641).

Andreas Lemos

In this section, we will discuss a case related to the definition of piracy and the disputes raised from it. Andreas Lemos ship was hijacked by the pirates while commuting in internal waters of the country Bangladesh. The ship owner attends the insurance company for getting compensation, having the ship insurance covering all insurance terms including war insurance and piracy insurance. The ship owner claim that his ship has all terms of insurance including the insurance of internal war in the countries, revolution, rebellion, uprising, conflict and civil strife, as well as piracy, and the insurance company has to pay for the damage in case of occurrence of any of the situations above. The ship owner attended insurance company for piracy attack and seizing the ship by pirates. By investigation in this regard, the insurer deduced that the ship was commuting in the waters of Bangladesh country at the time of hijacking, and insurance doesn`t include Andreas Lemos based on the definition of piracy which has to occur in free waters.

As it can be seen, the problem in comprehensive and unique definition of piracy causes such disputes in insurance contracts and their implementation in case of accidents. It is clear that the ship owner has no intention other that insurance and financial guarantee of his property for the accidents mentioned above at the time of his original property insurance, and the just the effect of discrepancy and paradox in various definitions of piracy in different regulations and conventions caused such disputes and, therefore such expenses for ship owners, and the ship became seized by the pirates; defects and discrepancies in rules causes such judgments.

Hill Harmony ship

In Hill Harmony ship, the ship commander chose a longer route instead of the standard route considered for the ship in order to prevent facing bad weather in crossing the Pacific Ocean. Meanwhile, the renter excluded the rent for the excess time resulted from changing the route and also the cost of excess fuel used from the original rent of the ship, and eventually the England court voted for eligibility of the renter (EWHC, 2012: 215).

Such a decision taken for Hill Harmony not only limits the commander in decision making for determining the route, but also makes the captain responsible for the safety of the ship at all times during travel. The problem of the ship commander in Hill Harmony took place since he didn`t have a good reason in terms of safety or a legitimate proof for choosing the shorter route. If the ship commander had paid more attention to the notifications of International Maritime Organization such as the notification related to piracy attack, and had stated his reason of changing the route to prevent confronting to pirates, there would have a been a totally different situation and changing the ship route would have been acceptable and logical with this reason (EWHC, 2012: 215).

IRAN DIANAT SHIP AND SIRUS STAR TANKER

Iran Dianat Ship is an example of piracy which occurred in Iran Republic Islamic Shipping in 2008. The Iran Dianat ship was moving from China to the Netherlands on 22 August while carrying 42500 tons of different industrial minerals, when it was hijacked by Somali pirates in the international waters in the Gulf of Aden. The ship and its personnel were seized by Somali pirates for 7 weeks, and eventually the ship owner was obliged to pay a compensation to the pirates, and this way could liberate the ship on 11 October, 2008. Due to extreme differences in shipbuilding contracts and related insurance investigation of this case has not reached to the ultimate conclusion about this ship and the costs imposed on it[2].

Somali pirates freed the giant Saudi oil tanker after getting 3 million dollars, and after 2 months of international effort. The Associated Press reports that the Sirus Star Ship and its 25 personnel were hijacked in 15 November, 2008. This ship with dimensions as an aircraft which carried 2 million barrels of oil worth 100 million dollars belonged to "Aramco" Oil Company of Saudi, and is the world`s biggest ship ever hijacked. The mentioned ship was hijacked in 830 km south east of Mombasa in Kenya, and since it is the first time that a big ship is attacked by pirates away far away from coast of Africa, it has raised some concerns. Now, after nearly seven years of this event, the final verdict of the court have failed in this case because of differences and disputes between the ship owner and insurance in this case, which was due to the fact that the piracy happened out of the war zone[3].

As can be inferred from these two cases, piracy and its regulations, and also differences and disputes in legal clauses in shipbuilding contracts and the insurances related to that caused international courts to verdict easily in this particular case, and these disputes would persist as long as there is no integrated law.

Effect of Pirates on Execution of the Contract in Lease Time Contract

The nature of the lease time contract of the ship is so that all risks are on the renter, and the basic rules state that the renter is responsible for the risk of all potential delays in lease time contract. The general rule of lease agreement is so that the renter has to pay his rent to the ship owner during the contract time. There are also some exceptions for paying the rent. As in all exceptions, the Off-hire or out of service ship is one of the exceptions in lease time contract. In a lease time contract, the renter, or the tenant commands the ship to move towards which port, although full authority of the ship is on the commander who directs the ship to the desired direction. The commander and/or captain of the ship has to prove his goodwill and impartiality in important decisions honestly to the ship owner and tenant. Here, the piracy can affect contracts since making a ship out of service while hijacking does not include in piracy clauses, therefore the responsible person for paying the rent in the contract may also face some problems in implementation of the contract and paying the rent, which is the effect of piracy on implanting of contract.

THE FINAL ANALYSIS OF PIRACY EFFECTS ON SHIPBUILDING CONTRACTS

Investigating the available contract analysis for shipbuilding contracts and limitations applied on the standard form in the particular case of piracy, and the problems existing in these limited forms have made the renters to set some conditions for ship owners to consider in contracts, which are sometimes the reason of opposition of the owners and not reaching the ultimate consensus in contract. Because as it was mentioned earlier, in the standard forms of BIMKO and INTERTANKO, the renter is responsible for paying the rent to the owner when the ship is in the hands of pirates. This results in their discontent and makes the more cautious at the time of setting the contract since there is no comprehensive and fair law.

Here, in order to clarify the problem and effect of piracy on implementing contract, and the losses that incurred for marine transportation companies in this regard, we will focus on a sample analysis of contract trend done in one of Iranian companies for leasing their ship to the renters.

National Iranian Tanker Company has 55 ocean-going ships. Considering this number of ships, it is assumed that one of these ships does not reach consensus in contract because of the piracy clause in INTERTANKO standard form which states the rent has to be paid by the renter during the time the ship is in hands of pirates, and the renter disagrees to this form or this clause and finally no contract would be made.

Now assuming the rent of this ship is $50,000 for a 3 month rent, so the national tanker company would lose $4,500,000 for leasing this ship, and according to the elicit explanations above, the reason is the differences in regulations and lack of a comprehensive and transparent law regarding piracy.

On the other hand, if the renter takes the ship along with the lease time contract, so that agrees with the ship owner on each of the standard forms

covering piracy, and the ship becomes hijacked by the pirates while moving in Gulf of Aden in compliance with all security issues, the renter is obliged to pay the rent to the owner for 90 days based in the BIMKO standard form, though the ship is not any longer under his control. This will cost $4,500,000 for the tenant according to the $50,000 daily rent.

THE FINAL OUTCOME OF THE LEGAL EFFECT OF STANDARD FORMS BIMKO AND INTERTANKO

As explained in this article, the condition of piracy drafted by BIMKO and INTERTANKO can be used in clarifying the legal issued regarding piracy. However, the comprehensiveness and of these forms and not existing any defect in them cannot be verified, because there are many errors in the clauses of these forms which cause some disputes among contract correspondents.

The BIMKO contract condition about piracy aims to serve justice among contract correspondents during signing the contract, and states that while a ship is in hands of pirates, or in other words, the ship is hijacked by the pirates, the rent belongs to the ship owner as an in service ship up to 90 days from the start of hijacking, meaning the ship belongs to the pirates after 90 days, it will be out of service, and off hired. There is another possibility for contract correspondents regarding this issue in which they can choose the article related to the Gulf of Aden which allows them to make the ship out of service after 60 days, instead of 90.

In INTERTANKO contract condition, it also can be concluded from investigating its clauses and comparing them with BIMKO contract terms that all clauses are almost the same, but the main difference of these two is that the time in which the ship is in service while it is in hands of the pirates is specified in BIMKO, but it has not been specified in INTERTANKO when the ship would be out of service.

Another important is to dismiss the contract or not to implement the shipbuilding contract in case of disaster, which was explained in details previously.

Contractual Obligations should change without any mistake by contract correspondents, which implies if the ship or its cargo is lost, it will cause some fundamental changes in the obligations of the ship owner for sure. For example, in lease time contract of the ship, the ship owner wouldn`t be able to deliver the cargo to the target port in case of hijacking the ship by the pirates, and eventually there would be no buyer. The main problem is that whether delay in delivering the goods (after liberating the ship by the hijackers and the resulted delay) can cancel the lease agreement or freight contract.

Here, the piracy method in Strait of Malacca[4] and Coast of Somalia and their differences matters. As it was mentioned earlier, the purpose of Somali pirates was to get the money for compensation, or the proposed money by the ship owner to set free the ship, its personnel, and cargo. But the piracy in Strait of Malacca was totally different, in which they tended to keep the ship and its cargo for their own use, sale, or trafficking.

So the Somali pirates can be considered as catchpoll pirates while pirates of the Strait of Malacca are thief pirates who steal other`s property with the intention of permanently depriving its owner. According to this difference, it can be concluded that there is more chance to retake the ship, its personnel and cargo from Somali pirates.

Therefore, if the ship is hijacked by the Somali pirates, the delay that will occur in delivery when the ship is seized cannot cancel the shipbuilding contract or the contract for carriage of goods easily since the Somali pirates will set the ship and its cargo free after getting the ransom money. Whereas the pirates of the Strait of Malacca will keep the ship for their own use and sell its cargo, so in this case the contract correspondents decide to cancel the contract after a short while from ship hijacking.

COMPARING THE RESULTS OF THIS RESEARCH WITH THE SIMILAR STUDIES

According to the literature review and the related studies and comparing them with this research, it can be concluded that in Ghorbanpour`s

research (2009), the only approach to prevent piracy is the cooperation of the concerned countries for strengthening preventive measures in order to prevent attack taking the ships hostage by pirates and enforcing the central government of Somalia in order to concur internal problems, by reconstruction of this country and its institutions in the form of long-term solutions to eradicate piracy in this part of the world, but nothing was mentioned regarding the current problems in good transportation contracts and also shipbuilding contracts and finding a plan for reducing the effects of such a disaster in sea freight. Moreover, comparing with Taghizadeh`s research (2010) named "Combating piracy off the coast of Somalia from the perspective of international law with an emphasis on Security Council actions", which considers various factors responsible for creating challenges in the fight against piracy, including the main challenges for the safety and security of commercial fleet against pirates in this region, lack of integrated regional and international political will to strengthen the regional institutions and mechanisms in support of the suppression of this phenomenon in the Horn of Africa, Insufficient available capacities, lack of effective and integrated programs to fight pirates, lack of a single legal framework, border and ethnic disputes and too much sensitivity towards sovereignty, and doesn`t mention the effects of this insecurity and lack of efficient planning and lawlessness in maritime transport and the global economy and shipping and shipbuilding contracts above all, and there is a common consensus on stability in Somalia and the presence of strong central government. But what has to done for these problems as long as this global desire has not been fulfilled? The study carried out on Aydin, 2011 noted using standard forms, and again mentioned the political stability is the Somalia as the only solution. In report of the speech gathered by Mohammadreza Hosseini in the Study of International Law Center about piracy from the prospect of international law, they concluded that the only solution to eradicate piracy in Somalia is to return peace and stability to this country and this responsibility is on United Nations Security Council, and the international society and United Nations above all have to modify the social and economic condition in this country in order to dry out the roots of piracy, which are poverty and lawlessness. Eradication of poverty and stability in Somalia will dry out the roots of piracy for sure, but several studies must be done looking for a way to reduce the impact of this phenomenon on the global economy till then. Applying new rules in maritime transport contracts and also international cooperation in generating a transparent law and a united judicial procedure, and also developing principles for marine insurance contracts which can contribute to the problems and fix them significantly are some of the approaches to deal with before developing a powerful and legislator state in Somalia. This research tries to figure out the problems among ship owners and renters related to this phenomenon in the world and to reveal its impact on shipbuilding contracts, and also challenges the current laws and judicial procedure and discrepancies in the terms of shipbuilding contracts and insurance regulations, and this way hopes administrators and officials to think of a solution for this problem and fill legal and contractual gaps and even insurance about the phenomenon of piracy.

CONCLUSION

Considering the whole data and existing regulations, we concluded that there is no unique judicial procedure to deal with piracy in courts, and also there are much legal gaps about that. The approach of dealing sea insurances, as explained in the text, causes some problems for ship owners and renters, and even owners of the cargo. Furthermore, the discrepancies in terms of standard forms of renting ships about piracy has added to this problem. By carefully investigating the different types of standard forms, we concluded that piracy does not results in off hiring the ship in any case, and the contract correspondents can decide freely on rules and terms of shipbuilding contracts in the vicinity of the desired countries. Generally, using standard forms and adding some contract terms to these forms by Large Marine Forum can help contract correspondents significantly. However, no comprehensive and complete law has been developed yet by the international regulatory bodies, and contract correspondents have to use the standard forms which piracy has been mentioned in the, for example: the ship owner and renter include the risk of piracy in the contract. In BIMKOW and INTERTANKO

standard forms, one contract term has been added for ship owner and renter related to piracy which can be used, but this terms has its own problems as well which could eventually be detriment to of one of the parties of the contract. However, we still have to expect some disputes in this regard among ship owners and tenants in implementing contracts.

SUGGESTIONS

According to the results of this research, the approaches for solving this problem are:

- Fundamental modification of all standard forma in renting ships and updating legal and contractual terms associated with piracy.
- Applying a consistent law in this regard by international regulators so that all marine transportation companies can reach a common consensus referring to that.
- Marine insurances can also help the international marine transport community significantly to solve this problem by developing their own terms.
- The contract correspondents should also include the issue of off hiring and changing the direction of the ship in case of piracy in signing the contract.
- Following a unique judgmental procedure in all international courts about piracy is another solution for this problem.
- The cooperation of international organizations in solving economic problems of Somalia and eradicating the prevailing poverty in this country which are the main reasons of tending to piracy.

REFERENCES

1. Bigdeli, M., General international law, Ganje Danesh Publications, 22nd edition, Tehran, 876 pages.

2. Pournouri, M. and Habibi, M., The international Law of the sea: Convention on the law of the sea 1982, Khane Ketab Publications, 2ndn edition, Tehran, 216 pages.

3. Taghizadeh, Z., 2012, Development of anti-piracy from the perspective of international law, Ganje Danesh Publications, 1st edition, Tehran, 239 pages.

4. Sadeghi Neshat, Marine Insurance Law, Educational hipping institution of Iran Republic Islamic, 2000.

5. Sadeghi Moghaddam, Mohammad Hissein, Changes in the terms of the contract, Dadgostar Publications, 2000.

6. Seddigh, Hossein, The general principles of maritime law, Jangal Publications, 2014.

7. Saffarzadeh, M., Abolbashar, A., and Shahba, M., 2006, Sea Freight, Asrare Danesh Publications, 567 pages.

8. Farmanfarmaian, Abolbashar, Maritime law, analytical discussion about Iran`s sea law, Khorrami Publications, 1970.

9. Ghorbanpour, M., 2009, Performance analysis of the international community in response to the actions of pirates off the coast of Somalia and the Gulf of Aden, Journal of International Law, 215-242.

10. Resolution No. 1851, The suppression of piracy and armed robbery at sea, UN Security Council, 2010.

11. Katoozian, N., 2001, General principals of contracts. Dissolving contracts, Volume V, Sahamie Enteshar Publications, Tehran, 392 pages.

12. Kass·h, Antonio, International criminal law, translation: Hossein Piran, Ardeshir Amirarjmand, Zahra Mousavi, Jangal Publications, 2008.

13. The International Maritime Organization report on piracy in Somalia, IMO, 2011.

14. Louis Baisun et. al., International Law of the Sea, translated by Muhammed Habibi Mojandeh, Tehran, Jangal Publications, 2011.

15. Mashhadchi, Majid, Shipping and Sea Transport, Iran Republic Islamic Shipping Press, 1982.

16. Najafiasfad, M., 2008, Maritime law, The organization of the study of humanities and

designing books in universities, Tehran, 362 pages.

Persian Journals

17. Beigzadeh, A., 2010, Piracy from the perspective of international law, Proceedings of the Iranian Association of UN Studies, 11-13 June, Tehran.

18. Tavazonizadeh, Abbas, Maritime law and the need to review it, Bandar o Darya, 19th year, No. 82-83, 2001.

19. Hosseini, Mohammadreza, Report of conference of piracy from the perspective of international law, Behengam Quarterly, Tehran, winter 2009.

20. Rouzbeh Mirmohammadi, Charter party, owners` obligations, tenants` obligations, Transportation industry, No 88.

21. Rouzbeh Mirmohammadi, Shipbuilding contract or charter party, terms and modifications, Transportation industry, No. 84-85.

22. Rouzbeh Mirmohammadi, Freight payment requirements, the consequences of delay, not paying the rent, Transportation industry, No. 89.

23. Shademan, A., 2011, Global cost of piracy, Journal of the National Iranian Tanker Company, 30-35.

24. Events Group, Safety at sea with a particular view to piracy, Payame Darya, No. 205, Tehran, 2011.

25. Report Group, Piracy, coordination and reactions, Bandar o Darya, No. 177, Tehran, 2010.

26. Mottaki, Manouchehr; Sabzian, Morteza; Sanzian, Hadi, Piracy from the perspective of international law of the seas and approaches to fight against it the Gulf of Aden, Fourteenth Conference on Marine Industry (MIC 2012), Tehran, 2012.

27. Mehrata, Reza, The international community against a scourge, piracy in international law, Payame Darya, No. 208, 2011.

28. Journal of National Iranian Tanker Company, 2011, Pirates report within a year, Journal of National Iranian Tanker Company, 16-19.

29. Journal of National Iranian Tanker Company, 2011, Investigating strategies of using armed security forces in the workgroup PMO, Journal of National Iranian Tanker Company, 33:63-43.

30. Nouamin, Amiesaeid; Kazemi Asiabar, Alireza, Investigating the effects of piracy on maritime trade, Payame Draya, No. 201, Tehran, 2011.

31. Yekdelepour, Hossein, Piracy phenomenon from the perspective of international law, Bandar o Darya, No. 181, 2011.

Theses

32. Taghizadeh, Z., 2010, Fighting against piracy off the coast of Somalia from the perspective of international law with an emphasis on Security Council action, M.Sc. thesis in the field of International Law, Allameh Tabatabaei University, 84 pages.

Websites

33. www.aja.ir

34. www.bimco.org

35. www.dodna.ir

36. www.edwardjones.com

37. www.farsnews.com

38. www.hamshahrionline.ir

39. www.icc-ccs.org

40. www.iranway.com

41. www.khabaronline.ir

42. www.maritimenews.com

43. www.Marsh.Com

44. www.orsam.org

45. www.parsine.com

46. www.Shippinglbc.Com

47. www.tabnak.ir

English References

48. Annual report, ICC IMB, 2003. Piracy and armed robbery against ships, annual report, ICC IMB, jan1-Dec, 87p.

49. Anonymos, 1991. Yearbook of the international law commission (1956, II) commentary to Article 39, 397p.

50. Anonymos, 2010. cosco bulk carrier co ltd v team-up owning co ltd(the saldanha)2010, p. 5

51. Aydin, I. 2011. Piracy and its effect on charter party contract, M.Sc. Thesis, Faculty of Law Lund University, 64p

52. Beck, R. and arend, a. 2004. dont tread on us: international law and forcible state responses to terrorism, oxford publishing, londan, 269p.

53. Continued U.S. Navy operation against pirates of Somalia, the American journal of International Law, Vol. 102, No.1 (Jan., 2008), PP.169-170.

54. Contracts for the carriage of goods by seA. bsp professional books, 1375p.

55. Convention on the High Seas 1958, Done at Geneve on 29 April 1958. Entered into force on 30 September 1962., United Nations, Treaty Series, vol. 450, p. 11, , p. 82.

56. Edward jones https://www. edwardjones. com/cgi/getHTML. cgi?page =intax. html)date, 15/03/2013. Time, 10:45.

57. EWCA, 2011. england wale high court of appeal decision. masefield AG v amlin corporate member ltd (the bunga melati dua) – Curt of Appeal (Rix, Mopre – aBick, Patten Lgg) {2011}EWCA Civ24.

58. EWHC, 2010. england wale high court decision 1340(comm), oxford publishing, London, 992p.

59. http://www. shipping;bc. Com / content / up;oads / members – documents / piracy – g. pbf (intertanko voyage), date, 09/09/2013.

60. IMO Circulars: MSC. 4/Circ. 133, 19 MSC. 4/Circ. 152, 29, March2010, MSC.4/Circ.169, 1 April 2011 and MSC.4/Circ180, 1 March 2012.

61. Lloyds, 1983. Rep, 483. Atens Maritime Enterprises Grop v Hellenic Mutual War risk Assn (Bermuda) Ltd (the AN DREAS LEMOS) 1983. QB647.

62. Maclachlan, M. 2004. The ship masters business companion. Published by the nautical institute, England, 816p.

63. Michel, K. 2008. Legal Issues Relating to Time Charter Parties, edited by Rhidian Thomas, Informa Law, London 298p.

64. Piracy and the charterer, Marsh's Global marine Practice, www.marsh.Com.

65. Ronzitti, N. 1980. (ed). Maritime terrorism and International Law, Kluwer Academic Publishers 218 p.

66. Singapore publishing, 1989. Halsburys Laws of Singapore (Carriers), vo1 3, Singapore publishing, Singapore, p. 463

67. Todd, P. 2010. Maritime Fraud and Piracy, 2nd ed. Lloyds List. London 174p.

68. UNCLOS, 1982. Arts. 86, 208p.

69. UNCLOS, 1982. arts87. 89, 209p.

70. Whisler International Ltd. V. Kawasaki kisen kaisha Ltd. (The Hill Harmony) (2001) 1 AC.

71. Wilford, m. and coghlin. t. & Kimball. J. D1989. Time charters. 3rd Edition. Lloyds of London press, London 673p.

72. Wilson, F. 2008. Carriage of Goods by Sea, BSP professional Books liverpool836p.

---

[1] For more information, see: www.hamshahrionline.ir visited on 16.06.2015.

[2] For more information, refer to: (www.icc-ccs.org), reviewed on 2015.08.11, 15:15 P.M.

[3] For more information, refer to: (www.icc-ccs.org), reviewed on 2015.08.11, 15:15 P.M.

[4] Strait of Malacca is the name of a waterway between Sumatra and Malay Peninsula which connects the Andaman Sea in the Indian Ocean to the South China Sea in the Pacific Ocean. Singapore is located at the southernmost point of the strait. The Strait is named after the port of

Malacca in Malaysia which was of significant importance during 16th and 17th century. The Strait of Malacca is funnel like with the narrowest part in south of the strait and widens towards north. Strait of Malacca is known to be one of the world`s most important sea crossings, and more than a quarter of the world`s crudes cargos passes through this strait. It is considered to be the most important transport highway of oil at sea in the world after Strait of Hormuz.

INTERNATIONAL CONFERENCE ON ADVANCES IN SCIENCE AND ARTS ISTANBUL 2017
29 – 31 MARCH 2017, Istanbul, Turkey

IMPEDANCE ANALYSIS AND NO GAS SENSING PERFORMANCE OF ZEOLITE DEPOSITED

ZN0.75CU0.25O THIN FILM

Tuğba Çorlu[1], Irmak Karaduman[1], Sezin Galioglu[2], Burcu Akata[2], Memet Ali Yıldırım[3], Aytunç Ateş[4], Selim Acar[1*]

[1]Department of Physics, Science Faculty, Gazi University, Ankara, Turkey
[2]Department of Micro and Nanotechnology, Middle East Technical University, Ankara, Turkey
[3]Department of Electric Electronics Engineering, Engineering Faculty, Erzincan University, Erzincan, Turkey
[4]Department of Material Engineering, Engineering and Natural Sciences Faculty, Yıldırım Beyazıt University, Ankara, Turkey

ABSTRACT

In this study, the $Zn_{0.75}Cu_{0.25}O$ thin film for 40 cycles was produced by SILAR method and deposited with zeolite. The gas sensing properties of the $Zn_{0.75}Cu_{0.25}O$ thin film were measured at different operating temperatures and different gas concentrations in air. Impedance measurements were also performed for NO gas presence and absence. It can be seen that the sample exhibited good sensing performances to 20 ppb NO gas concentration. Thus, our detailed investigation shows zeolite deposited $Zn_{0.75}Cu_{0.25}O$ thin film has potential for the highly sensitive NO gas sensing applications.

Keywords: Zeolite, Zinc oxide, Copper, Gas Sensor
** Corresponding author: sofue@gazi.edu.tr*

INTRODUCTION

Electronic nose is a device intended to detect, identify and quantify odors. Desirable qualities such as high sensitivity, selectivity, and speed of response of the sensors are important for electronic nose applications. An alternative with respect to selectivity is the combination of n-type [1] or p-type [2] metal oxide semiconductors (MOS) with a zeolite films on top. Several groups investigated zeolites as filters for gas sensors [3–4]. However, in these cases the zeolite deposite layer is applied only due to its adsorbing properties in order to improve the selectivity of commonly used sensing materials or sensing principles.

MOS thin films for gas sensing applications, have been prepared by various techniques such as electro chemical method, spray pyrolysis, molecular-beam epitaxy, sol gel, etc. Most of these techniques require high temperature and pressure hence, limits the kind of substrate that can be used for the deposition.

On the contrary this methods, SILAR is capable of producing metal oxide films at relatively low temperature, is relatively simple, does not require expensive equipment, and there is minimal waste of chemicals as compared with other methods. The deposition rate and thickness of the film can be easily controlled by changing the deposition cycle (figure 1). There is no restriction on the substrate material, dimensions, or surface profile to be used [5].

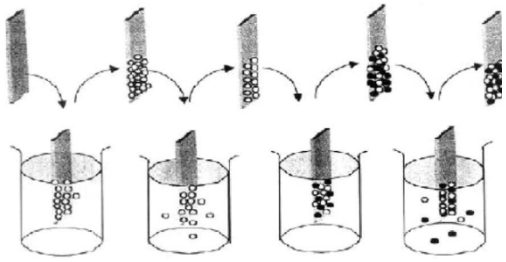

Figure 1. The schematic diagram of SILAR cycle

RESULTS AND DISCUSSION

In this study, the $Zn_{0.75}Cu_{0.25}O$ thin film for 40 cycle was produced by SILAR method on the glass substrate and then deposited with zeolite. Surface morphology was studied using the FEI Quanta FEG 450 model SEM. Nanoflowers were clearly seen from the SEM image.

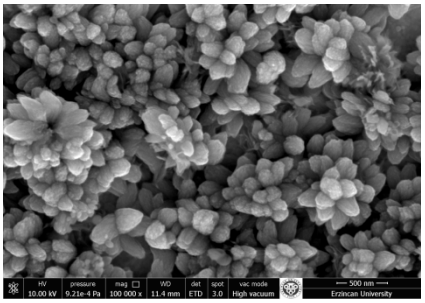

Figure 2. SEM image of $Zn_{0.75}Cu_{0.25}O$ thin film

The gas sensing performance of the sensor was tested using a special computer controlled measurement system. The gas sensing measurement system consists of Mass flow controllers (MKS Series) for controlling gas concentrations, a LakeShore

325 temperature controller for maintaining a constant temperature, a Keithley 2400 SourceMeter for monitoring the data continuously, a Honeywell HIH-4000 humidity sensor for using the relative humidity being constant (25%), as shown in Figure 3.

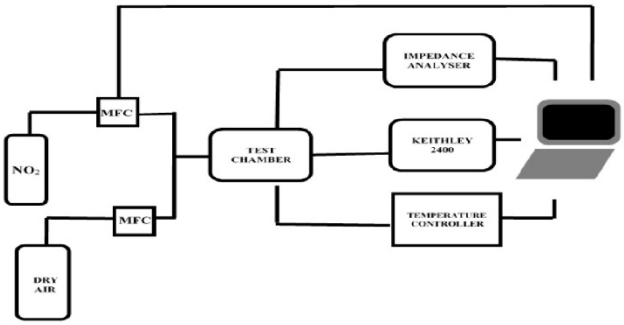

Figure 3. Gas sensing measurement system.

The gas-sensing performance of $Zn_{0.75}Cu_{0.25}O$ thin film at different temperatures and gas concentrations investigated. The sample shows acceptable response over to 50 °C. Selectivity is important factor for the practical application of a gas sensor, a sensor with good selectivity means that one can detect the target gas even in a multicomponent gas environment. The gas sensing measurements were performed to NO, CO, NH_3 and H_2 at 55 °C The sample has the highest response to NO compared to CO, NH_3 and H_2. But the sensor has slightly response CO and NH_3 gases. To enhance response and selectivity the sample covered with zeolite. At room temperature response changes for different gases of zeolite modified sensor are given Figure 4. The sensor shows good sensitivity and selectivity for 20 ppb NO gas at room temperature. This case related to the increase in the amount of zeolite pores per unit surface area available to interact.

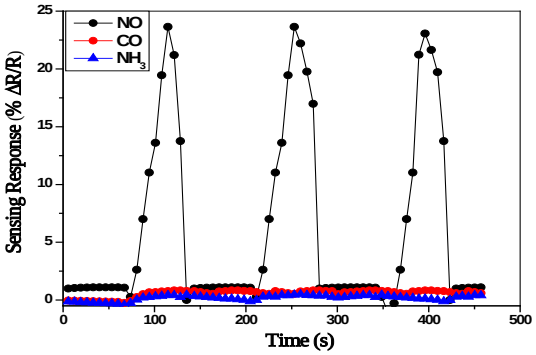

Figure 4. Transient responses of sensors tested to different gas in air at the room temperature.

Also impedance analyses are carried out room temperature for 20 ppb NO gas presence and absence. Figure 5 shows the impedance spectrum room temperature, real component of impedance (Zr/ and imaginary component (Zi/ in the complex plan for sensor. In order to separate out the bulk and grain boundary contribution to the total conductivity, the impedance measurements are done. Figure 5 shows sample a semicircle. According to Shinde *et. al.* [6] the semicircle at higher and lower frequencies represents bulk and electrode process, respectively, while those at intermediate frequencies represent grain boundary contribution. The sizes of these semicircles depend upon the grain size and the number of grains and the resistance of grain attribute to diameter of semicircle.

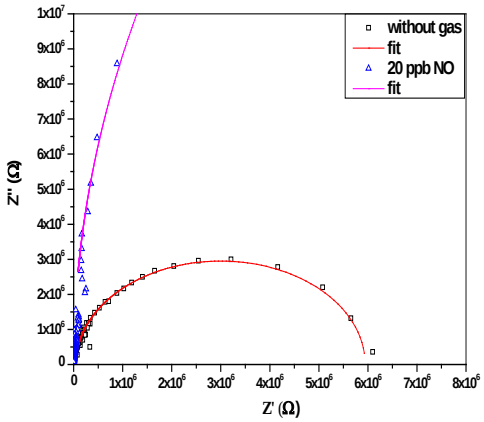

Figure 5. Nyquist plots of sensor at room temperature

CONCLUSION

The gas sensing properties of the $Zn_{0.75}Cu_{0.25}O$ thin film were measured at different operating temperatures and different gas concentrations in air. Impedance measurements were performed versus NO gas presence and absence. It can be seen that the sample exhibited good sensing performances to 20 ppb NO gas concentration. Thus, our detailed investigation shows zeolite deposited $Zn_{0.75}Cu_{0.25}O$ thin film has potential for the highly sensitive NO gas sensing applications.

ACKNOWLEDGMENTS

This work is supported by The Scientific and Technological Research Council of Turkey (TUBİTAK) under Project No, 115M658 and Gazi University Scientific Research Fund under project no 05/2016-21.

NOMENCLATURE

ZnO	Zinc Oxide
NO	Nitric Oxide
ppm	Parts Per Million
SEM	Scanning Electron Microscope
SILAR	Successive Ionic Layer Adsorption and Reaction

REFERENCES

[1] J. Trimboli, P. Dutta, Oxidation chemistry and electrical activity of Pt on titania: development of a novel zeolite-filter hydrocarbon sensor, Sens. Actuators B Chem. 102 (2004) 132–141.

[2] K. Sahner, R. Moos, M.M. Matam, J. Tunney, M. Post, Hydrocarbon sensing with thick and thin film p-type conducting perovskite materials, Sens. Actuators B Chem. 108 (2005) 102–112.
[3] N. Szabo, H. Du, S. Akbar, A. Soliman, P. Dutta, Microporous zeolite modified yttria stabilized zirconia (YSZ) sensors for nitric oxide (NO) determination in harsh environments, Sens. Actuators B Chem. 82 (2002) 142–149.
[4] N. Szabo, P. Dutta, Strategies for total NO*x* measurement with minimal CO interference utilizing a microporous zeolitic catalytic filter, Sens. Actuators B Chem. 88 (2003) 168–177.
[5] A.C.Nwanya, P.R.Deshmukh, R.U.Osuji, M.Maaza, C.D. Lokhande, F.I.Ezema: Synthesis, characterization and gas-sensing properties of SILAR deposited ZnO-CdO nano-composite thin film, Sens. Actuators B Chem. 206(2015)671–678
[6] Shinde S S, Korade A P, Bhosale C H, et al. Influence of tin doping onto structural, morphological, optoelectronic and impedance properties of sprayed ZnO thin films. J Alloys Compd, 2013, 551: 688 033002

INTERNATIONAL CONFERENCE ON ADVANCES IN SCIENCE AND ARTS ISTANBUL 2017
29 – 31 MARCH 2017, Istanbul, Turkey

CHEMICAL QUALITY OF WATER IN THE TRADITIONAL BATHS AND ITS EFFECTS ON THE SKIN

***Khedidja Benouis**
University of Djillali Liabes
Sidi Bel Abbes, Algeria

Nadia Ramdani
University of Djillali Liabes
Sidi Bel Abbes, Algeria

Latifa Mahieddine
University of Djillali Liabes
Sidi Bel Abbes, Algeria

Fadila Boukhobza
University of Djillali Liabes
Sidi Bel Abbes, Algeria

Hadjer Cherif Otsmane
University of Djillali Liabes
Sidi Bel Abbes, Algeria

Keywords: Chemical quality, Water, Skin, Traditional bath, Algeria.

** Corresponding author:*
E-mail address: benouiskhadidja@yahoo.fr

ABSTRACT

Taking a Turkish bath is a great way to improve our physical and mental well-being. The steam and heat generated in the Turkish bath improves the acceleration of the body's metabolic functions by improving blood circulation and stimulating the nervous, respiratory and endocrine systems.

In Algeria, a Maghreb country, traditional Turkish baths are frequented regularly by users, at least once a week to relax and to eliminate toxins from the body through moisture-saturated air. However, the bath must also be a place of purification and relaxation without the risk of contracting dermatoses. In this context, the water quality plays an important role; it should not be neglected because it can have in some cases negative effects on human health, especially on the skin.

In this study we are interested in the chemical quality of water in the traditional Algerian baths and its possible effects on the skin of users.

INTRODUCTION

Since centuries, many doctors have been interested in the curative properties of immersion of the body in warm water.

The hammam is a one of the different public place where people can take a hot bath with warm water.

The authentic hammam, introduced in the East by the Turks, it is a bath at 50 ° C, saturated with humidity and with two rooms: a steam room and a more lukewarm. The practice is still alive in many countries of the East and Maghreb and is developing in Europe.

Several studies have been interested in the quality of water in traditional baths [1, 2, 3, 4,5].

The hot water of the bath has several effects on the human body especially on the skin which is an external organ of the human body protects internal organs from damage due to external aggressions such as UV rays, chemicals, contaminants and bacteria, but it is almost constantly subjected to these aggressions. The hot water and the humidity of the bath favor the opening of the pores of the skin and allow the substances dissolved in water to penetrate such as mineral salts, metals and even bacteria.

In the present study, and according to its different physicochemical parameters, we discussed the possible effect of water used for bathing in the traditional Hammams in Algeria, on the skin of users.

MATERIALS AND METHODS

The study area has several public baths. The wells feeding the water baths have a depth that varies from one neighborhood to another. In this study, we chose 10 Hammams regularly frequented by the users.

The research of water quality was based on the study of the heat of bathhouses and the temperature and mineral elements dissolved in water. Used for bathing.

Selected parameters analyses are: temperature, pH, salinity, hardness and chloride.

Measurements of temperature and pH which could be modified during transport were made directly in the bathroom using a Multi-parameter analyzer.

The salinity and TDS of the water samples are measured using an InoLab Cond Level 1 conductivity meter (graphite measuring cell with a constant of 0.475 / cm ± 1.5%).

Hardness and mineral content are determined by standard protocols [6, 7].

RESULTS AND DISCUSSION

The results of the physicochemical analyses are shown in Table I and II.

Table I. Temperatures Of Bathrooms, Of Waters And Ph.

HAMMAM	TEMPERATURE OF THE BATHROOM (°C)	TEMPERATURE OF WATER (°C)	pH
H1	41	40	7.55
H2	45	43	7.85
H3	50	46	7.60
H4	52	50	7.15
H5	48	44	7.65
H6	50	41	7.90
H7	44	47	7.70
H8	51	45	7.85
H9	50	52	7.20
H10	48	48	7.50

Table 2. **Tds, Hardness And Chloride In Water.**

HAMMAM	TDS (mg/L)	TH °f	CHLORIDE (mg/L)
H1	970	80,25	395
H2	161	83.41	193
H3	908	68.33	221
H4	1197	104.25	502
H5	3167	159.33	431
H6	788	70.83	281
H7	887	63.16	341
H8	161	83.41	193
H9	195	74.16	291
H10	102	49.16	72

Temperature T

The temperature in the bathrooms varied between 41 °C and 52°C, while the temperature of the water used for bathing in the Hammams oscillates between 40° C and 52° C (figure 1).

In humans, temperature values between 36 ° C and 37.5 ° C correspond to optimum conditions for the proper functioning of the body, but the hot water and the hot steam used for the bath can be beneficial for the health of the users, it releases all the muscular tensions, it is recommended to those who suffer from rheumatological diseases, it is a cure for osteoarthritis because tuning in the water from time to time helps to alleviate the pain of inflammation.

In contact with water at high temperature, the heart begins to beat substantially faster , it is a sort of sports session for the organ, which allows a better circulation of the blood in the organism. In healthy people, hot baths can lower heart pressure and improve heart function. When the water is very hot and the heart beats fast, the oxygen supply increases and the water vapor cleans the sinuses and lungs.

The warmth of a bath can also help relieve pain caused by hemorrhoids and anal fissures. The high temperature helps the sphincter to relax and accelerate the healing of post-operative wounds.

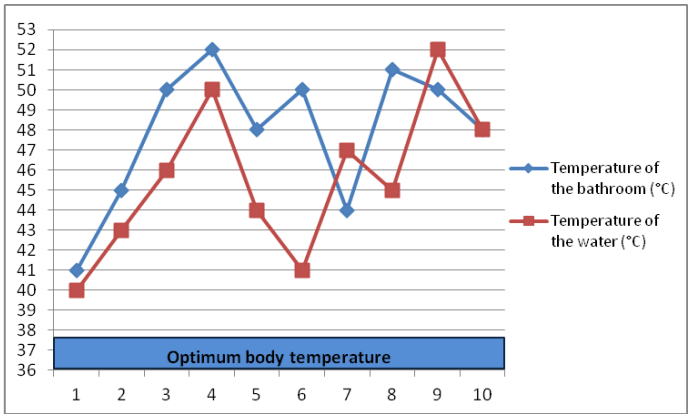

Figure 1. Temperature Of Bathrooms And Of Waters

pH of normal adult skin varies depending on the type of skin; it is somewhat acidic, having an approximate pH range of 4 to 6. This acidity is due to the presence, on the most superficial part of the epidermis, of a hydrolipidic film, a layer consisting of lipids (sebum) and water (perspiration), whose role is to preserve the hydration of the skin. This part of the skin is called the "acid mantle", it is maintained by the different glands and the normal flora of the skin [8]. pH acid leaching fulfills several protective functions of the skin, one of which is killing unwanted bacteria.

The pH of the water is practically neutral; it varied between 7.15 and 7.9, which respects the natural balance of the skin.

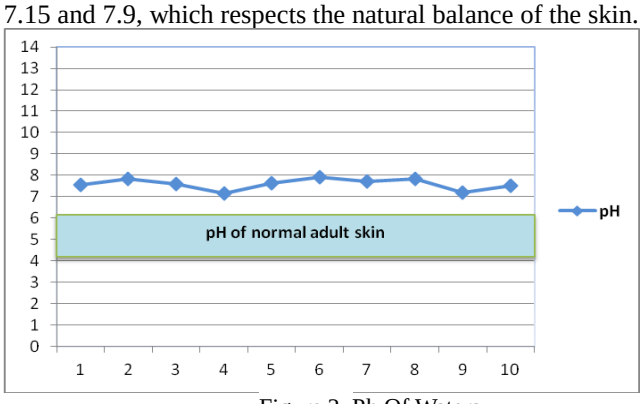

Figure 2. Ph Of Waters

Hardness

The waters are classified hard and very hard, their TH varies between 49.16 °f and 159.33 °f (figure 2).

A bath with hard water can cause irritations, itching, and dermatological problems, on the skin like the scalp, the hair become more rough, dull and brittle.

The mineral crystals present in the hard water are invisible to the naked eye, peck the skin, and cause some unpleasant sensations,

Hard water can also be a factor favouring pathologies such as psoriasis, eczema or dermatitis.

On sensitive skin, it can still cause scaling, peeling of the superficial layer of the epidermis.

It is not recommended for people suffering from psoriasis.

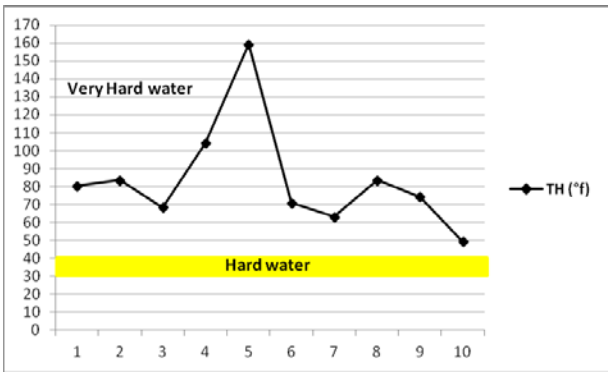

Figure 3. Th Of Waters

Chloride

The chloride levels recorded vary between 72 mg/L and 502 mg/L (figure 3). Salt water has harmful effects on the skin; this causes an irregular dryness of the epidermis, itching, acne, irritation and an imbalance of healthy and natural bacteria on the skin.

On sensitive skin, it also causes the appearance of red patches, the hair becomes dry and brittle; They also affect their color, dark hair becomes lighter, tinted hair loses color and the color of blonde hair is damaged.

In addition to this, it is not uncommon for chlorine to cause the bursting of micro-blood vessels in the eyes, making them red.

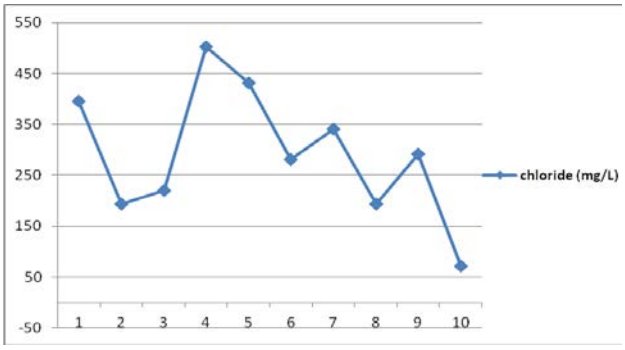

Figure 4. Chloride In Waters

CONCLUSION

The water used for personal hygiene in traditional baths has beneficial and disadvantageous characteristics for the skin health of users. The analyses showed that pH respects the natural balance of the skin. Hardness and chloride are high in some samples, which can have undesirable effects on the skin.

These characters must be regularly monitored by the owners of the Hammams to maintain a sufficient mineralization while avoiding excessive hardness.

REFERENCES

[1]. Leyla Benammar, Taha Menasria, Amel Chergui, Ammar Ayachi. Indoor fungal contamination of traditional public baths (Hammams). International Biodeterioration & Biodegradation 117C (2017):115-122.

[2]. Benouis.K, Benabderrahmane.M, Harrache-Chettouh.D, Benabdeli.K. Peut-on boire les eaux de bains maures « Hammam » ? : Cas des bains de la ville de Sidi-Bel-Abbès. Cahiers Santé. Vol. 18, n° 2, (2008). doi: 10.1684/san.2008.0112

[3]. Rhazi Filali F, Zaid Zerhouni M. Contamination bactérienne des bains traditionnels publics. Objectif Med 1996 : 6-12 ; (spécial Maroc, Casablanca).

[4]. Rhazi Filali F, Zaid A, Zerhouni M. Contamination bactérienne des bains traditionnels publics. Objectif Med 1996 : 6-12 ; (spécial Maroc, Casablanca).

[5]. Laraqui CE, Caubet A, Benghalem A, et al. Hygiène, conditions de travail et risques professionnels dans les bains maures « Hammams » à Marrakech. Sante; 10 : 19-26. (2000).

[6]. Rodier J. L'analyse de l'eau, 8e éd. Paris : Bordas, (1984).

[7]. Alexeev V. Analyse quantitative. Éditions Mir ; (72-256). 1980

[8]. W. Joachim et al. Stratum corneum pH: Formation et fonction du manteau acide. Dermatologie Exogène 2002; 1 (4): 163-75.

[8]. N. Schurer, M. Bock. Abaisser lésionnel pH de surface dans l' acné: Un nouveau traitement pour Modalité Herpifix. Journal de traitement dermatologique 2009; 20 (1): 27-31.

INTERNATIONAL CONFERENCE ON ADVANCES IN SCIENCE AND ARTS ISTANBUL 2017
29 – 31 MARCH 2017, Istanbul, Turkey

NO GAS SENSING PROPERTIES OF $ZN_{1-X}SN_XO$ NANOSTRUCTURE THIN FILMS SYNTHESIZED BY SILAR METHOD

Irmak Karaduman[1], Tuğba Çorlu[1], Memet Ali Yıldırım[2], Aytunç Ateş[3], Selim Acar[1*]

[1]Department of Physics, Science Faculty, Gazi University, Ankara, Turkey
[2]Department of Electric Electronics Engineering, Engineering Faculty, Erzincan University, Erzincan, Turkey
[3]Department of Material Engineering, Engineering and Natural Sciences Faculty, Yıldırım Beyazıt University, Ankara, Turkey

Keywords: Gas Sensors, Electrical Characterization, NO
** Corresponding author: Selim Acar*
E-mail address: sacar@gazi.edu.tr

ABSTRACT

In this work, $Zn_{1-x}Sn_xO$ nanostructure thin films with 20 cycle were synthesized by SILAR method and investigated their NO gas sensing properties. The morphological and structural characteristics of the samples were characterized by scanning electron microscopy (SEM) and UV-absorbance measurement. The effect of operating temperature and concentration of the NO were analyzed for sensing performance of synthesized nanostructure thin films. The operating temperature was found at 105 °C. The maximum response was found 28 % for $Zn_{0.75}Sn_{0.25}O$ film. $Zn_{0.75}Sn_{0.25}O$ nanostructure thin film was showed the highest gas detection response toward NO for 25 ppm than that of the other nanostructure thin films.

INTRODUCTION

Gas sensors have been extensively researched due to the widespread application areas of safety control requirements, environmental monitoring, detecting for inflammable (explosive or toxic) gases, chemical process control, medical and food quality analysis, and personal safety, etc. [1-2]. Metal-oxide semiconductors provide an appealing coupling of chemical, electrical, and optical properties that can be exploited in the design of gas sensors [3-5].

A prominent and well-studied example for metal oxide nanomaterials is tin dioxide (SnO_2), which is an important n-type wide-band gap (Eg = 3.6 eV, at 300 K) semiconductor with broad applications also in lithium rechargeable batteries [6], photocatalyst [7], and gas sensing [8]. Oxide semiconductor materials in nanoparticle form have been extensively investigated because of their unique size dependent electronic, optical, and electrochemical properties [9]. Therefore, Fabrication method is one of the important factor foraffecting the sensor performance [10]. Many synthetic methods have been employed for the preparation of metal oxide semiconductors including: sol–gel processes, chemical spray pyrolysis and SILAR [11]. Several research groups have reported the different growth methods to product of ZnO incomposite films for gas sensor applications with different gases but there are very few reports on NO gas sensing properties of ZnO nanostructure grown by SILAR method. Currently, SILAR method is favorable and considered to be a chemical methods to deposit a variety of compound materials in a nanomaterial form for metal oxide gas sensors [12]. The SILAR method is low cost, simple and suitable for large area deposition. As a low-temperature process, it also avoids oxidation and corrosion of the substrate.

Nowadays, decoration or doped a semiconducting metal oxide (SMO) with other metal oxide or noble metal nanoparticles is widely accepted as a powerful strategy to enhance sensitivity and selectivity of gas sensors. Doping with extrinsic dopants is a facile and effective way to modify. The change in chemical, structural or electronic surface composition by doping provides many opportunities for creating surfaces with tailored physicochemical properties, for tuning the electronic properties of semiconductor material, and for enhanced detection of a target analyte [13-14]. In this work, $Zn_{1-x}Sn_xO$ nanostructure thin films were synthesized by SILAR method. Gas sensing properties of these nanostructures towards to low level NO gas concentration are investigated as a function of Zn doping.

EXPERIMENTAL

The thin films were prepared using SILAR method at room temperature and ambient pressure. In order to prepare ZnO, $Zn_{0.75}Sn_{0.25}O$, $Zn_{0.5}Sn_{0.5}O$, $Zn_{0.25}Sn_{0.75}O$ and SnO2

nanostructure thin films, aqueous zinc-ammonia complex ions ($[Zn(NH_3)_4]^{2+}$), aqueous and tin-ammonia complex ions ($[Sn(NH_3)_4]^{2+}$) were chosen for the cation precursors, in which analytical reagents of $ZnCl_2$ (%99) of 0.1M, $SnCl_2$ (%99) of 0.1M and concentrated ammonia (NH_3) (25-28%) were used. The double distilled water was used as a solvent and the molar ratio of Sn-Zn:NH_3 is 1:10 that obtained as a result of several experiments [15]. The obtained $[Zn(NH_3)_4]^{2+}$ and $[Sn(NH_3)_4]^{2+}$ complexes were mixed in proper proportion according to the composition for ZnO, $Zn_{0.75}Sn_{0.25}O$, $Zn_{0.5}Sn_{0.5}O$ and $Zn_{0.2\,5}Ni_{0.75}O$ thin films.

To prepare nanostructure thin films, one SILAR preparation cycle involves the four following steps: (1) immersing the substrate in the Sn-Zn species to create a thin liquid film containing Zn and Sn-Zn ammonia complex ions on the substrate, respectively; 2) immersing immediately the withdrawn substrates in hot water (~ 90℃) for 7 s to form nanostructure layers; 3) drying the substrate in the air for 60 s and 4) rinsing the substrate in a separate beaker for 40 s to remove large and loosely bonded particles. Thus, one SILAR cycle of nanostructure thin films preparation was completed. The nanostructure films were prepared by repeating 20 SILAR cycles.

For the structural analysis, a FEI Quanta FEG 450 model Scanning Electron Microscope (SEM) was used. The absorption measurements were carried out using a Perkin Elmer UV / VIS Lambda 2S Spectrometer with a wavelength resolution better than ±0.3 nm at room temperature. The gas sensing performance of the samples was tested using a special computer controlled measurement system, which was described in detail by. [16] Nanostructure thin films were evaluated by measuring the resistance change at various NO concentrations from 0.1 to 25 ppm. The gas concentration in the test chamber was controlled by mass flow controllers (MKS Series). A LakeShore 325 temperature controller with platinum RTDs was used to maintain a constant temperature. The current of the sample was continuously monitored with a computer-controlled system using the Keithley 2400 Source Meter and data was collected in real-time using a computer with corresponding data acquisition hardware and software. The relative humidity was being constant 25% and monitored by a Honeywell HIH-4000 humidity sensor.

RESULTS AND DISCUSSION

SEM can provide detailed information on the surface morphology of the films. Figure 1 shows the SEM images of as synthesized nanostructure thin films. It is seen that there is a change in the morphology with the addition of Sn. It seems that the morphology is starting to slide towards the nanoflower to nanocubes.

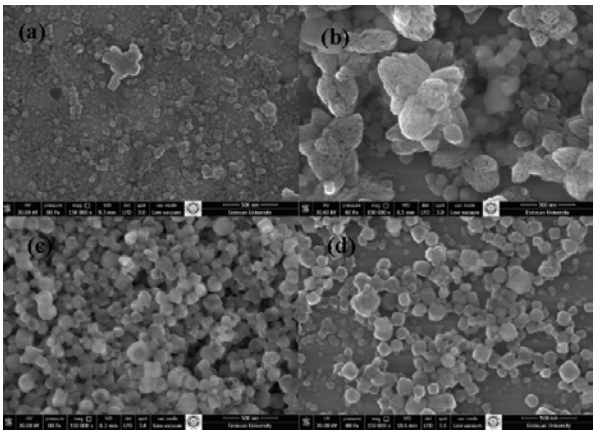

Figure 1. SEM images of the SnO_2 (a), $Zn_{0.75}Sn_{0.25}O$ (b), $Zn_{0.5}Sn_{0.5}O$ (c) and $Zn_{0.25}Sn_{0.75}O$ (d) nanostructure thin films

The optical band gap energy for undoped and doped ZnO has been calculated using Tauc's relation [17]. The plot of (αhν)2 as a function of hυ for all samples is shown in Fig. 2. Extrapolating the straight line portion of the plot of $(\alpha h\nu)^2$ against hν to energy axis for zero absorption coefficients gives optical band gap energy of material. E_g values of thin films were calculated as 3.93 eV, 3.87 eV , 3.72 eV and 3.57 eV for SnO_2 $Zn_{0.75}Sn_{0.25}O$, $Zn_{0.5}Sn_{0.5}O$ and $Zn_{0.25}Sn_{0.75}O$, respectively. E_g values of the films decreased with doping material.

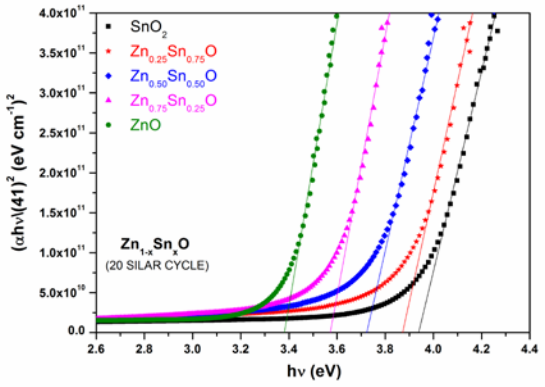

Figure 2. The plot of (αhν)2 as a function of hυ for SnO_2, $Zn_{0.75}Sn_{0.25}O$, $Zn_{0.5}Sn_{0.5}O$ and $Zn_{0.25}Sn_{0.75}O$ nanostructure thin films, respectively

The effects of working temperature on their sensing performances were investigated on the samples to obtain the optimum conditions, because the operating temperature has an apparent influence on gas response [18]. Figure 3 presents the typical response characteristics of all the fabricated gas sensors to 25 ppm of NO under the operating temperature varies from 35 ◦C to 135 ◦C.

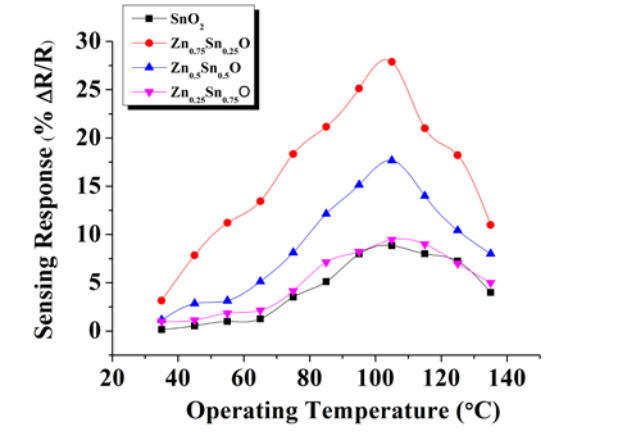

Figure 3. The response of nanostructure thin films as a function of operating temperature

The experimental results show that the sensing responses of all the sensors increase at the beginning and then decrease with the increasing of operating temperature, and all the sensors response reach maximum value at 105 °C, which displays that the optimum operating temperature is determined to be about 105 °C for all the gas sensors. Moreover, $Zn_{0.75}Sn_{0.25}O$ sensor exhibits the highest response than other sensors. The measured results indicate that the $Zn_{0.75}Sn_{0.25}O$ sensor is very promising for the detection of NO. The gas-sensing performances of nanostructure thin films at 105 °C were investigated. Figure 4 indicates the response of nanostrucure thin films to different NO gas concentrationsfrom 0.1 ppm to 25 ppm at 105°C.

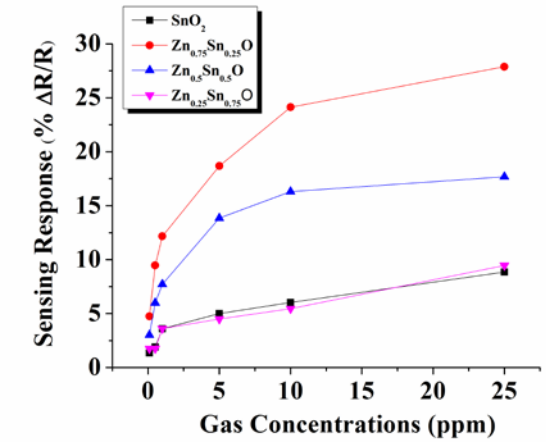

Figure 4. The response of nanostructure thin films as a function of gas concentrations

It can be seen that the response increases with increasing gas concentration. The responses for 25 ppm NO gas concentrations were calculated 9 %, 28 %, 17 % and 9% for SnO_2, $Zn_{0.75}Sn_{0.25}O$, $Zn_{0.5}Sn_{0.5}O$ and $Zn_{0.25}Sn_{0.75}O$ nanostructure thin films, respectively, whereas the response for 0.1 ppm were calculated 1.5 %, 5%, 3 % and 1.7 %, as shown in Figure 5. The results indicated that $Zn_{0.75}Sn_{0.25}O$ nanostructure thin film was showed the highest gas detection response toward NO for 0.1 ppm than that of the other nanostructure thin films.

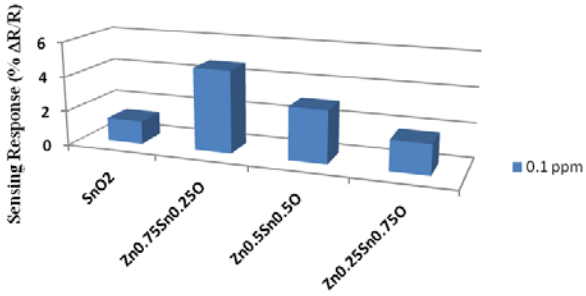

Figure 5. The response of 0.1 ppm NO gas concentration for all nanostructure thin films

The resistance of n-type metal oxide semiconductor will be changed when oxygen or testing gas molecules are adsorbed on its surface. In our testing process, oxygen molecules will be adsorbed on the surface when the sensors are exposed to air . The adsorbed oxygen molecules will capture free electrons from the conduction band, and then form adsorbed oxygen (O2-, O and O2-) . The formation of the adsorbed oxygen results in a depletion layer near the surface. The existence of the depletion layer blocks the electron conduction and leads to the increase of the resistance. When the surface are exposed to NO, the adsorbed oxygen will react with the NO molecules and then release electrons [19-20].

Subsequently, while exposing to the oxidizing gas, the NO molecules would capture electrons from the conductance band on their activesites in the form of adsorbed NO, resulting in the potential barrier formed in depletion layer and the concentration decrease of free charge carriers, leading to an increase of the resistance. Moreover, there is a potential barrier to electronic conduction at each grain boundary. When the sensor is exposing to the oxidized gas of NO, the trapping electrons would also lead to the increasing of the height of the potential barrier, then the resistance increases [21-22].

CONCLUSION

Nanostructure $Zn_{1-x}Sn_xO$ thin films were synthesized using the SILAR method with 20 cycle and the NO gas sensing properties were studied. The results indicated that $Zn_{0.75}Sn_{0.25}O$ nanostructure thin film was showed the highest gas detection response toward NO than that of the other nanostructure thin films. The characteristic parameters of the gas sensing properties of films were related to the film morphologies. The

larger surface/volume ratio is caused the higher sensitivity in sensor materials.

ACKNOWLEDGMENTS

This work is supported by The Scientific and Technological Research Council of Turkey (TUBİTAK) under Project No, 115M658 and Gazi University Scientific Research Fund under project no 05/2016-21.

NOMENCLATURE

NO	Nitric Oxide
ppm	Parts Per Million
SEM	Scanning Electron Microscope
SILAR	Successive Ionic Layer Adsorption and Reaction

REFERENCES

[1] V.S. Vaishnava, S.G. Patel, J.N. Panchal, Sens. Actuators, B: Chem. 206 (2015)381.

[2] J. Mitrovics, H. Ulmer, U. Weimar, W. Gopel, Acc. Chem. Res. 31 (1998) 307.

[3] Z. Wang, Y.M. Hu, W. Wang, X. Zhang, B.X. Wang, H.Y. Tian, Y. Wang, J.G. Guan,H.S. Gu, Int. J. Hydrogen Energy 37 (2012) 4526.

[4] L.Z. Kou, T. Frauenheim, C.F. Chen, J. Phys. Chem. Lett. 15 (2014) 2675.

[5] L. Liu, C.C. Guo, S.C. Li, L.Y. Wang, Q.Y. Dong, W. Li, Sens. Actuators, B: Chem.150 (2010) 806.

[6] S.Q. Tian, F. Yang, D.W. Zeng, C.S. Xie, J. Phys. Chem. C 116 (2012) 10586.

[7] S.M. Niu, Y.F. Hu, X.N. Wen, Y.S. Zhou, F. Zhang, L. Lin, S.H. Wang, Z.L. Wang, Adv. Mater. 25 (2013) 3701.

[8] T.F. Jiang, T.F. Xie, W.S. Yang, H.M. Fan, D.J. Wang, J. Colloid Interface Sci. 405 (2013) 242.

[9] T. Senthil, S. Anandhan, J. Colloid Interface Sci. 432 (2014) 285.

[10] I. Sta, M. Jlassi, M. Kandyla, M. Hajji, P. Koralli, R. Allagui, M. Kompitsas and H. Ezzaouia, , *J. Alloy. Compd.* 626, 87 (2015).

[11] B. Güzeldir, M. Sağlam and A. Ateş, *Turk J Phys* 35, 1 (2011).

[12] H.M. Pathan and C.D. Lokhande, *Bull. Mater. Sci.* 27(2), 85 (2004).

[13] L.-Y. Hong, H.-W. Ke, C.-E. Tsai and H.-N. Lin, *Mater. Lett.* 185, 243 (2016).

[14] S. Xu, J. Gao, L. Wang, K. Kan, Y. Xie, P. Shen, L. Li and K. Shi, *Nanoscale* 7, 14643(2015).

[15] Y. Akaltun and T. Çayır, *J. Alloy. Compd.* 625, 144 (2015).

[16] I.Karaduman, O. Barin, M. Ozer and S. Acar, *J. Electron. Mater.* 45, 8 (2016).

[17] W. Chen, H. Gan, W. Zhang and Z. Mao, *Journal of Nanomaterials* 291273 (2014).

[18] C. Liewhiran and S. Phanichphant, *Sensors* 7, 185 (2007).

[19]A. Mirzaei, S. Park, G.-J. Sun, H. Kheel and C. Lee, *Journal of Hazard. Mater.* 305, 130 (2016) .

[20] D. Zhang, J. Lıu and B. Xıa, *J. Electron. Mater.* 45, 8 (2016).

[21] P. Li, H. Fan and Y. Cai, *Sens. Actuators B* 185, 110 (2013).

[22] N. Nithyavathy, S. Arunmetha, M. Vinoth, G. Sriram and V. Rajendran, *J. Electron. Mater.* 45, 4 (2016).

INTERNATIONAL CONFERENCE ON ADVANCES IN SCIENCE AND ARTS ISTANBUL 2017
29 – 31 MARCH 2017, Istanbul, Turkey

THE EFFECT OF ELECTRIC FIELD ON THE TRANSPORT PROPERTIES OF THE POROUS ZEOLITE MICROSTRUCTURE

B. Soltabayev[1], M. Ozer[1], U. Bunyatova [2], I.C. Koçum [2], B.G. Salamov [1, 3], S. Acar [1*]

[1]Department of Physics, Science Faculty, Gazi University, Ankara, Turkey
[2] Department of Biomedical Engineering, Faculty of Engineering, Baskent University, Baglica, Ankara, Turkey [3]
Azerbaijan Academy of Science, Institute of Physics, AZ0143 Baku, Azerbaijan

Keywords: Zeolite, dc electric field, resistance, temperature
** Corresponding author: sacar@gazi.edu.tr*

ABSTRACT

This study explores, the influence of DC electric field on the conductivity of natural clinoptilolite at room temperature. Zeolite samples were exposed to an electric field, E_p = 2 kV cm^{-1} in an air atmosphere for 24 hours. The influence of temperature (from 27 to 260 ^{0}C) and DC electric field on the dc conductivity was described. During some time the transport properties is restored, which indicates on the electret behavior of clinoptilolite samples. These changes are observed within a few days consequently, there is long-term dynamics of the transport properties changes.

INTRODUCTION

Investigation of electret state in solid state field is carried out for a long time [1]. Electret is an interesting natural phenome-non which is important not only for solid state physics, it is pre-sently extensive use in optoelectronic application as well. There are several fields which electrets are used such as, micropho-nes, headphones and loudspeakers), motors and generators, air filters [2], electret floppy disc for storing digital information [3], as well as dosimeters. Although the applications are mainly restricted to polymer electrets, there is also a considerable interest to nonorganic electrets [4] since they exhibit better mechanical properties and may operate in a wider temperature range, as well as in aggressive atmospheres [5].

Zeolite is a natural mineral which has well defined pore sizes and internal cavities (≈4A) and have the ability to ion exchange as a good sorbent based on this porosity. Zeolite has a sponge like structure with a pore volume of up to 50% of the volume of the framework. There are several cations in these channels which are Na^+, K^+, Mg^{2+}, Ca^{2+} compensating the negative char-ges of the framework and a large number of molecules of H_2O-water. Zeolites are material-resistant to blockage of cation movement because of three dimensional structures of pores [6].

During dehydration and under the influence of an external elec-tric field, the cations in cages, which compensate the negative charges of the framework, are mobile and may move to new positions. Thus, the main purpose of this study is to investigate the influence of DC electric field and time storage on the transport property and stability of electret state of naturel zeolite (NZ) samples. Furthermore, electret properties, such as stability of electret charge, depend on the structure and phase composition, as well as condition of polarization (i.e. intensity of applied electrical field, temperature, atmosphere, etc.).

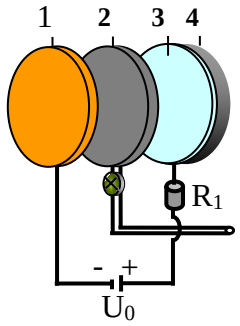

Figure 1. Schematic view of the cell: 1- Cu electrode; 2- Zeolite plate; 3- SnO_2 contact; 4- Flat glass disc.

RESULTS AND DISCUSSION

In order to have a discussion, we want to note that ions, which are the carriers of charge in the zeolite, are not capable of reaching to the metal electrode. Therefore, some authors in their works discuss the depolarization field raising in substance, with the ionic conductivity, after the influence of external electric field. For the calculation of the impact of the depolari-zation field, it is necessary to considerate the gap capacity bet-ween the border of sample and metal electrode. The results are presented in Figs 2-3.

During electret formation, polarizati-on current was measured as a function of time and temperature. In clinoptilolite plate a homocharge is formed by charges depo-sited on the surface of the ZP from the gas gap between the electrode and the specimen. The plot of resistance (R) of NZ (i.e. clinoptiloliıte CL) vs. temperature is given in Fig. 2.

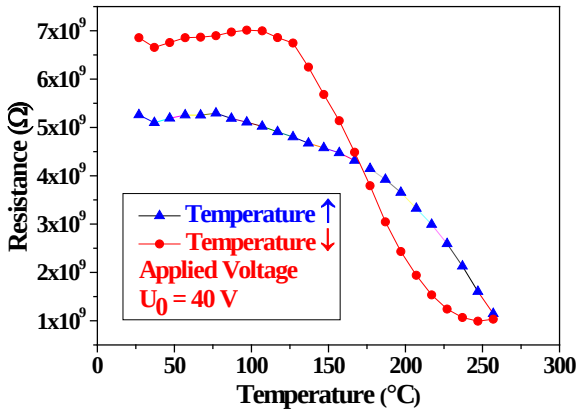

Fig. 2. Hysteresis behavior of the NZ at different temperatures.

The resistance of CL was measured in the temperature range of 27–260 ^{0}C. As may be seen from Fig. 2, at low temperatures a heterocharge is observed in the CL present in an atmosphere of air, which is converted to a homocharge with an increase in temperature. The hysteresis loop increases when NZ samples exposed to an electric field. When the applied voltage U_0 was 300 V, the corresponding widths of the hysteresis loop is maximum. The wide hysteresis windows localized nature of the surface state by charging and discharging these surface states, one can change the NZ conductivity. Long life nitrogen metastables might also play a role in the hysteresis phenome-non; this hypothesis would need a dedicated study.

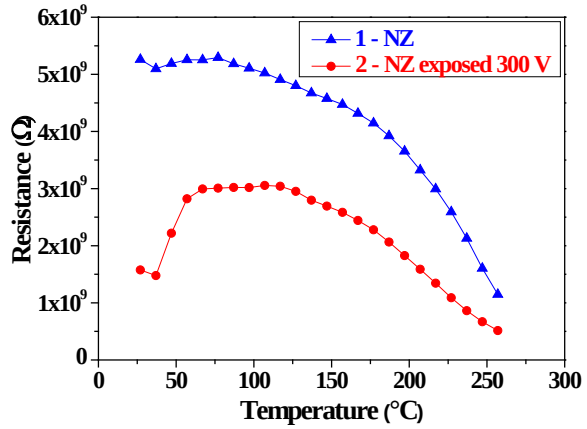

Fig. 3. The temperature dependence of resistance of the NZ.

The obtained samples were also exposed to an electric field. For this purpose they were placed in the cassette with the two push electrodes to which from dc power supply was applied up 300 V during 24 hours. After this procedure we again measured the values of resistance dielectric response across different time intervals (i.e. when an external electric field is applied through the 1 hour; after 3 days and after 5 days). The study showed that the DC electric field has influence only on the conductivity of the CL samples. When we applied external electric field (E = 2 kV.cm^{-1}) to the CL samples the resistance is decreases. Moreover, this decrease depends on the time after turning off the DC electric field.

Figure 3 shows the temperature dependence of the resistance for NZ plate after turning off the DC electric field. The curve 1 corresponds to the measurements on the sample that is not subjected to the effects of electric field and the curve 2 correspond to measurements on the sample after the field is switched off. The existence of the thermoelectret effects has been found in the system zeolite-air. The thermoelectret effects are caused by both the accumulation of charges in the specimen and the adsorption of molecules in the electric field.

In the feedback temperature, the charges captured by surface of NZ provide an important contribution to the conductivity. With the forward increment and reverse decrement temperatures, results obtained from the effect of electric field have led to the dramatic increase and expansion (U_0 = 300 V) in the hysteresis loop of NZ at atmosphere pressure for temperature range from 110 to 260 C. In the feedback temperature, a considerable decrease in conductivity with the passage of time (2 h) was not noted for temperature range from 100 to 30 ^{0}C.

In the hydrated NZ the adsorbed molecules are distributed over the external surface of crystalline particles. Thus, the relaxa-tion process can be compared with the desorption and subse-quent adsorption of molecules at the active sites on the external surface of crystalline particles of the NZ. If molecules present in the voids of the crystalline zeolite particles are responsible for polarization, then they may transfer during relaxation from some active sites to others, remaining in the voids.

CONCLUSION

The influence of thermal treatment atmosphere on the resistance and stability of electret charge of NZ was investigated. The resistance decreased from 7x10^9 to 1x10^9 Ω whiles the temperature increased from 27^{0}C to 260 ^{0}C which is associated with the ionic mobility. NZ samples remain polarized in time. The heat treatment atmosphere has an important effect on effective surface density of free charge. Atmosphere air promotes creation of oxygen defects, which have a significant role in the formation of dipole polarization,and also on the resistance and stability of electret states in NZ. During some time the transport properties is restored, which indicates on the electret behavior of clinoptilolite samples.

ACKNOWLEDGMENTS

The authors thank the Turkish Scientific and Technological Research Council of Turkey (TUBITAK) for the financial support of this work through BIDEB-2221.

NOMENCLATURE

NZ Naturel zeolite

CL Clinoptilolite

U_0 Applied voltage

E Electric field

REFERENCES

[1] M.Eguchi, On the permanent electret, Philosophical Magazine 49 (1925) 178–192.

[2] G.M. Sessler, J.E.West, Applications, in: G.M. Sessler (Ed.), Electrets, second ed., Springer-Verlag, Berlin/Heidelberg/New York/London/Paris/ Tokyo, 1987, pp. 347–453.

[3] H. Amjadi, C.-P. Franz, An electret floppy disk for digital information storage, J. Electrostatics 50 (2001) 265–277.

[4] A.N. Gubkin, G.I. Skanavi, Fabrication and behaviour of new electrets from inorganic dielectrics, Solid State Physics 22 (1958) 330–342 (in Russian).

[5] A.N. Gubkin, G.I. Skanavi, On inorganic electrets problem, Solid State Physics 3 (1961) 297–304 (in Russian).

[6] H. Jobic, Molecular motions in zeolites, Spectrochim. Acta, A 48, (1992) 293

INTERNATIONAL CONFERENCE ON ADVANCES IN SCIENCE AND ARTS ISTANBUL 2017
29 – 31 MARCH 2017, Istanbul, Turkey

ELECTROCHROMIC PROPERTIES OF NICKEL OXIDE FILM PREPARED BY SUCCESSIVE IONIC LAYER ADSORPTION AND REACTION METHOD

* **Turan Taşköprü**
Çankırı Karatekin University
Çankırı, Turkey

Evren Turan
Anadolu University
Eskişehir, Turkey

Keywords: SILAR, Electrochromism, NiO
** Corresponding author: Tel: +90(376) 218 95 00/ 8125:, Fax:+90 376 218 95 09:*
E-mail address: turanian@rocketmail.com

ABSTRACT

In this study, electrochromic NiO film was deposited on fluorine-doped tin oxide (FTO) coated glass substrates using the successive ionic layer adsorption and reaction (SILAR) method. XRD analysis revealed that the film was polycrystalline with cubic phase with (200) orientation. Raman study shows that the deposited film was almost stoichiometric with the presence of LO mode at 518 cm^{-1}. The electrochemical properties of the film were studied by cyclic voltammetry. The electrochromic reversibility was found to be 79%. The change in optical density at λ= 630 nm was 1.21.

INTRODUCTION

NiO is one of the most popular transition metal oxides having a varying band gap (3.6 - 4.0 eV) [1]. NiO has been extensively studied material as being an optically active material in electrochromic devices, gas sensors, magnetic materials, and fuel cell electrodes. The physical and chemical properties of nickel oxide nanostructures strongly depend on their size and shape. The synthesis of nanoporous NiO is in the focus to improve the specific surface area and enhance the corresponding performance [2]. To prepare NiO films, several deposition methods were studied such as sputtering, electrodeposition, thermal evaporation, chemical vapor deposition, sol-gel, chemical bath deposition, and successive ionic layer adsorption and reaction (SILAR) [3]. The SILAR method offers many advantages for the fabrication of thin films including simplicity, control of stoichiometry, cost-effectiveness, and feasibility of deposition on large-area substrates. In this study, NiO film was produced after annealing the as-deposited sample of nickel hydroxide. We have discussed the structural and the electrochemical properties of the film.

DETAILS EXPERIMENTAL

NiO film was prepared on ultrasonically cleaned FTO-coated conductive glass substrate by SILAR method. For the deposition of the film, 0.1 M nickel nitrate solution in double distilled water is used as cationic precursor. As an oxidizing agent diluted KOH is used which acts as anionic precursor. The deposition was carried out at room temperature. A SILAR cycle involves two following steps: (1) immersing the substrate in cationic precursor $Ni(NO_3)_2.6H_2O$ solution for 5 s so that the nickel ions were adsorbed on the surface of the substrate, (2) immersing the substrate in anionic precursor KOH solution for 10 s for nickel ions to react with the adsorbed OH- ions on the glass substrate resulting in the formation of nickel hydroxide. Nickel hydroxide film has produced for 5 SILAR cycles. The as-deposited films were annealed at 400ºC for two hours in air.
For the the crystal structure analysis of the films, X-ray diffractometer (Bruker D8 Advance XRD) and Raman scattering (Bruker Senterra Dispersive Raman Microscope) were used. For transmittance and the absorbance spectra of films were taken by UV–Vis spectrophotometer (UV-2550). The electrochemical measurements were done with cyclic voltammetry using three electrode cell arrangement using Electrochemical Quartz Potentiometer (CHI440B). NiO film deposited on FTO, platinum wire and Ag/AgCl electrode was used as working, counter and reference electrodes, respectively.

RESULTS AND DISCUSSION

The XRD patterns NiO film grown on FTO-coated glass substrate is shown in Fig. 1. XRD pattern shows 4 peaks corresponding face centered cubic crystal structure with diffraction peaks at (111), (200), (220), and (311) (JCSPD 47-1049). Other peaks in the pattern belong to FTO.

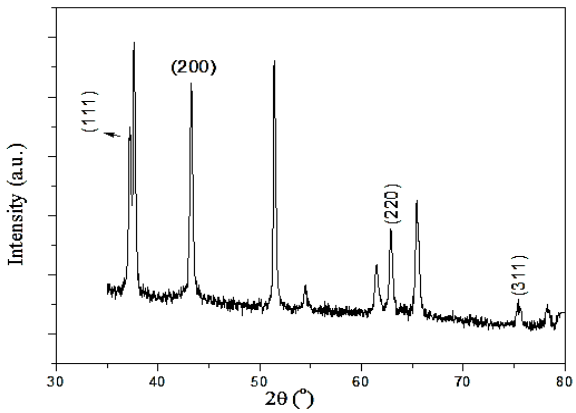

Figure 1. XRD pattern of NiO (other peaks belong to FTO)

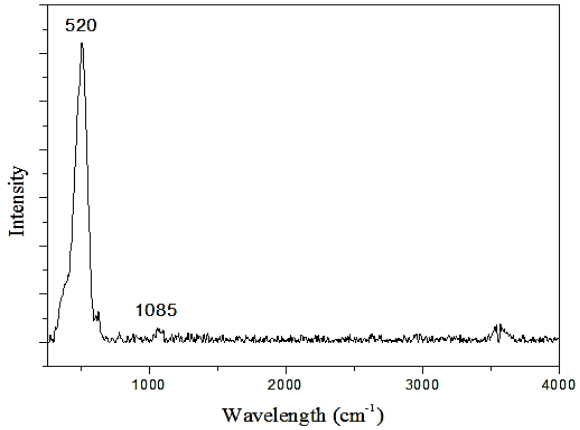

Figure 2. Raman spectrum of NiO film

Fig.2. shows the Raman spectrum for NiO film. Raman peaks located around 518 cm^{-1} and 1100 cm^{-1} could be assigned to LO and 2LO phonon modes of NiO, respectively. The LO mode at 518 cm^{-1} showed that the NiO film is almost stoichiometric [4].

For the electrochemical characterization, the standard three-electrode electrochemical cell was used. Fig. 3 shows cyclic voltammograms (CV) recorded in 0.3 M KOH electrolyte. Typical CV spectra measured during 1st, 25th, and 50thcycles between the potential range -0.6 to 1.4 V versus SCE at 100 mV/s scan rate. During the anodic potential scan, oxidation of Ni^{2+} to Ni^{3+} takes place and causes brown coloration (Fig. 4.) of the film, consequently transmittance of the film decreases

The surface of NiO particles is converted into $Ni(OH)_2$ when immersed in an electrolyte. In aqueous KOH solution, a change between NiOOH and $Ni(OH)_2$ occurs. These forms correspond to the material being colored and bleached according to the following chemical reaction [5];

$$Ni(OH)_2 \leftrightarrow NiOOH + H^+ + e^- \quad (1)$$

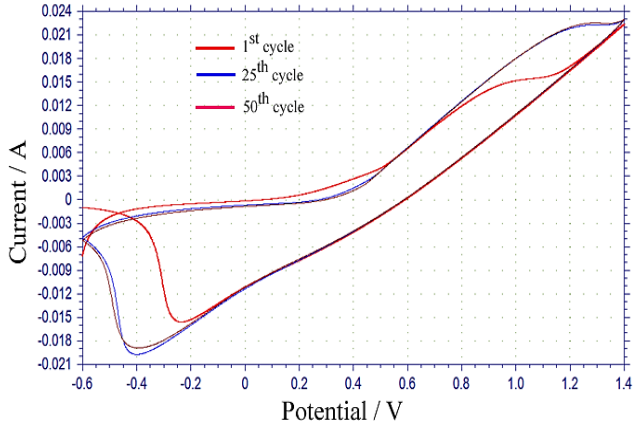

Figure 3. Voltammograms of NiO in 0.3 M KOH at a scan speed of 100 mV/s.

During the cathodic scan, bleaching of the film takes place. Coloration and bleaching of NiO film are associated with insertion and de-insertion of OH^- ions and electrons in the film.

Figure 4. Photograph of the NiO film in the colored state (Left part of photo)

The increase in the intensities of the cathodic and anodic peaks implies that in the first cycles there is a growth of the charge capacity of the film. This may be interpreted as a transformation of the nickel oxide to nickel hydroxide.

From values of a number of charges intercalated (Q_a) during oxidation (O_x) and the amount of charges deintercalated (Q_c) during reduction (R_x), electrochromic reversibility was estimated. The estimated values for reversibility of the film was given in Table 1 as a function of a number of cycles. The reversibility varies between 87 and 79%.

Table 1. Potential and charge values for anodic and cathodic peaks of NiO film.

	1st cycle		25th cycle		50th cycle	
	O_x	**R_x**	**O_x**	**R_x**	**O_x**	**R_x**
Ep	0.88	-0.25	1.07	-0.42	1.08	-0.43
Q(10^{-3} C)	3.9	-16	5.5	-11	1.5	-1.9
Qa/Qc	0.26		0.50		0.79	

The transmittance spectra of the samples in the colored and bleached states were recorded in the wavelength range of 350–1200 nm, at the room temperature as seen in Fig. 5. The change in optical density at λ= 630 nm was found to be 1.21.

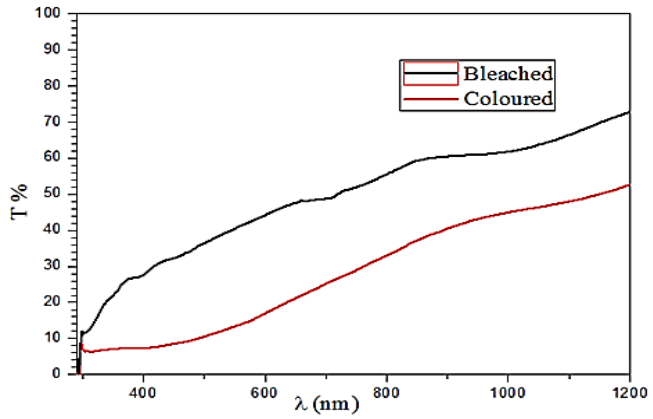

Figure 5. Transmittance spectra of the beached and the colored state of NiO film.

CONCLUSION

The electrochromic NiO film was successfully deposited by SILAR method on FTO-coated conducting glass substrate. The the structural, and electrochemical properties of the NiO film was investigated. The analysis of XRD patterns revealed that NiO has a face-centered cubic phase with (200) preferred orientation. NiO film has shown good electrochemical reversibility with %79 coulombic efficiency. The change in optical density was 1.21 at λ= 630 nm.

ACKNOWLEDGMENTS

Authors are thankful to Assoc. Prof. Ali Özcan form Anadolu University, Eskişehir, Turkey, for providing the facilities for electrochemical analysis.

REFERENCES

[1] D. Adler, J. Feinleib, Electrical and optical properties of narrow-band Materials, Phy Rev B, 2 (1970) 3112- 3134.

[2] P.C. Yu, C.M. Lampert, In-situ spectroscopic studies of electrochromic hydrated nickel oxide films, Sol. Energy Mater,19 (1989) 1-16.

[3] Taskopru, T., Bayansal, F., Sahin, B., Zor, M. (2015). Structural and optical properties of Co-doped NiO films prepared by SILAR method. Philosophical Magazine, 95,32-40.

[4] Gary,H. (2003). Chemical solution deposition of semiconductor films. Marcel Dekker Inc.

[5]Oliva P, Leonardi J, Laurent J.F, Delmas C, Braconnier J.J, Figlarz M, Fievet F., Guibert A. Review of the structure and the electrochemistry of nickel hydroxides and oxy-hydroxides. J. Power Sources 1982; 8: 229-255

INTERNATIONAL CONFERENCE ON ADVANCES IN SCIENCE AND ARTS ISTANBUL 2017
29 – 31 MARCH 2017, Istanbul, Turkey

ALTERNATIVE APPROACH TO WASTE EDIBLE OIL MANAGEMENT: BIOLUBRICANT PRODUCTION VIA GREEN PROCESSES

Bahar Gürkaya Kutluk
Department of Chemical Engineering, Kocaeli University, 41380 Kocaeli, Turkey

***Togayhan Kutluk**
Department of Chemical Engineering, Kocaeli University, 41380 Kocaeli, Turkey

Nurcan Kapucu
Department of Chemical Engineering, Kocaeli University, 41380 Kocaeli, Turkey

Keywords: Biolubricant, candida antartctica, lipase, polyol esters, trimethylolpropane ester

** Corresponding author:, Phone:,+902623033526 Fax: +902623591262*
E-mail address: togayhan.kutluk@kocaeli.edu.tr

ABSTRACT

Biolubricants (esters) are a reasonable attitude to flinch the environmental menace of petroleum based lubricants annihilation. In this work, we examined that the synthesis of biolubricants via esterification reaction between trimethylolpropane (TMP) and free fatty acids (FFAs) from waste sunflower oil (WSO). Immobilized *Candida Antarctica* (Novozyme 435) lipase was used as a biocatalyst. The effects of biocatalyst content, oil /alcohol mole fraction and reaction time on the esterification were investigated. After the experimental studies, the maximum WSO FFAs conversion was obtained 90% at 3/1 oil/alcohol molar fraction 15% biocatalyst content and 24 h reaction time.

INTRODUCTION

Biodegradable lubricants, which can be used instead of existing lubricants, have begun to attract attention due to the drastic reduction of oil resources and increased sensitivity to environment. Although its use with legal regulations is increasing, it is disadvantageous for users as price in comparison with petroleum derived products. With economic reasons and not widespread use, they are taking place in the world market with a rapid increase every year. In this sense, efforts to meet both increasing demand and new and more economical products are dominant. Considering the destruction given to nature by traditional lubricants, biofuels become even more important [1]. As a result of these investigations, it can be seen that 100% decolor lubricants can be obtained in short time in the nature and the performance can be at a level that can compete with mineral oils. 95% of biodegradable lubricants are degraded in nature in one year. The use of biodegradable lubricants is up to 2% of total lubricant use, with an annual increase of about 5-10%. The transesterification method is used in the production of many biodegradable products. In this method, the glycerol in the vegetable oil is replaced with another polyol alcohol such as trimethylolpropane, neopentyl glycol or pentaerythritol. In the production of biolubricants, mainly acid and base catalysts have been studied. Enzyme-catalyzed studies are limited in number and have been performed with free or commercial arrested lipase forms [2,3]. Biolubricants may be produced via chemical or enzymatic catalysis. Enzyme catalysis; despite more complex; affords different avdantages; reactions are selective; specific and environmentally friendly such are mild reaction temperature and low pressure[4]. Using a lipase catalysis more effective than chemical catalysis because their high activity and stability. There are limited reports on the lipases used for production of biolubricants from vaste edible oils in literature. However; most of these biolubricants synthesis studies have been undertaken with soybean; sunflower and rapeseed [5,6].Thus; based on limited knowledge in literature about enzymatic production of biolubricants ; we suggest in this paper to the enzymatic synthesis of biolubricants from WSO FFAs and TMP with immobilized lipase *Candida antarctica* lipase. Reaction conditions, such as lipase content, oil/alcohol molar ratio and reaction time were studied.

MATERIALS AND METHODS

MATERIALS

WSO with %1.4 FFA content collected from local restaurants in Kocaeli/TURKEY. *Candida Antarctica* (Novozyme 435) and *Thermomyces lanuginosus* (Lipozyme TL IM) as a gift from Novozymes Denmark. BSTFA, TMP, NaOH, phenolphthalein,

ethanol (%99), and all other chemical which were used in experimental studies were purchased from Merck.

ESTERIFICATION REACTIONS

FFAs was synthesised by hydrolysis reaction via Lipozyme TL IM (*Thermomyces lanuginosus)* catalyst. Optimum hydrolysis parameters were clearly described our previous studies [7,8]. Esterification reactions were kept in 50 mL open flasks with the 400 rpm agitation speed ,initial water content (% substrate, w/w) 1% and 40 C° temperature. Reaction time, lipase content and acid alcohol molar ratio were studied in this study.

DETERMINATION OF FFA CONTENT

Fatty acids analyses was performed that potassium hydroxide KOH titration according to the ASTM-D5555-95 standard.

RESULTS AND DISCUSSION

EFFECT OF LIPASE AMOUNT

The amount of enzyme used in enzymatic reactions is an important parameter. The use of more enzymes than necessary improves the process cost. Depending on the coagulation of the excess enzymes in the reaction media and the decrease of their activity, the yield also drops [1,9]. Failure to use the lipase in sufficient concentration will cause the conversion to be slow. The effect of the amount of enzyme (1-25)% on the esterification reaction of free fatty acids was investigated. Experiments were carried out at a temperature of 40 ºC at a molar ratio of 3/1 fatty acid / TMP Initially there is no water in the reaction media. The effect of the amount of enzyme on the esterification reaction of waste fatty acids with TMP is shown in figure 1.

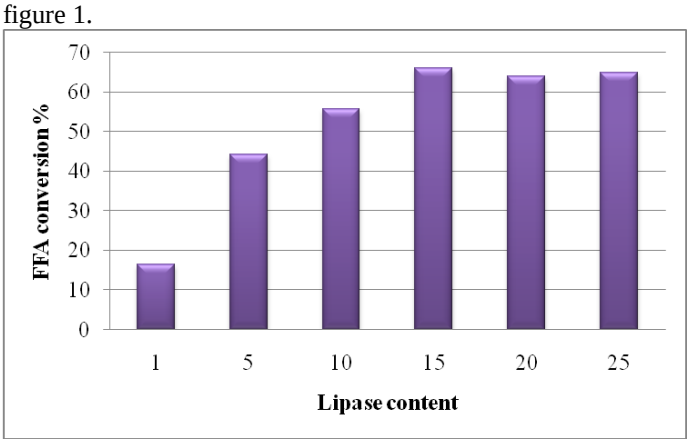

Figure 1. Effect of lipase amount on esterification of WSO FFAs

As the amount of enzyme increases, the conversion of free fatty acid increases before and then decreases. when the optimum amount of enzyme was 15%, the highest FFA conversion value(65%) was reached. The increase in the amount of enzyme also brought about the problem of mixing. Thus, the mass transfer limitations between the enzyme substrate and the free fatty acid conversion degrading effect were clearly observed.

EFFECT OF FFA/ALCOHOL MOLAR RATIO

The fatty acid / TMP molar stoichiometric ratio in the production of biolubricant from fat sites is 3/1. In this study, the effects of different amounts (3 / 1, 4 / 1, 6 / 1, 8 / 1) on the fatty acid / TMP molar ratios to biolubricant production were investigated. The reaction was carried out at 400 rpm agitation speed for 24 hours. Lipase content 15% and 40 ° C temperature The effect of the fatty acid / TMP mol ratio on esterification reaction is showed in Figure 2.

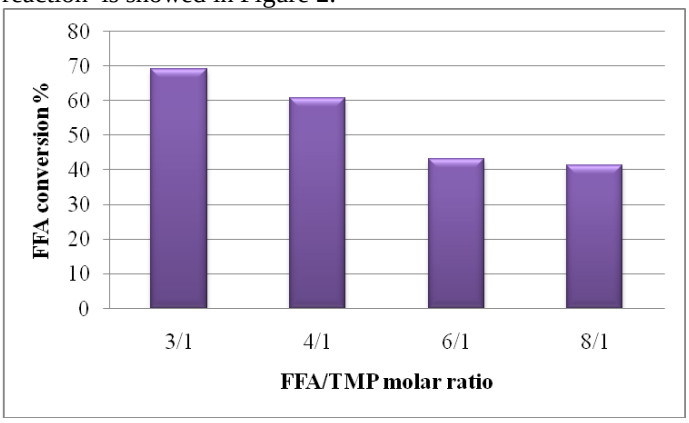

Figure 2. Effect of FFA/alcohol molar ratio on esterification of WSO FFAs

The increase in fatty acid / TMPmol ratio negatively affected the conversion of free fatty acids. The highest conversion (70%) was achieved at a molar ratio of 3/1 fatty acid / TMP. Similar results have been reported in literature [9-10]. Reaction temperature 40 ° C is insufficient for reaction. In order to increase the FFa conversion temperature was settled 60 ° C and at the end of the 24h. maximum FFa conversion (90%)was obtained.

EFFECT OF REACTION TIME

To determine the effect of the reaction time, and by taking samples at specific time intervals from the reaction medium Reaction was implemented that a mixing ratio of fatty acid / TMP of 3/1, an amount of starting water of 1% of enzyme by 15%, and a stirring speed of 400 rpm at 40 ° C.(Fig.3)

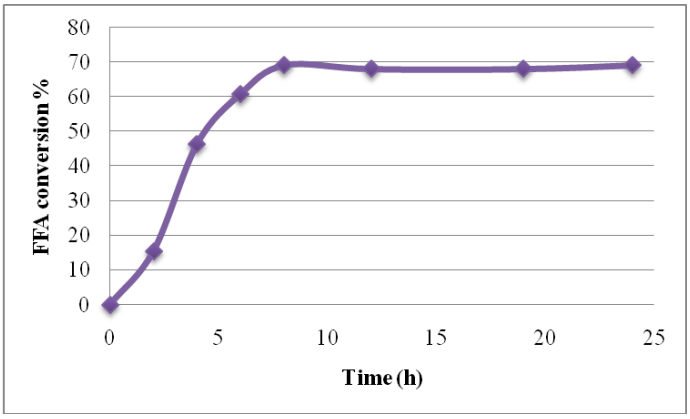

Figure 3. Effect of reaction time on esterification of WSO FFAs

It is clear from the graph that the conversion takes place in the first 12 hours. The highest free fatty acid conversion (70%) was obtained at the end of 24 h. There is no change after 12th hour. Comparable results in literature about enzymatic esterification reactions were exist [1,9,10].

CONCLUSION

Biolubricant has been successfully produced from WEO FFAs via environmentally friendly process with lipase catalyst. The paper clarifies the applicability of using enzyme catalysis are sustainable for biolubricant synthesis. In addition to this more work has to be done for optimize lipase catalyzed esterification the processes contidions and determine the mono di tri ester content in ester product which is important parameter for lubrication industry. Our investigations are still going on in our laboratory.

ACKNOWLEDGMENTS

We thank to Novo Nordisk for presenting Lipozyme TL 100L and Novozyme 435.

REFERENCES

[1] Åkerman C. O., Hagström A. E. V., Mollaahmad M. A., Karlsson S., Hatti-Kaul R., Biolubricant synthesis using immobilised lipase: Process optimisation of trimethylolpropane oleate production, Process Biochemistry, 2011, 46, 2225–2231

[2] Linko Y.-Y., Tervakangas T., Lämsä M., Linko P., Production of trimethylolpropane esters of rapeseed oil fatty acids by immobilized lipase, Biotechnology Techniques,1997, 11, 889–892.

[3] Kutluk G. B., Biyoyağlama Yağlarının Tutuklanmış Lipaz Katalizli Üretimi, Yüksek Lisans Tezi, Kocaeli Üniversitesi, Fen Bilimleri Enstitüsü, Kocaeli, 2012.

[4] Bokade V. V., Yadav G. D., Synthesis of bio-diesel and bio-lubricant by transesterification of vegetable oil with lower and higher alcohols over heteropolyacids supported by clay (K-10), Process Safety Environment Protect,2007, 85, 372–377.

[5] Syaima M.,T.S, Ong K.H., Ishenny M.,N., Zamratul M.,I.,M., Brahim S.,A., Hafizul M.,M., " The synthesisofbio-lubricant based oil byhydrolysis and non-catalytic of palm oil mill effluent (POME) using lipase", Renewable and Sustainable Energy Reviews, 44,2015,669–675.

[6] Dossat, V. Combes, D. Marty, A. Efficient lipase catalysed production of a lubricant and surfactant formulation using a continuous solvent-free process, J. Biotechnol. 97 2002, 117–124.

[7] Kutluk T., Uyar B., Kapucu N., Synthesis of trimethylolpropane ester from waste edible oil FFAs 10th international clean energy Symposium 24-26th October, İstanbul, Turkey, 2016.

[8] Karasungur N., Guler F., Kutluk T., Uyar B., Kapucu N., Atık yagdan lipaz katalizli yağ asitleri sentezi, 12.Ulusal Kimya Mühendisliği Kongresi 23-26 Ağustos, İzmir,Türkiye, 2016.

[9] Chowdhury A., Chakraborty R., Mitra D., Biswas D., " Optimization of the production parameters of octyl ester biolubricantusing Taguchi's design method and physico-chemical characterizationof the product", Industrial Crops and Products 52 2014 783– 789.

[10] Richetti, A., Leite, S.G.F., Antunes, O.A.C., Lerin, L.A.,Dallago, R.M., Emmerich, D., Luccio, M.D., Oliveira, J.V. Treichel, H., & Oliveira, D. , Assessment of process variables on 2-ethylhexyl palmitate production using Novozym 435 as catalyst in a solvent-free system, Bioproc. Biosyst. Eng., 33, 331–3, 2010.

INTERNATIONAL CONFERENCE ON ADVANCES IN SCIENCE AND ARTS ISTANBUL 2017
29 – 31 MARCH 2017, Istanbul, Turkey

EFFECT OF DIFFERENT PARAMETERS ON GROWTH MICROALGAE *CHLORELLA VARIABILIS*

Necla Altın

Department of Chemical Engineering, Kocaeli University, 41380 Kocaeli, Turkey

***Togayhan Kutluk**

Department of Chemical Engineering, Kocaeli University, 41380 Kocaeli, Turkey

Başar Uyar

Department of Chemical Engineering, Kocaeli University, 41380 Kocaeli, Turkey

Nurcan Kapucu

Department of Chemical Engineering, Kocaeli University, 41380 Kocaeli, Turkey

Keywords: Microalgae**,** *Chlorella Variabilis,* N starvation
** Corresponding author:, Phone:,+902623033526 Fax: +902623591262*
E-mail address: togayhan.kutluk@kocaeli.edu.tr

ABSTRACT

Biochemical composition of live mass in microalgae cultures is dependent on growth conditions such as environmental factors, medium, temperature, salinity, pH and light. Nitrogen sources and levels are known to be one of the most important factors affecting growth and biochemical composition in algal cultures. The effect of different Nitrogen concentrations in the nutrient medium on the development of microalgae of the species *Chlorella Variabilis* was studied in laboratory conditions. In this study, the values of nitrogen and BG11 nutrient media (1.5 g / L) were investigated by adding nitrogen to the microorganism. It was seen that it increased when growing by increasing nitrogen amount. Growth of 0.57 g / L in the absence of nitrogen, 3.62 g / L of microorganism growth at 670 hours in the nitrogen atmosphere was investigated. It was observed that KH_2PO_4 in different amounts did not significantly change the microorganism pH. The lowest pH value was 0.080 g / L KH_2PO_4 and the highest pH value was 0.020 g / L KH_2PO_4. After 525 hours, the pH remained constant at 8-10.

INTRODUCTION

Algae has been used in different areas for many years. Because of the proteins, carbohydrates, fatty acids, vitamins, minerals, pigments and many other important metabolites they accumulate in the cells, they are used for different purposes to be the main food supplements for humans. For this reason II. The world's warfare grower has benefited from the nutritional richness of microalgae in developed countries such as the United States, Japan, England, Germany and Norway. (Becker, 1994). With the search for different energy sources in the 1970's, solar energy collects on the interest of the world. Algae are living organisms that use solar energy most effectively, and for this reason, interest in microalgae production technology is increasingly being explored for the discovery of new components in different microalgae species. Microalgae, which produce the first organic substances as primary producers in sea and lakes, are consumed as antioxidants due to their valuable metabolites in the cells, as well as being evaluated as supporting food, due to their pigments, oils, fatty acids, polysaccharides and immunity. In recent years, studies on mass production have been accelerated in recent years as energy source and fertilizer to be evaluated in fields such as feedstuffs and wastewater treatment, because they can be cultivated year-round, can be cultivated in unsuitable areas, and are systems that use water and solar energy most efficiently. The first microalgae culture study in our country started with *P. tricornutum*. (Gökpınar 1980) (Gökpınar ve Durmaz, 2001).

Microalgae are able to produce oil using sunlight and carbon dioxide, but with this they multiply by hours and grow more productive than black plants because they can be produced throughout the year. These photosynthetic organisms are the resultant photosynthetic oxygen and give changes in their metabolism in response to adverse environmental conditions. Biochemical composition of live mass in microalgae cultures is dependent on growth conditions such as environmental factors, medium, temperature, salinity, pH and light. (Sukenik, 1991).

Nitrogen sources and levels are known to be one of the most important factors affecting growth and biochemical composition in algal cultures. (Xu ve ark., 2001). Nitrogen sources and concentrations affect growth of algae cultures and

biochemical composition, and in particular cause changes in fatty acid values and carotenoid content. In addition, since the nitrogen limitation is associated with cellular fatty acids and cellular growth, nitrogen restriction is effective in enriching fatty acids. The most important nitrogen sources that can be used by cells in microalgae cultures are nitrate nitrogen, ammonium nitrogen and urea nitrogen. (Gökpınar, 1991; Levasseur ve diğ., 1993; Grobbelaar., 2000). Ilman et al. Investigated the effect of incomplete nitrogen application on growth and lipid content in some species of *Chlorella* species in their studies carried out in 2000. According to this; *C. vulgaris* showed the best improvement compared to the other four species studied under both normal conditions and low nitrogen application.

Optimization of biotechnological processes is, in most of the cases, related with the establishment of optimum conditions that maximize the involved microorganism's performance. In this context, pH is one of the most important parameters in microalgal growth. In most cases microalgae prefer pH values close to 7.0, but there are staggering exceptions. For example, the optimal pH for the growth of the microalga *Dunaliella salina* is close to 11.5, while for *Dunaliella acidophila* it is between 0.0 and 3.0 (Varshney et al., 2014). The acclimation of a microalgal strain to a certain environment plays a major role in its yield. For instance, in the study of Nancucheo and Johnson (2012) two acidophilic algae, identified as strains of *Chlorella protothecoides* and Euglena mutabilis, were isolated from abandoned copper mines. When the *Chlorella* isolate was cultivated in pH-controlled bioreactors, it grew optimally at pH 2.5, even though in the study of Liang et al. (2011) the optimal pH for the growth of a *C. protothecoides* strain, cultivated under laboratory conditions was found to be 5.0. Therefore, depending on the environment where the microalga has been adapted, each strain has a unique pH range in which it can grow and function properly. An interesting effect of pH on microalgae is observed at pH higher than 9.0, where flocculation of cells takes place. . It can happen deliberately with the addition of a strong base, or spontaneously in microalgal cultures as a result of pH increase due to photosynthetic CO_2 depletion. To sum up, although pH is one of the parameters that determine the microalgal growth, it has been hard to draw a general rule for optimum pH, as it is highly dependent on the species grown and the cultivation conditions. Even in reference to a particular strain, such as *Chlorella vulgaris*, the literature is somewhat confusing. However, it is safe to say that at pH controlled cultivation conditions, the microalgae's performance is improved both in terms of growth and intracellular product formation.

In this study, it was aimed to investigate the effect of nitrogen restriction applied to the nutrient medium on microglial growth of *Chlorella variabilis* species. No such study has been found in the literature that examines the effect of *Chlorella variabilis* on microalbuminemia. In this respect, it is aimed to examine the parameters affecting the microalgae growth by determining the content of suitable medium for growing microorganisms.

MATERIALS AND METHODS

MATERIALS

Microalgae species *was donated from Dr.Turgay Çakmak* Department of Molecular Biology and Genetics of Istanbul Civilization University. Microalga growth curve Blue Green Medium (BG 11) was monitored in the nutrient medium. The chemical composition of this medium (g/L); $NaNO_3$, 1.5; KH_2PO_4, 0.04; $MgSO_4.7H2O$, 0.075; $CaCl_2.2H2O$, 0.036; H_3BO_3 0.0029; Na_2CO_3, 0.02; Fe(III)citrate, 0.006; citric acid 0.006; The chemicals used in the study are in analytical purity.

CULTIVATION

Chlorella variabilis were cultured in 650 ml-volume batch run media. Ambient temperature of cultures is set at 25 ± 2 ºC. The pH value of the medium was initially measured at 7.76. The cultures were ventilated via a compressor. The experimental setup is shown in Figure 1. Growth was monitored daily by absorbance and pH measurements at 600 nm with UV-VIS spectrophotometer in cultures grown for 14, and 20 days.

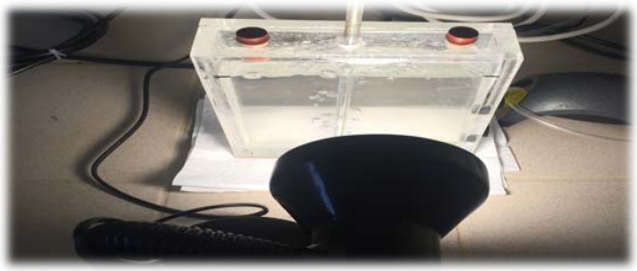

Figure 1. Experimantal setup *Chlorella variabilis* cultivation

Chlorella variabilis were cultured in 125 ml-volume batch run media. Ambient temperature of cultures is set at 25 ± 2 ºC. $NaNO_3$ (non-Nitrogen and 1.5 g/L) and KH_2PO_4 (0.005 g/L, 0.020 g/L, 0.080 g/L, and 0.160 g/L) were applied at different ratios to observe the growth of microorganisms in the cultures and growth of the cultures was observed. 200 rpm stirring was applied. The cultures were monitored daily with UV-VIS spectrophotometer at 600 nm by measuring absorbance and pH.

HARVESTING OF MICROORGANISMS

In cultures, the logarithmic phase of the universe and the monitoring of the pause phase are made according to the optical density values. Immediately after termination of the assay, a centrifuge suitable for large volumes was used and the cultures were centrifuged at 4000 rpm for 30 minutes.

DRYING PROCES OF MICROORGANISMS

The wet material in each centrifuged batch was dried in a drying cabinet.

RESULTS AND DISCUSSION

Nutrients and concentrations used in culture media with environmental conditions can cause changes in microalgae growth and microalgae biochemical structure. It affects growth as well as nutrient concentration in the nutrient medium. (Brown ve diğ., 1989). The difference in nitrogen source and concentrations is known to be effective in microalgae growth and biochemical structures. Gökpınar, 1991; Fidalgo ve diğ., 1995; Valenzuela-Espinoza ve diğ., 1999; Xu ve diğ., 2001). In the study conducted, the effect of Nitrogen limitation on the development of microalgae cultures was observed. Growing up in culture with non-Nitrogen restriction is very rare, and it is seen that this growth is caused by nitrogen from the mains water. Growth in culture with 1.5 g/L Nitrogen constraint continues at normal course and is thought to be caused by contaminants. Figure 2 shows the effects of different nitrogen stresses on microorganism growth.

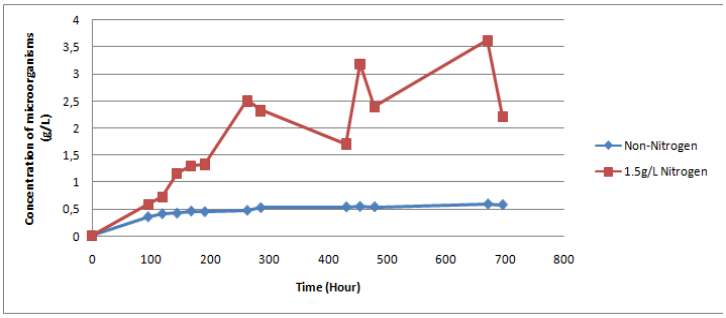

Figure 2. Effect of nitrogen stress on growth of microalgae of the species *Chlorella variabilis* in the medium prepared with water.

As can be understood from the figure, it is seen that the microorganism does not show improvement in the non-nitrogen environment and that the growth is increased by increasing the amount of nitrogen. It is thought that non-Nitrogen-restricted growth is caused by contamination from network water, and 1.5g /L nitrogen-restricted deviations are from contamination.

The effect of KH_2PO_4 (0.005g/L, 0.020g/L, 0.080g/L; and 0.160g/L) on pH was investigated at different ratios. Figure 3. results are shown.

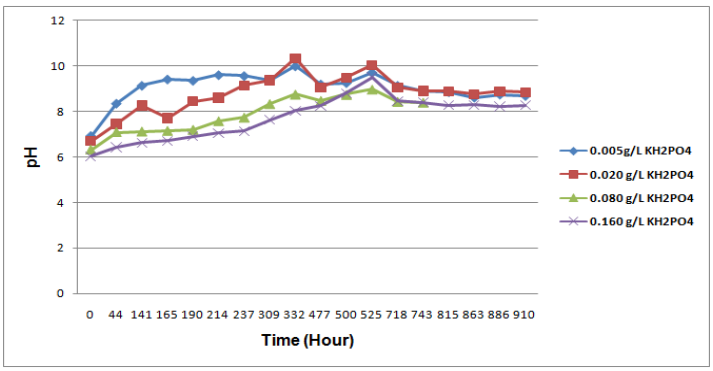

Figure 3: Effect of different proportions of KH_2PO_4 on microalgae of *Chlorella variabilis* species

As is apparent from the figure, the quantitative changes did not change significantly on the pH.

CONCLUSION

Chlorella variabilis, a freshwater microalgae, was cultured in laboratory conditions and nutritional differential treatments were applied to determine its effect on growth. In the study in the absence of nitrogen, 0.57 g / L growth was observed. On the contrary, with the fluctuating growth observed in the experiments performed in the nitrogen environment, a growth of 3.62 g / L microorganism was observed after 670 hours. The effect of KH_2PO_4 (0.005g / L, 0.020g / L, 0.080g / L; and 0.160g / L) pH on different ratios was investigated .It has been observed that the KH_2PO_4 values tested in different amounts do not show a significant change in pH values. pH up to 525 hours. After 525 hours, it remained stable at pH 8-10. The lowest pH increase occurred at 0.080 g / L KH_2PO_4 feed. The highest pH increase occurred at 0.020 g / L KH_2PO_4 feed, despite fluctuations.

REFERENCES

[1] Sakarika, M., & Kornaros, M. (2016). Effect of pH on growth and lipid accumulation kinetics of the microalga Chlorella vulgaris grown heterotrophically under sulfur limitation. Bioresource Technology, 219, 694-701.

[2] Bulut, Y.,"Chlorella'da(Chlorophyceae) Yağ Miktarının arttırma olanaklarının araştırılması", Biyoteknoloji Anabilim Dalı Yüksek Lisans Tezi, Çukurova Üniversitesi, Fen Bilimleri Enstitüsü, Adana, 2009.

[3] Uslu, L., Isik, O., & Mutlu, Y. (2012). Besleyici element kompozisyonundaki değişikliklerinin mikroalglerde lipid içeriğine etkisi /The Effects of the Changes in the Composition of Nutrient on Lipid

Content of Microalgae. Journal of FisheriesSciences. com, 6(3), 176.

[4] Durmaz, Y. (2006). Azot Kaynakları ve Konsantrasyonlarının Nannochloropsis oculata (Droop, 1955)(Eustigmatophyceae)'nın Büyüme ve Pigment Komposizyonuna Etkisi. EÜ Su Ürünleri Dergisi, 23(3-4), 295-299.

[5] Illman, A.,M., Scragg, A.,H., Shales, S.,W., Increase in Chlorella strains calorific values when grown in low nitrogen medium. Enzyme and Microbial Technology. 27: 631-635, 2000.

INTERNATIONAL CONFERENCE ON ADVANCES IN SCIENCE AND ARTS ISTANBUL 2017
29 – 31 MARCH 2017, Istanbul, Turkey

THE INFLUENCES OF FORCES DURING ELECTROSPINNING ON NANOFIBER FORMATION

Saide Başak Arıkan
Bülent Ecevit University,
Faculty of Engineering, Food Engineering Dept.
Zonguldak, Turkey

Sercan Dede
Mustafa Kemal University, Faculty of Agriculture Food Engineering Dep.
Hatay, Turkey

Filiz Altay*
Istanbul Technical University,
Chemical and Metallurgical Faculty,
Food Engineering Dept.
Istanbul, Turkey

Keywords: Electrospinning, nanofiber, electrostatic force, Coulomb force, viscoelastic force, surface tension
** Corresponding author: Phone: 212 285 6948, Fax: 212 285 7333*
E-mail address: lokumcu@itu.edu.tr

ABSTRACT

Electrospinning is the one of the nanofiber production techniques providing fibers with diameters less than 1 µm. It is an easy, simple, versatile and relatively low cost method. The affecting forces during electrospinning are electrostatic force, coulombic force, viscoelastic force, surface tension force, gravitational force and air drag force. These forces influence the formation of fibers and their properties. To tailor the functional properties of electrospun nanofibers, these forces and their effects on the electrospinning must be taken into account. In this review, therefore, these forces will be presented.

INTRODUCTION

Fibers which have less than 1 µm diameter are called as 'nanofibers'. Nanofibers can be produced by electrospinning method. Electrospinning is a novel, simple, cheap and reliable method of especially, one-dimensional nanostructure (fibers) formation (Li &Wang, 2013). The process is conducted under electric field intensity. After the polymer solution is filled in a capillary tube, it comes to the tip of the needle and takes a 'Taylor Cone' shape due to the electrical voltage. The solvent of polymer solution begins to evaporate and the fibers form in such patterns as cross-sectional shapes, beads, branches or zigzags (Reneker & Yarin, 2008; Valizadeh & Farkhani, 2014).

The patterns and the properties of the collected fibers are depended on various forces. First, the electrostatic force is main affecting force during electrospinning process. The electrostatic force comes from applied electrical field (Wannatong et al., 2004). By execution of electric field, the positive ions of feed solution move to the negatively charged electrode, and negatively charged ions of feed solution go to positively charged electrode. The distinction between the numbers of opposite ions causes excess charge (Reneker et al., 2000). With overcoming the surface tension forces of feed solution by electrostatic charges, a jet moves to the nearest electrode of opposite polarity (Deitzel et al., 2001). The process is realized under applied electrical voltage that provides surface charge on the jet resulted in differentiation on the diameter of nanofibers (Okutan et al., 2014). The composite electrostatic force can be calculated from Equation (1).

$$\Sigma F = k\lambda\lambda_0 \left[\left(2r_1/a\right)-1\right] / \left[\left(r_1/a\right)-\left(r_1^2/a^2\right)\right] \quad (1)$$

In the equation 1; k, λ, λ_0, r_1, a are constant, linear charge density of fibers, linear charge density of electrodes, distance between O and upper boundary, length of the isolated area, respectively (Zhang et al., 2008).

Another kind of the electrostatic forces affecting jets is the coulombic forces implemented by the electrical field and it is likely to be the force that affects the fiber diameter (Jarusuwannapoom et al., 2005; Garg & Bowlin, 2011; Lipol & Rahman, 2016). If this force is increased, fiber diameter decreases and the stretching of the charged jet increases (Veleirinho et al., 2008; Shahreen & Chase, 2015). The coulombic force on the fiber can be calculated by Equation (2):

$$F = k\lambda^2 / r^2 \quad (2)$$

where k, λ and r are constant, linear charge density and the distance between two interacted forces (Zhang et al. 2008).

The electrostatic and coulombic forces are depended on a number of charge carriers. With an increase in the concentration of the feed solution, an increase of a number of charge carriers results in an increase also in the electrostatic force and the Coulombic force (Jarusuwannapoom et al., 2005). These two of

them also the most responsible ones for the "Taylor Cone" shape of the droplets (Garg & Bowlin, 2011).

The third affecting force is the viscoelastic force. Viscoelastic forces provide resistance to rapid deformation of fibers occurred on the collector plate (Fong et al., 1999). Viscoelasticity is influenced by the concentration of the polymer solution, the viscosity and the molecular weight of the polymer (Wannatong et al., 2004). If the viscosity of feed solution increase, the nanofiber formation gets better in terms of beads (Fong et al., 1999).

The fourth affecting force is the surface tension. It is the conclusion of localized surface forces (Brackbill et al., 1992). These surface forces charge the jet of the polymer solution electrically and it moves to the nearest electrode of the opposite polarity. Thus, the surface tension coefficient is related with polymer and solvent. The higher surface tension resulted in the more bead formation and the smaller diameter (Fong et al., 1999; Deitzel et al., 2001; Wannatong et al., 2004).

Of the forces affect the formation of nanofibers, only the coulombic, the viscoelastic and the surface tension forces influence on bead formation, fiber diameter and/or shrinking of the jets between the needle and the collector plate (Wannatong et al., 2004; Jarusuwannapoom et al., 2005).

The fifth force is the gravitational force or body force. The gravitational force is an external force on the jet. The jet moves to the collector under the effects of gravity and electrical field (Hohman et al., 2001; Jarusuwannapoom et al., 2005). The gravity force of per unit length can be emphasized by Equation (3).

$$f_g = \rho g \pi a^2 \quad (3)$$

In the equation, ρ, g, a are the liquid density, gravity acceleration and cross-section radius (Reneker et al., 2000).

Adding the ambient conditions to the account such as temperature, humidity (both of them affect to the concentration of the feed solution) and air velocity (revealed the air drag force) in the electrospinning chamber (Huan et al., 2015). The air drag force is the last effective force on nanofiber formation that relates aerodynamic characteristics on the working conditions. Reneker et al.,(2000) revealed the air drag force for each jet length that implies the jet along its axis by Equation (4) and added that when compared to the stretchings due to the gravity and electrical forces, the jet axis of the air drag is pretty smaller. Therefore, the value of air drag force shall be ignorable due to the much higher effect of electrical forces.

$$f_a = \pi \alpha \rho_a \boldsymbol{\upsilon}^2 0.65(2\boldsymbol{\upsilon} a/\nu_a)^{-0,81} \quad (4)$$

In the equation, α, ρ_a, $\boldsymbol{\upsilon}$, ν_a are surface tension coefficient, air density, the jet velocity, kinematic viscosity of air, respectively (Reneker et al., 2000).

Xu (2009) made some mathematical analysis for electrospinning process. According to the momentum equation the velocity of jet can be calculated with Equation (5):

$$\rho(du/dt) = \nabla t + \rho f + q_e E + (\nabla E)P + F_m + F_v + F_f \quad (5)$$

where ρ, u, t, q_e, E, P, F_m , F_v and F_f are in order of density of the jet, velocity of the jet, stress tensor, electrical charge, electrical field, polarization, magnetic force, vibration force and electric force.

CONCLUSION

During electrospinning process, six basic forces have their own roles in the process for the resulted fiber formation. The electrostatic and coulumbic forces make the jets evaporate to the collector and give the conical shape of the droplets. The viscoelastic and the surface tension forces relate to the bead formation and deformation of the fiber on the collector. The gravitational and the air drag forces are the natural effects on the fiber formation. The air drag of these two are ignored due to the prominent presences of both gravitational and electrical forces.

REFERENCES

[1] Brackbill, J. U., Kothe, D. B., & Zemach, C. 1992. A continuum method for modeling surface tension. *Journal of computational physics*, *100*(2), 335-354.

[2] Deitzel, J. M., Kleinmeyer, J. D., Hirvonen, J. K., & Tan, N. B. 2001. Controlled deposition of electrospun poly (ethylene oxide) fibers. *Polymer*, *42*(19), 8163-8170

[3] Fong, H., Chun, I., & Reneker, D. H. 1999. Beaded nanofibers formed during electrospinning. *Polymer*, *40*(16), 4585-4592.

[4] Garg, K. & Bowlin, G. L. 2011. Electrospinning jets and nanofibrous structures. *Biomicrofluids*, 5, 013403-1-19. doi:10.1063/1.3567097

[5] Hohman, M. M., Shin, M., Rutledge, G., & Brenner, M. P. 2001. Electrospinning and electrically forced jets. I. Stability theory. *Physics of fluids*, *13*(8), 2201-2220.

[6] Huan, S., Liu, G., Han, G., Cheng, W., Fu, Z., Wu, Q. and Wang, Q. 2015. Effect of Experimental Parameters on Morphological, Mechanical and Hydrophobic Properties of Electrospun Polystyrene Fibers. *Materials*, *8*, 2718-2734. doi:10.3390/ma8052718

[7] Jarusuwannapoom, T., Hongrojjanawiwat, W., Jitjaicham, S., Wannatong, L., Nithitanakul, M., Pattamaprom, C., Koombhongse, P.; Rangkupan, R. & Supaphol, P. 2005. Effect of solvents on electro-spinnability of polystyrene solutions and morphological appearance of resulting electrospun polystyrene fibers. *European Polymer Journal*. 41, 409–421.

[8] Li, Z. & Wang, C. One-Dimensional Nanostructures - Electrospinning Technique and Unique Nanofibers, *Springer* Berlin Heidelberg, Berlin, Germany, 2013, pp. 1–70.

[9] Lipol, L. S. & Rahman, Md. M. 2016. Electrospinning and Electrospun Nanofibers. *World Journal of Nano Science and Engineering*, 6, 45-50. Published Online June 2016 in SciRes. http://www.scirp.org/journal/wjnse http://dx.doi.org/10.4236/wjnse.2016.62005

[10] Okutan, N., Terzi, P., & Altay, F. 2014. Affecting parameters on electrospinning process and characterization of electrospun gelatin nanofibers. *Food Hydrocolloids*, 39,19-26.

[11] Reneker, D. H., Yarin, A. L., Fong, H., & Koombhongse, S. 2000. Bending instability of electrically charged liquid jets of polymer solutions in electrospinning. *Journal of Applied physics*, *87*(9), 4531-4547.

[12] Reneker, D. H. & Yarin, A. L. 2008. Electrospinning jets and polymer nanofibers. *Polymer*, 49, 2387-2425.

[13] Shahreen, L. & Chase, G. G. 2015. Effects of Electrospinning Solution Properties on Formation of Beads in Tio2 Fibers with PdO Particles. *Journal of Engineered Fibers and Fabrics*. Volume 10, Issue 3, 136-145.

[14] Valizadeh, A., & Farkhani, S. 2014. Electrospinning and electrospun nanofibres. *IET nanobiotechnology*, *8*(2), 83-92.

[15] Veleirinho, B., Rei, M. F. & Lopes-Da-Silva, J. A. 2008. Solvent and Concentration Effects on the Properties of Electrospun Poly(ethylene terephthalate) Nanofiber Mats. *Journal of Polymer Science: Part B: Polymer Physics*, Vol. 46, 460–471.

[16] Xu, L. (2009). A mathematical model for electrospinning process under coupled field forces. *Chaos, Solitons & Fractals*, *42*(3), 1463-1465.

[17] Wannatong, L., Sirivat, A., & Supaphol, P. 2004. Effects of solvents on electrospun polymeric fibers: preliminary study on polystyrene. *Polymer International*, 53(11), 1851-1859.

[18] Zhang, J. F., Yang, D. Z., & Nie, J. (2008). Effect of electric potential and coulombic interactions on electrospinning

[19] nanofiber distribution. *Polymer International*, *57*(10), 1194-1197.

.

INTERNATIONAL CONFERENCE ON ADVANCES IN SCIENCE AND ARTS ISTANBUL 2017
29 – 31 MARCH 2017, Istanbul, Turkey

THE INVESTIGATION OF BRAND AND CONSUMER COMMUTICATION OF DIGITAL MARKETING IN TURKEY

***Derya YONDAR KARABEYOGLU**
Istanbul University
Istanbul, Turkey

Ruya SAMLI
Istanbul University
Istanbul, Turkey

Keywords:Digital Marketing, Brand Assessment, Social Media
** Corresponding author:*
E-mail address: deryayondar@gmail.com, ruyasamli@istanbul.edu.tr

ABSTRACT

In this study, the effect of digital marketing tools in Turkey and the interaction of brands with the consumer, is examined. In this concept, the definition of digital marketing is defined, the development process of digital marketing is explained briefly and the situation of digital marketing in Turkey is mentioned. Then, a questionnaire about digital marketing was conducted to analyse the users' situation and the relationship between the users of the various brands in various sectors and the relation of various campaigns with digital marketing.

INTRODUCTION

Social media and digital marketing partnerships are now a force in itself, along with ever-increasing user numbers. There is a huge technology gap between the days we communicate with mobile phones via SMS (text messaging) and the period when we make video calls over smartphones, although there is not a huge difference in time. For the unilateral advertising world like radio and television, the interactive world remains very active. They are trying to integrate marketing strategies into these platforms, which are changing every day and renewing themselves.

Web marketing, online marketing, e-marketing or internet marketing; means various products or services on the internet. Internet marketing has gained a number of different initiatives, the most important of which is that the internet can provide the most massive amounts of money to reach the cheapest, and the marketing strategies on this side changes over and over. Through the internet, companies can instantly respond to their customers and customers can also receive feedback in a serial fashion. Of course, on the other side, many of the services that come with online marketing require control and proper behaviour (this is known as online customer relationship management).

Today's brands are striving to be among the ones that are suitable for them, from social networks that are constantly renewing, especially Facebook. The first steps brands take in social networks are to increase their brand awareness. With the time past, brands came to the race to put campaigns into digital experiences that enable customers to live under the roof of their own digital marketing activities.

Contrary to what had been thought a few years ago, everyone has noticed that digital change does not just mean the adaptation of new technologies, the opening of a new sales channel, or the social media interaction. The combination of tools such as smartphones and tablets that have become indispensable parts of our lives with trends such as social media, mobile applications, cloud applications and advanced analytics competencies provide consumers with unlimited access to information that they can use while performing their daily purchasing activities. At this point, it is far beyond just building a new website or creating an e-commerce platform that is considered along with the digital change. Digital change refers to the processing of destructive technologies into the DNA of companies, and the consumers are confronted with a phenomenon

involving the improvement of the experience of everyone to the worker, supplier to the customer [1].

When we looked at the development in Turkey only in the last one year; We Are Social has received a 10% increase in the number of active internet users and active social media users since January 2015, according to international organisations. [2].

The inevitable rise of digital marketing reveals the importance of highly gained markets in the field of marketing, from purchased media. Today, everybody has their social media channels they can share their content in the way they want. The same applies to brands. This should lead to the idea of aligning digital marketing communication with the corporate image before communicating with a brand consumer.

Other digital communication channels, especially social media, which managed to settle quickly in the centre of routine life in a short period of 20 years; Inevitably brought about the change of traditional marketing. Consumers' direct communication with brands has made the use of digital marketing and social media channels for brands an indispensable one. Regardless of the geographical coverage of the globally, all brands develop digital marketing and social media strategies to take part in a few of the digital channels that fit their vision and mission. One of the most important ways to sell for brands is now a successful digital marketing and social media strategy.

Digital marketing is the name given to marketing using internet resources. It has become a very important element in today's technology age. It is possible that we can see how important digital marketing has to be, taking into account only 1 year's use of internet in Turkey, which has a steady increase in its place in the digital world. When internet usage is taken into account, 82.4% of individuals who use the internet in the first three months of 2016 have a social networking profile, send a message, 65.5% with 65.5%, searching for information about goods and services with 65.5%, and sharing information with other people, while sharing content, watching videos from sharing sites with 74.5%, reading online news, newspapers or magazines with 69.5% Followed by internet listening (web radio) with 63.7%. While the users in Turkey spend 4.2 hours per day on desktop computers, it is known that they spend 2.6 hours on their mobile devices.

It is observed that in digital marketing, brands have two main purposes: to gain respect for the brand; to win the love of the consumer.

Digital marketing has two major advantages if you do not consider it a potential to have billions of users on the internet:

1) Ability to target your target audience:
When the target audience is identified, it is possible to reach and interact with them using the internet tools. This is a feature not found in traditional marketing. It is not possible to run an advertisement in a printed newspaper advertisement such as "Show it only to occupational doctors". However, sites such as Linkedin can be limited by occupational groups. If the target audience is housewives, it is possible to achieve the advertisement by putting contents on the website for them.

2) Measurable access to actions and targets:
In a market, any customer can pick up a product and then put it back in place without thinking that it is not suitable for him. Nobody knows about this. However, in the virtual world, every move of the visitor can be recorded. Which pages did it open? Which products looked more often? Which linkage did you click on? According to this information, information can be obtained to make more sales by knowing what the visitor thinks and what they are interested in. Here, the great power of measurement is revealed [3].

Facebook is the most used social network in Turkey with 32% of the world. Followed by Facebook with 17%, Instagram with 16%, Google Plus with 15% and Linkedin with 9% [4].

It is called a virtual authentication social network, in which people define themselves on the internet and

communicate with other people, and at the same time symbols that represent a number of movements in normal social life [5]. "Some of them are connected nature, some succeed in building connections, others are not confident they are not still connected," says Strategy Business Magazine's "Network Theory's New Math." Everyone is connected by social networks. Each individual is a node or centre in the social network of another person. Much of the quality of our experience is influenced by the quality of our social networks. Our standard of living depends on the standards of our social networks. "We form our social networks, and then our social networks shape us" [6], suggesting that Marshall McLuhan's "Global Village"

According to the report prepared by the Global Web Index data, 3,419 billion people are connected to the internet in the world, 2,307 billion users are actively involved in social media. It is also known that 3,790 billion mobile device users use social media over mobile devices for 1,968 billion [7].

Accordingly, social media is seen as a link that strengthens communication between people. It is observed that in digital marketing, brands have two main purposes: to gain respect for the brand; to win the love of the consumer. In digital marketing as well as in traditional marketing, the most desirable brands are to increase their sales and at the same time to increase the consumer's love for the brand.

Taking this into consideration, marketers are developing new digital marketing strategies that are highly transparent to the digital world. A communication language that empowers emotions and experiences and uses brand communication as the only basis for communication will help motivate consumers and interact with brands in the way markets want. When all these are taken into consideration, it is necessary to determine the right contents to communicate directly with the target group and deliver them to the consumer. The content created should create a conversation with the consumer and the communication of the conversation with the brand should be carried out on all channels in a similar way.

The first names that come to mind when Social Media Marketing is said are Facebook and Twitter. Facebook ads, pages, groups and applications are the marketing methods that Facebook offers in its own right. Nevertheless, thanks to Facebook's application-enabling structure, applications can become an important feature that makes a difference in terms of companies. Facebook has become an area where the advertising industry can not ignore, with the ability to create fan pages for brands and companies within the site, to publish ads on the page according to users' profile information, and to be a very suitable medium for viral campaigns. Facebook provides users with the opportunity to advertise the information to their target audience by sharing their information with advertisers via Facebook ads service. Small-budget businesses, where advertising costs are lower than traditional media tools, can also reach their target audience on Facebook [8].

With this study, we will focus on the relationship of brands with consumers in digital marketing in our country which has developed rapidly in digital marketing field. Positive or negative examples of brand and consumer communications will take place over other digital communication channels, especially social media channels.

At the same time, the introduction of these types of communication and the examples of the momentum of digital marketing of changing marketing will be given. The efficiency of marketing through digital platforms and evaluation of consumer behaviour will be tried to be done. The communication between the consumer and the brand through digital channels and the effect of this communication on consumer behaviour in the purchasing process will be examined.

RESULTS AND DISCUSSION

In Turkey, both digital platforms and social media can be used for marketing purposes. It was determined that Turkey's digital marketing awareness is high because of the questionnaire containing 22 questions and 229 participants. Survey questions can be grouped into demographic characteristics (sex, age

range, education status), job information (working status and occupational information), daily internet usage frequency, social media information and online shopping information.

Some findings from the questionnaire are as follows: 40,09% of the consumers who participated in the survey stated that they spend 3-5 hours on the internet and 30,63% of them have 6-11 hours. 16.67% of the consumers remained connected to the Internet for 1-2 hours, while the rate of 12 hours and over remained 12.61%.

96.94% of the users participating in the survey are accessing social media accounts from their smartphones while 46.72% are accessing from computers. While 4.80% have pointed to the other answer.

39.91% of the respondents indicated that they were shopping over the internet in the last month. The percentage of shoppers who shopped in the last week was 37.61%, while 22.48% said they shopped online over the past year.

While 56.14% of the respondents said that they were affected by social media during the buying process, 43.86% said they were not affected.

While 60.18% of the consumers who participated in the survey thought that they would not buy products from the social media platforms, the share of imports was 39.18%.

Per a survey conducted in 2013, Turkey was 6. in the world about usage of Facebook; 11. About usage of Twitter; 14. about Youtube and 20. about Pinterest. These results show how much the users in Turkey consider social media. Per Euromonitor's report, Technology, Communications and Media in Turkey, Facebook was the most visited website in Turkey in 2012. Following Facebook in order; it comes from Google, Youtube and Twitter. The bank used by 80% of the approximately 29 million Facebook users in Turkey is likely to follow the graduated school, the brands they like, the mobile operator they use, and many pages that are integrated into their lives [9].

There is a need for a medium for social media to exist as well as traditional media. We can call these invitations as social media tools in general. These tools, where different technologies and different methods are used, are perhaps the only common point to provide top-level sharing services for all users. We can list these tools as: wikis, social networks, blogs, social management sites, content sharing sites, microblogging and life stream [10].

Users using the social media platform have made social media a viable way to create marketing activities by sharing real information about themselves, such as where they live, their personal characteristics, financial situation, interests, age, gender, profession. In line with this information, the diversity of marketing activities that can be carried out in social media is numerous, and it is not only marketing based on advertising but also many different methods [11].

CONCLUSION

In this study, various data related to digital marketing were obtained in Turkey. For this purpose, a questionnaire consisting of various questions was applied to 229 people from various age and occupation groups and the results were analysed. As a result, it is clear that digital marketing is developing in Turkey; There are consequences as everyone adopts, regardless of age group and profession group.

All digital marketing channels, especially social media, have very serious effects on consumers. As stated in this study, there is a great effect on the consumers as well as the digitalization of the traditional marketing with the internet. When digital marketing and social media channels are used correctly, they provide important services for consumers. Although social media channels in Turkey are not yet very effective channels for sales, they seem to be the biggest channel for your near future.

REFERENCES

[1] Digital Exchange CEO Glance Report on Turkey Deloitte, 2016.

[2] Booz Allen Hamilton, Network Theory's New Math, Strategy Business, 2003.

[3] Ertan Kayalar: Digital Marketing Book: Part 1.

[4] GlobalWebIndex, 2015

[5] Vikipedia- (Kasım 2016). https://tr.wikipedia.org/wiki/Sosyal_a%C4%9F

[6] Booz Allen Hamilton, Network Theory's New Math, Strategy Business, 2003.

[7] Internet and Social Media Usage Statistics 2016

[8] Altındal, 2013: 1149

[9] Deloitte Social Media Banking

[10] Murat Kahraman (Eylül 2014) Sosyal Media 101 2.0. İstabul: Kapital Media.

[11] Society for new Communications Research: New Media, New Influencers and Implications For Public Relations, S. 16

INTERNATIONAL CONFERENCE ON ADVANCES IN SCIENCE AND ARTS ISTANBUL 2017
29 – 31 MARCH 2017, Istanbul, Turkey

GAMMA IRRADIATION AND ITS TEXTILE APPLICATIONS

Ece Kalayci
Pamukkale University Textile Engineering Department
Denizli, Turkey

***Arzu Yavas**
Pamukkale University Textile Engineering Department
Denizli, Turkey

Ozan Avinc
Pamukkale University Textile Engineering Department
Denizli, Turkey

Ali Nurdogan Koroglu
Pamukkale University Textile Engineering Department
Denizli, Turkey

Melek Gundogan
Pamukkale University Buldan Vocational Training School, Fashion and Design Department, 20070, Denizli, Turkey

Keywords: gamma irradiation, gamma ray, surface modification, textile
** Corresponding author: E-mail address: aozerdem@pau.edu.tr*

ABSTRACT

Radiation treatments are increasingly being used for adding value in coloration, antifielding, printing and coating of textile materials and gamma ray is one of the promising surface modification methods especially for textile applications. Gama rays have the smallest wavelengths and the highest energy levels (above 100 keV and wavelength less than 10 picometers) in the electromagnetic spectrum. These waves which are generated by radioactive atoms and nuclear explosions can be used for various purposes in textile treatments. In this paper, gamma irradiation and its textile applications were explored and reviewed.

INTRODUCTION

Physical and chemical surface modifications are promising applications for textile industry. Recently, scientists and researchers have been focused on quality enhancement for textile materials by using such new generation modification methods. Particularly, textile materials lately are being used as functional/technical textiles with an increasing quantity day by day. Exceptional properties may be required from textile materials for their special applications and surface modifications may lead to textile materials for gaining different qualifications.

Radiation treatments such as plasma, gamma irradiation, etc. are increasingly used for adding value to textile materials. These irradiation processes have some commercial applications in various fields for instance in the metal coating, effluent decolorization, printing, wood finishing, and textile finishing.

GAMMA RAYS AND GAMMA IRRIDATION

Gama rays have the smallest wavelengths and the highest energy (above 100 keV and wavelength less than 10 picometers) in the electromagnetic spectrum. This energy normally come from the spontaneous disintegration of radionuclides. Cobalt-60 is the radionuclide which is generally used for the gamma irradiation processes. Gamma rays are produced by neutron bombardment in a nuclear reactor of the metal cobalt-59. After that, it is encapsulated in a stainless steel tank (pencils) to prevent any leakage during its use in a radiation plant [1].

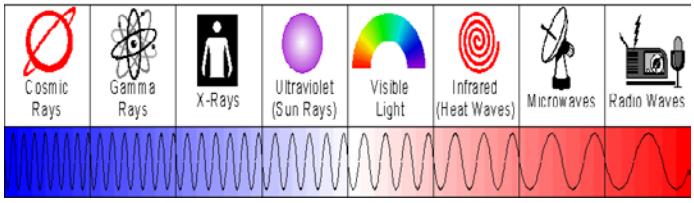

Figure 1: The electromagnetic spectrum [2]

Gamma irradiation technology has been used for many years in different areas and it is widely used for sterilization processes and radiation treatments of cancer disease.

Radioactive substances are be able to emit gamma rays all the time. Gamma ray source is needed to be stored in a pool of water which absorbs the radiation harmlessly and completely, when it is not in use. In order to gamma irradiation process, gamma ray source is pulled out of the water into a chamber with massive concrete walls that keep any rays from escaping. Material/product which is brought into the chamber are exposed to the gamma rays for a defined period of time for gamma

irradiation process. After process, gamma ray source is returned to the water pool.

Gamma rays are able to pass through different dense materials, including human tissue. Lead is commonly used as shielding to slow or stop gamma photons as a result of its dense character [1].

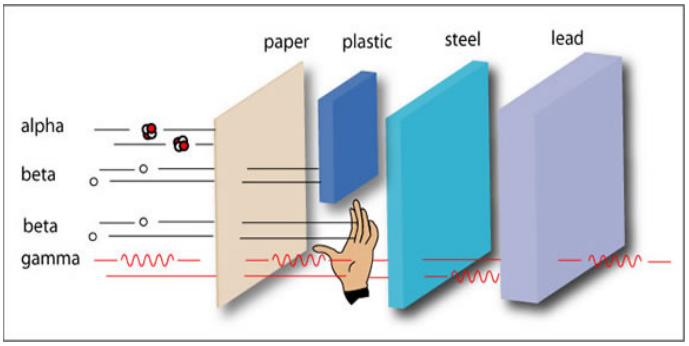

Figure 2: Gamma rays are able to pass through different dense materials [1]

GAMMA IRRIDATION IN TEXTILE APPLICATIONS

Researchers have been focused on the surface modifications and adding functional properties or structures to the material by using surface modification for many years. The excellent mechanical properties, heat and oxidation resistance, and environmental stabilities can be obtained with radioactive irradiations. Gamma irradiation, a kind of radioactive irradiation, is a simple, green, and versatile novel technique [3].

Recently, gamma irradiation has been started to be used in textile industry and it is becoming more important day by day for the future of textile industry especially for textile finishing processes. In this study, gamma irradiation usage in textile processes was explored and reviewed. Gamma irradiation is an easy method to obtain evenly functionalized fabric surface. It was reported that gamma irradiation process is more uniforme than traditional electrochemical methods [3]. Blouin and Arthur (1960) explained that gamma irradiation penetration power at oxygen atmosphere results in unique oxidative degradation in the cellulose molecules of cotton fiber compared to ordinary chemical oxidations [4].

Improvement of hydrophilic character

Surface modifications are generally applied to synthetic fiber in order to improve their hydrophilic character. For this reason, gamma irradiation is usually applied on the synthetic fibers for enhancing their water absorption capacity. However, not only synthetic fibers but also many natural fibers may be applied to gamma irradiation for better hydrophilic properties. Particularly, gamma irradiation has a great importance for reinforced composite materials which are required superior features.

Improvement of dyeability

Dyeability or printability is a character directly depending on the relationship between textile material and dye. Even though, cellulosic textile materials can be easily dyed, it is possible to increase their dyeability/ printability with gamma irradiation. Gamma irradiation pretreatment application on cellulosic fabric led to darker shades with deeper colors. Bhatti et. Al. (2010) investigated the influences of gamma irradiation on the natural dyed cotton fabrics' color strength and fastness properties and it is reported that gamma irradiation improved the color strength and fastness properties of cotton fabric while minimizing the mordant concentration [5]. Naz and Bhatti (2011) expressed that gamma irradiation had a potential to enhance fastness properties (washing, light and rub fastness) and natural dyeability (eucalyptus bark powder) of cotton fibers [6].

Gamma irradiation can be used for dyeability enhancement for textile materials with surface modification. Especially synthetic textile materials face difficulties during dyeing processes. For this reason, this situation has been investigated by many researchers in order to find an optimum ecofriendly solution. Zodhy (2005) reported that it was possible to enhance dyeability of polyester fabric for disperse dyes without effecting the chemical and physical properties of polyester fabrics [7].

Zahid et Al. (2016) investigated effects of gamma radiation on the cotton fabric and compared the dyeability of gamma irradiated fabric with that of chemically mercerized fabric using reactive dye. It was stated that gamma irradiated cotton fabric has high color strength at 60 °C while dyeing for 40 min. It was also stated both mercerization and irradiation treatments increased the surface area of cotton fibers that substantially elevated the dyeing performance and fastness properties [8].

Textile waste water

Waste water has been a serious problem for textile industry from the ecological point of view. Waste water released by wet-processing textile companies generally contains toxic residues and/or non-degradable dyes. These hazardous substances are required to be removed from waste water for more sustainable and ecofriendly textile production [9]. Gamma irradiation is an alternative method for cleaning textile waste water [10-14].

Gamma irradiation provides approximately 76–80% reduction in chemical oxygen demand (COD) of reactive dye solutions [10]. Also, Gamma irradiation caused higher removal of organic pollutant when gamma irradiation dose was increased [14].

Textile waste water which is released during scouring and bleaching processes in the textile pretreatment applications may applied to gamma irradiation. Bhuiyan et. Al. (2014) investigated gamma irradiation of scouring and bleaching waste water. Moreover, reuse performance of textile wastewater after gamma irradiation had been investigated. It was reported that gamma irradiated waste water can be used for the scouring and bleaching of textile materials with acceptable whiteness degrees [15].

Sterilization processes of textile materials

Sterilization processes have vital importance especially for surgeries and medical issues. It is known that many textile materials can be used during surgery as medical textiles and these textile materials are needed to be sterilized as well as their biocompatible characters. Gamma irradiation can be used for medical device sterilization and this sterilization process sometimes may cause differences in the structure or the properties of the materials. Ferraira et Al. (2002) reported that gamma irradiation applications resulted in degradation on medical textile materials therefore their mechanical properties have changed [16].

Gamma irradiation treatment is one of the popular sterilization methods for medical textile materials. Sterilization can also be achieved with heat, chemicals and electron radiation [17]. Gamma-irradiation can be combined with various other treatments such as alkali treatment, cationization for modification of textile materials. [7, 18].

CONCLUSION

Gama rays which are generated by radioactive atoms and nuclear explosions have the smallest wavelengths and the highest energy. These waves can be used for various purposes in textile treatments such as surface modification, waste water cleaning, sterilization, improvement of hydrophilic properties and improvement of dyeability. Gamma irradiation has a great potential for the future textile applications.

REFERENCES

[1]<http://www.arpansa.gov.au/RadiationProtection/Basics/gamma.cfm>, (accessed March.2017).

[2] The Food irradiation process. <https://uw-food-irradiation.engr.wisc.edu/Process.html>, (accessed March.2017).

[3] S. Shahidi, J. Wiener, Radiation Effects in Textile Materials, in: W.A. Monteiro (Ed.), Radiation Effects in Materials, INTECH Open Access Publisher2016.

[4] F.A. Blouin, J. Arthur Jr, Degradation of cotton in an oxygen atmosphere by gamma radiation, Journal of Chemical and Engineering Data (US) 5 (1960).

[5] I.A. Bhatti, S. Adeel, M.A. Jamal, M. Safdar, M. Abbas, Influence of gamma radiation on the colour strength and fastness properties of fabric using turmeric (Curcuma longa L.) as natural dye, Radiation Physics and Chemistry 79(5) (2010) 622-625.

[6] S. Naz, I.A. Bhatti, Dyeing properties of cotton fabric using un-irradiated and gamma irradiated extracts of Eucalyptus camaldulensis bark powder, Indian Journal of Fiber & Textile Research 36(132-136) (2011).

[7] M.H. Zohdy, Cationization and gamma irradiation effects on the dyeability of polyester fabric towards disperse dyes, Radiation Physics and Chemistry 73(2) (2005) 101-110.

[8] M. Zahid, I.A. Bhatti, S. Adeel, S. Saba, Modification of cotton fabric for textile dyeing: industrial mercerization versus gamma irradiation, The Journal of The Textile Institute (2016) 1-7.

[9] D. Şolpan, O. Güven, E. Takács, L. Wojnárovits, K. Dajka, High-energy irradiation treatment of aqueous solutions of azo dyes: steady-state gamma radiolysis experiments, Radiation Physics and Chemistry 67(3–4) (2003) 531-534.

[10] D. Şolpan, O. Güven, Decoloration and degradation of some textile dyes by gamma irradiation, Radiation Physics and Chemistry 65(4–5) (2002) 549-558.

[11] M.A. Khalaf, Biosorption of reactive dye from textile wastewater by non-viable biomass of Aspergillus niger and Spirogyra sp, Bioresource Technology 99(14) (2008) 6631-6634.

[12] L.A.W. Abdou, O.A. Hakeim, M.S. Mahmoud, A.M. El-Naggar, Comparative study between the efficiency of electron beam and gamma irradiation for treatment of dye solutions, Chemical Engineering Journal 168(2) (2011) 752-758.

[13] H. Jo, S. Lee, H. Kim, E. Park, J. Kim, H. Chung, J. Jung, Modification of textile wastewater treatment system by gamma-irradiation, Journal of Industrial and Engineering Chemistry-Seoul- 12(4) (2006) 615.

[14] S. Selambakkannu, K.A. Bakar, T.M. Ting, J. Sharif, K.Z. Dahlan, Effect of gamma irradiation on textile waste water, J. Nucl. Relat. Technol. 8 (2010) 21-25.

[15] M.R. Bhuiyan, M.M. Rahman, A. Shaid, M. Khan, Application of gamma irradiated textile wastewater for the pretreatment of cotton fabric, Environment and Ecology Research 2(3) (2014) 149-152.

[16] L. Ferreira, M. Casimiro, C. Oliveira, M.C. Silva, M.M. Abreu, A. Coelho, Thermal analysis evaluation of mechanical properties changes promoted by gamma radiation on surgical polymeric textiles, Nuclear Instruments and Methods in Physics Research Section B: Beam Interactions with Materials and Atoms 191(1) (2002) 675-679.

[17] Y. Qin, Medical Textile Materials, Woodhead Publishing, Cambridge, 2016.

[18] E. Takács, L. Wojnárovits, C. Földváry, P. Hargittai, J. Borsa, I. Sajó, Effect of combined gamma-irradiation and alkali treatment on cotton–cellulose, Radiation Physics and Chemistry 57(3–6) (2000) 399-403.

INTERNATIONAL CONFERENCE ON ADVANCES IN SCIENCE AND ARTS ISTANBUL 2017
29 – 31 MARCH 2017, Istanbul, Turkey

THE EFFECTS OF PECTINASE ENZYME TREATMENT ON THE HYDROPHILICITY PROPERTIES OF PINEAPPLE FABRICS

Ece Kalayci
Pamukkale University Textile Engineering Department
Denizli, Turkey

Arzu Yavas
Pamukkale University Textile Engineering Department
Denizli, Turkey

***Ozan Avinc**
Pamukkale University Textile Engineering Department
Denizli, Turkey

Melek Gundogan
Pamukkale University Buldan Vocational Training School, Fashion and Design Department, 20070,
Denizli, Turkey

Keywords: pineapple fiber, natural fiber, pectinase enzyme, absorption capacity, hyrdrophilization
** Corresponding author: E-mail address: oavinc@pau.edu.tr*

ABSTRACT

Environmental bell rings for danger about the world future sustainability. Every people in the world has an important role for sharing today's resources with future generations so the usage of eco-friendly materials and production methods are becoming more and more important for sustainable future. Pineapple fiber is a natural fiber which is extracted from pineapple plant leaves. Leaves are generally obtained as agricultural wastes during pineapple fruit planting. Pineapple fibers that are used as textile materials are treated with various chemicals during textile production processes. Enzymes generally can be effectively used as an alternative to chemicals in the textile wet processes. Pectinase enzymes are commonly used for enzymatic scouring applications of cellulosic textile fibers instead of alkaline treatment. In this study, pineapple fabrics were treated with pectinase enzymes and then absorption capacities, whiteness and yellowness indexes of pineapple fabrics were evaluated in comparison with alkaline treated control fabric sample. According to obtained results, the absorption capacities of pectinase enzyme treated pineapple fabrics were mostly higher than that of alkaline treated pineapple fabric sample. On the other hand, pectinase enzyme treated pineapple fabrics were measured as more yellowish and less white compared with alkaline treated pineapple fabric. Pectinase enzymes can be recommended instead of alkaline chemicals for hydrophilicity enhancement on pineapple fabrics but with yellower appearance.

INTRODUCTION

Sustainability is becoming more and more important day by day. Every people in the world has the same responsibility and this responsibility is to ensure today's resources to reach for future generations. Today, unfortunately there is no optimistic scene for our future due to some serious environmental problems such as global warming, climate change, decline in resources, the wrong usage of our sources, etc. For this reason, environmentally friendly materials and production methods are getting more valuable for industrial areas. Products from renewable resources, especially agro-waste and lignocellulosic materials has gained importance due to sustainability and renewability [1-3]. Researchers has been focused on developing sustainable, biodegradable, eco-friendly new materials. At this point pineapple fiber is a promising material which is extracted from pineapple leaves and every year tones of pineapple leaves emerge as agro-waste during pineapple fruit farming [4, 5].

Pineapple fiber is a less known natural lignocellulosic fiber. It is cultivated in tropic and sub-tropic countries mostly for its exotic fruit [4, 6, 7]. Even it is so popular and worthy as a textile material especially in Philippines, there is a limited usage of pineapple fiber in other world regions. Lately, researchers have been focused on its availability and usability in composites since natural composites become important. According to the

studies, pineapple fibers contain 70-82% cellulose, 16-22,2% hemicellulose, 5-13% lignin, 2,5-3,5% wax and others and also of course these amounts are related to climate conditions, soil, age of plant and harvesting time [6, 8].

Eco-friendly productions and methods are essential as much as environmentally friendly materials. Chemical agents are frequently used during textile wet processing and there is a serious water and energy consumption during these processes. The usage of biological substances instead can save water and energy.

Enzymes have been used for centuries in industrial applications [9]. Pectinase enzymes are a complex group of enzymes and they are capable of removing impurities from natural cellulosic fibers. Pectin and pectic substances are complex polysaccharides that are mainly located in the plant cell walls [10, 11]. Natural cellulosic fibers possess some other impurities such as protein and wax. Pectinase enzymes are capable to hydrolase these pectins, pectic substances and other components. Therefore, they can be utilized for retting, degumming and pretreatment applications. It is reported that pectinase enzyme treated cotton fabric exhibited soft handle and enhanced hyrophilicity [11]. Also, it is more safe and eco-friendly when compared with alkali chemicals [9, 11, 12].

MATERIAL METOD

Natural cellulosic fibers usually contain some substances (pectin, lignin, protein and vax,) that reduce the hydrophilicity of fibers and pineapple fiber, as a natural cellulosic fiber, contains some impurities reducing water absorption. For this reason, some pre-treatment applications are general applied in order to enhance the hydrophilicity of pineapple fibers. In this study, 100% natural pineapple fiber woven fabric was utilized. The weight of woven pineapple fabric was 32.06 g/m^2. Conventional alkaline treatment with sodium hydroxide was carried out as a control process for comparison with pectinase enzyme applications. Pineapple fabric sample was treated with 1 ml/l nonionic surfactant and 2% (owf) NaOH at 90^{o}C for 30 minutes with a liquor ratio of 1:40. Then sample washed at 80^{o}C for 2 minutes and at 40^{o}C for 5 minutes, respectively. Afterwards, the sample was subjected to cold washing.

Two different commercial available pectinase enzymes were used and application duration, temperature, and concentration were determined as it was recommended in commercial applications according to the producers' suggestions. These enzymes will be expressed as "pectinase A" and "pectinase B" in the study. "pectinase A" treatments (0.5%, 2% and 4%, owf) were carried out at 55^{o}C and pH 8 for 20 minutes with 1 g/l non-ionic surfactant following rinsing at 55^{o}C for 10 minutes in order to deactivate the pectinase enzymes. "pectinase B" treatments (0.2%, 0.4% and 1%, owf) were carried out at 55^{o}C and pH 8 for 30 minutes with 1 g/l non-ionic wetting agent and 1 g/l sequestering agent followed by final rinsing at 90^{o}C for 30 minutes in order to again deactivate pectinase enzymes. All samples then washed successively at 80^{o}C for 2 minutes and at 40^{o}C for 5 minutes and finally with cold water.

Ultimately, color properties and absorption capacities of treated pineapple fabrics were analyzed. Absorption capacity was measured according to EDANA 10.3.99 Standard [13]. Whiteness and yellowness indexes were measured using a DataColor 600 spectrophotometer (DataColor International, Lawrenceville, NJ, USA).

RESULTS AND DISCUSSION

Colorimetric properties

Colorimetric properties (whiteness degrees, yellowness index and lightness values) of pineapple fabrics are given at Table 1 and Figure 2. Both alkali treatment and pectinase enzyme treatment resulted in slightly yellower leading to less white appearance. As also reported earlier, degradation of chlorophylls, pigments and lignin in the cellulosic fiber structure with alkali solution could cause such yellowing effect. Both studied pectinase enzymes caused more yellowing effect than alkali treatment. In the samples treated with pectinase A, yellowness slightly increased in relation to the increase on enzyme concentration, whereas yellowness levels of pineapple fabric treated with pectinase B slightly reduced with again an increase on enzyme concentration. However, yellowness index of 1% pectinase b enzyme treated fabric was higher than that of untreated pineapple fabric.

Absorption Capacity

Absorption capacities of pineapple fabrics are given at Table 2 and Figure 3. Alkali treatment and pectinase enzyme treatments were effective for water absorption capacity increment on cellulosic fibers. These applications ensure decomposition of impurities which cause lower hydrophilic character leading to hydrophilicity improvement. Absorption capacities of pineapple fabrics treated with pectinase enzymes were higher than that of alkali treated sample. Both pectinase enzymes increased the hydrophilicity of pineapple fabric with fairly similar values. It is observed that absorption capacity of alkali treated pineapple fabric increased with the subsequent enzyme treatment.

Table 1: Color properties of pectinase enzyme treated pineapple fabrics

	Pectinase A treated			Pectinase B treated		
	Whiteness Index (Stendsby)					
	% 0.5 Enzyme	% 2 Enzyme	% 4 Enzyme	% 0.2 Enzyme	% 0.4 Enzyme	% 1 Enzyme
Non-treated	39.74	39.74	39.74	39.74	39.74	39.74
Alkali treated	38.48	38.48	38.48	38.48	38.48	38.48
Pectinase treated	34.85	34.29	32.33	35.8	36.66	37.33
Alkali + Enzyme treated	36.03	34.77	31.76	34.03	34.19	34.07
	Yellowness Index (E313)					
	% 0.5 Enzyme	% 2 Enzyme	% 4 Enzyme	% 0.2 Enzyme	% 0.4 Enzyme	% 1 Enzyme
Non-treated	32.82	32.82	32.82	32.82	32.82	32.82
Alkali treated	33.43	33.43	33.43	33.43	33.43	33.43
Pectinase treated	37.39	38.25	39.81	36.62	36.02	35.05
Alkali + Enzyme treated	37.41	37.86	40.77	40.45	40.2	40.82
	L*					
	% 0.5 Enzyme	% 2 Enzyme	% 4 Enzyme	% 0.2 Enzyme	% 0.4 Enzyme	% 1 Enzyme
Non-treated	80.18	80.18	80.18	80.18	80.18	80.18
Alkali treated	76.21	76.21	76.21	76.21	76.21	76.21
Pectinase treated	74.7	75.48	74.32	74.98	75.16	76.06
Alkali + Enzyme treated	75.56	76.02	74.95	75.23	75.72	75.76

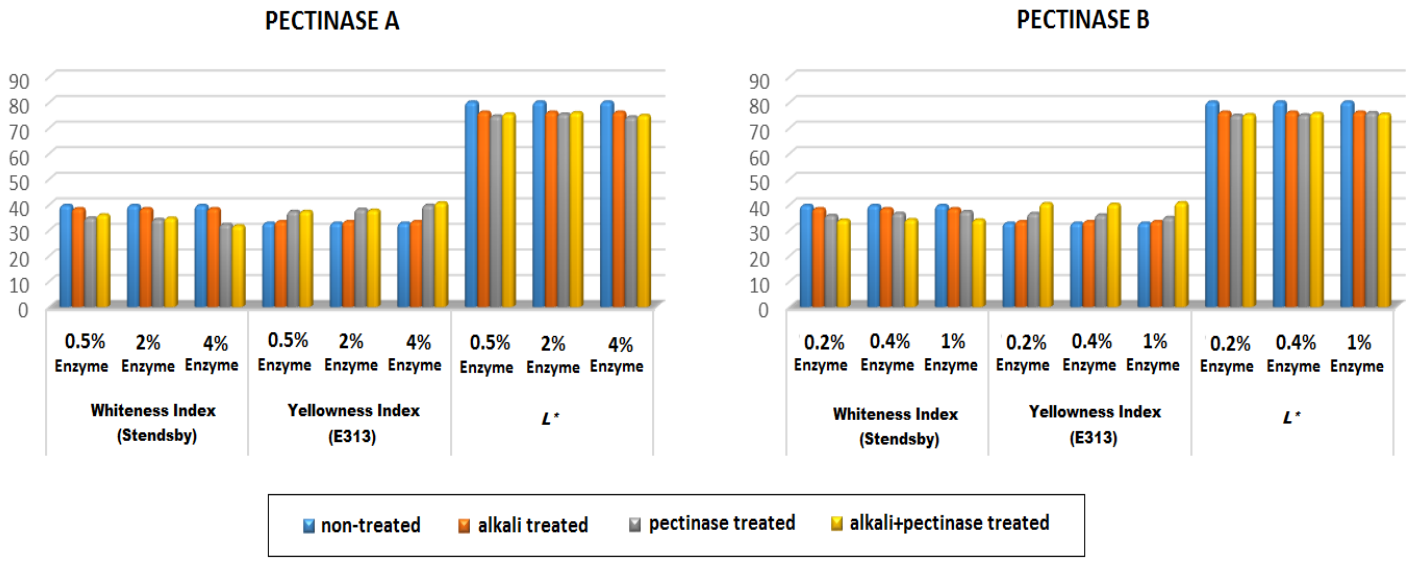

Figure 1: Color properties of pectinase enzyme treated and alkali treated pineapple fabric

Table 2: Absorption capacities of pineapple fabric samples

	Absorption Capacity (%)					
	Pectinase A treated			Pectinase B treated		
	% 0.5 Enzyme	% 2 Enzyme	% 4 Enzyme	% 0.2 Enzyme	% 0.4 Enzyme	% 1 Enzyme
Non-treated	205	205	205	205	205	205
Alkali treated	291	291	291	291	291	291
Pectinase treated	308	314	346	291	315	341
Alkali + Enzyme treated	325	326	346	325	326	359

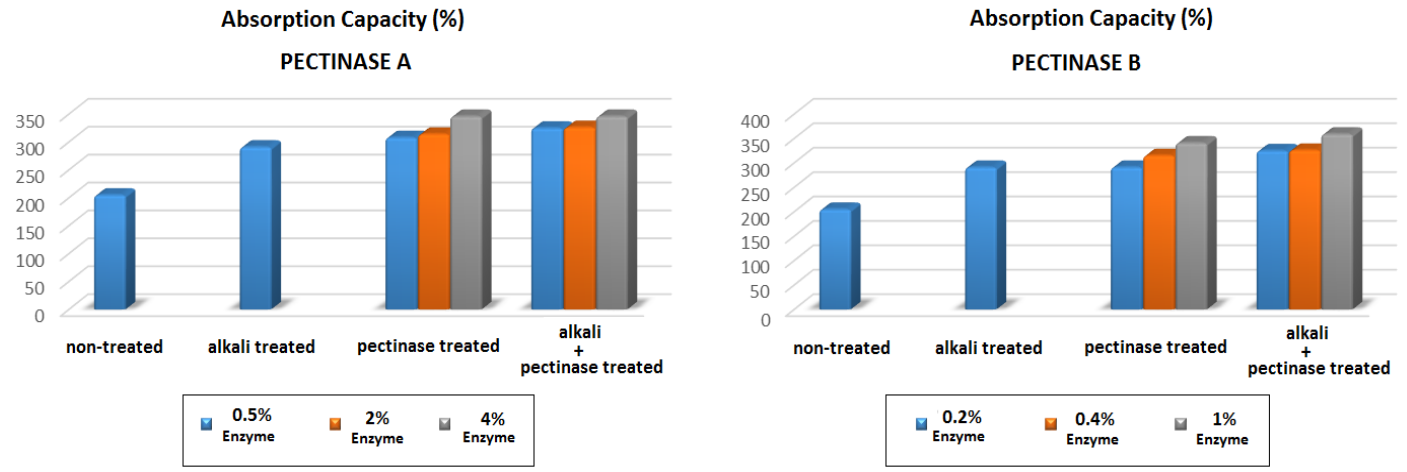

Figure 2: Absorption capacities of pineapple fabric samples

CONCLUSION

Pineapple fabric samples were hydrophilized with pectinase enzymes versus alkali solution (NaOH). After hydrophilization process, water absorption capacities of pineapple fabrics were evaluated. The results show that water absorption capacities of pectinase enzymes treated pineapple fabrics were higher than alkali treated pineapple fabric. Both, hydrophilization process caused slightly yellower shade on pineapple fabrics but pectinase enzyme caused yellower shade than alkali treatment. Pectinase enzymes can be recommended instead

ACKNOWLEDGMENTS

The authors extend their appreciation to the Scientific Research Project at Pamukkale University for funding the work through the project PAU-BAP No. 2015-FB020.

REFERENCES

[1] R.S. Blackburn, Sustainable textiles: Life cycle and environmental impact, Elsevier, Cambridge, 2009.
[2] R.S. Blackburn, Biodegradable and sustainable fibres, Woodhead Publishing Limited, Cambridge, 2005.
[3] E. Ganglberger, Environmental aspects and sustainability, Handbook of Natural Colorants (2009) 353-366.
[4] S. Mishra, A.K. Mohanty, L.T. Drzal, M. Misra, G. Hinrichsen, A review on pineapple leaf fibers, sisal fibers and their biocomposites, Macromolecular Materials and Engineering 289(11) (2004) 955-974.
[5] A. Mohamed, S. Sapuan, M. Shahjahan, A. Khalina, Characterization of pineapple leaf fibers from selected Malaysian cultivars, Journal of Food, Agriculture & Environment 7(1) (2009) 235-240.
[6] E. Kalaycı, O.O. Avinç, A. Bbozkurt, A. Yavaş, Tarımsal atıklardan elde edilen sürdürülebilir tekstil lifleri: Ananas

yaprağı lifleri, Sakarya Üniversitesi Fen Bilimleri Enstitüsü Dergisi 20(2) (2016) 203-221.
[7] A. Mohanty, P. Tripathy, M. Misra, S. Parija, S. Sahoo, Chemical modification of pineapple leaf fiber: Graft copolymerization of acrylonitrile onto defatted pineapple leaf fibers, Journal of applied polymer science 77(14) (2000) 3035-3043.
[8] E. Bozacı, T. Öktem, N. Seventekin, Ananas Yaprak Lifi, Tekstil & Konfeksiyon 3 (2007) 167-170.
[9] K. Mojsov, Application of enzymes in the textile industry: a review, Tekstilec 58(1) (2011) 47-56.
[10] E. Kalaycı, Ananas liflerinin ön terbiyesinin araştırılması, Textile Engineering Department, Pamukkale University, Denizli, 2017.
[11] S.R. Karmakar, Chemical technology in the pre-treatment processes of textiles, Elsevier, Amsterdam, 1999.
[12] E. Karapinar, M.O. Sariisik, Scouring of cotton with cellulases, pectinases and proteases, Fibres and Textiles in Eastern Europe 12(3) (2004) 79-82.
[13] S. Pulan, S. Kaplan, S. Ulusoy, Islak Mendil Üretiminde Kullanılan Dokusuz Yüzey Kumaşların Sıvı Absorbsiyon ve Transfer Özelliklerinin İncelenmesi Tekstil ve Mühendis 22(100) (2015) 13-22.

INTERNATIONAL CONFERENCE ON ADVANCES IN SCIENCE AND ARTS ISTANBUL 2017
29 – 31 MARCH 2017, Istanbul, Turkey

FLUORESCENCE LIFETIME DISTRIBUTION CHANGES OF "N-(1-PYRENYL)MALEIMIDE (PM) – BOVINE SERUM ALBUMIN (BSA); PM-BSA" COMPLEX BY THE PROTEOLYTIC EFFECTS OF FREE AND POLYACRYLIC ACID (PAA)-CONJUGATED TRYPSIN

***Ümmügülsüm Polat**
Yıldız Technical University
İstanbul, Türkiye

İbrahim Ethem Özyiğit
Yıldız Technical University
İstanbul, Türkiye

Emine Karakuş
Yıldız Technical University
İstanbul,Türkiye

Keywords: Trypsin, Fluorescence, Bovine Serum Albumin
** Corresponding author: Emine Karakuş 05301807573*
E-mail address eminekaraku@gmail.com

ABSTRACT

Surrounding of a fluorophore by more than one polar molecule results a variation in fluorescence lifetimes showing a distribution profile. Proteins provide different chemical environments to fluorophores and exhibit specific fluorescence lifetime distributions. Hydrolysis of proteins by proteases causes specific distribution profiles depending on the peptide content of the hydrolysates [1]. Conjugation with polymers may provide a higher thermal stability to enzymes [2,3] and at this point, it is important to know whether if the enzyme activity was changed by the conjugation. The distributional data may be used for tracking the proteolysis processes and may enable to monitor the changes in activity of the proteases by conjugation with polymers.

INTRODUCTION

In this work we studied the changes of the activity of trypsin by conjugation with polyacrylic acid (PAA), by using the fluorescence lifetime distributions of PM-BSA complex by using time resolved spectrofluorometer. The aim of the study is to detect whether if there were remarkable differences between the proteolytic effects of free trypsin and PAA-conjugated trypsin on the fluorescence lifetime distributions of PM-BSA complex.

RESULTS AND DISCUSSION

The fluorescence lifetime distribution of the hydrolysate produced from PM-BSA by the proteolytic activity of PAA-trypsin conjugate showed a longer distribution profile according to the hydrolysate produced by free trypsin. The result indicates uncompleted hydrolysis. The conjugation may have caused the active side of trypsin to be partially covered.

CONCLUSION

According to the resultant fluorescence lifetime distribution of the hydrolysate, the covalent modification of trypsin with PAA may not be proper conjugation method.

NOMENCLATURE

For synthesis of polymer-protease conjugates, the covalent conjugation method needs to be approached carefully because it may cause inhibition and fluorescence lifetime distribution analysis may be useful tool to monitor the differences between the proteolytic hydrolysates.

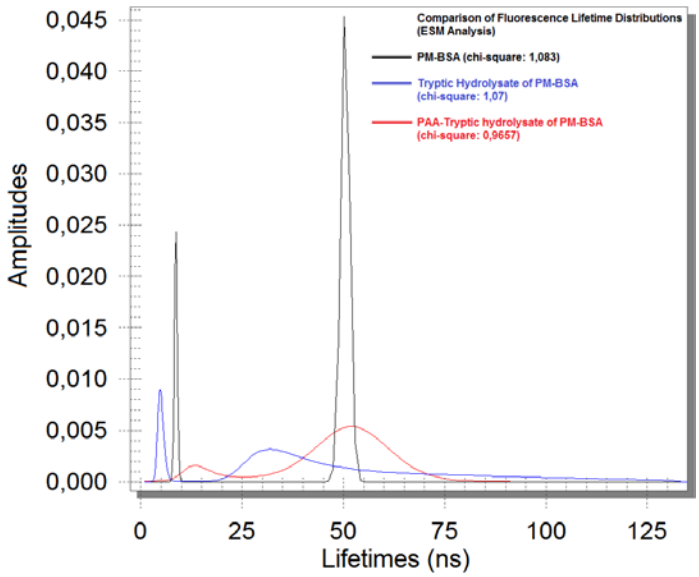

Figure 1. Fluorescence Lifetime Distributions

REFERENCES

1. J.R. Lakowicz, Principles of Fluorescence Spectroscopy, third edition, Springer Science+Business Media, LLC, New York (2006).
2. B. Jung and P. Theato, (2013) “Chemical Strategies for the Synthesis of Protein–Polymer Conjugates”, Adv Polym Sci, 253: 37–70.
3. G.T. Hermanson, Bioconjugate Techniques, second edition, Academic Press, Elsevier Inc., New York (2008).

PHYSICOCHEMICAL PROPERTIES OF NEW BIOBASED (FURANO-PYRIDINIC) COPOLYMERS

S. Abid and A. Bougarech

Laboratoire de Chimie Appliquée, Faculté des Sciences de Sfax, Université de Sfax, Tunisie

ABSTRACT

Polymers containing pyridinic moieties can be applied as sensor, in metal absorption or in biomedical application: antimicrobial activity, gene delivery[1]. As a part of our research conducted in the frame of the biobased furanic copolymers, we report herein the synthesis of a new family of furano-pyridinic copolyesters performed by melt polycondensation between 5,5'-isopropylidene-bis(ethyl 2-furoate) (DEF), dimethyl 2,6-pyridinedicarboxylate (DEPy) and ethanediol (ED)[2].The microstructure of the resulting copolyesters was investigated and the statistic repartition of monomer units was evidenced by NMR analysis.

As introduction of pyridine moiety into furanic copolyesters backbone modify the polymer properties, a study on the relationship between the copolyesters structure and their physicochemical properties was achieved. Thus, thermal properties, solubility properties and degradation were investigated. Globally, the pyridinic moieties render the copolyesters backbone more flexible and consequently the copolyesters are amorphous and have a low Tg ranging from 62 to 67°C. For the same reason, both hydrolytic and oxidative (as in-vivo degradation model) degradations are enhanced when the pyridinic unit content increases. All these results suggest that these novel copolyesters should be suitable for biological applications.

Submitting author: Souhir ABID, University of Sfax, 3000 Sfax, Tunisia.

E-mail: abidsouhir@yahoo.fr

References

[1] S. Kumar, J. Dutta, P. K. Dutta, *Int. J. Biol. Macromol.*, *45*, 330 (2009).

[2] A. Bougarech, M. Abid, F. Gouanvé, E. Espuche, S. Abid, R. El Gharbi, E. Fleury, P*olymer*, 54, 5482 (2013).

AB-INITIO INVESTIGATION OF THE STRUCTURAL, ELASTIC, ELECTRONIC, PHONON AND THERMODYNAMIC PROPERTIES OF LIBEBI IN *A* PHASE

F. Soyalp[1], G.Uğur[2] and Ş. Uğur[2]

Yuzuncu Yil University, Faculty of Education, Theoretical Physics Research Laboratory, Van, Turkey, fsoyalp@yyu.edu.tr
[2]Gazi University, Faculty of Science, Department of Physics, Ankara, Turkey, gokay@gazi.edu.tr
[2]Gazi University, Faculty of Science, Department of Physics, Ankara, Turkey, suleugur@gazi.edu.tr

ABSTRACT

By means of first principles calculations within density functional theory, we have studied the structural, elastic, electronic, phonon and thermodynamic properties of the LiBeBi in α phase. Bulk properties including lattice constants, static bulk modulus, first-order pressure derivative of the bulk modulus are reported and compared with available literature values. The second-order elastic constants, the electronic band structures and the related total and partial density of states are presented. Then, a linear-response approach to the density functional theory is used to derive the phonon dispersion curves and phonon partial and total density of states. Atomic displacement patterns for LiZnAs at the Γ point are also presented. The thermodynamical properties of LiBeBi have been successfully calculated in the whole temperature range from 0 to 500 K.

INTERNATIONAL CONFERENCE ON ADVANCES IN SCIENCE AND ARTS ISTANBUL 2017

29 – 31 MARCH 2017, ISTANBUL, TURKEY

BOSE-EINSTEIN DISTRIBUTION AND ENERGY SPECTRAL DENSITY WITHIN PADÉ APPROXIMATION

Bouserhane Adnane[1], Yahiaoui Abdelaziz[2]

[1]Université Tahri Mohammed de Béchar, adnray1965@yahoo.fr
[2]Université Tahri Mohammed de Béchar, abdelaziz_yahiaoui26@yahoo.com

ABSTRACT

A theorem due to Padé stipulate that all of the fonction which pocess a Maclaurin expansion, can be approched within its Padé approximants of the form

$P[n,m] = h_n(x)/k_m(x)$ avec $n + m + 1 \leq l$ the degree of the polynom of Maclaurin

We try to apply such a theorem about rational fractions in the case of black body electromagnetic radiation. We try to show that the evaluation of Bose-Einstein distribution and enrgy spectral density radiated by a black body can be approched as far as possible in a determined frequencies interval of the electromagnetic radiation spectrum.

Key words: black body, Distribution of Planck, energy density, rational fraction, Padé approximants.

POLY(PYRROLE) FILMS EFFICIENTLY ELECTRODEPOSITED USING NEW MONOMERS DERIVED FROM 3-BROMOPROPYL-N-PYRROL AND DIHYDROXYACETOPHENONE - ELECTROCATALYTIC REDUCTION ABILITY TOWARDS BROMOCYCLOPENTANE

Djouhra Aggoun, Ali Ourari

Laboratoire d'Electrochimie, d'Ingénierie Moléculaire et de Catalyse Redox (LEIMCR), Faculté de Technologie, Université Ferhat ABBAS de Sétif-1 19000 - Algeria.

ABSTRACT

Three monomers 6-[3'-N-pyrrolpropoxy]-2-hydroxyacetophenone **(1)**, 5-(3'-N-pyrrol propoxy)-2-hydroxyacetophenone **(2)** and 4-(3'-N-pyrrolpropoxy)-2-hydroxyacetophenone **(3)** were synthesized and their poly(pyrrole) films were electrodeposited on glassy carbon (GC) and Indium tin oxide (ITO) conductive electrodes by anodic oxidation in acetonitrile solutions containing n-Bu)$_4$N$^+$ClO$_4^-$ (TBAP 0.1 M). These films, currently called modified electrodes (noted ME), were obtained by the successive cycling at the appropriate potentials. These films contain chelating sites such as carbonyl group bearing the phenolic function which could play an important role in coordination chemistry. The electrodeposited poly(pyrrole) films on the ITO conductive glass electrodes offer some analytical advantages as the optical and electronic properties. Consequently, these new materials of electrodes were characterized by cyclic voltammetry while the morphology of these films was studied by FT-IR spectroscopy, scanning electron microscopy (SEM), dispersive energy X-ray spectroscopy and atomic force microscopy (AFM). The AFM studies show that the morphology of polypyrrole (PPy) films, electrodeposited on ITO surface, depends on the specific structure of the compound deriving from the monoalkylated dihydroxyacetophenone **1**, **2** and **3**. The coordination of copper was performed by electroreduction reaction in presence of ligand (**3**) and copper acetate salt. The resulting electrode material was tested towards the electrocatalytic activity in the reduction of bromocyclopentane.

Key-words: *Anodic oxidation, Poly(pyrrole) films, SEM and AFM, Dispersive energy X-ray spectroscopy, Copper complex, Electrocatalytic reduction .*

INTERNATIONAL CONFERENCE ON ADVANCES IN SCIENCE AND ARTS ISTANBUL 2017

29 – 31 MARCH 2017, ISTANBUL, TURKEY

SYNTHESIS, ELECTROCHEMICAL AND THEORETICAL STUDY OF (+)-(1R,4S)-3-NAPHTHOYLCAMPHOR LIGAND

Sabrina Bendia* **and Kamel Ouari**

Laboratoire d'Electrochimie, d'Ingénierie Moléculaire et de Catalyse Rédox (LEIMCR), Faculté de Technologie, Université Ferhat Abbas Sétif 1, DZ-19000 Sétif, Algeria.

Keywords: Camphor; B-diketone; Synthesis; Cyclic voltammetry; DFT

** Corresponding author : +213 550803331, Sabrina_bendia@univ-setif.dz*

ABSTRACT

The b-diketonates are a flexible class of chelating ligands which have been used in transition metal chemistry for more than 100 years [1]. In recent decades, organic-inorganic supramolecular compounds have attracted considerable attention and developed rapidly as a new kind of material in the coordination chemistry field [2-4]. The synthesis of coordination supramolecular compounds with different metal ions and ligands has led to intriguing structures with a variety of potential applications, such as molecular wires, catalysts, biosensors, gas storage and separation media, and luminescence [5-9].

The calculated structural parameters is some difference between the experimental and calculated parameters. It should be noted that the experimental data are for the solid phase, whereas the calculated data correspond to the isolated molecule in the gas phase. However, the experimental and computational data clearly show that both sets of data differ only slightly from each other. The electrochemical technique hase been used to show the oxido-reduction potential of the b-diketone ligand.

References

[1] R.C. Mehrotra, R. Bohra, D.P. Gaur, Metal b-Diketonates and Allied Derivatives, Academic Press, New York, 1978.
[2] V. Safarifard, A. Morsali, Coord. Chem. Rev. 292 (2015) 1-14.
[3] Y. Wei, Y. Yu, K. Wu, Cryst. Growth Des. 7 (2007) 2262-2264.
[4] J.C. Tan, A.K. Cheetham, Chem. Soc. Rev. 40 (2011) 1059-1080.
[5] S. Satapathi, S. Chattopadhyay, K. Bhar, S. Das, R. Krishna Kumar, T.K. Maji, B.K. Ghosh, Inorg. Chem. Commun. 14 (2011) 632-635.
[6] S.R. Batten, B.F. Hoskins, B. Moubaraki, K.S. Murray, R. Robson, Chem. Commun. (2000) 1095-1096.
[7] H.S. Patel, V.C. Patel, Eur Polym J. (2001) 2263-2271.
[8] B. Klenke, M.Barrett Stewart, M.P. Brun, R. Gilbert, J. Med. Chem. 44 (2001) 3440-3452.
[9] H. Hosseini-monfared, F. Mojtabazadeh, R. Bikas, V. Eigner, M. Dusek, A. Gutierrez, J. Coord. Chem. 67 (2014) 3510-3518.

INTERNATIONAL CONFERENCE ON ADVANCES IN SCIENCE AND ARTS ISTANBUL 2017

29 – 31 MARCH 2017, ISTANBUL, TURKEY

SYNTHESIS, SPECTROSCOPIC ANALYSIS AND X-RAY STRUCTURAL DETERMINATION OF SOME AZO-COMPOUNDS.

***H. BOUGUERIA*[1,2]** , *S. CHETIOUI*[1] , *S.E. BOUAOUD*[1], *H. MERAZIG*[1] , *L. Ouahab*[3].

[1]*Unité de Recherche de Chimie de l'Environnement et Moléculaire Structurale-CHEMS-*

Faculté des Sciences exactes. Département de Chimie. Université Mentouri-Constantine. Algérie.

[2] *Centre universitaire abd el hafid boussouf Mila, 43000 Mila, Algérie.*

[3]*LCSIM / UMR 6511 CNRS, Université de Rennes I.*

**E-mail :bougueriahassiba@gmail.com.*

Key word: azo dyes, Diazotation, Copulation, Chromophores, X-ray diffraction.

The preparation of compounds with use tinctorial and the improvement of their properties and their quality always stay a vast domain of investigating that doesn't quit developing.

In this work we will especially interest to structures containing the -N=N- chromophore on which carried our synthesis, our analytic studies of characterization usual spectrometric as well as a resolution structural by X-ray diffraction.

The interest and the valorization of this class of compounds exist in their big utilization on international plan in many agro-sanito-industrial domains: environment, pharmacy, medicine, feeding microscopy, textile, photograph, cosmetic, dye, plastics industry….

By diazotation reaction of primary arylamines, follow-up by copulation on β-naphthol [1] according the following diagram which permit to present a series of structures restraints for exploitation and Characterization.

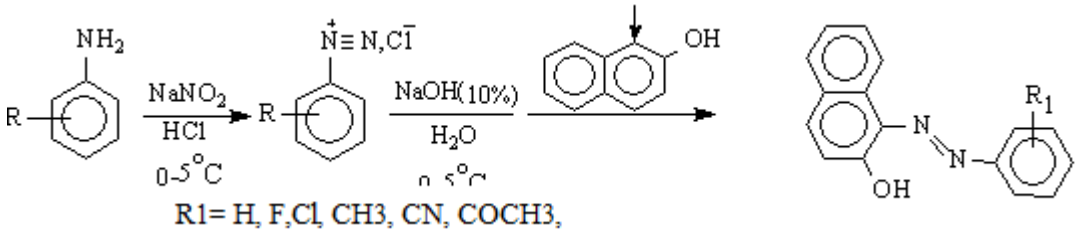

R1= H, F,Cl, CH3, CN, COCH3,

The identification of the different substances synthesized is especially put in relief in this work.

INTERNATIONAL CONFERENCE ON ADVANCES IN SCIENCE AND ARTS ISTANBUL 2017

29 – 31 MARCH 2017, ISTANBUL, TURKEY

THE THERMODYNAMIC AND VIBRATIONAL PROPERTIES OF AL_2SM

Sule Uğur[a] and Gökay Uğur[a]

[a]Department of Physics, Faculty of Science, Gazi University, TR-06500, Ankara, Turkey

ABSTRACT

We have calculated the electronic, elastic, thermodynamic, and vibrational properties of the Al_2Sm using first-principles calculations within the density functional theory. The electronic structure and partial density of states of Al_2Sm have been obtained and compared with the available theoretical calculations. The mechanical properties such as ductility and brittleness are further analyzed. The results for the phonon dispersion curves of Al_2Sm along several high-symmetry lines together with the corresponding phonon density of states are displayed. The temperature-dependent behavior of heat capacity obtained from phonon density of states for Al_2Sm is also presented.

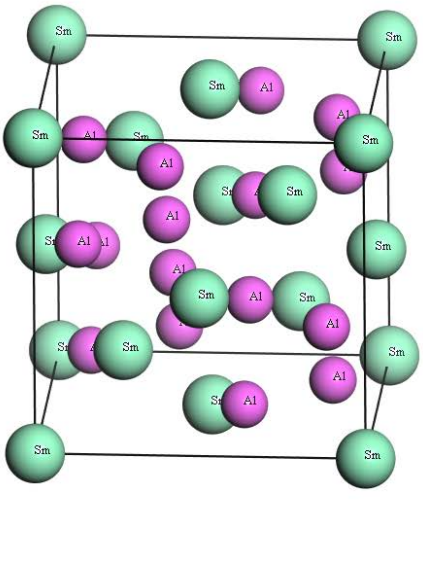

Fig. 1. Crystal structure of Al_2Sm.

INTERNATIONAL CONFERENCE ON ADVANCES IN SCIENCE AND ARTS ISTANBUL 2017

29 – 31 MARCH 2017, ISTANBUL, TURKEY

FIRST-PRINCIPLES STUDY ON ELASTIC, ELECTRONIC, AND PHONON PROPERTIES OF AU_4AL

Şule Uğur[a]

[a]*Department of Physics, Faculty of Science, Gazi University, TR-06500, Ankara, Turkey*

ABSTRACT

The structural, elastic, electronic and phonon properties of the Au_4Al at zero pressure are investigated by using a generalized gradient approximation of the density functional theory and ab initio pseudopotentials. The ground state properties, including, lattice constants, bulk modulus are in reasonable agreement with the available theoretical data. Electronic band structures and partial and total densities of states have been derived for Au_4Al. The partial density of states (PDOS) of Au_4Al is in good agreement with the earlier ab-initio calculations. The band structures show metallic character; the conductivity is mostly governed by Au-5d states. Phonon dispersion curves and their corresponding total densities of states were obtained using a linear response in the framework of the supercell approach.

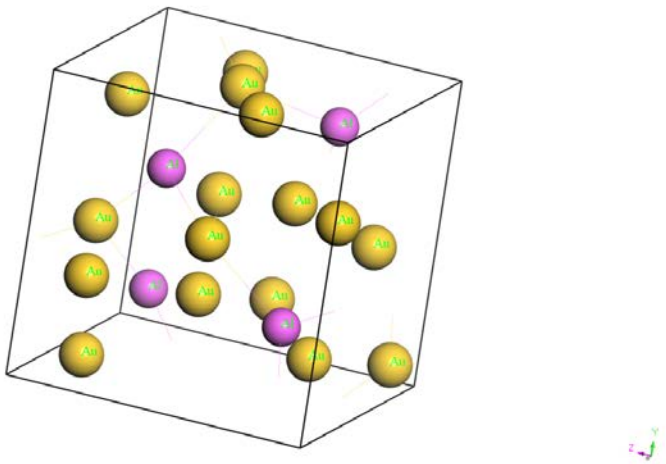

Fig. 1. Crystal structure of cubic Au_4Al unit cell.

INTERNATIONAL CONFERENCE ON ADVANCES IN SCIENCE AND ARTS ISTANBUL 2017

29 – 31 MARCH 2017, ISTANBUL, TURKEY

THEORETICAL STUDIES OF ELECTRONIC, ELASTIC, AND PHONON PROPERTIES OF KESTERITE CU_2ZNSNS_4

Gökay Uğur[a] , H. Yaşar Ocak[b] and Şule Uğur[a]

[a]*Department of Physics, Faculty of Science, Gazi University, TR-06500, Ankara, Turkey*

[b]*Department of Physics, Faculty of Arts and Science, Dumlupınar University, TR-43100, Kütahya, Turkey*

ABSTRACT

The structural, electronic, elastic, and phonon properties of Cu_2ZnSnS_4 (CZTS) were explored through first-principles calculations within the generalized gradient approximation (GGA). Comparison of the calculated equilibrium lattice constants and experimental data shows very good agreement. The stress-strain method was used to calculated elastic constants. The mechanical modulus, such as the bulk modulus (*B*), shear modulus (*G*) and Young's modulus (*E*) were discussed. The phonon dispersion curves of the Cu_2ZnSnS_4 (CZTS) were obtained using the direct method.

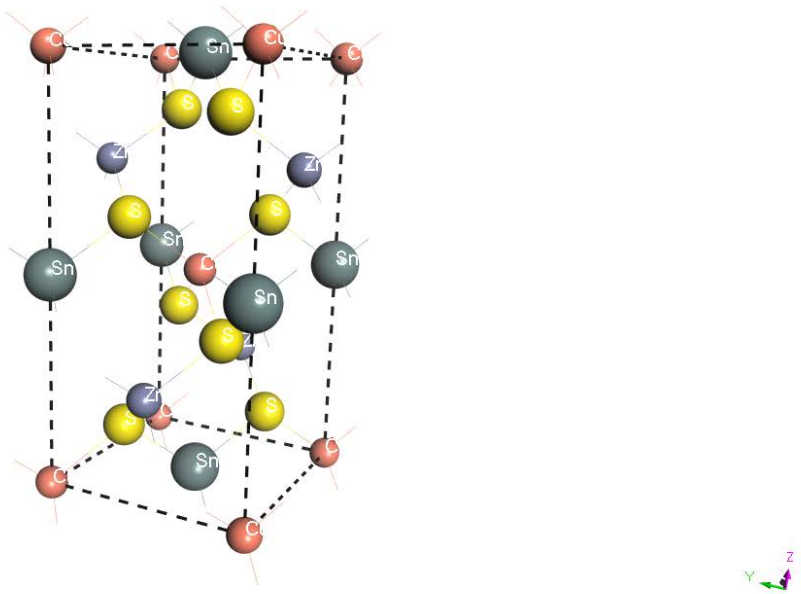

Fig. 1. Unit cells of kesterite Cu_2ZnSnS_4.

References

[1] A. Ritscher, J. Just, O. Dolotko, S. Schorr, M. Lerch, Journal of Alloys and Compounds, 670 (2016) 289.

INTERNATIONAL CONFERENCE ON ADVANCES IN SCIENCE AND ARTS ISTANBUL 2017

29 – 31 MARCH 2017, ISTANBUL, TURKEY

STRUCTURAL, ELASTIC, ELECTRONIC AND PHONON PROPERTIES OF *CMCM*-MOALB: AN *AB INITIO* STUDY

Gökay Uğur[a] , H. Yaşar Ocak[b] and Şule Uğur[a]

[a]*Department of Physics, Faculty of Science, Gazi University, TR-06500, Ankara, Turkey*

[b]*Department of Physics, Faculty of Arts and Science, Dumlupınar University, TR-43100, Kütahya, Turkey*

ABSTRACT

A first principles study has been performed to calculate the structural, elastic, electronic, and phonon properties of *Cmcm*-MoAlB. The results showed that the structural and elastic properties (i.e., bulk modulus, elastic constants, shear modulus and Young's modulus) derived by the GGA method were in good agreement with the available experimental and theoretical values. The electronic band structure reveals metallic conductivity and the major contribution comes from Mo-d states, with some contributions from B-p states. The phonon dispersion of MoAlB has been performed using the density functional theory and the direct method.

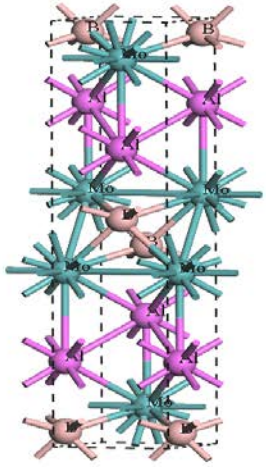

Fig. 1. Crystal structures of the *Cmcm*-MoAlB.

ULTRASTRUCTURE OF THE FEMALE REPRODUCTIVE SYSTEM IN *AELIA ALBOVITTATA* FIEBER, 1868 (HETEROPTERA: PENTATOMIDAE)

Nurcan ÖZYURT KOÇAKOĞLU, DAMLA AMUTKAN, IRMAK POLAT, ZEKİYE SULUDERE, SELAMİ CANDAN

Gazi University, Faculty of Science, Department of Biology, ANKARA, TURKEY

ABSTRACT

The stink bug *Aelia* genus contains approximately 15 species in Turkey and they are referred to as "wheat bug" indicating. *Aelia albovittata* Fieber, 1868 (Heteroptera: Pentatomidae) is a pest on *Inula* sp., *Poterium* sp. and graminaeous plants and weeds. *A. albovittata* is economically important insect, so, in order to combat with *A. albovittata* need to well-know the structure of the reproductive system of this insect. Therefore the present study aims to describe the ultrastructure of the female reproductive system in *A. albovittata* under the light microscopy and the scanning electron microscopy (SEM). Adults of *A. albovittata* were collected from Ankara, Kazan in June-July, 2016 and transferred to the laboratory in the Department of Biology (Gazi University, Ankara, Turkey). For the light microscopic examination, the reproductive systems of females were fixed in Formaldehyde. Thereafter, the tissues were washed, dehydrated and embedded in paraffin. Paraffin sections were cut into 6 µm thick slides and stained with Mallory's triple stain. The sections were viewed and photographed by using a Olympus BX51 microscope. For SEM, cleaned and dried samples with Critical Point Dryer (Polaron CDP 7501) were mounted with double-sided tape on SEM stubs, coated with gold using a Polaron SC 502 Sputter Coater, and examined with a Jeol JSM 6060 LV SEM. We observed that the female system of *A. albovittata* had two ovaries, two lateral oviducts, a common oviduct, a spermathecal, a pair of accessory glands and a genital chamber. The paired ovaries of *A. albovittata* are composed of 6 telotrophic. An each ovariole is differentiated into a terminal filament, germarium, vitellarium and pedicel (ovariolar stalk). The vitellarium contains 3-4 oocytes of different developmental stages: previtellogenesis, vitellogenesis and choriogenesis.

Keywords: Ovary, oocyte, insect, light microscope, electron microscope.

INTERNATIONAL CONFERENCE ON ADVANCES IN SCIENCE AND ARTS ISTANBUL 2017
29 – 31 MARCH 2017, Istanbul, Turkey

AN X-RAY DIFFRACTION (XRD) STUDY ON THE EFFECT OF CO-ADDITIVES OF Mg AND Zn ON THE CRYSTAL STRUCTURE OF HYDROXYAPATITE

*** HANİFİ KEBİROĞLU**
Firat University
Elazig, Turkey

Niyazi BULUT
Firat University
Elazig, Turkey

Serhat KESER
Firat University
Elazig, Turkey

Omer KAYGILI
Firat University
Elazig, Turkey

Tankut ATES
Firat University
Elazig, Turkey

Keywords: X-ray diffraction; wet chemical method; crystal structure
**Phone: +905315057534*
E-mail address: hanifi007@hotmail.com

ABSTRACT

The present study deals with a detailed X-ray diffraction (XRD) investigation of the effect of co-dopants of Mg and Zn on the cell parameters, unit cell volume and crystallinity degree of hydroxyapatite (HAp) synthesized via wet chemical process. The XRD results show that the values of all the as-mentioned parameters decreases significantly with increasing Mg and Zn contents.

INTRODUCTION

Hydroxyapatite (HAp) is one of the most used bioceramic sample, and its chemical composition is very similar to natural bone. Recently, to improve and to control of its characteristic properties, HAp has been doped or co-doped with elements such as Mg, Ni, Cd, Zn and Co [1,2]. In this work, Mg/Zn co-doped HAps were prepared using wet chemical method, and investigation of the effects of these co-dopants on the cell parameters, unit cell volume and crystallinity degree were carried out using XRD technique.

RESULTS AND DISCUSSION

As can be seen from the XRD data of the as-prepared HAps, all the investigated parameters including the cell parameters, unit cell volume and crystallinity degree are decreased. These decreases point out the introduction of the co-dopants of Mg and Zn into HAp structure [3]. As known, the ionic radii of these co-dopants (0.065 nm for Mg and 0.074 nm for Zn) are smaller than that of Ca (0.099 nm). For this reason, the as-observed decreases are quite consistent.

CONCLUSION

Using XRD results of the Mg/Zn co-doped HAps produced via wet chemical synthesis, it can be conclude that both additives significantly affect the cell parameters, unit cell volume and crystallinity degree of HAp. In other words, the aforementioned parameters may be controlled by the amount of these co-dopants.

NOMENCLATURE

HAp: Hydroxyapatite
XRD: X-ray diffraction

REFERENCES

[1] S.V. Dorozhkin, Calcium Orthophosphates: Applications in Nature, Biology, and Medicine. Pan Stanford, Singapore, 2012.

[2] O. Kaygili, S. Keser, T. Ates, A.A. Al-Ghamdi, F. Yakuphanoglu, Controlling of dielectrical and optical properties of hydroxyapatite based bioceramics by Cd content, Powder Technol 245 (2013) 1-6.

[3] S. Kannan, F. Goetz-Neunhoeffer, J. Neubauer, J.M.F. Ferreira, Ionic substitutions in biphasic hydroxyapatite and β-tricalcium phosphate mixtures: structural analysis by Rietveld refinement, J. Am. Ceram. Soc. 91(2008) 1–12.

INTERNATIONAL CONFERENCE ON ADVANCES IN SCIENCE AND ARTS ISTANBUL 2017
29 – 31 MARCH 2017, Istanbul, Turkey

THE EFFECTS OF DIFFERENT IMMERSION PERIODS IN SIMULATED BODY FLUID (SBF) ON THE CRYSTALLINITY OF CITRIC ACID CONTAINING HYDROXYAPATITES

***Hanifi KEBIROGLU**
Firat University
Elazig, Turkey

Niyazi BULUT
Firat University
Elazig, Turkey

Omer KAYGILI
Firat University
Elazig, Turkey

Serhat KESER
Firat University
Elazig, Turkey

Keywords: Hydroxyapatite; simulating body fluid
** Phone: +905315057534*
E-mail address: hanifi007@hotmail.com

ABSTRACT

Citric acid containing hydroxyapatite (HAp) samples were prepared via sol-gel technique. Then, the as-prepared HAp samples were immersed in simulated body fluid (SBF) prepared by Kokubo's recipe in different periods. X-ray diffraction (XRD) measurements of the samples before and after soaking in SBF were taken. The crystallinities of the samples, as well as the unit cell parameters, were computed using XRD data, and the as-calculated values were compared with each other. It is seen that the immersion period in SBF affects significantly the crystallinty of HAp.

INTRODUCTION

Hydroxyapatite ($Ca_{10}(PO_4)_6(OH)_2$, HAp), which is a member of calcium phosphate family, has been widely used in medical applications due to its excellent properties such as high biocompatibility and non-toxicity [1,2]. Citric acid, which is a chelating agent, has affected the biocompatibility and mechanical properties of calcium phosphate cement [3]. Simulated body fluid (SBF) is a solution having an ion concentration close to that of human blood plasma and has been used to test the bioactivity of the materials since 1991 [4].

The present study focuses on the effects of citric acid on the crystallinity of HAp before and after immersion in SBF.

RESULTS AND DISCUSSION

The crystallinity values estimated by the relation derived from Landi et al. [5] decrease with increasing citric acid content. The lattice parameters are affected by citric acid content and immersion period in SBF. These changes are in a good agreement with Bayraktar and Tas [6].

CONCLUSION

Citric acid-assisted HAps were prepared by sol-gel route. It is found that citric acid content affects the crystal structure of HAp. Additionally, the immersion period of HAp sample in SBF causes the significant changes in the lattice parameters and crystallinity.

NOMENCLATURE

HAp: Hydroxyapatite
XRD: X-ray diffraction
SBF: Simulated body fluid

REFERENCES

[1] O. Kaygili, S. Keser, Sol–gel synthesis and characterization of Sr/Mg, Mg/Zn and Sr/Zn co-doped hydroxyapatites. Materials Letters, 141 (2015) 161-164

[2] S.V. Dorozhkin, Calcium Orthophosphates: Applications in Nature, Biology, and Medicine. Pan Stanford, Singapore, 2012.

[3] A. Yokoyama, S. Yamamoto, T. Kawasaki, T. Kohgo, M. Nakasu, Development of calcium phosphate cement using chitosan and citric acid for bone substitute materials, Biomaterials 23 (2002) 1091-1101.

[4] T. Kokubo, Bioactive glass ceramics: properties and applications, Biomaterials 12 (1991) 155–163.

[5] E. Landi, A. Tampieri, G. Celotti, S. Sprio, J. Eur. Ceram. Soc. 20 (2000) 2377–2387.

[6] D. Bayraktar, A.C. Tas, Chemical preparation of carbonated calcium hydroxyapatite powders at 37 °C in urea-containing synthetic body fluids, J Eur Ceram Soc 19 (1999) 2573–2579.

INTERNATIONAL CONFERENCE ON ADVANCES IN SCIENCE AND ARTS ISTANBUL 2017
29 – 31 MARCH 2017, Istanbul, Turkey

DIELECTRIC PROPERTIES OF Gd/Ag CO-DOPED HYDROXYAPATITES

***Hanifi KEBIROGLU**
Firat University
Elazig, Turkey

Serhat KESER
Firat University
Elazig, Turkey

Niyazi BULUT
Firat University
Elazig, Turkey

A. Birkan SELÇUK
Nuclear Research and Training Center
Ankara, Turkey

Omer KAYGILI
Firat University
Elazig, Turkey

Keywords: Hydroxyapatite; gamma irradiation; relative permittivity
** Phone: +905315057534*
E-mail address: hanifi007@hotmail.com

ABSTRACT

Ag and Gd co-doped hydroxyapatites (HAps) were synthesized by wet chemical method. Then, the as-synthesized samples were irradiated at different doses using a ^{60}Co gamma source. The effects of gamma irradiation on the dielectric properties of HAps co-doped with Ag and Gd were investigated in the frequency range from 40 Hz to 10 MHz. The changes in the dielectric permittivity and ac conductivity were observed.

INTRODUCTION

Hydroxyapatite (hereinafter HAp), which is a main component of the hard tissues in human body, has been extremely used in medical applications as bone repairing material [1,2]. As known, bone is a dielectric material [3]. For this reason, the investigation of dielectric properties of HAp, especially the relative permittivity, gains a major importance. Additionally, resistance to ionizing radiation for a bioceramic material is a desired property [4].

Taking into consideration the above-mentioned situations, in the present work, the effects of gamma irradiation on the dielectric properties of HAp co-doped with Ag and Gd were investigated in detail.

RESULTS AND DISCUSSION

The graphs of relative permittivity vs. frequency show that there is a decrease in the relative permittivity with increasing frequency. It is affected by the co-dopant content, as well as the applied radiation. Contrary to the relative permittivity, the ac conductivity, which obeys Jonscher's universal power law [5], increases with increasing frequency. The applied irradiation causes some variations in the relative permittivity and ac conductivity of HAps doped with Ag and Gd.

CONCLUSION

HAps co-doped with Ag and Gd were successfully synthesized by wet chemical method. Gamma irradiation at various doses affected significantly both relative permittivity and ac conductivity. With increasing frequency, the relative permittivity decreases whereas ac conductivity increases. The dielectric properties and ac conductivity can be controlled by the amount of co-additives.

NOMENCLATURE

HAp: Hydroxyapatite

REFERENCES

[1] S.V. Dorozhkin, Calcium Orthophosphates: Applications in Nature, Biology, and Medicine. Pan Stanford, Singapore, 2012.

[2] O. Kaygili, S.V. Dorozhkin, S. Keser, Synthesis and characterization of Ce-substituted hydroxyapatite by sol–gel method, Mater. Sci. Eng. C, 42 (2014) 78-82.

[3] P.M. Meaney, T. Zhou, D. Goodwin, A. Golnabi, E.A. Attardo, K.D. Paulsen, Bone dielectric property variation as a function of mineralization at microwave frequencies, Int. J. Biomed. Imaging 2012 (2012) 649612.

[4] H. Badran, I. S. Yahia, M. S. Hamdy, and N. S. Awwad, Lithium-doped hydroxyapatite nano-composites: Synthesis, characterization, gamma attenuation coefficient and dielectric properties, Radiat. Phys. Chem., 130 (2017) 85-91.

[5] A.K. Jonscher, The 'Universal' Dielectric Response, Nature, 267 (1977) 673–679.

INTERNATIONAL CONFERENCE ON ADVANCES IN SCIENCE AND ARTS ISTANBUL 2017

29 – 31 MARCH 2017, ISTANBUL, TURKEY

A TRIGONOMETRIC FOUR VARIABLE PLATE THEORY FOR FREE VIBRATION OF RECTANGULAR COMPOSITE PLATES WITH PATCH MASS

Kada Draiche [1,2], Abdelouahed Tounsi [*1,3] and Y. Khalfi [1]

[1] *Material and Hydrology Laboratory, University of Sidi Bel Abbes, Faculty of Technology, Civil Engineering Department, Algeria*

[2] *Département de Génie Civil, Université Ibn Khaldoun Tiaret, BP 78 Zaaroura, 14000 Tiaret, Algérie*

[3] *Laboratoire des Structures et Matériaux Avancés dans le Génie Civil et Travaux Publics, Université de Sidi Bel Abbes, Faculté de Technologie, Département de génie civil, Algeria*

ABSTRACT

The novelty of this paper is the use of trigonometric four variable plate theory for free vibration analysis of laminated rectangular plate supporting a localized patch mass. By dividing the transverse displacement into bending and shear parts, the number of unknowns and governing equations of the present theory is reduced, and hence, makes it simple to use. The Hamilton's Principle, using trigonometric shear deformation theory, is applied to simply support rectangular plates. Numerical examples are presented to show the effects of geometrical parameters such as aspect ratio of the plate, size and location of the patch mass on natural frequencies of laminated composite plates. It can be concluded that the proposed theory is accurate and simple in solving the free vibration behavior of laminated rectangular plate supporting a localized patch mass.

Keywords: laminated plates; free vibration; four variable plate theory; patch mass

INTERNATIONAL CONFERENCE ON ADVANCES IN SCIENCE AND ARTS ISTANBUL 2017

29 – 31 MARCH 2017, ISTANBUL, TURKEY

PRODUCTION OF *TRICHODERMA HARZIANUM* SPORES BY LF AND SSF

AlMI H[1], DEHIMAT L[1], KACEM CHAOUCHE N[1], SABRI A[2] and THONART P[2]

[1]Laboratory of Mycology, Biotechnology and Microbial Activity, SNV, University of Mentouri Constantine, 25000 Algeria

[2]Walloon Centre for Industrial Biology, Agro-Biotech, University of Liege, Belgium

Kaywords : Trichoderma harzianum, liquide fermentation, solide state fermentation.

Trichoderma harzianum is one of the best microorganisms (Fungi) used as a fungicide. It used for foliar application, seed treatment and soil treatment for suppression of various diseases causing fungal pathogens like *Botrytis, Fusarium* and *Penicillium* sp..

The production of *Trichoderma harzianum* spores was carried out after Screening and selection of strains collared on agricultural soils in the Constantine region –Algeria-. Tens strains were isolated and tested for their antifungal capacity and only two were selected and identified.

The first step of the production began with liquid fermentation (LF) for production / multiplication of biomass on M2 medium with optimized conditions. The biomass obtained, was collected under aseptic conditions after seven days of fermentation.

The fresh mycelia mass obtained from the LF was mixed with an equal amount of Wheat Bran (sterile) to form the solid state fermentation (FMS) trays. The prepared trays were incubated under aseptic conditions for an undetermined time. The solid fermentation was stopped when the trays become dry with a brittle structure and a green color.

Finally, the last step of production involved the separation of the spores of *T. harzianum* from their fermentation substrate: Wheat Bran.

INTERNATIONAL CONFERENCE ON ADVANCES IN SCIENCE AND ARTS ISTANBUL 2017
29 – 31 MARCH 2017, ISTANBUL, TURKEY

SCHIFF BASE AS CORROSION INHIBITOR FOR STEEL XC48 IN H_2SO_4 SOLUTION

BENGHANEM Fatiha

Laboratoire d'Electrochimie, d'Ingénierie Moléculaire et Catalyse Redox (LEIMCR).
Département de Génie des Procédés Faculté de Technologie UFA Sétif-1 Algérie

benghanem_f@yahoo.fr

ABSTRACT

The corrosion protection of steel in acidic media is a challenging task for researchers in materials engineering in view of satisfying environmental requirements and for industrial facilities. The use of organic compounds as corrosion inhibitors for mild steel has assumed great significance due to their application in preventing corrosion under different corrosive environments. The adsorption of such molecules depends mainly on certain physicochemical properties of the organic molecules such as the presence of nitrogen, oxygen, sulfur, and phosphorus heteroatoms, or the existence of multiple bonds, as well as aromatic rings in the molecule through which they are adsorbed on the metal surface.

The inhibition effect of new synthesized Schiff base on the corrosion of steel XC48 in H_2SO_4 0.5 M been investigated using electrochemical impedance spectroscopy, Tafel polarization and weight loss measurements. The inhibition efficiencies obtained from all methods employed are in good agreement with each other. Tafel polarization studies showed that the Schiff base is mixed type inhibitor. The adsorption of the compound onto the surface of steel XC48 in 0.5 M H_2SO_4 M obeys the Langmuir isotherm. Adsorption thermodynamic parameters reveal that the adsorption of inhibitor is chemical adsorption.

Keywords: Corrosion, inhibitor, Schiff base, steel

INTERNATIONAL CONFERENCE ON ADVANCES IN SCIENCE AND ARTS ISTANBUL 2017

29 – 31 MARCH 2017, Istanbul, Turkey

AEROBIC BIODEGRADATION OF BTEX COMPOUNDS BY ACTINOBACTERIA ISOLATED FROM ACTIVATED SLUDGE

BOUDEMAGH Allaoueddine [(1,*)]; HOCINAT Amira [(1,2)] ; ALI-KHODJA Hocine [(2)]

[(1)] Faculty of nature and life sciences, Department of Microbiology, University of Mentouri Brothers, Constantine 1. Constantine, Algeria.

[(2)] Laboratory of pollution and water treatment, Faculty of exact sciences, Department of chemistry, University of Mentouri Brothers, Constantine 1. Constantine, Algeria.

Keywords: Actinobacteria, biodegradation, BTEX, activated sludge.

* *Corresponding author:* BOUDEMAGH Allaoueddine *Phone:* +213 771 206 765, email: boudemaghallaoueddine@yahoo.fr

ABSTRACT

Benzene, toluene, ethyl benzene and xylene (known as BTEX) constitute an important family of volatile organic compounds. These xenobiotics contaminate several ecosystems such as soil, surface water, groundwater and various natural environments. BTEX compounds are highly hazardous to health because they are carcinogenic, neurotoxic and genotoxic. The US Environmental Protection Agency classified them as priority environmental pollutants, making their removal necessary from polluted sites. The destruction of these compounds by thermochemical methods has serious disadvantages. In contrast, biological processes have significant economic and environmental benefits. Biodegradation of these pollutants by aerobic and anaerobic bacteria has been studied for more than two decades. Initially, several ri studies focused on the biodegradation of BTEX components individually. However, BTEX are known to occur as a mixture in contaminated sites. Thus, for bioremediation applications, it could be advisable and advantageous to study the biodegradation of BTEX mixes by isolated microorganisms. Actinomycetes are known to degrade complex and varied substrates thanks to their rich enzymatic systems. They may therefore be important agents of various types of biodegradation in the most diverse ecosystems. In the present study we tested the degradation of BTEX by the actinobacteria isolated from samples of activated sludge from a wastewater treatment plant. The results show that 19 *Streptomyces* were capable of using at least one compound of BTEX as a sole source of carbon and energy. Among them, three strains from activated sludge degraded *in vitro* in aerobic conditions all of these volatile organic compounds at initial concentrations ranging from 1400 to 1500 mg/L. On the basis of the sequence analysis of the 16S rRNA genes, two active strains were identified as *Streptomyces griseobrunneus and Streptomyces flavogriseus*, and one as *Streptomyces* sp. These strains could represent excellent candidates in bioremediation techniques for aquatic sites polluted by such xenobiotics.

Key words: Actinobacteria, biodegradation, BTEX, activated sludge.

INTERNATIONAL CONFERENCE ON ADVANCES IN SCIENCE AND ARTS ISTANBUL 2017

29 – 31 MARCH 2017, Istanbul, Turkey

ANTIBIOTIC ACTIVITY OF ACTINOBACTERIA ISOLATED FROM THE SALINE SOILS OF CHOTT MELGHIR IN EL-OUED (ALGERIA)

BENSOUICI Karima [(*)], KITOUNI Mahmoud and BOUDEMAGH Allaoueddine

(1) Faculty of Natural and Life Sciences. University Abbes Laghrour, Khenchela, Algeria.

(2) Laboratory of Microbiological Engineering and Applications Faculty of Nature and Life Sciences, Department of Microbiology, University of Mentouri Brothers, Constantine, Algeria.

(3) Department of Microbiology, Faculty of Nature and Life Sciences, University of Mentouri Brothers, Constantine 1, Constantine, Algeria.

Email: kbensouici@yahoo.fr; mahmoudkitouni@yahoo.fr;boudemaghallaoueddine@yahoo.fr

Key words: Actinobacteria, antibacterial activity, antifungal activity, chott Melghir.

ABSTRACT

The investigations carried out in recent years on the discovery of new antibiotic molecules are in a considerable progress in microbiology. The main reasons are the emergence of new pathogens and the proliferation of resistant microorganisms which escape the inhibitory action of the antibiotic molecules currently used. The most extreme and less studied ecosystems can provide molecules with new potentialities. In this context, we have been interested in isolating actinobacteria known as the major producer of antibiotics, from the saline soils of chott Melghir in the El-Oued region of Algeria. This rough place is characterized by a very high degree of salinity and a temperature that varies from 50 to 60°C in the morning to reach 0 to -3°C throughout the night. These Saharan ecosystems are poorly studied and can hide unlimited secrets. Thus, 15 actinomycetes were isolated and purified on the selective media. The technique of agar disks has been used to study the antibacterial activity of these isolates against four multiresistant test bacteria coming from the Ibn Badis University Hospital of Constantine (Algeria): *Streptococcus feacalis, Staphylococcus aureus, Klebsciella pneumonea* and *Pseudomonas aeruginosa*. The antifungal activity was revealed by the double layer technique against *Aspergillus niger* and *Fusarium oxysporum*. The macroscopic and microscopic identification tests used on our isolates confirm the belonging of these bacteria to the actinobacteria. The results indicate that these microorganisms have the ability to produce secondary metabolites of high anti-cellular activity. Of all the purified strains, 13 showed an activity against at least one test bacterium with a percentage of about 86%. Four active strains called SH 1, SH 2, SH 4, SH 6 showed antibacterial activity against all tested bacteria. The action against the fungi tested in this study is relatively low. Indeed, no activity has been observed against *Aspergillus niger*, but 30% of actinobacteria exhibit an antifungal activity against *Fusarium oxysporum.* Our results are very promising and show that

this saline ecosystem can be a source of new bioactive molecules with very important potentialities.

INTERNATIONAL CONFERENCE ON ADVANCES IN SCIENCE AND ARTS ISTANBUL 2017

29 – 31 MARCH 2017, ISTANBUL, TURKEY

CONVERGENCE OF THE CORRELATED CALCULATİONS WİTH CORRELATİON ENERGY AND TOTAL ENERGY: A FİRST PRİNCİPLES STUDY

Salih Akbudak[a], Gökay Uğur[b], H. Yaşar Ocak[c], and Şule Uğur[b]

[a]Department of Physics, Faculty of Arts and Science, Adiyaman University, TR-02100, Adiyaman, Turkey

[b]Department of Physics, Faculty of Science, Gazi University, TR-06500, Ankara, Turkey

[c]Department of Physics, Faculty of Arts and Science, Dumlupınar University, TR-43100, Kütahya, Turkey

Abstract:

All explicitly correlated methods suffer from slow convergence of total energy and correlation energy with respect to basis set size. This slow convergence is more severe for heavy elements. Because heavy elements have high number of electrons which increase the effects of electron-electron interactions. However, all density functional and wave function based methods have a common problem of difficulty in explaining the electron-correlation effects. So, in this study we have systematically investigated the performance of correlation consistent basis sets in describing the correlation and total energy of Zn_2, Cu_2 and Mn_2. We analyzed the importance of unfreezing the second order valence shells going beyond frozen-core approximations. For all calculations we have used frozen-core random phase approximation (RPA) method. We have observed a good convergence pattern for RPA correlation energy and RPA total energy which is comparable to light elements.

[1] Perdew J. P. and Schmidt K., 2001. “Density Functional Theory and its Application to Materials”, edited by V. Van Doren, C. Van Alsenoy, and P. Geerlings, AIP, Melville, NY)

[2] Kritikou, S., Hill, J.G., 2015. “Auxiliary Basis Sets for Density Fitting in Explicitly Correlated Calculations: The Atoms H-Ar”, Journal of Chemical Theory and Computation, 11, 5269-5276.

[3] Usvyat, D., 2013.”Linear-scaling explicitly correlated treatment of solids: Periodic local MP2-F12 method”, Journal of Chemical Physics, 139, 194101-15.

[4] Hill, J.G, Peterson, K.A, Knizia, G., Werner, H.J., 2009. “Extrapolating MP2 and CCSD explicitly correlated correlation energies to the complete basis set limit with first and second row correlation consistent basis sets”, Journal of Chemical Physics, 131, 194105-13.

[5] Klopper, W, Manby, F.R, Ten-No, S., Valeev, E.F, 2006. “R12 methods in explicitly correlated molecular electronic structure theory”, International Reviews In Physical Chemistry, 25, 427-468.

[6] Dunning T.H., 1989.”Gaussian basis sets for use in correlated molecular calculations. I. The atoms boron through neon and hydrogen”, Journal of Chemical Physics, 90, 1007–23.

INTERNATIONAL CONFERENCE ON ADVANCES IN SCIENCE AND ARTS ISTANBUL 2017

29 – 31 MARCH 2017, ISTANBUL, TURKEY

ASSESMENT OF RESOLUTİON OF IDENTİTY (RI) METHOD İN DESCRİBİNG BİNDİNG ENERGY OF HOMONUCLEAR DİATOMİCS; A CASE STUDY OF AR_2 AND H_2

Salih Akbudak[a], Şule Uğur[b] and Gökay Uğur[b]

[a]*Department of Physics, Faculty of Arts and Science, Adiyaman University, TR-02100, Adiyaman, Turkey*

[b]*Department of Physics, Faculty of Science, Gazi University, TR-06500, Ankara, Turkey*

Abstract:

Binding energies of Ar_2 and H_2 molecules have been investigated using correlation consistent cc-pVXZ and aug-cc-pVXZ basis sets together with Coupled Cluster with Singles Doubles with Perturbative Triples (CCSD(T)) and Coupled Cluster with Singles Doubles (CCSD) methods respectively. Two point extrapolations to complete basis set limit has been applied to to speed up calculations and reduce the basis set incompleteness (BSIE) error. To alleviate basis set superposition errors (BSSE) counterpoise (CP) correction method was assessed. Obtained CP-corrected and uncorrected binding energy values were compared to experimental values in literature. Discrepancy of our theoretical binding energy values from existing experimental binding energy values for Ar_2 observed to be less than 5. 2 meV and for H_2 less than 0. 14 eV.

[1] Dunning T.H., 1989."Gaussian basis sets for use in correlated molecular calculations. I. The atoms boron through neon and hydrogen", Journal of Chemical Physics, 90, 1007–23.

[2] Feller, D., Peterson, K. A., Hill, J. G., 2011. "On the effectiveness of CCSD(T) complete basis set extrapolations for atomization energies", Journal of Chemical Physics, 135,044102-18.

INTERNATIONAL CONFERENCE ON ADVANCES IN SCIENCE AND ARTS ISTANBUL 2017

29 – 31 MARCH 2017, ISTANBUL, TURKEY

SYNTHESIS AND ELECTROCHEMICAL STUDY OF TETRADENTATE SCHIFF BASE COMPLEX

Salima MESSALI* **and Ali OURARI**

Laboratoire d'Electrochimie, d'Ingénierie Moléculaire et de Catalyse Rédox (LEIMCR), Faculté de Technologie, Université Ferhat Abbas Sétif 1, DZ-19000 Sétif, Algeria.

Keywords: Schiff base; Tetradentate; Complex; Synthesis; Cyclic voltammetry;

* *Corresponding author : +213 550803331, Salima_messali@univ-setif.dz*

ABSTRACT

Complexes containing Schiff bases have not only found extensive application in design and synthesis of organic molecules [1], but these compounds exhibit several of significant electrical conductivity [2], host-guest chemistry [3], sensors [4], and biological activity [5]. In recent years Schiff base ligands received enormous attention due to their wide application in the field catalyst [6,7] and anti-microbial and anti-tumors activity[8] and recently reported as nano sized Schiff base complexes for medical applications [9].

The present work amid to synthesis and characterization of three Schiff base complexes derived from reaction of salicylaldehyde with 1,2-diaminoethane bis(methylamine) included N2O2 donor site and their complex. The CV methods provided a good tool to reveal the complementary nature of structure of complex and electron-transfer reactions of the oxidized and reduced species of new electroactive Schiff -base complex.

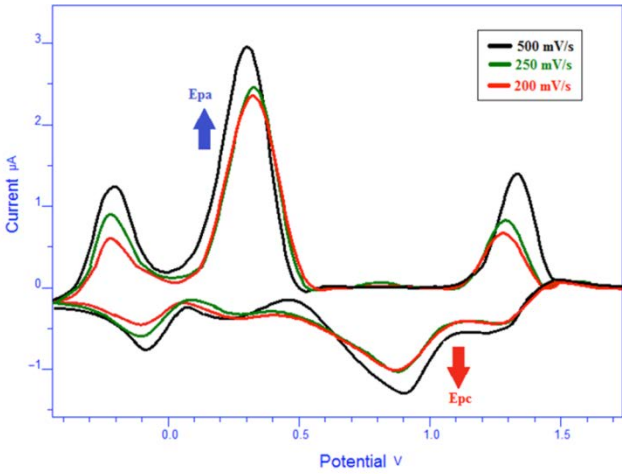

INTERNATIONAL CONFERENCE ON ADVANCES IN SCIENCE AND ARTS ISTANBUL 2017
29 – 31 MARCH 2017, ISTANBUL, TURKEY

THERMALLY EVAPORATED Sn-DOPED In_2O_3 THIN FILMS: OPTICAL, ELECTRICAL AND ELECTROTHERMAL PROPERTIES

Murat OLUTAŞ[1,*], Atılgan ALTINKÖK[2]

[1] Abant İzzet Baysal University, Department of Physics, Bolu, Turkey
[2] Giresun University, Department of Electrical and Electronics Engineering, Giresun, Turkey
** Presenter, Phone: +903742541000, Fax: +903742534642,*
E-mail address: olutas_m@ibu.edu.tr

Transparent semiconducting oxide materials have extended their broad spectrum of applications in the material science world due to the unique combined properties of transparency to visible light and electrical conductivity. Coatings on glass with highly transparent conductive oxide films (TCO) are mostly performed with indium tin oxide (ITO) which is commonly used oxide material in applications such as transparent film heaters (TFHs) where both high electrical conductivity and optical transmittance are essential. However, electrical and optical properties of ITO films are sensitive to production conditions, and they are fabricated by several methods such as molecular beam epitaxy (MBE), DC and RF magnetron sputtering.

In this study, we aimed to investigate structural, optical, electrical and electrothermal properties of semiconductor Sn-doped In_2O_3 (i.e., ITO) thin films fabricated on glass substrate by thermal evaporation method. Scanning elelctron microscope (SEM) and x-ray diffraction (XRD) spectroscopy were used for elucidation of their structural characterizations such as surface morphology, grain size and crystal structure . On the other hand, current-voltage (I-V) and temperature dependent resistivity (ρ-T) measurements were carried out for electrical characterization of the ITO thin films. Furthermore, the optical parameters such as transmittance, refractive index and energy gap were also determined. In addition, electrothermal performance of the fabricated ITO film having 95% transmittance was investigated and analyzed using infrared thermography method for the transparent film heaters (TFHs) applications.

ACKNOWLEDGMENTS

This work was supported by the Research and Development Foundation of Abant İzzet Baysal University under project number 2016.03.02.1092 and Giresun University Research Fund under project number FEN-BAP-A-140316-55.

INTERNATIONAL CONFERENCE ON ADVANCES IN SCIENCE AND ARTS ISTANBUL 2017
29 – 31 MARCH 2017, ISTANBUL, TURKEY

A COMPARATIVE STUDY ON REVERSIBLE AND IRREVERSIBLE EFFECTS IN ELECTRICAL TRANSPORT CHARACTERISTICS OF POLYCRYSTALLINE TYPE-2 SUPERCONDUCTORS

Murat OLUTAŞ[1,*], Atılgan ALTINKÖK[2], Atilla KILIÇ[1], Kıvılcım KILIÇ[1]

[1] Abant İzzet Baysal University, Department of Physics, Bolu, Turkey
[2] Giresun University, Department of Electrical and Electronics Engineering, Giresun, Turkey
** Presenter, Phone: +903742541000, Fax: +903742534642,*
E-mail address: olutas_m@ibu.edu.tr

ABSTRACT

Detailed investigations on type-II superconductors reveal that the flux line dynamics are governed by two distinct mechanisms. One of them is the repulsive interaction between flux lines (i.e., vortices) and the other is the interplay between vortices and pinning centers. It is well known that the type and distribution of the pinning centers inside the superconducting sample influence strongly the motion of vortices and also the measured dissipation induced by them. Therefore, the pinning and depinning of vortices are considered as the main mechanisms of the dissipation, provided that the thermal fluctuations are negligible compared to pinning. In addition, experimental, theoretical and computer simulation studies show that the transport current can cause an increase or a decrease in the order of moving flux line configuration. When the vortices are set in motion with an applied current, the reorganization of moving flux line configuration can develop gradually and can take some time depending on the magnitude of applied current.

In this study, the flux dynamics and reversible/irreversible effects in polycrystalline sample of MgB_2 have been studied by current-voltage (I-V) measurements for different sweep rates (dI/dt) of transport current, and transport relaxation measurements (V-t curves) as a function of transport current (I), temperature (T) and external magnetic field (H). In order to understand better the flux dynamics, the experimental results for polycrystalline MgB_2 sample were compared to our previous similar studies on polycrystalline high-temperature superconductors (e.g., YBCO). The results show that current-voltage characteristics of MgB_2 exhibit nearly reversible behavior for both slow and high dI/dt cases, and their evolution is nearly independent of dI/dt. The current-voltage (I-V) measurements were also carried out by reverse procedure, and the standard and reverse procedures of $I - V$ measurements reveal that there is no significant difference between them. These findings suggest that the weak links between grains and surface weak links in polycrystalline MgB_2 do not have a considerable effect on the evolution of the $I - V$ curves and also on the other transport measurements (e.g., V-t curves) as compared to the polycrystalline high-temperature superconductors.

INTERNATIONAL CONFERENCE ON ADVANCES IN SCIENCE AND ARTS ISTANBUL 2017

29 – 31 MARCH 2017, Istanbul, Turkey

THE SELECTIVE ISOLATION OF ACTINOBACTERIA FROM THE ALGERIAN DESERT SOIL

BOUDEMAGH Allaoueddine [(1,*)]; BENSOUICI Karima[(2,3)]

(1) Faculty of nature and life sciences, Department of Microbiology, University of Mentouri Brothers, Constantine 1**.** Constantine, Algeria.

(2) Laboratory of Microbiological Engineering and Applications Faculty of Nature and Life Sciences, Department of Microbiology, University of Mentouri Brothers, Constantine, Algeria.

(3) Faculty of Natural and Life Sciences. University Abbes Laghrour, Khenchela, Algeria.

Keywords*: Actinobacteria, Desert soil, Selectif isolation*

* *Corresponding author:* BOUDEMAGH Allaoueddine *Phone:* +213 771 206 765, email: boudemaghallaoueddine@yahoo.fr

ABSRACT

Actinobacteria are microorganisms of great biotechnological, environmental, agronomic and medical interest. This is due to the incredible diversity of their primary and secondary metabolites such as antibiotics, enzymes and antitumor molecules. However, selective isolation of these bacteria from their ecosystems poses serious difficulties, mainly because of their rather long generation times. This characteristic promotes the growth of the fastest microorganisms, such as fungi and other bacteria. Several methods have been used to promote the isolation of actinomycetes and to inhibit invading organisms. The preheating of soil samples is a technique widely used in many screening programs for actinomycetes isolation, because of the high resistance of their spores to drying and high temperatures. The addition of antibacterials and antifungals and the choice of selective isolation media are also widely used. According to our knowledge, research on the isolation of actinobacteria from arid soils is rare and studies focusing on the optimal conditions for the isolation of these bacteria from these very special ecological places are even rarer. The aim of this study is to define the effects of preheating of soil samples and the addition of antibacterials and antifungals in isolation media. It is also a matter of choosing among the commonly used isolation media those which are most adapted to desert soils. Thus, two soil samples were prepared. The first was heated to 110 °C. for 10 minutes and the other was not subjected to any heat treatment. The isolation of actinomycetes was performed on the casein starch medium supplemented with a combination of antifungal agents (nystatin and amphotericin B) and antibacterials (nalidixic acid, polymexin B sulphate and sodium penicillin). The following isolation media (Glucose-yeast extract-malt, Benett, Water-yeast extract-agar, Glucose-asparagin and Pridham medium) were also tested in order to select the most favourable. The results show that treatment of soil with heat is not recommended because the number of actinomycetes isolated was 92.10^4 ufc.g^{-1} before heating and became 38.10^4 ufc.g^{-1} when the samples are heated. Thus the preheating reduces the actinomycetes to more than 50%. The antifungal and antibacterial agents which allow the elimination of undesirable germs are nystatin and nalidixic acid at concentrations of 50µg/ml and 10µg/ml respectively. The most favourable isolation medium for of actinomycetes from desert soils in the study area is glucose-yeast-malt (GLM). These results are very important, they allow to isolate and to study the maximum of the biodiversity of the actinobacteria in the desert soils.

INTERNATIONAL CONFERENCE ON ADVANCES IN SCIENCE AND ARTS ISTANBUL 2017

29 – 31 MARCH 2017, ISTANBUL, TURKEY

CALORIMETRIC RESEARCHES OF STABILITY OF COMPLEXES DPPC LIPOSOMES WITH VITAMIN C AND VITAMIN E

E.Shekiladze[1,2] T.Mdzinarashvili[1,2] M. Khvedelidze[1,2]

1- Faculty of Exact and Natural Sciences, I. Javakhishvili Tbilisi State University, Tbilisi 0179, Georgia

2- Institute of Medical and Applied Biophysics, I. Javakhishvili Tbilisi State University, Tbilisi 0179, Georgia

ABSTRACT

The modern nanotechnology was used to encapsulate vitamins (C, E) in DPPC liposomes. Proportions of vitamins and DPPC lipids were selected one vitamin per one lipid molecule. In liposome structure the hydrophobic vitamin E was placed in hydrophobic part of liposome and the hydrophilic vitamin C - on a surface of a bilayer of liposomes' membrane. The formation of the complex is confirmed with either calorimetric or biological experiments. In particular, calorimetric curve of the complex differs considerably from calorimetric peak profiles of the pure DPPC liposomes, that further emphasize the existence of vitamins and liposomes complex. Thanks to the biological experiments, behavior of the complex nanoparticles (vitamin E and DPPC lipid complex) against tumorous Jurkat cells became more effective than adding the same amount of pure vitamin E, which is a quite significant result.

INTERNATIONAL CONFERENCE ON ADVANCES IN SCIENCE AND ARTS ISTANBUL 2017

29 – 31 MARCH 2017, ISTANBUL, TURKEY

NOVEL SCHIFF BASE COMPLEXES, SYNTHESIS, ELECTROCHEMICAL, CATALYTIC AND ANTIMICROBIAL ACTIVITIES

SABRINA BENDIA* AND KAMEL OUARI

Laboratoire d'Electrochimie, d'Ingénierie Moléculaire et de Catalyse Rédox (LEIMCR), Faculté de Technologie, Université Ferhat Abbas Sétif 1, DZ-19000 Sétif, Algeria.

Keywords: Synthesis ; Complex ; Electrochemistry ; Catalytic activities

** Corresponding author : +213 550803331, Sabrina_bendia@univ-setif.dz*

ABSTRACT

Compounds containing an azomethine group (-CH=N-), known as Schiff bases are formed by the condensation of a primary amine with a carbonyl compound. Schiff bases appear to be an important intermediate in a number of enzymatic reactions. A large number of Schiff bases and their complexes have been investigated for their interesting and important properties, such as their ability to reversibly bind oxygen [1], catalytic activity in the hydrogenation of olefines [2], photochromic properties [3,4] and complexing ability towards some toxic metals [5]. Schiff bases are a special class of ligands with a variety of donor atoms exhibiting interesting coordination modes towards various metals [6- 8]. The azomethine linkage in Schiff bases is responsible for the biological activities such as antitumor, antibacterial, antifungal and herbicidal activities [9]

The complexes of the type bidentate Schiff base ligand have been prepared and characterised by analytical, spectral (I.R., electronic, 1H-, 13C- N.M.R.) and electrochemical data. The new complexes are effective catalysts for the oxidation of alcohols to carbonyl compounds but are unable to oxidise alkenes in the presence of TBHP as oxidant. The antimicrobial activity of the ligands and complexes have also been tested against six microorganisms.

INTERNATIONAL CONFERENCE ON ADVANCES IN SCIENCE AND ARTS ISTANBUL 2017

29 – 31 MARCH 2017, ISTANBUL, TURKEY

DESIGN, SPECTRAL CHARACTERIZATION, ELECTROCHEMICAL AND ELECTROCATALYTICAL PROPERTIES TOWARDS ALCOHOLS OXIDATION OF A NOVEL TETRADENTATE COPPER(II)-SCHIFF BASE COMPLEX CONTAINING PYRROL RING

DJOUHRA AGGOUN, ALI OURARI

Laboratoire d'Electrochimie, d'Ingénierie Moléculaire et de Catalyse Redox (LEIMCR), Faculté de Technologie, Université Ferhat Abbas, Route de Béjaia Sétif 19000-Algérie.

Abstract

New tetradentate copper(II)-Schiff base complex (**Cu(II)-L**) containing N_2O_2 donor atoms have been prepared from 6-[3'-(N-pyrrol)propoxy]-2-hydroxyacetophenone and diaminoethane by refluxing in absolute ethanol after that an ethanolic solution of an appropriate amount of Copper(II) acetate monohydrated was dropwisely added under stirring. The obtained complex was characterized by elemental and spectral analysis such as FT-IR, UV–Vis, mass spectra and cyclic voltammetry. The molecular structure of **Cu(II)-L** has been confirmed by X-ray diffraction, showing a triclinic space group P, a = 7.9688 (4), b = 12.8433 (9), c = 14.5166 (11)Å, α = 102.075 (3), β = 90.486 (4), γ = 96.270 (4), Z = 2, R = 0.035. The electrochemical behavior of copper (II) complex containing pyrrole groups has been investigated in DMF and acetonitrile solvents by cyclic voltammetry. Electrochemical reduction of copper(II) complex in acetonitrile produces conducting polymeric films at the electrode surface. The modified electrodes were electrochemically and morphologically characterized and their electrocatalytical properties have been examined. The AFM studies showed that the morphology of polypyrrole (PPy) films on indium tin oxide (ITO) electrodes depends on the number of cyclical scans. The catalytic activity of this complex was found to be efficient towards the electro-oxidation of several organic molecules especially isopropanol than the other kinds of alcohols (ethanol, benzyl alcohol and methanol) and for the reduction of dioxygen and carbon dioxide.

KEY WORDS: *copper (II) complex, mass spectra, X-ray diffraction, modified electrodes, AFM studies, oxidation of alcohols.*

INTERNATIONAL CONFERENCE ON ADVANCES IN SCIENCE AND ARTS ISTANBUL 2017

29 – 31 MARCH 2017, ISTANBUL, TURKEY

OPTICAL PROPERTIES AND TDDFT STUDY OF NOVEL COUMARINS DYES

Houcine AMMAR

Applied Chemistry Laboratory, Faculty of Sciences of Sfax, University of Sfax, *Soukra, BP1170, 3000 Sfax, Tunisia*

Abstract: Coumarin derivatives are an important class of heterocyclic compounds obtained from both nature and synthetic origin. The growing popularity of these compounds, is due to their inherent photochemical characteristics, good solubility and reasonable stability. Coumarin derivatives were also studied for their electronic and photonic applications such as charge-transfer agents, laser dyes, solar energy collectors and nonlinear optical materials, photosensitizers, … They are a key species for organic fluorescent chromophores which are used widely as fluorescent labels and pigments, as fluorescent probes for physiological. Fluorescence characteristic of these compounds can be changed with substitution of different functional groups at the 3- and/or the 7-position of coumarin skeleton. Generally fluorescent coumarin compounds contain an electron donor group at the 7-position like hydroxy, amino and methoxy. At 3-position the modification of the electron-accepting ability of the substituent (benzothiazole, benzimidazole or benzoxazole ring…) improves the fluorescence properties of the coumarins. On the other hand the photophysical properties are extremely dependent of the electron withdrawing substituents, such as formyl group in 3-position. Various researches suggest that extended conjugated system in 3 position of coumarin ring appears quite promising for the optical properties. In this study, six new coumarins dyes were prepared. The structures of the synthesized compounds were confirmed by ^{1}H NMR, ^{13}C NMR spectral data, IR and elemental analysis. Optical properties were studied in dimethyl sulfoxide by UV/Vis absorption and fluorescence spectroscopy. And finally the calculated ultraviolet absorption spectrum is in good agreement with the experimental data.

E-mail: Houcine.Ammar@fss.rnu.tn

INTERNATIONAL CONFERENCE ON ADVANCES IN SCIENCE AND ARTS ISTANBUL 2017

29 – 31 MARCH 2017, ISTANBUL, TURKEY

PHYSICAL PROPRETIES OF NEW POLYESTERS OBTAINED BY R.O.P POLYCONDENSATION

M. Abid, A. Bougarech and S. Hbaieb

Laboratoire de Chimie Appliquée HCGP, Université de Sfax, 3000 Sfax, Tunisie

ABSTRACT

The present study has undertaken the synthesis of Furano-Aliphatic copolyesters (Biomaterials), such as poly(propylene furanic)-co-(polycaprolactone) (PPF-co-PCL), Poly(propylene furanic)-co-(polylactide) (PPF-co-PLA) and Poly(propylene furanic)-co-(polyglycolide) (PPF-co-PGA) were prepared by ring opening polymerization (R.O.P.) using monomers derived from renewable resources[1].

It was established that the choice of catalysts, namely tin octoate, as the most efficient catalyst, is helpful to efficiently control etherification side reactions and obtain high molecular weights. The microstructure of the resulting copolyesters was studied and the random or blocky character of the copolyesters was evidenced. This study has also clearly shown the importance of combining furanic and aliphatic units emphasizing the major role of these units on the thermal properties of the copolymer, and the behavior of degradation by hydrolysis and oxidation. The oxidative degradation proved a mass loss of about 50%.

Submitting author: Majdi ABID, University of Sfax, 3000 Sfax, Tunisia.

E-mail: majdi.abid@fss.rnu.tn

References

[1]. S. Hbaieb, W. Kammoun, C. Delaite, M. Abid, S. Abid, R. El Gharbi, J. Macromol. Sci. Part A, 52, 365 (2015).

INTERNATIONAL CONFERENCE ON ADVANCES IN SCIENCE AND ARTS ISTANBUL 2017
29 – 31 MARCH 2017, ISTANBUL, TURKEY

INVESTIGATION OF COMPATIBILIZER LOADING LEVEL ON THE PROPERTIES OF RECYCLED LOW DENSITY POLYETHYLENE/TPS BLENDS

Barış Öner[1], Tolga Gökkurt[2], Ayşe Aytaç [1,3]
[1] Kocaeli University, Polymer Science and Technology Master Program, 41380 Kocaeli
[2] Polipro Plastic SAN, 41400, Gebze/Kocaeli
[3] Kocaeli Üniversitesi, Chemical Engineering Department, 41380 Kocaeli
baris_oner@windowslive.com

ABSTRACT

In recent years, the growing environmental awareness has encouraged the development of biodegradable polymers to replace synthetic polymers in many applications. As is known, great amount of synthetic polymers has been thrown away from the domestic wastes and this waste creates important environmental problems. One of the solutions of this problem is blended biodegradable materials with synthetic polymers to reduce the amount of synthetic polymers. Another solution is recycling, which is also a good process to reduce the pollution. The aim of this study is using both of these methods and produces a material will be used an environmentally friendly bio-recycled garbage bags. Polyethylene, one of the most vastly used polymer on packaging industry and its wastes are obtained easily. Thermoplastic starch (TPS), being an inexpensive and renewable product and it has good potential as biodegradable filler for synthetic polymers. However, these materials are not compatible due to the difference in their chemical nature, polarity and their blends results in poor mechanical properties. In order to increase compatibility, it is necessary to use a compatibilizer. In this study, the effect of compatibilizers on the properties of recycled polyethylene (r-LDPE) and thermoplastic starch (TPS) blends were investigated. Polyethylene-grafted-Maleic anhydride (LDPE-g-MA), Maleic anhydride modified EPM(EPM-g-MA), Ethylene Maleic Anhydride Copolymer were selected as compatibilizer and they were used two different loading level as 5wt% and 10wt%. r-LDPE/TPS blends were prepared by using a twin screw extruder and characterized by means of mechanical, thermal tests and morphological analyses. It was found that the tensile strength values of the compatibilized blends were slightly changed. In addition the elongation at break values greatly increased as at 2000% with in the groups that contains (LDPE-g-MA).

Key Words: *Recycled LDPE / TPS Blends, Recycled LDPE, Compatibilizer*

INTERNATIONAL CONFERENCE ON ADVANCES IN SCIENCE AND ARTS ISTANBUL 2017
29 – 31 MARCH 2017, ISTANBUL, TURKEY

PROTECTIVE EFFECTS OF VITAMINS C AND E ON BENDIOCARB INDUCED TESTICULAR TOXICITY IN RATS

Gizem BAŞPINAR[1], Enver Kerem DİRİCAN[2], Yusuf KALENDER[1]

[1]Gazi University, Faculty of Science, Department of Biology, 06500, Ankara-Turkey

[2]Akdeniz University, Department of Gynecology and Obstetrics, Antalya, TURKEY

ABSTRACT

Bendiocarb pertains to in a category of pesticides go by the name of carbamates. They are used in gardens, agriculture and homes and also inhibit acetylcholinesterase allowing accumulation of acetylcholine. Oxidative stress is a result of imbalanced reproduction and degradation of ROS inside the body. Vitamin E and vitamin C are recognized as antioxidants, several works have been carried out to specify whether they can protect cells against pesticides' toxic effects. This experimental study on rats was performed with approval of the Animal Experiments Local Ethics Committee followed protocols for ethical standards for the use of laboratory animals. In this study, 8 groups (6 animals in each group) were composed. These groups were control group, vitamin C (100 mg/kg) treated group, vitamin E (100 mg/kg) treated group, vitamin C+vitamin E treated group, bendiocarb (0,8 mg/kg 1/50 LD_{50}) treated group, bendiocarb+vitamin C treated group, bendiocarb+vitamin E treated group, bendiocarb+vitamin C+vitamin E treated group. During 28 days (experimental period) bendiocarb, vitamin C and vitamin E were given to rats daily by gavage. At the end of 4^{th} week, malondialdehyde (MDA) levels, antioxidant enzyme activities [superoxide dismutase (SOD), catalase (CAT), glutathione peroxidase (GPx), glutathione-S-transferase (GST)], investigated compared to control group. No significant differences were observed between control, vitamin C and vitamin E treated groups. By the end of the fourth week, bendiocarb increased the levels of MDA while decrease in SOD, CAT, GPx and GST activities compared with the control group rats. In the present study we found that a carbamate pesticide bendiocarb caused testicular toxicity in rats, vitamins C and E treatment reduced bendiocarb induced toxicity but not protect completely.

Key Words: Bendiocarb, Testicular toxicity, Oxidative stress, Antioxidant Enzymes, Lipid peroxidation

INTERNATIONAL CONFERENCE ON ADVANCES IN SCIENCE AND ARTS ISTANBUL 2017

29 – 31 MARCH 2017, ISTANBUL, TURKEY

PROTECTIVE ROLE OF VITAMINS C AND E ON BENDIOCARB-INDUCED LUNG TOXICITY IN RATS

Merve CEFA, Yusuf KALENDER

Gazi University, Faculty of Science, Department of Biology, 06500, Ankara-Turkey

ABSTRACT

Xenobiotics, including pesticides, are known to enhance the production of reactive oxygen species (ROS), which in turn generate oxidative stress in different tissues. Bendiocarb is a carbamate insecticide known to produceoxidative stress in different human and animal cells. Bendiocarb also induces oxidative stress, and in rat studies this results in the accumulation of lipid peroxidation products in different organs. Cells have several ways to alleviate the effects of oxidative stress. In this study, 8 groups (6 animals in each group) were composed. These groups were control group, vitamin C (100 mg/kg) treated group, vitamin E (100 mg/kg) treated group, vitamin C+vitamin E treated group, bendiocarb (0,8 mg/kg 1/50 LD_{50}) treated group, bendiocarb+vitamin C treated group, bendiocarb+vitamin E treated group, bendiocarb+vitamin C+vitamin E treated group. This experimental study on rats was performed with approval of the Animal Experiments Local Ethics Committee followed protocols for ethical standards for the use of laboratory animals. During 28 days (experimental period) bendiocarb, vitamin C and vitamin E were given to rats daily by gavage. At the end of 4^{th} week, malondialdehyde (MDA) levels and antioxidant enzyme activities [superoxide dismutase (SOD), catalase (CAT), glutathione peroxidase (GPx), glutathione-S-transferase (GST)] and histopathological changes of lung were investigated compared to control group. No significant differences were observed between control, vitamin C and vitamin E treated groups. Light microscopic investigations revealed that 4 weeks of bendiocarb exposure induced numerous histopathological alterations in the lung. By the end of the fourth week, bendiocarb increased the levels of MDA while decrease in SOD, CAT, GPx and GST activities compared with the control group rats. Milder histopathological changes and oxidative damages were observed in animals co-treated with bendiocarb. Thus, it appears that vitamin C and vitamin E ameliorate bendiocarb-induced lung toxicity but not completely**.**

Key Words: Pesticide, Bendiocarb, Lung, Oxidative stress, Histopathology

INTERNATIONAL CONFERENCE ON ADVANCES IN SCIENCE AND ARTS ISTANBUL 2017

29 – 31 MARCH 2017, ISTANBUL, TURKEY

PROTECTIVE ROLE OF VITAMINS C AND E ON BENDIOCARB-INDUCED CARDIOTOXICITY IN RATS

Çağla OCAK, Yusuf KALENDER

Gazi University, Faculty of Science, Department of Biology, 06500, Ankara-Turkey

ABSTRACT

Agrochemicals used in agriculture with a wide diversity of products for plant nourishment, protection of crops and animals. Such substances are also insecticides. Bendiocarb pertains to in a category of pesticides go by the name of carbamates. The toxicity of carbamates which are insecticidally active to animals is based upon their property to inhibit acetylcholinesterase allowing accumulation of acetylcholine. Vitamin E and vitamin C are known as antioxidants, several works have been carried out to specify whether they can protect cells against pesticides' toxic effects. Antioxidant enzymes such as SOD, CAT, GST and GPx protect cellular homeostasis from oxidative damage by ROS generated through the reduction of molecular oxygen. This experimental study on rats was performed with approval of the Animal Experiments Local Ethics Committee followed protocols for ethical standards for the use of laboratory animals. In this study, 8 groups (6 animals in each group) were composed. These groups were control group, vitamin C (100 mg/kg) treated group, vitamin E (100 mg/kg) treated group, vitamin C+vitamin E treated group, bendiocarb (0,8 mg/kg 1/50 LD_{50}) treated group, bendiocarb+vitamin C treated group, bendiocarb+vitamin E treated group, bendiocarb+vitamin C+vitamin E treated group. During 28 days (experimental period) bendiocarb, vitamin C and vitamin E were given to rats daily by gavage. At the end of 4^{th} week, malondialdehyde (MDA) levels and antioxidant enzyme activities [superoxide dismutase (SOD), catalase (CAT), glutathione peroxidase (GPx), glutathione-S-transferase (GST)] and histopathological changes of heart were investigated compared to control group. No significant differences were observed between control, vitamin C and vitamin E treated groups. Light microscopic analyses revealed that bendiocarb induced several histopathological changes in hearth tissues of rats. In co-treatment groups there were mild pathological changes. And also bendiocarb caused increase of MDA level while decrease of antioxidant enzymes. Co-treatment of vitamins C and E provided more ameliorative effects. In the present study we found that bendiocarb caused

cardiotoxicity in rats, vitamins C and E treatment reduced this toxicity, but not protect completely.

Key Words: Pesticide, Bendiocarb, Heart, Oxidative stress, Histopathology

INTERNATIONAL CONFERENCE ON ADVANCES IN SCIENCE AND ARTS ISTANBUL 2017

29 – 31 MARCH 2017, ISTANBUL, TURKEY

THE EFFECT OF DISTORTIONAL DEFORMATION ON THE ELASTIC LATERAL BUCKLING OF THIN-WALLED BOX BEAM

Abdelkader SAOULA[a], Sid Ahmed MEFTAH[a], Amine OSMANI[a], A.BENYAMINA[a]

[a] Laboratoire des Structures et Matériaux Avancés dans le Génie Civil et Travaux Publics, Université de Djellali Liabes, Sidi Bel Abbes, Algérie.

ABSTRACT

The effect of distortional deformation on the elastic lateral buckling of thin-walled box beam elements under combined bending and axial forces is investigated in this paper. For the purpose, an analytical model is developed for the stability of laterally unrestrained box beams according to higher order theory. Ritz and Galerkin's methods are applied in order to discretize the governing equilibrium equations and then the buckling loads are obtained by requiring the singularity of the tangential stiffness matrix. The different solutions are discussed and then compared to the finite element simulation using Abaqus software where shell elements are used in the mesh process.The numerical results reveal that classical stability solutions as those adopted in Eurocode 3 overestimate the real lateral buckling resistance of thin-walled box beam members, particularly for the ones with high ratios between the height and the thickness of the cross-section.

Keywords: Distortion deformation;Lateral-Torsional buckling; box beam; Galerkin's method; Ritz's method.

INTERNATIONAL CONFERENCE ON ADVANCES IN SCIENCE AND ARTS ISTANBUL 2017

29 – 31 MARCH 2017, ISTANBUL, TURKEY

ELECTROCHEMICAL AND MOLECULAR DYNAMICS SIMULATION STUDIES ON THE CORROSION INHIBITION AT CARBON STEEL/HCL INTERFACE USING 2-PYRAZOLINE DERIVATIVE

I. Selatnia[1] , A. Sid[1], M. Benahmed[2]

[1]Laboratory of Analytical Sciences, Matrials and Envirromental (LSAME). Material Structure Departement. Larbi Ben M'Hidi University. Oum El Bouaghi. 04000. Algeria.

[2] Laboratory of Bioactif Molecules and Applications. Tebessa University, Route de Constantine, 12000 Tebessa, Algeria.

ABSTRACT

The inhibition performance of a new synthesized 2- pyrazoline derivative namely: **5-(2,4-dihydroxyphenyl)- 3-(2-acetonaphtone) 2- pyrazoline** (P2), for carbon steel in 1M HCl solution was carried out under various experimental conditions using weight loss, potentiodynamic polarization and EIS and and scanning electron microscopy (SEM) methods.The results indicated that the synthesized compound is an efficient mixed-type inhibitor and its inhibition efficiency increased with increasing the inhibitor concentration. The adsorption of the inhibitor on the carbon steel surface obeys Langmuir isotherm and the thermodynamic parameters were obtained. The interaction between the inhibitor and Fe (100) surface were performed by molecular dynamic simulations.

Key words: *carbon steel, corrosion ,EIS, pyrazoline derivative, MD simulation.*

INTERNATIONAL CONFERENCE ON ADVANCES IN SCIENCE AND ARTS
ISTANBUL 2017
29 – 31 MARCH 2017, ISTANBUL, TURKEY

DIFFERENT FORMULAS CHARACTERIZING TRADITIONAL MANUFACTURE OF COUSCOUS *LEMZEIET*

Fatima Zohra BECILA*; Rania BOUSSEKINE; Ryma MERABTI and Farida BEKHOUCHE

Laboratory of Biotechnology and Food Quality (BIOQUAL)
INATAA, UC1, Constantine, Algeria
Keywords: Fermented wheat, Couscous, Lemzeïet, Manufacture, Semolina
** Corresponding author: becila.fatima@gmail.com.*

ABSTRACT

In Algeria, couscous called *lemzeiet is made from* fermented wheat. Which is characterized by a brown color and a variety of particular flavors and aromas; it is part of our food habits. Its manufacture uses the traditional method. For it, we conducted a descriptive investigation in the cities of Constantine, Mila and Oum el Bouaghi (East of Algeria), with 144 women aged 21 to 98 years. These places were chosen on the basis of the previous investigations out on couscous *lemzeïet* and on fermented wheat (Bekhouche et *al*., 2013; Merabti, 2015). Our objective is to acquire information respecting the homogeneity in the steps of couscous manufacture which are carried out almost in the same manner and to evince the heterogeneity in the choice of the nature and proportions of the semolina used.

Following the results obtained through a statistical analysis which was performed out using XL-STAT Software, 2015.4; it emerges three production formulas are shown, which involve a mixture of fine semolina "*dkak*" (50%) with coarse semolina "*fetla*" (50%) of fermented wheat for forming the grains and to obtain 100% fermented couscous, Or the mixture of fine semolina "*dkak*" of fermented wheat (75%) with the coarse wheat semolina unfermented "*fetla*" (25%) or again the mixture of fine semolina "*dkak*" of fermented wheat (66,66%) with a white couscous (33.33%). It has been observed that the manufacturing schema described by the women interviewed represent the same steps: sizing, sieving, emoting, cooking and drying, and the same utensils used (traditionally manufacture) : *"guassaâ"*, "*steam-cooker*" and indispensable sieves named "*ezzraâ*", "*meâaoudi*", "*reffad*" and "*Sekkat*", which are respectively to: (2532 µm), (800 µm-1140 µm) , (600 µm-1110) and (1000 µm-1140 µm).and with a variable choice in the order of use of the first and last sieve. For each of these sieves a different role and a stitch opening qualifies it according to sieves that are available in the Algerian market; some studies (Bahchachi, 2002 ; Yousfi, 2002 ; Derouiche, 2003 ; Bekhouche et *al* ; 2013) have been carried out in some towns of East and South (in Algeria), which can define the stitch size of these sieves. At the end of the production the rest of the semolina not rolled, it is not recycled because this semolina becomes smooth in the form of the aggregates and impossible of to transformed into couscous. Overall this fraction used for manufactured the bread cake (*galette elmachrob*).

INTERNATIONAL CONFERENCE ON ADVANCES IN SCIENCE AND ARTS ISTANBUL 2017

29 – 31 MARCH 2017, Istanbul, Turkey

ADSORPTION OF ERYTHROSINE DYE FROM AQUEOUS SOLUTION BY COMMERCIAL ACTIVATED CARBON

H. Zeghache[*], *S. Hafsi*

Laboratoire de Chimie Appliquée et Technologie des Matériaux, Département des Sciences de la Matière, Faculté des Sciences Exactes et S.N.V.

Université Larbi Ben M'Hidi, 04000-Oum El Bouaghi, Algérie

E-mail :zeghache_hadjer@hotmail.fr

ABSTRACT

The aim of this research was to study the adsorption of erythrosine dye onto commercial activated carbon. The influence of different parameters, such as contact time, concentration of the dye, temperature and stirring speed have been studied to understand the kinetic of the process of adsorption. The equilibrium data were fitted to the Langmuir and Freundlich isotherm models to estimate the efficiency and capacity of the adsorption.

Keywords: Erythrosine; isotherm; adsorption; activated carbon.

References

[1] K. Jeyajothi. Removal of dyes from textile wastewater using Orange peel as adsorbent. Journal of Chemical and Pharmaceutical Sciences 0974-2115(2014).

[2] V.K. Gupta, A.Mittal , L. Kurup , J. Mittal. Adsorption of a hazardous dye, erythrosine, over hen feathers. Journal of Colloid and Interface Science 304 (2006) 52–57.

[3] M.V. Sureshkumar, C. Namasivayam. Adsorption behavior of Direct Red 12B and Rhodamine B from water onto surfactant-modified coconut coir pith. Colloids and Surfaces A: Physicochem. Eng. Aspects 317 (2008) 277–283.

.

INTERNATIONAL CONFERENCE ON ADVANCES IN SCIENCE AND ARTS
ISTANBUL 2017
29 – 31 MARCH 2017, Istanbul, Turkey

THERMAL AND THERMOMECHANICAL PROPERTIES OF POLY(LACTIC ACID)/ POLYCARBONATE BLENDS

Seda HAZER[1], Meral COBAN[1], Ayse AYTAC[1,2,✉]

[1] Kocaeli University, Chemical Engineering Department, Kocaeli-TURKEY

[2] Polymer Science and Technology Department, University of Kocaeli, TURKEY

Corresponding Author Email: aaytac@kocaeli.edu.tr, Phone: 02623033532

aaytac@gmail.com

ABSTRACT

In recent years, Poly(lactic acid) (PLA) becomes a more common biodegradable polymer due to its good mechanical properties and obtainable from renewable sources. Nevertheless, PLA has some disadvantages such as low thermal stability, toughness and hard to process. Polycarbonate (PC) is well known engineering polymer that has high thermal stability and impact strength properties. PLA has low toughness property so plasticizers and different polymers are used to overcome this issue such as poly(ethylene oxide), poly(ethylene glycol) (PEG), poly(propylene glycol), citrate esters and PC. In the literature, thermal and thermomechanical properties of PLA/PC blends have not been investigated in different loading levels of the PC. In this study, PC loading levels were changed at 10-90 wt% in the PLA/PC blends. The blends were prepared by extrusion process and molded by injection techniques. Characterization of the blends was operated by using Dynamic Mechanical Analysis (DMA), Differential Scanning Calorimetry (DSC), Thermogravimetric Analysis (TGA) and tensile test. Compatibility properties of blends were evaluated by using DMA. The glass transition temperature (T_g) values of PLA and PC are determined at 60 ^oC and 145 ^oC, respectively in DMA. Generally, two T_g values were observed for PLA/PC blends. However, some of the PLA/PC compositions (40/60, 80/20 and 90/10) were determined third T_g value. This peak may be explained as there is copolymerization between PLA and PC. The percentage crystallinity values of the blends were investigated by using DSC. The maximum percentage crystallinity (X_c) was calculated as 11,6% for 50/50 PLA/PC blend. T_m values of blends did not change significantly in DSC. Tensile strength values of the PLA/PC blends did not affected, increasing loading levels of the PC. Maximum elongation at break value was observed for 50/50 PLA/PC blend. Besides, elongation at break values of the PLA/PC blends were decreased by increasing the PC amount after 50/50 PLA/PC ratio.

Keywords - *poly(lactic acid), polycarbonate, mechanical properties*

INTERNATIONAL CONFERENCE ON ADVANCES IN SCIENCE AND ARTS ISTANBUL 2017

29 – 31 MARCH 2017, Istanbul, Turkey

THEORETICAL CALCULATIONS OF MAXIMUM STRESS VALUES IN EQUILIBRIUM FOR BCC FE AND FCC AL WITH RESPECT TO DIFFERENT PLANES

H. Yaşar Ocak[a], Ali Çetin [b], Salih Akbudak[c], Gökay Uğur[d] Şule Uğur[d] and Rahmi Ünal[e]

[a]Phone: 053637007014

hyasar.ocak@dpu.edu.tr

[a]Department of Physics, Faculty of Arts and Science, Dumlupınar University, TR-43100, Kütahya, Turkey

[b]Department of Physics, Faculty of Arts and Science, Osmangazi University, TR-26480, Eskişehir, Turkey

[c]Department of Physics, Faculty of Arts and Science, Adiyaman University, TR-02100, Adiyaman, Turkey

[d]Department of Physics, Faculty of Science, Gazi University, TR-06500, Ankara, Turkey

[e]Department of Mechanical Engineering, Faculty of Engineering, Gazi University, TR-06570, Ankara, Turkey

Abstract: At room temperature Fe has bcc while Al has fcc crystal structure. Lattice parameters for Fe and Al are 2.87 Å and 4.05 Å respectively. Inner exchange potential energies at equilibrium points are minimum. In this study, maximum stress acting on the crystals in equilibrium have been investigated according to crystal (hkl) surfaces. When crystals are in equilibrium, the difference between the C_{12} and C_{44} elastic constants is minimum. Moreover, $(C_{12} – C_{44})$ /2 term which is known as Cauchy relation defines the inner pressure acting on crystal. This pressure is zero or almost zero at equilibrium position. All the physical contributions to any of the system parameters come from crystal planes. We have calculated the maximum stress (T_{hkl}) of Fe and Al in equilibrium using second order elastic constants. Before this calculation, first of all Young constants (E_{hkl}) and Miller indices obtained separately for given planes. Furthermore, relying on the (hkl) Miller indices, dimensionless H parameter and according to Bragg's law β peak width have been calculated. Obtained results showed that Young constants have different ratios in different planes, contrary to this, maximum stress values did not increased or decreased in different planes for Fe and Al crystals. Lastly, possible reflections observed between (100) and (400) planes compared with the values in literature. For two crystals first plane values were in good agreement with experimental values. From these observations, we can infer that mechanical effects have impact on planes.

INTERNATIONAL CONFERENCE ON ADVANCES IN SCIENCE AND ARTS ISTANBUL 2017

29 – 31 MARCH 2017, Istanbul, Turkey

COMBUSTION AND THERMAL BEHAVIOR OF PLASTICIZED AND FLAME RETARDANT POLY(LACTIC ACID) WITH INCREASING NANOCLAY CONTENT

Meral COBAN[1], Ayse AYTAC[1,2, ✉]

[1] *Kocaeli University, Chemical Engineering Department, Kocaeli-TURKEY*
[2] *Polymer Science and Technology Department, University of Kocaeli, Turkey*

Corresponding Author Email: aaytac@kocaeli.edu.tr

ABSTRACT

Poly(lactic acid) (PLA) which is an aliphatic polyester with good mechanical properties and is a good candidate to replace petroleum-based polymers. Use of PLA is limited due to its easy flammability in various industrial areas owing to low limiting oxygen index (LOI) value. Because of the LOI value of PLA was only 19. It is known that the PLA has brittle structure and low toughness. In addition elongation at break value of PLA decreases by adding flame retardant materials to improve the flame resistance. In this study, the effects of increasing nanoclay (NC) content on gained flame retardancy property and plasticized PLA composites were investigated. Firstly, plasticized with polyethylene glycol (PEG) and gained flame retardancy with triphenyl phosphate (TPP) composites of PLA was prepared and then nanoclay was added at a changing loading level between 1-7 wt.%. Samples were produced by using extrusion and injection molding techniques. The thermal and flammability properties were studied. Thermal stability of the samples were analysed by Thermogravimetric Analysis (TGA) and the flammability evaluation was performed by using the limiting oxygen index (LOI), vertically burning (UL-94) and cone calorimeter. Cone calorimeter was employed to evaluate the burning behavior of composites. According to test results, the higher LOI value was observed as 33,4 for including 1 wt% NC sample and V-0 classification was observed by UL-94 test in this sample. The beginning of the decomposition temperatures and 50 wt% loss temperatures were not significantly changed for all prepared samples in TGA. Besides, the increasing to the loading level of NC enhanced of char residue. The results of cone calorimetry showed that the heat release rate (HRR), total heat release (THR), and the mass loss of PLA/PEG/TPP decreases remarkably compared with that of PLA/PEG.

Keywords - *Poly(lactic acid), flame retardant, triphenyl phosphate (TPP), nanoclay*

The authors thank Scientific Research Projects Unit of Kocaeli University (KOUBAP) for financial support under Project number 2015/043.

INTERNATIONAL CONFERENCE ON ADVANCES IN SCIENCE AND ARTS ISTANBUL 2017

29 – 31 MARCH 2017, Istanbul, Turkey

SYNTHESIS, CHARACTERIZATION, ELECTROCHEMISTRY AND CATALYTIC ACTIVITY OF IRON(III) AND MANGANESE(III) TETRADENTATE SCHIFF BASE COMPLEXES

Hana amira GUADOURI*, Sabrina BENDIA and Kamel OUARI

Laboratoire d'Electrochimie, d'Ingénierie Moléculaire et de Catalyse Rédox (LEIMCR), Faculté de Technologie, Université Sétif-1, DZ-19000 Sétif, Algeria

Keywords: Iron complex; Schiff base; Synthesis; Electrochemistry; Catalytic activity

* *Corresponding author : hanaamiraguadouri@gmail.com*

ABSTRACT

The chemistry of manganese and iron complexes is investigated recently since these metals are present in a various biological redox systems including peroxidases [1], catalases [2], superoxide dismutases [3], dioxygenases [4] and lipoxidases [5]. The manganese is also present in the oxygen evolving complex (OEC) in photosystem II of green plants which consists of a tetranuclear manganese cluster [6]. Iron proteins are significant functions in transport of oxygen [7] and electron transfer in a range of metabolic reactions [8]. The manganese-oxo species, which are produced in many biological systems, participate in various important biochemical processes.

The differences in catalytic ability of heme enzymes and thevariety of catalyzed reactions are ascribed to dissimilarities of theprosthetic group, the nature of the heme environment, and thesteric accessibility of the heme iron. A particular role is assignedto the identity of the proximally coordinated amino acid residue,which differs between enzymes, e.g. cysteine in cytochrome P450and chloroperoxidase, histidine in cytochrome c peroxidase andhorseradish peroxidase or tyrosine in catalase. Since this aspectseems to be especially crucial for the ability to cleave the O Obond of dioxygen or peroxide and catalyze different types of reac-tions, numerous studies on the nature of the proximal ligand onthe formation and reactivity of high-valent iron(IV) oxo species,were undertaken.

We are reporting here on the synthesis and characterization of new two iron(III) and manganese(III) complexes by IR, UV-Vis and H-NMR spectroscopic techniques. Electrochemical behavior has been investigated by cyclic voltammetry on glassy carbon electrode in DMSO at 100 mV/s scan rate.

INTERNATIONAL CONFERENCE ON ADVANCES IN SCIENCE AND ARTS ISTANBUL 2017
29 – 31 MARCH 2017, Istanbul, Turkey

SYNTHESIS, CHARACTERIZATION, CRYSTAL STRUCTURE AND ANTIMICROBIAL ACTIVITY OF NEW SCHIFF BASES DERIVED FROM ANTHRANILONITRILE

N. BENAROUS [a], A. CHEROUANA [a], E. AUBERT [b], P. DURAND [b], S. DAHAOUI [b]

[a] *Unité de Recherche de Chimie de l'Environnement et Moléculaire Structurale (CHEMS), Département de Chimie, Université des frères Mentouri, Constantine 1, 25000 Constantine, Algeria*

[b] *Cristallographie, Résonance Magnétique et Modélisations (CRM2), Faculté des Sciences et Technologies, Université de Lorraine, BP 70239, Boulevard des Aiguillettes, 54506 Vandœuvre-lès-Nancy Cedex, France*

E-mail : bbnesrine@gmail.com

Keywords: Schiff base, anthranilonitrile, FT-IR, UV–Vis, X-ray diffraction and antimicrobial activity.

Since their discovery, by the German chemist Hugo Schiff in 1864, Schiff bases have a wide application area. They have been used in areas such as, catalysis[1] corrosion inhibitors [2], coordination chemistry [3], Moreover; they have been widely used not only in inorganic and biological field [4], but also in developing new applications in the area of non-linear optical (NLO) materials [5] and as new molecular magnets [6].

As antibacterial, anticancer, antifungal, antiinflammatory, antimicrobial and antiviral, many Schiff bases are used as starting materials in the preparation of important pharmaceuticals and medicinal drugs.

In this work, three crystal structures of new Schiff bases (**Fig 1.**), prepared by the reaction of anthranilonitrile with corresponding aldehyde in ethanol are reported.

The (E)-2-(2,4-dichlorobenzylideneamino)benzonitrile, present two crystal structure, the first polymorph ***(I)***, crystallizing in the monoclinic space group $P2_1/c$, was obtained by slow evaporation of solution reaction, however, the crystal of the second one ***(II)***, who crystallize in the orthorhombic space group Pbca, was obtained in high temperature condition. On the other hand (E)-2-(4-nitrobenzylideneamino)benzonitrile ***(III)***, crystallizing in the monoclinic space group $P2_1/c$, was obtained in the same condition as ***(I)***.

The dihedral angles between the two aromatic rings are 4.81° in ***(I)***, 82.26 ° in ***(II)***, 27.77° and 39.35 ° in ***(III)*** respectively in molecule ***A*** and ***B***. An antimicrobial activity was estimated by determination of the minimal inhibitory concentration (***MIC***) using the well-diffusion method.

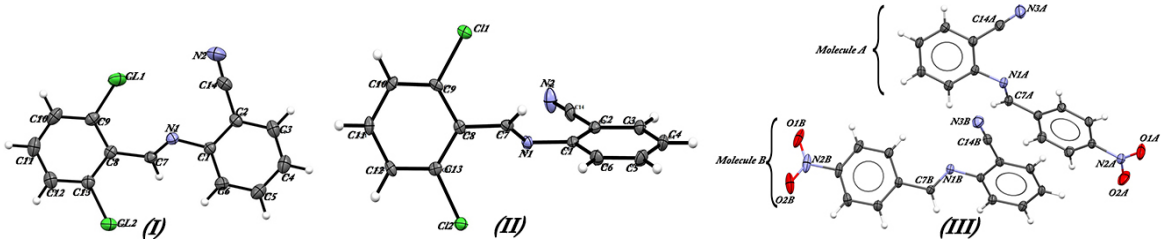

Fig. 1. ORTEP view of the asymmetric unit of ***(I)***, ***(II)*** and ***(III)***; Displacement ellipsoids are drawn at the 50% probability level.

INTERNATIONAL CONFERENCE ON ADVANCES IN SCIENCE AND ARTS ISTANBUL 2017
29 – 31 MARCH 2017, Istanbul, Turkey

CRYSTAL STRUCTURE, VIBRATIONAL AND MAGNETIC PROPERTIES OF A NOVEL ORGANIC-INORGANIC HYBRID MATERIAL $(C_{15}H_{29}N_2O)_2CoCl_4$

Rim ESSALHI, Walid AMAMOU and Fatma ZOUARI

Laboratoire des Sciences des Matériaux et d'Environnement, Université de Sfax, BP 1171, 3000 Sfax, Tunisia

ABSTRACT

The single crystals of organic-inorganic hybrid compound (cyclohexyl(ethoxy)carbonoimidioyl)cyclohexanaminium)tetrachloroccobaltate (II) , was obtained by slow evaporation of an aqueous solution at room temperature and characterized by a single-crystal X-ray diffraction, IR, Raman spectroscopy and magnetic measurements. The entitled compound crystallizes into triclinic system of P-1 space group. The Co(II) ion of the $[CoCl_4]^{2-}$anion shows a tetrahedral coordinating geometry. The atomic arrangement can be described as the layers of the organic and inorganic groups. The cohesion of the atomic arrangement is ensured by hydrogen bonding (N-H…Cl). The room temperature infrared and Raman spectra were recorded and analyzed on the basis of literary data to gain more information about the entitled compound. The magnetic susceptibility measurements in the temperature range 2-100 K shows that the complex displays a weak antiferromagnetic exchange interaction at very low temperatures.

Key words: Magnetic, X-ray diffraction, hydrogen bonds, Infrared and Raman.

INTERNATIONAL CONFERENCE ON ADVANCES IN SCIENCE AND ARTS ISTANBUL 2017

29 – 31 MARCH 2017, Istanbul, Turkey

INVESTIGATIONS OF MODES AND RELATIVE REFRACTIVE INDEX DIFFERENCE IN WEAKLY GUIDING OPTICAL FIBERS

Ali ÇETİN[1]* and Hamza Y. OCAK[2]

[1] Physics Department, Faculty of Science and Letters, Eskisehir Osmangazi University, Eskisehir, Turkey

[2] Physics Department, Faculty of Science and Letters, Dumlupinar University, Kutahya, Turkey

*Correspondence author: acetin@ogu.edu.tr

ABSTRACT

This study presents an investigation on modes and relative index difference in weakly guiding optical fiber waveguides. Optical fiber waveguide is one of media that light is guided inside. This waveguide is composed two elements that named core and cladding. If the difference between refractive indexes the core and the cladding is very small, these optical fibers are referred weakly guiding fibers. Some simple numerical computations are presented in order to propagate the light inside this structure efficiently. Refractive index profiles and mode numbers in optical fibers investigated. The variation of the relative refractive index difference in an optical fiber with respect to the wavelength, refractive index and radius is examined.

Key words: Optical fiber, Refractive index, Modes

INTERNATIONAL CONFERENCE ON ADVANCES IN SCIENCE AND ARTS ISTANBUL 2017

29 – 31 MARCH 2017, Istanbul, Turkey

PRODUCTION AND CHARACTERIZATION VANADIUM OXIDE FILMS BY SPRAY PYROLYSIS

Olcay Gençyılmaz[1]*, Enis Sert[1]

[1]Çankırı Karatekin University, Department of Material and Material Process, Çankırı,

ogencyilmaz@karatekin.edu.tr

[1]Çankırı Karatekin University, Department of Physics, Çankırı,

esert@karatekin.edu.tr

ABSTRACT

In this study, vanadium oxide thin films, which are promising for production of novel electrochemical capacitors and other novel devices, were produced by ultrasonic spray pyrolysis technique over glass substrates at 300 °C. In order for development of the physical properties of the produced films, they were annealed at 500 °C in air ambient. Structural, optical, electrical and surface properties of the films were investigated using different techniques such as XRD, optical transmittance, absorbance, four probe methods and atomic force microscopy, respectively. The effect of annealing on the optical, structural, electrical and surface properties of the films was also investigated.

INTERNATIONAL CONFERENCE ON ADVANCES IN SCIENCE AND ARTS ISTANBUL 2017

29 – 31 MARCH 2017, Istanbul, Turkey

STRUCTURAL CHARACTERIZATION OF COPPER/NICKEL OXIDE FILMS DEPOSITED BY SILAR PROCESS

TURAN TAŞKÖPRÜ

Department of Physics, Çankırı Karatekin University, Çankırı, Turkey
E-mail :turanian@rocketmail.com

In this study, Ni-doped copper oxide films were deposited onto glass substrates using the successive ionic layer adsorption and reaction (SILAR) method. The effect of Ni doping on structural properties of CuO was investigated. The films have been examined to evaluate the structural properties. X-ray diffraction spectra have revealed the presence of both the CuO (Tenorite, Monoclinic) and (Cu0.2Ni0.8)O (Copper Nickel Oxide, Cubic) phases for the film doped with 5 at. % concentration of Ni. The average crystallite size was calculated using the Scherrer's formula as 52 nm and 25 nm for the CuO and $Cu_{0.2}Ni_{0.8}O$ phases, respectively.

INTERNATIONAL CONFERENCE ON ADVANCES IN SCIENCE AND ARTS ISTANBUL 2017

29 – 31 MARCH 2017, Istanbul, Turkey

STUDY OF THE ANTI-CORROSIVE POWER OF A NEW SCHIFF BASE MOLECULE 4-4' –BIS (2-PYRROLE CARBOXALDEHYDE) DIPHENYL DIIMINO ETHER ON MILD STEEL X48 IN HCL MEDIUM

Imene Benmahammed[1], Tahar Douadi[2] and Saifi Issaadi[3].

[1.2] Laboratoire d'Electrochimie des Matériaux Moléculaires et Complexes LEMMC, Département de Génie des Procédés, Faculté de Technologie, Université Ferhat Abbas Sétif-1, 19000-Algérie.

[3] Faculté des sciences, Département de Chimie, Université Ferhat Abbas Sétif-1, 19000- Algérie.

Email[1] : imene.benmahammed@yahoo.fr

ABSTRACT

Mild steel is a major construction material in various industries including food, petroleum, and power production, chemical and electrochemical industries. The acidic solutions are widely used to remove the rust and scales from the corroded mild steel for further uses such as rolling, galvanizing etc. This process of rust removal is pronounced as acid pickling and the acid pickling requires use of corrosion inhibitors in order to protect metals from aggressive dissolution. Due to their ease synthesis and high effectiveness, organic compounds containing hetero atoms particularly oxygen (O), nitrogen (N) and sulfur (S) have been reported as good corrosion inhibitors for mild steel in acidic media [1–2].

Literature survey reveals that a large number of organic compounds having heteroatoms have been utilized as effective corrosion inhibitors for mild steel in acidic media.

The inhibition effect of a new Schiff base, namely 4,4'-Bis (2-Pyrrole Carboxaldehyde) Diphenyl Diimino Ether has been studied against the corrosion of mild steel in the solution HCl 1M. The results were analyzed by using the curves of polarization, the electrochemical impedance and the method of weight loss. The curves of polarization indicate that the examined compound is a mixed inhibitor; this last showed an inhibitory efficacy of 91.85% at 5.10^{-3} M. the adsorption of this compound obeys Langmuir adsorption isotherm**.**

Keywords: Schiff base, corrosion, mild steel, HCl medium, inhibitory efficacy.

References

[1] S.A. Ali, M.T. Saeed, S.V. Rahman, Corros. Sci. 45 (2003) 253–266.

[2] M.A. Quraishi, I. Ahamad, A.K. Singh, S.K. Shukla, B. Lal, V. Singh, Mater. Chem. Phys. 112 (2008) 1035–1039.

INTERNATIONAL CONFERENCE ON ADVANCES IN SCIENCE AND ARTS ISTANBUL 2017
29 – 31 MARCH 2017, Istanbul, Turkey

EFFECTS OF PAA-CHYMOTRYPSIN CONJUGATE ON FLUORESCENCE LIFETIME DISTRIBUTIONS OF PM-BSA COMPLEX

***Sama Amer Abbas**
Yıldız Technical University
İstanbul, Türkiye

Ümmügülsüm Polat
Yıldız Technical University
İstanbul, Türkiye

İbrahim Ethem Özyiğit
Yıldız Technical University
İstanbul, Türkiye

Emine Karakuş
Yıldız Technical University
İstanbul, Türkiye

Keywords: PAA, Fluorescence, Chymotrypsin
* Corresponding author: Sama Amer Abbas, Phone: 05378267502 Fax:
E-mail address: smsmamer99@yahoo.com

ABSTRACT

The properties and application areas of biomacromolecules can be further expanded and improved by attaching synthetic polymers. Immobilization of enzymes has been taken to improve catalytic stability of enzymes and can expand the application of the neutral catalysts. There are many materials, including synthetic organic polymers, biopolymers, hydrogels, inorganic supports, and smart polymers, to be used to immobilize enzymes, and good activity retention, and enhanced thermo-stability are often observed [1]. A range of functional groups, which can be used in the covalent immobilization of enzymes, including amino, hydroxyl, carboxyl and phenolic groups. The physical structure and chemical composition of support can also influence the microenvironment of the immobilized species and consequently their biological properties [2]. Fluorescence lifetime distributions may be useful tool to monitor the changes of enzyme activity by the conjugation with polymers. Fluorophores which are embedded in different regions of proteins have different chemical environments and exhibit varying fluorescence lifetimes that produce a specific fluorescence lifetime distribution profile. The changes of the distribution by free and conjugated protease activity may provide useful information about the hydrolysis process of the protein substrate [3].

INTRODUCTION

Conjugation and immobilization of enzymes with polymers may provide wide range industrial applications in medicine, diagnosis, life sciences, microelectronics and material sciences [4]. In this work we examined the activity of covalent conjugate of chymotrypsin with polyacrylic acid (PAA) on fluorescence lifetime distributions of PM-BSA complex by using time resolved spectrofluorometer. The aim of the study is to research whether if there were remarkable differences between the proteolytic effects of free chymotrypsin and PAA-conjugated chymotrypsin on the fluorescence lifetime distributions of PM-BSA complex.

RESULTS AND DISCUSSION

The lifetime distributions exhibited different profiles in varying range of lifetime scales. The lifetime distribution produced by the activity of PAA-conjugated chymotrypsin has shifted to the longer lifetime ranges than the one produced by the activity of free chymotrypsin; that means the polarity range of the peptides in the hydrolysate produced from the conjugate shifted to the shorter scale relatively. This phenomenon indicates that the conjugation with PAA has decreased the proteolytic capacity of chymotrypsin.

CONCLUSION

According to the differences between the lifetime distributions produced from free and conjugated chymotrypsin, the covalent modification of chymotrypsin with PAA may not be convenient application to improve the kinetic properties. The remarkable differences between the fluorescence lifetime distributions revealed that lifetime distribution analysis may provide valuable and useful information to track the changes in proteolytic activities by conjugation.

NOMENCLATURE

Covalent modification may not be proper operation for every polymer-protease synthesis. Lifetime distribution analysis may be very useful tool to track the changes in proteolytic activities by conjugation.

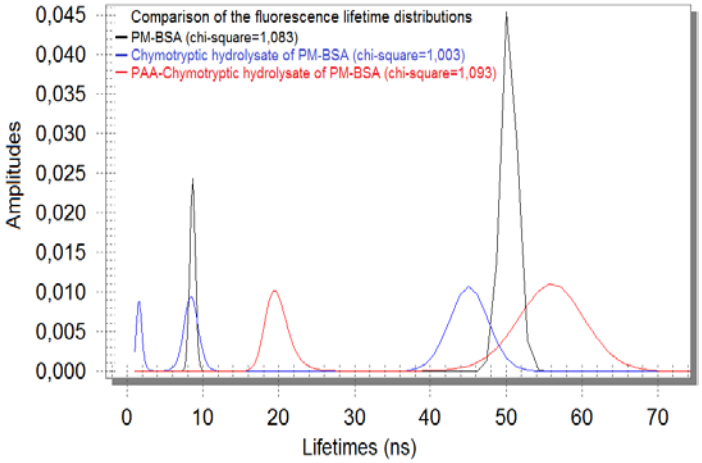

Figure 1. Fluorescence Lifetime Distributions

REFERENCES

1. Y. Zhang, L. Fan, T. Zhi, , L. Zhang, H. Huang and H. Cheni. J.Polym. Sci. 47, 3232-40 (2009).
2. Y. Chen, E.T. Kang, K.G. Neoh and K.L. Tan. European Polymer Journal, 36, 2095-2103 (2000).
3. J.R. Lakowicz, Principles of Fluorescence Spectroscopy, third edition, Springer Science+Business Media, LLC, New York (2006).
4. G.T. Hermanson, Bioconjugate Techniques, second edition, Academic Press, Elsevier Inc., New York (2008).

INTERNATIONAL CONFERENCE ON ADVANCES IN SCIENCE AND ARTS ISTANBUL 2017

29 – 31 MARCH 2017, Istanbul, Turkey

INVESTIGATION THE INHIBITORY ACTION OF 6-METHYL -3 - [3 (2'-THIOFÈNYL) PROP-2-ENOYL)] PYRAN-2, 4-DIONE FOR MILD STEEL IN *1M OF* H_2SO_4

Salima Tabti[a*], Amel Djedouani [b], Amira hamimid[c] and Lamia Semmari[c].

[a] *Laboratoire Matériaux et systèmes électroniques, Universite Mohamed el Bachir El Ibrahimi, El Anasser, 34000, Bordj Bou Arreridj, Algeria*
[b]*Laboratoire de Physicochimie Analytique et Cristallochimie des Materiaux Organometalliques et Biomoleculaires, Universite Constantine 1, 25000, Constantine, Algeria*
[c]*Departement SM, Faculté des Scienc, Universite Mohamed el Bachir El Ibrahimi, El Anasser, 34000, Bordj Bou Arreridj, Algeria*

**For correspondence: Email: thabti_sa@yahoo.fr (S. TABTI); Phone: +213663495071;*

ABSTRACT

Heterocyclic compounds offer a high degree of structural diversity and have proven to be broadly and economically useful as therapeutic agents, energy, materials inhibitors..

The synthesis of 6-METHYL -3 - [3 (2'-THIOFÈNYL) PROP-2-ENOYL)] PYRAN-2, 4-DIONE derivatives of dehydroacetic acid which has several sites coordinations electron donors (oxygen, sulfur), allowed us to make their characterization by various spectroscopic methods (IR, UV-Vis, XRD and NMR: H^1) and electrochemical methods.

The study of the inhibitory pathway of organic materials has given us an idea of application of our material synthesized to study the interface electrode / electrolyte and their inhibitory effect on even a mild-steel (MS) in H_2SO_4 by potentiodynamic polarization and electrochemical impedance spectroscopy (EIS).

Experience has shown us clearly that our material is a good inhibitor against corrosion control in low concentrations

Keywords: DHA, IR, XRD, NMR, corrosion inhibitor.

INTERNATIONAL CONFERENCE ON ADVANCES IN SCIENCE AND ARTS ISTANBUL 2017
29 – 31 MARCH 2017, Istanbul, Turkey

EFFECTS OF PAA-CHYMOTRYPSIN CONJUGATE ON FLUORESCENCE LIFETIME DISTRIBUTIONS OF PM-BSA COMPLEX

***Sema Amer**
Yıldız Technical University
İstanbul, Türkiye

Ümmügülsüm Polat
Yıldız Technical University
İstanbul, Türkiye

İbrahim Ethem Özyiğit
Yıldız Technical University
İstanbul, Türkiye

Emine Karakuş
Yıldız Technical University
İstanbul, Türkiye

Keywords:PM-BSA,Chymotrypsin,Fluorescence
** Corresponding author:Emine Karakuş,05301807573*
E-mail address: eminekaraku@gmail.com

ABSTRACT

The properties and application areas of biomacromolecules can be further expanded and improved by attaching synthetic polymers. Immobilization of enzymes has been taken to improve catalytic stability of enzymes and can expand the application of the neutral catalysts. There are many materials, including synthetic organic polymers, biopolymers, hydrogels, inorganic supports, and smart polymers, to be used to immobilize enzymes, and good activity retention, and enhanced thermo-stability are often observed [1]. A range of functional groups, which can be used in the covalent immobilization of enzymes, including amino, hydroxyl, carboxyl and phenolic groups. The physical structure and chemical composition of support can also influence the microenvironment of the immobilized species and consequently their biological properties [2]. Fluorescence lifetime distributions may be useful tool to monitor the changes of enzyme activity by the conjugation with polymers. Fluorophores which are embedded in different regions of proteins have different chemical environments and exhibit varying fluorescence lifetimes that produce a specific fluorescence lifetime distribution profile. The changes of the distribution by free and conjugated protease activity may provide useful information about the hydrolysis process of the protein substrate [3].

INTRODUCTION

Conjugation and immobilization of enzymes with polymers may provide wide range industrial applications in medicine, diagnosis, life sciences, microelectronics and material sciences [4]. In this work we examined the activity of covalent conjugate of chymotrypsin with polyacrylic acid (PAA) on fluorescence lifetime distributions of PM-BSA complex by using time resolved spectrofluorometer. The aim of the study is to research whether if there were remarkable differences between the proteolytic effects of free chymotrypsin and PAA-conjugated chymotrypsin on the fluorescence lifetime distributions of PM-BSA complex.

RESULTS AND DISCUSSION

The lifetime distributions exhibited different profiles in varying range of lifetime scales. The lifetime distribution produced by the activity of PAA-conjugated chymotrypsin has shifted to the longer lifetime ranges than the one produced by the activity of free chymotrypsin; that means the polarity range of the peptides in the hydrolysate produced from the conjugate shifted to the shorter scale relatively. This phenomenon indicates that the conjugation with PAA has decreased the proteolytic capacity of chymotrypsin.

,

ABSTRACT

The properties and application areas of biomacromolecules can be further expanded and improved by attaching synthetic polymers. Immobilization of enzymes has been taken to improve catalytic stability of enzymes and can expand the application of the neutral catalysts. There are many materials, including synthetic organic polymers, biopolymers, hydrogels, inorganic supports, and smart polymers, to be used to immobilize enzymes, and good activity retention, and enhanced thermo-stability are often observed [1]. A range of functional groups, which can be used in the covalent immobilization of enzymes, including amino, hydroxyl, carboxyl and phenolic groups. The physical structure and chemical composition of support can also influence the microenvironment of the immobilized species and consequently their biological properties [2]. Fluorescence lifetime distributions may be useful tool to monitor the changes of enzyme activity by the conjugation with polymers. Fluorophores which are embedded in different regions of proteins have different chemical environments and exhibit varying fluorescence lifetimes that produce a specific fluorescence lifetime distribution profile. The changes of the distribution by free and conjugated protease activity may provide useful information about the hydrolysis process of the protein substrate [3].

INTRODUCTION

Conjugation and immobilization of enzymes with polymers may provide wide range industrial applications in medicine, diagnosis, life sciences, microelectronics and material sciences [4]. In this work we examined the activity of covalent conjugate of chymotrypsin with polyacrylic acid (PAA) on fluorescence lifetime distributions of PM-BSA complex by using time resolved spectrofluorometer. The aim of the study is to research whether if there were remarkable differences between the proteolytic effects of free chymotrypsin and PAA-conjugated chymotrypsin on the fluorescence lifetime distributions of PM-BSA complex.

RESULTS AND DISCUSSION

The lifetime distributions exhibited different profiles in varying range of lifetime scales. The lifetime distribution produced by the activity of PAA-conjugated chymotrypsin has shifted to the longer lifetime ranges than the one produced by the activity of free chymotrypsin; that means the polarity range of the peptides in the hydrolysate produced from the conjugate shifted to the shorter scale relatively. This phenomenon indicates that the conjugation with PAA has decreased the proteolytic capacity of chymotrypsin.

CONCLUSION

According to the differences between the lifetime distributions produced from free and conjugated chymotrypsin, the covalent modification of chymotrypsin with PAA may not be convenient application to improve the kinetic properties. The remarkable differences between the fluorescence lifetime distributions revealed that lifetime distribution analysis may provide valuable and useful information to track the changes in proteolytic activities by conjugation.

NOMENCLATURE

Covalent modification may not be proper operation for every polymer-protease synthesis. Lifetime distribution analysis may be very useful tool to track the changes in proteolytic activities by conjugation.

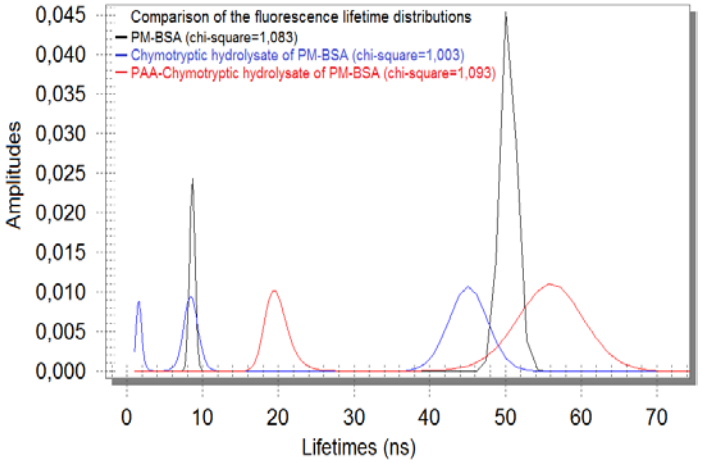

Figure 1. Fluorescence Lifetime Distributions

REFERENCES

1. Y. Zhang, L. Fan, T. Zhi, , L. Zhang, H. Huang and H. Cheni. J.Polym. Sci. 47, 3232-40 (2009).
2. Y. Chen, E.T. Kang, K.G. Neoh and K.L. Tan. European Polymer Journal, 36, 2095-2103 (2000).
3. J.R. Lakowicz, Principles of Fluorescence Spectroscopy, third edition, Springer Science+Business Media, LLC, New York (2006).
4. G.T. Hermanson, Bioconjugate Techniques, second edition, Academic Press, Elsevier Inc., New York (2008).

INTERNATIONAL CONFERENCE ON ADVANCES IN SCIENCE AND ARTS ISTANBUL 2017
29 – 31 MARCH 2017, Istanbul, Turkey

FLUORESCENCE LIFETIME DISTRIBUTION CHANGES OF "N-(1-PYRENYL)MALEIMIDE (PM) – BOVINE SERUM ALBUMIN (BSA); PM-BSA" COMPLEX BY THE PROTEOLYTIC EFFECTS OF FREE AND POLYACRYLIC ACID (PAA)-CONJUGATED TRYPSIN

***Ümmügülsüm Polat**
Yıldız Technical University
İstanbul, Türkiye

İbrahim Ethem Özyiğit
Yıldız Technical University
İstanbul, Türkiye

Emine Karakuş
Yıldız Technical University
İstanbul, Türkiye

Keywords:Fluorecence, Trypsin, PM-BSA
Corresponding author: Emine Karakuş, 05301807573
E-mail address: eminekaraku@gmail.com

ABSTRACT

Surrounding of a fluorophore by more than one polar molecule results a variation in fluorescence lifetimes showing a distribution profile. Proteins provide different chemical environments to fluorophores and exhibit specific fluorescence lifetime distributions. Hydrolysis of proteins by proteases causes specific distribution profiles depending on the peptide content of the hydrolysates [1]. Conjugation with polymers may provide a higher thermal stability to enzymes [2,3] and at this point, it is important to know whether if the enzyme activity was changed by the conjugation. The distributional data may be used for tracking the proteolysis processes and may enable to monitor the changes in activity of the proteases by conjugation with polymers.

INTRODUCTION

In this work we studied the changes of the activity of trypsin by conjugation with polyacrylic acid (PAA), by using the fluorescence lifetime distributions of PM-BSA complex by using time resolved spectrofluorometer. The aim of the study is to detect whether if there were remarkable differences between the proteolytic effects of free trypsin and PAA-conjugated trypsin on the fluorescence lifetime distributions of PM-BSA complex.

RESULTS AND DISCUSSION

The fluorescence lifetime distribution of the hydrolysate produced from PM-BSA by the proteolytic activity of PAA-trypsin conjugate showed a longer distribution profile according to the hydrolysate produced by free trypsin. The result indicates uncompleted hydrolysis. The conjugation may have caused the active side of trypsin to be partially covered.

CONCLUSION

According to the resultant fluorescence lifetime distribution of the hydrolysate, the covalent modification of trypsin with PAA may not be proper conjugation method.

NOMENCLATURE

For synthesis of polymer-protease conjugates, the covalent conjugation method needs to be approached carefully because it may cause inhibition and fluorescence

lifetime distribution analysis may be useful tool to monitor the differences between the proteolytic hydrolysates.

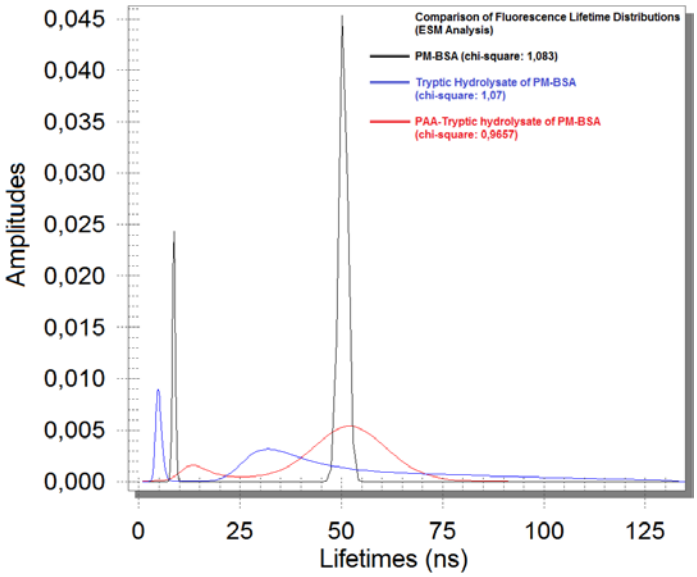

Figure 1. Fluorescence Lifetime Distributions

REFERENCES

1. J.R. Lakowicz, Principles of Fluorescence Spectroscopy, third edition, Springer Science+Business Media, LLC, New York (2006).
2. B. Jung and P. Theato, (2013) “Chemical Strategies for the Synthesis of Protein–Polymer Conjugates”, Adv Polym Sci, 253: 37–70.
3. G.T. Hermanson, Bioconjugate Techniques, second edition, Academic Press, Elsevier Inc., New York (2008).

INTERNATIONAL CONFERENCE ON ADVANCES IN SCIENCE AND ARTS ISTANBUL 2017
29 – 31 MARCH 2017, Istanbul, Turkey

THERMAL AND SMALL-SCALE EFFECTS ON VIBRATION OF EMBEDDED ARMCHAIR SINGLE-WALLED CARBON NANOTUBES.

*** Tayeb BENSATTALAH**
University of Ibn Khaldoun, Faculty of applied Sciences, Civil Engineering Department, Tiaret-Algeria

Mohamed ZIDOUR
University of Ibn Khaldoun, Faculty of applied Sciences, Civil Engineering Department, Tiaret-Algeria

Tahar hassaine DAOUADJI
University of Ibn Khaldoun, Faculty of applied Sciences, Civil Engineering Department, Tiaret-Algeria

Abdelouahed TOUNSI
Hydrology Laboratory, University of Sidi Bel Abbes, Faculty of Technology, Civil Engineering Department, Algeria

El Abbas ADDA BEDI
Hydrology Laboratory, University of Sidi Bel Abbes, Faculty of Technology, Civil Engineering Department, Algeria

Keywords: Nano-composite, vibration, armchair, elasticity, small-scale
** Corresponding author:, Phone: +213 794679266*
E-mail address: t_satal@yahoo.fr

ABSTRACT

The non-local Timoshenko beam theory (TBT) has been implemented to investigate the free vibration of armchair single-walled carbon nanotubes (SWCNTs) embedded in an elastic medium including the thermal effects. The mechanical properties of nano-composite (carbon nanotubes and polymer matrix) are treated as the functions of temperature change and the analytical solution is derived according to the governing equations of non-local Timoshenko beam models. Influence of small-scale coefficient, the vibrational mode number, the matrix of nano-composite and aspect ratio on the frequency ratio of the armchair (SWCNTs) including the thermal effect are studied and discussed. The research work reveals the significance of the small-scale coefficient, the vibrational mode number, the elastic medium and aspect ratio of length to diameter on the frequency ratio. It is also demonstrated that some properties of free vibrations of the armchair (SWCNTs) are dependent on the change of temperature.

INTRODUCTION

Since the single-walled carbon nanotube (SWCNT) and multi-walled carbon nanotube (MWCNT) are discovered by Iijima[1,2]. A new era has been evolved in the field of nano science and technology. Carbon nanotubes are cylindrical macromolecules composed of carbon atoms in a periodic hexagonal arrangement which have received tremendous attention from various branches of science. Varieties of experimental, theoretical, and computer simulation approaches indicate that carbon nanotubes (CNTs) possess superior electronic, thermal and mechanical properties[3,4], others studies have showed that they have good properties so they can be used for nanoelectronics, nanodevices and nanocomposites[5,6].

Due to difficulties encountered in experimental methods to predict the responses of nanostructures under different loading conditions, the molecular dynamics (MD) simulations are used. But the computational problem here is that the time steps involved in the (MD) simulations are limited by the vibration modes of the atoms to be of the order of femto-seconds (10-15 s) [7]. Jin et al.8 used (MD) and force-constant approach and reported the Young's modulus of (SWCNTs) to be about 1236±7GPa.

The continuum mechanics methods have been effectively used to study mechanical behaviors of not only single-walled carbon nanotubes (SWCNTs) but also MWCNTs [9,10]. Recently, the continuum mechanics approach has been widely and successfully used to study the responses of nanostructures, such as the static [11,12], the buckling [13,14], free vibration15,16, wave propagation17, 18 and thermo-

mechanical analysis of (CNTs)[19, 20]. More recently, utilize a continuum shell model to predict the mechanical behavior of single and multi-walled carbon nanotubes embedded in a polymer or metal matrix and their results are compared with molecular dynamics simulations. Fu et al.[21] have studied the nonlinear vibration analysis of embedded carbon nanotubes.

In this study the equivalent Young's and shears modulus of armchair (SWCNTs) using an energy-equivalent model obtained by Wu et al[22] is used in the formulations.

The vast majority of structural theories are derived using the constitutive assumptions that the stress at a point depends only on the strain at the point. On the other hand, nonlocal elasticity theory, advanced by Eringen[23,24], is based on the hypothesis that the stress at a point is a function of strains at all points in the continuum. Tounsi et al25, Boumia et al[26] and Heireche et al[27] ,Zidour et al28 have used the nonlocal elasticity constitutive equations to study vibration and buckling of CNTs. There are some studies for vibration of (CNTs), which assumes (CNT) as a cylindrical shell. On those researches, wave propagation in (CNTs) raises a significant and challenging. Natsuki et al.[29] investigated sound wave propagation in (CNTs) by means of a simplified shell theory. Benzair et al [30] have analyzed the thermal effect on vibration of single-walled carbon nanotubes using nonlocal Timoshenko beam theory

This study is concerned with the use of the non-local Timoshenko elastic beam model to analyse the wave propagation of armchair single-walled carbon nanotubes (SWCNTs) embedded in an elastic medium. The characteristic of transverse wave propagating in (CNTs) is investigated and the effects of both small scale parameter and elastic medium including the temperature change are discussed. The vibrational mode number and aspect ratio of the (SWCNTs) are studied and discussed using the nonlocal Timoshenko beam model.

ARMCHAIR SINGLE-WALLED CARBON NANOTUBE ATOMIC STRUCTURE:

A single-walled carbon nanotube (SWCNT) is theoretically assumed to be made by rolling a graphene sheet Figure 1. The fundamental structure of carbon nanotubes can be classified into three categories as zigzag, armchair and chiral in terms of the chiral vector ($\vec{C}_h$) shown in Figure 1.

The chiral vector can be expressed in terms of base vectors ($\vec{a}_1$) and ($\vec{a}_2$) Figure 1:

$$\vec{C}_h = m\vec{a}_1 + n\vec{a}_2 . \quad (1)$$

where the integer pair (n, m) are the indices of translation, which decide the structure around the circumference.

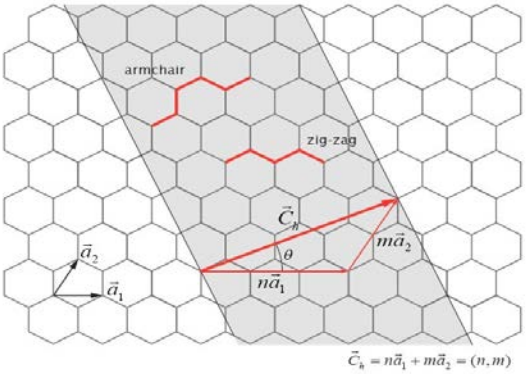

Fig 1. Hexagonal lattice of graphene sheet including base vectors.

The diameter of armchair (SWCNTs) for (n=m) is given by [31]:

$$d = \frac{3na}{\pi} \quad (2)$$

where (a) is the length of the carbon–carbon bond which is(0.142×10^{-9} m).

Based on the link between molecular mechanics and solid mechanics, Wu et al22 developed an energy-equivalent model for studying the mechanical properties of SWCNTs. Using the same method, the equivalent Young's modulus of armchair nanotube are expressed as

$$E_a = \frac{4\sqrt{3}}{3}\frac{KC}{3Ct + 4Ka^2t\left(\lambda_{a1}^2 + 2\lambda_{a2}^2\right)} \quad (3)$$

whereKandCare the force constants,t is the thickness of the nanotube, and the parameters λ_{a1}, λ_{a2} and λa are given by

$$\lambda_{a1} = \frac{4-\cos^2(\pi/2n)}{16+2\cos^2(\pi/2n)},$$

$$\lambda_{a2} = \frac{\sqrt{12-3\cos^2(\pi/2n)}\cos(\pi/2n)}{32+4\cos^2(\pi/2n)} \quad (4)$$

Letting $n\to\infty$, the expressions of Young's modulus of a graphite sheet is given by

$$E_g = \frac{8\sqrt{3}KC}{18Ct + Ka^2t} \quad (5)$$

NONLOCAL ELASTICITY THEORY OF (SWCNTS):

Based on Eringen nonlocal elasticity model[32,24] the stress at a reference point is considered to be a functional of the strain field at every point in the body. In the limit when the effects of strains at points other than x are neglected, one obtains classical or local theory of elasticity. For homogeneous and isotropic elastic solids, the constitutive

equation of non-local elasticity can be given by[24]. Non-local stress tensor (t) at point (x') is defined by:

$$\sigma_{ij,j} = 0$$

$$\sigma_{ij}(x) = \int K(|x-x'|,\ \tau) C_{ijkl}\varepsilon_{kl}(x')dV(x'), \quad \forall x \in V$$

$$\varepsilon_{ij} = \frac{1}{2}\left(u_{i,j} + u_{j,i}\right)$$

(6)

where (Cijkl) is the classical, macroscopic stress tensor at point x', σij and εij are stress and strain tensors respectively. $K(|x-x'|,\ \tau)$ is the kernel function and ($\tau = e0a/l$) is a material constant that depends on internal and external characteristic length (such as the lattice spacing and wavelength)., where (e0) is a constant appropriate to each material, a is an internal characteristic length, e.g., length of (C–C) bond, lattice parameter, granular distance, and (l) is an external characteristic length.

As solving of integral constitutive equation (4) is difficult, a simplified equation in one-dimensional differential form is used as a basis of all nonlocal constitutive formulation,

$$\left(1 - e0a^2\frac{\partial^2}{\partial x^2}\right)\sigma_x = E\varepsilon_x$$

(7)

$$\left(1 - e0a^2\frac{\partial^2}{\partial x^2}\right)\tau_{xz} = G\gamma_{xz}$$

(8)

where (E) and (G) are the Young's and shear modulus of the material respectively, and (γ) is the shear strain. Thus, the scale coefficient (e0a) in the modelling will lead to small-scale effect on the response of structures at nano size.

The expressions of the axial strain and the shear strain are33

$$\varepsilon_x = z\frac{\partial\psi}{\partial x}, \quad \gamma_{xz} = \frac{\partial w}{\partial x} + \psi \qquad (9)$$

where (ψ) is the rotation angle of cross-section of the beam and (w) is the transverse displacement.

The shear force and the bending moment can be defined by:

$$M = \int_A z\sigma_x dA, \quad T = \int_A \tau_{xy} dA \qquad (10)$$

Based on Equations. 7, 8, 9 and 10 the bending moment (M) and the shear force (T) for the non-local model can be expressed as

$$\left(1 - e0a^2\frac{\partial^2}{\partial x^2}\right)M = EI\frac{d\psi}{dx} \qquad (11)$$

$$\left(1 - e0a^2\frac{\partial^2}{\partial x^2}\right)T = \beta GA\left(\frac{dw}{dx} + \psi\right)$$

(12)

$$I = \int_A z^2 dA$$

where (A) is the moment of inertia, (A) is the cross-section area of the beam, and (β) the shear correction factor which is used to compensate for the error due to the constant shear stress assumption is (9/10) for a circular shape of the cross area.34

NONLOCAL TIMOSHENKO BEAM MODEL FOR EMBEDDED SWCNTS USING THERMAL EFFECT

Using Timoshenko beam theory, the force equilibrium equations and the moment on the one-dimensional structure for transverse vibrations of an elastic beam can be easily provided follows:

$$\frac{\partial T}{\partial x} - \rho A\frac{\partial^2 w}{\partial t^2} + f(x) + N_t\frac{\partial^2 w}{\partial x^2} = 0$$

(13)

$$\frac{\partial M}{\partial x} - T = \rho I\frac{\partial^2\psi}{\partial t^2}$$

(14)

where (x) is the axial coordinate, (w) is the transverse deflection of the (SWCNT), (M) and (T) are the resultant bending moment and shear force, respectively (Ψ) is the rotation angle of cross section of the beam, (ρ) is the mass density of the material, (A) is the area of the cross section of the nanotubs beam, (I) the second moment of inertia,. f(x) is the interaction pressure per unit axial length between the nanotube and the surrounding elastic medium, (Nt) denote an additional axial force and is dependent on temperature θ and thermal coefficient α of the nanotube; the force can be expressed as35

$$N_t = -\alpha EA\theta \qquad (15)$$

Based on Equations. (11), (13) and (14), the following relation can be obtained:

$$M = EI\frac{\partial\psi}{\partial x} + e0a^2\left[\rho A\frac{\partial^2 w}{\partial t^2} - f(x) - N_t\frac{\partial^2 w}{\partial x^2} + \rho I\frac{\partial^3\psi}{\partial x\partial t^2}\right.$$

(16)

Substituting Equation. (12) into Equation. (13), we can obtain

$$T = \beta AG\left(\frac{\partial w}{\partial x} + \psi\right) + e0a^2\left[\rho A\frac{\partial^3 w}{\partial x\partial t^2} - \frac{\partial f(x)}{\partial x} - N_t\frac{\partial^3 w}{\partial x^3}\right]$$

(17)

Substituting Equation. (17) into Equation. (13), we can obtain

$$\beta AG\left(\frac{\partial^2 w}{\partial^2 x}+\frac{\partial \psi}{\partial x}\right)-\left(1-e0a^2\frac{\partial^2}{\partial x^2}\right)\left[\rho A\frac{\partial^2 w}{\partial t^2}-f(x)-N_t\frac{\partial^2 w}{\partial x^2}\right]=0 \quad (18)$$

Based on Eqs. (16), (17) and (14), it can be derived that

$$EI\frac{\partial^2 \psi}{\partial x^2}-\beta AG\left(\frac{\partial w}{\partial x}+\psi\right)-\left(1-e0a^2\frac{\partial^2}{\partial x^2}\right)\left[\rho I\frac{\partial^2 \psi}{\partial t^2}\right]=0 \quad (19)$$

Since finding an analytical solution is possible for simply supported boundary conditions for the present problem, the (SWNT) beam is assumed simply supported. As a result, the boundary conditions have the following form16:

$$w(x,t)=\overline{W}e^{i\omega t}\sin(\lambda x), \qquad \psi(x,t)=\overline{\psi}e^{i\omega t}\cos(\lambda x), \qquad \lambda=\frac{N\pi}{L} \quad (20)$$

Where ($\overline{W}$) is the amplitude of deflection of the beam and ($\overline{\psi}$) is the amplitude of the slope of the beam due to bending deformation alone. In addition, (ω) is the frequency. In addition the pressure per unit axial length, acting on the outermost tube due to the surrounding elastic medium, can be described by a Winkler-type.

$$f=-kw \quad (21)$$

Substitution of Equation.(18) into Equations. (18) and (19) gives two branches of wave dispersion relation and the correspondent frequencies via nonlocal Timoshenko beam model are as follows;

$$\omega_{NT}=\sqrt{\frac{1}{2}\left(\alpha_n\pm\sqrt{(\alpha_n)^2-4\beta_n}\right)} \quad (22)$$

With

$$\alpha_n=\frac{\beta IG\lambda^2+\beta AG+EI\lambda^2}{\rho I\left(1+e0a^2\lambda^2\right)}+\frac{k+N_t\lambda^2}{\rho A},$$

$$\beta_n=\frac{E\beta G\lambda^4}{\rho^2\left(1+e0a^2\lambda^2\right)^2}+\frac{\left(\beta GA+EI\lambda^2\right)\left(k+N_t\lambda^2\right)}{\rho^2 AI\left(1+e0a^2\lambda^2\right)}$$

THE MATERIAL PROPERTIES OF ARMCHAIR SINGLE-WALLED CARBON NANOTUBE:

The proposition for the material properties used in continuum beam models in CNTs will be studied through an analysis of a single walled nanotube shown in Figure 2. The length of the SWNT is (L), and the diameter of the mid-surface is (d), the effective thickness of (CNTs) taken to be 0.258×10^{-9} m , the mass density ρ =2300 kg/m3, the poisson ratio υ=0.25 and the thermal expansion coefficient at high temperature $\alpha0=1.1\times10^{-6}C^{-1}$. Another, Young's modulus, thermal expansion coefficients of CNTs and The spring constant of polymer matrix, under temperature changes environments, which may be a function of temperature change as follows36:

$$E=E^0\left(1-0.0005\theta\right), \quad \alpha=\alpha^0\left(1+0.002\theta\right) \text{ and } k=k^0\left(1-0.0003\theta\right) \quad (23)$$

where E0 and α0 express elastic modulus and thermal expansion coefficient of CNTs under a high temperature, respectively. k^0 is spring constant of polymer matrix under a temperature environment.

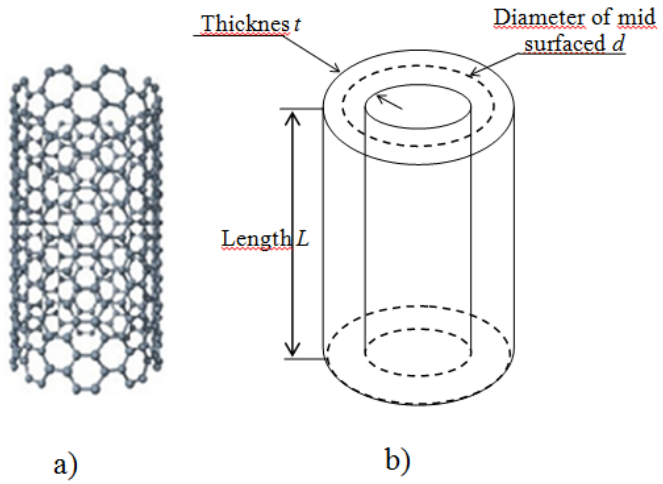

Fig 2. Single and Layout of single-walled nanotubes of carbone a) Single nanotubes type armchair (10,10). b) Layout of a single-walled carbon nanotube.

RESULTS AND DISCUSSIONS

Based on the formulations obtained above with the nonlocal Timoshenko beam model, the vibration properties of single-walled nanotubes (SWCNTs) are discussed here. In addition, the results including the effect of small-scale coefficient, the vibrational mode number and aspect ratio of the (SWCNTs).

To investigate the effect of scale parameter, elastic medium and temperature change on vibrations of single-walled nanotubes, the results including and excluding the nonlocal parameter, the thermal effect and the elastic parameter are compared. It follows that the ratios of the results are respectively given by:

$$\chi_N=\frac{\omega_{NT}}{\omega_{LT}}, \qquad \chi_{th}=\frac{(\omega_{NT})_{nth}}{(\omega_{NT})_{th}}, \qquad \chi_k=\frac{(\omega_{NT})_{nk}}{(\omega_{NT})_k} \quad (24)$$

Where (ω_{LT} , ω_{NT}) are the frequency based on the local and nonlocal Timoshenko beam respectively. $(\omega_{NT})_k$, $(\omega_{NT})_{th}$ are the frequency based on the nonlocal Timoshenko beam with the thermal and elastic medium effect respectively. Furthermore, ($(\omega_{NT})_{nk}$, $(\omega_{NT})_{nth}$) are the frequency based on the nonlocal Timoshenko beam model without the thermal effect (θ = 0) and elastic medium (k=0).

In the present study, the figure 3 depicts the values of Young's modulus for various chirality of single armchair carbon nanotube under temperature change. It can be concluded that as the chirality of armchair carbon nanotube increase the Young's modulus increase and the rate of this increase reduces for higher values of chirality. This significance is attributed to the influence of diameter, because the stiffness of carbon nanotube increase when the diameter increase. In additional it is observed that as temperature change increase the Young's modulus decrease. The reason for this decreasing of Young's modulus is attributed to the effect of temperature change on the fundamental atomics structure of carbon nanotubes.

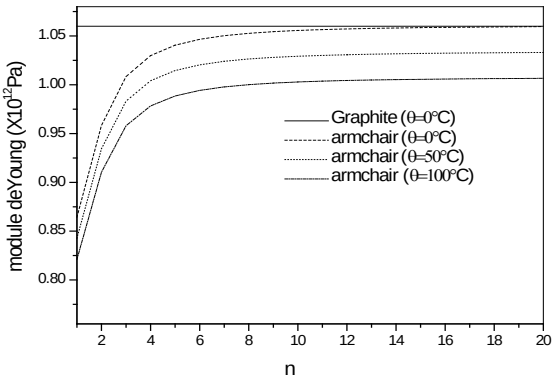

Fig 3. The distributions of Young's modulus for armchair nanotube under thermal effect.

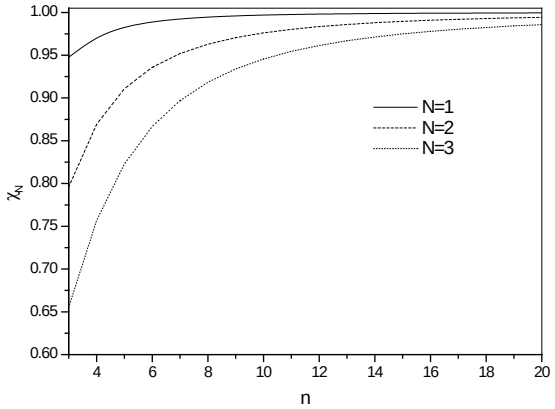

Fig 4. The distributions of ratio (χ_N) for different mode number (N) and armchair chirality (n) in the case of high temperature where (e0a=0.5×10-9m, L/d=10).

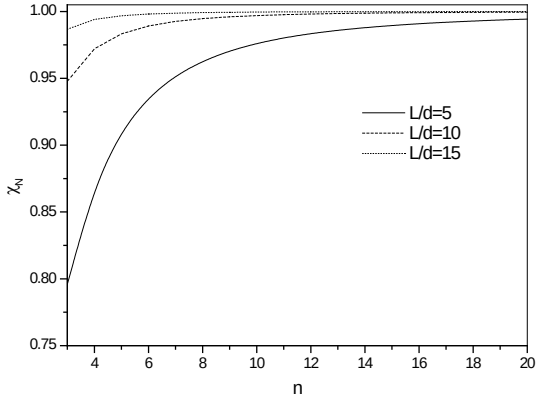

Fig 5. Effect of aspect ratio and chirality of carbon nanotube on the values of ratio (χ_N) in fundamental mode and high temperature where (e0a=0.5×10-9m).

Figures 4 and 5 shows the dependence of the frequency ratios (χN) on the chirality of armchair carbon nanotube (n) for high temperature. The frequency ratio (χN) serves as an index to assess quantitatively the scale effect on CNT vibration solution. It is observed from Figures 4 and 5 that the frequency ratios (χN) are less than unity. This means that the application of the local Timoshenko beam model for CNT analysis would lead to an overprediction of the frequency if the scale effect between the individual carbon atoms in CNTs is neglected. The frequency ratios (χN) exhibit a dependence on the structure characteristic of armchair carbon nanotube n. However for armchair CNTs with larger values of n, this dependence becomes very weak. The reason for this phenomenon is that a carbon nanotube with smaller lattice indices of translation n has a larger curvature, which results in a more significant distortion of C–C bonds. Furthermore, the chirality of nanotube has not obvious effect on the ratio (χN) when the fundamental mode is considered.

It can be seen from Figure 4 that the scale effect on the frequency ratios (χN) diminishes with increasing the index of translation (n) and becomes more significant with the increase of the vibrational mode N. However, the scale effect becomes less significant with the increase of the length-to-diameter ratio (L/d) as shown in Figure 5. Therefore, it is clear that the small scale effect is significant for short CNTs. It can be noted that for these types of CNTs (short CNTs), the transverse shear strain becomes important, and thus, the nonlocal Euler-Bernoulli beam theory cannot be used.

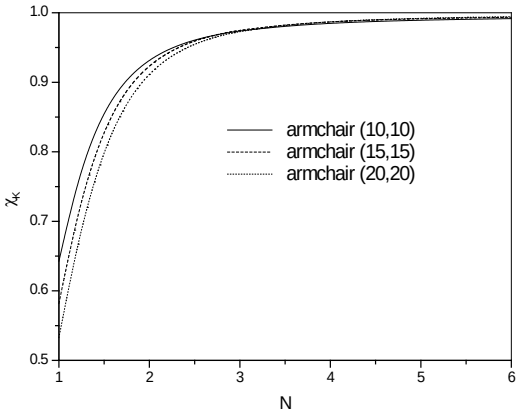

Fig 6. Relation between the values of ratio (χ_K), the mode number (N) and chirality of carbon nanotube embedded in an elastic medium. The value of (L/d) is 10 and (e0a=2×10-9m).

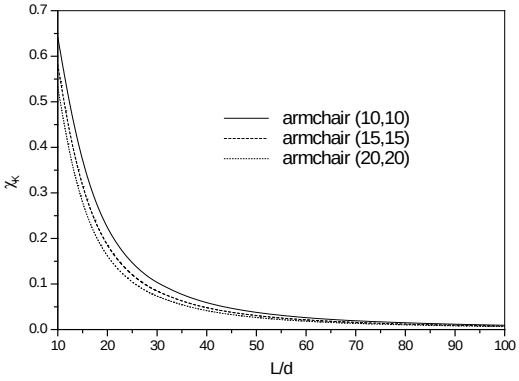

Fig 7. Relation between the values of ratio (χ_K), the aspect ratio (L/d) and chirality of carbon nanotube embedded in an elastic medium in fundamental mode where (e0a=2×10-9m).

In figures 6 and 7 the frequency ratio (χk) serves as an index to assess quantitatively the elastic medium effect on CNT vibration solution. The figure 6 illustrate the dependence of the frequency ratios (χk) on the chirality and vibrational mode number of armchair (SWCNTs) embedded in an elastic medium. It is clearly seen from Figure 6 that the frequency ratios (χk) are less than unity. This means that the frequency of nonlocal Timoshenko beam model with elastic medium is big then the frequency if the elastic medium is neglected. It can be concluded that the availability of elastic medium decrease the frequency of (SWCNTs). In additional, the ranges of the frequency ratios (χk) for this chirality of carbon nanotube are quite different. For armchair (15,15), the range is the smallest for armchair (20,20), but the range is the largest for armchair (10,10). The reason for this difference is that the increasing or decreasing of carbon nanotube diameter. Furthermore, it is clearly that as the vibrational mode number increases, the Winkler modulus parameter effect on the frequency ratios (χN) decreases. This significance of elastic medium effects in higher modes is attributed to the influence of small wavelength for higher modes. For smaller wavelengths, interactions between atoms are increasing and this leads to an decrease in the Winkler modulus parameter effect.

Figure 7 for fundamental mode of armchair (SWNTs) and scale coefficient (e0a=2×10-9m) shows the dependence of the frequency ratio (χN) versus on the aspect ratio (L/d) (length-to-diameter ratios). However for (CNTs) with low values of diameters, this dependence becomes littel weak. The reason for this phenomenon is that a carbon nanotube with smaller diameter has a larger curvature, which results in a more significant distortion of (C–C) bonds.

In additional, it can be seen from the figure 7 that as the aspect ratios of armchair (SWCNT) increase the effect of elastic medium increases. However, it is observed, that the elastic medium effect on the frequency ratios (χk) is more affected by low aspect ratio values. Therefore, it is clear that the scale effect is significant for long (CNTs).

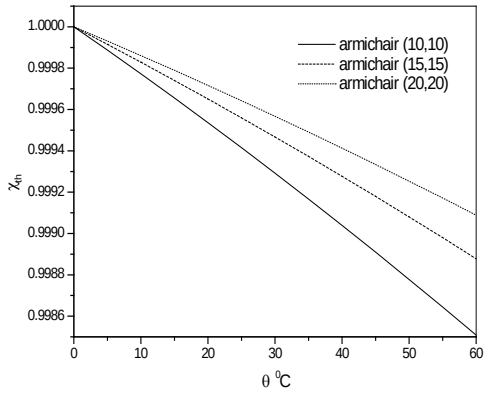

Fig 8. Thermal effects on vibration frequencies for different armchair SWCNTs with fundamental mode and L/d= 10 in the case of high temperature.

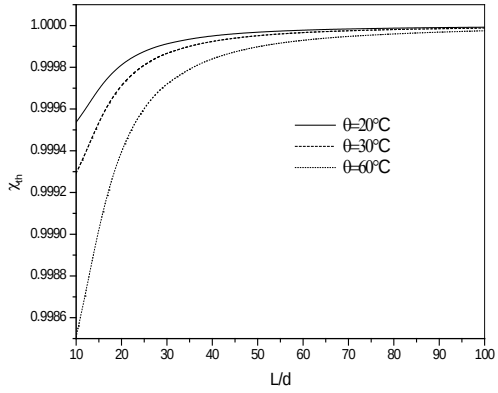

Fig 9. Thermal effects on vibration frequencies for different aspect ratios (L/d) of nanotube with the vibrational

mode number N = 1and e0a=2×10^{-9}m, in the case of high temperature.

The effect of temperature change on the vibration frequencies for case of high temperature are shown in Figure 8 with the aspect ratio L/d= 10 and the vibrational mode N= 1. It can be seen that the frequency ratios (χth) is vary linearly with the temperature change. The ratio χth increases monotonically as the temperature increases, indicating that the effect of temperature change leads to an increase of the fundamental frequency and especially for the armchair nanotubes with higher index of translation (n).

With the vibrational mode number N=1 and the scale effect e0a=2×10-9m, the relationship among the ratio (χth) , the temperature change θ and the aspect ratio L/d is indicated in Figure 9 for case of high temperature. It is clearly seen from Figure 9, that the frequency ratios (χth) exhibit a dependence on the temperature change. However for armchair CNTs with larger values of L/d, this dependence becomes very weak and becomes more significant with the increase of the aspect ratio L/d. Therefore, it is clear that the small scale effect is significant for short CNTs.

Table 1. Lists the values of frequency ratios (χ_N) for different chirality's, and aspect ratios (L/d) of armchair carbon nanotube with and without elastic medium using nonlocal Timoshenko beam model (e0a=0.5×10-9m, θ=25°C, N=1).

	Without elastic medium		With elastic medium	
(n,m) armchair	L/d =10	L/d =30	L/d =10	L/d =30
(3,3)	0.542341	0.887281	0.668700	0.995323
(4,4)	0.652581	0.931650	0.770124	0.998033
(5,5)	0.732798	0.954607	0.836646	0.998996
(6,6)	0.790938	0.967799	0.881042	0.999420
(7,7)	0.833449	0.976016	0.911314	0.999636
(8,8)	0.864996	0.981523	0.932433	0.999756
(9,9)	0.888811	0.985306	0.947503	0.999829
(10,10)	0.907101	0.988033	0.958489	0.999875
(11,11)	0.921381	0.990082	0.966658	0.999906
(12,12)	0.932705	0.991631	0.972844	0.999927
(13,13)	0.941811	0.992861	0.977606	0.999943
(14,14)	0.949230	0.993837	0.981325	0.999954
(15,15)	0.955343	0.994662	0.984271	0.999963
(16,16)	0.960435	0.995317	0.986632	0.999970
(17,17)	0.964718	0.995813	0.988546	0.999975
(18,18)	0.968350	0.996277	0.990113	0.999979
(19,19)	0.971457	0.996629	0.991407	0.999982
(20,20)	0.974133	0.996958	0.992486	0.999984

The values of ratio (χ_N) of armchair (CNTs) with different length-to-diameter ratios and different chirality type armchair with and without elastic medium based on the non-local Timoshenko beam model are listed in Table 1. A constant value of nonlocal parameter, (e0a=2×10-9m) and vibrational mode number (N=1). The results show the dependence of the frequency ratios (χN) on the different chirality's of carbon nanotube, aspect ratio and, Winkler modulus parameter. In addition, the values of frequency ratios also increase as the value of diameter of carbon nanotubes increases for different chirality's of carbon nanotube. Therefore, it can be found that the values of frequency ratios are slightly larger for the higher length-to-diameter ratios and are very larger for the lower length-to-diameter ratios.

The detailed comparisons of frequency ratios (χ_{th}) for different chirality's of armchair carbon nanotube and mode number (N) including the thermal effect using nonlocal Timoshenko beam model are listed in Table 2. The ratio of the length to the diameter, (L/d), is 10 and the scale coefficients, (e0a=2×10^{-9}m).

Table 2. Lists the values of frequency ratios (χ_{th}) for different chirality and mode number (N) of armchair carbon nanotube including the thermal effect using nonlocal Timoshenko beam model (e0a=2×10-9m, L/d=10).

	N=1			N=6		
(n,m)	θ=0	θ=30	θ=60	θ=0	θ=30	θ=60
armchair						
(3,3)	0.999404	0.998146	0.996089	0.997988	0.993714	9866690
(4,4)	0.999538	0.998561	0.996965	0.998784	0.996205	0.991965
(5,5)	0.999617	0.998808	0.997488	0.999185	0.997458	0.994620
(6,6)	0.999669	0.998970	0.997830	0.999414	0.998172	0.996134
(7,7)	0.999706	0.999085	0.998071	0.999556	0.998617	0.997075
(8,8)	0.999733	0.999170	0.998251	0.999651	0.998911	0.997698
(9,9)	0.999755	0.999237	0.998393	0.999717	0.999116	0.998132
(10,10)	0.999772	0.999292	0.998508	0.999764	0.999265	0.998445
(11,11)	0.999787	0.999337	0.998604	0.999800	0.999375	0.998679
(12,12)	0.999799	0.999376	0.998687	0.999827	0.999460	0.998858
(13,13)	0.999810	0.999410	0.998758	0.999848	0.999526	0.998998
(14,14)	0.999820	0.999440	0.998821	0.999865	0.999579	0.999110
(15,15)	0.999828	0.999467	0.998878	0.999878	0.999622	0.999200
(16,16)	0.999836	0.999491	0.998928	0.999890	0.999657	0 999274
(17,17)	0.999843	0.999512	0.998973	0.999899	0.999686	0.999336
(18,18)	0.999850	0.999532	0.999015	0.999907	0.999710	0.999387
(19,19)	0.999855	0.999550	0.999053	0.999914	0.999731	0.999431
(20,20)	0.999861	0.999567	0.999089	0.999919	0.999749	0.999469

The results show the dependence of the frequency ratios (χth) on the mode number, temperature change and chirality's of armchair carbon nanotube. It is noted that the ratio (χth) increases as the temperature θ increases, and becomes more significant with the variation of chirality, in additional, It is clearly that the scale effect on the frequency ratios (χth) increases when the vibrational mode number increases.

CONCLUSIONS:

This paper studies the vibration analysis of armchair (SWCNTs) embedded in an elastic medium including the thermal effects, based on non-local Timoshenko beam theory. The theoretical formulations include the small scale effect, the vibrational mode number, the aspect ratio and the chirality number of armchair carbon nanotube. The governing equations and the boundary conditions for the (SWCNTs) are solved and the frequency ratios are obtained.

According to the study, the results showed the dependence of the frequency ratios (χN ,χk ,χth) on the chirality of carbon nanotube, small-scale coefficients, Aspect Ratio, the temperature change, mode number and Winkler modulus parameter. However, it is observed that the small scale effect on the frequency ratios (χN) is more affected by higher mode number and low aspect ratio values. The reason of this more affected is attributed to the influence of small wavelength and short (CNTs). Using the nonlocal Timoshenko beam model (NTB), the frequency ratios (χN) are affected by the increasing or decreasing of carbon nanotube diameter. The reason for this phenomenon is that a carbon nanotube with smaller diameter has a larger curvature, which results in a more significant distortion of (C–C) bonds. For case of high temperatures, the ratio (χ_{th}) increases monotonically as the temperature θ increases, and becomes more significant with the variation of chirality. In additional, the rate of increase of frequency ratio reduces for higher values of Winkler modulus. The reason of this significant is that the elastic medium grips the single nanotube and forces it to be stiffer. Therefore, the small-scale effect is found to be more significant without the presence of elastic medium. The presented investigation may be is helpful in the application of (CNTs), such as nanoelectronics, nanodevices, mechanical sensors and nanocomposites.

ACKNOWLEDGMENTS

This research was supported by the Algerian National Thematic Agency of Research in Science and Technology (ATRST) and university of Sidi Bel Abbes (UDL SBA) in Algeria.

REFERENCES

[1] Iijima S. Helical microtubules of graphitic carbon. *Nature* 1991; 354: 56-8.

[2] Iijima S, Ichihashi T. Single-shell carbon nanotubes of 1 nm diameter. *Nature* 1993; 363: 603.

[3] Dresselhaus MS and Avouris P. Carbon nanotubes: synthesis, structure, properties and application. *Top Appl Phys* 2001; 80: 1-11.

[4] Bachtold A, Hadley P, Nakanishi T and Dekker C. Logic circuits with carbon nanotube transistors. *Science* 2001; 294(5545): 1317-21.

[5] Dai H, Hafner JH, Rinzler AG, Colbert DT and Smalley RE. Nanotubes as nanoprobes in scanning probe microscopy. *Nature* 1996; 384: 147-50.

[6] Thostenson ET, Ren Z and Chou TW. Advances in the science and technology of carbon nanotubes and their composites. *Compos. Sci. Technol*. 2001; 61: 1899-912.

[7] Ranjbartoreh AR, Ghorbanpour A and Soltani B. Double-walled carbon nanotube with surrounding elastic medium under axial pressure. *Physica E* 2007; 39: 230-239.

[8] Jin Y and Yuan FG. Simulation of elastic properties of single-walled carbon nanotubes. *Compos. Sci. Technol*. 2003; 63: 1507.

[9] Gafour Y, Zidour M, Tounsi A, Heireche H and Semmah A. Sound wave propagation in zigzag double-walled carbon nanotubes embedded in an elastic medium using nonlocal elasticity theory. *Physica E* 2013; 48: 118-123.

[10] Benguediab S, Tounsi A, Zidour M and Semmah A. Chirality and scale effects on mechanical buckling properties of zigzag double-walled carbon nanotubes. Composites Part B 2014; 57: 21-24.
[11] Wang X and Cai H. Effects of initial stress on non-coaxial resonance of multi-wall carbon nanotubes. Acta Mater. 2006; 54: 2067-2074.
[12] Reddy JN and Pang SD. Nonlocal continuum theories of beams for the analysis of carbon nanotubes. J. Appl. Phys. 2008;103: 023511.
[13] Tounsi A, Benguediab S, Adda Bedia E, Semmah A and Zidour M. Nonlocal effects on thermal buckling properties of double-walled carbon nanotubes. Advances in Nano Research, 2013;1(1): 1-11.
[14] Amara K, Tounsi A, Mechab I and Adda Bedia EA. Nonlocal elasticity effect on column buckling of multiwalled carbon nanotubes under temperature field. Appl. Math. Model. 2010; 34: 3933-3942.
[15] Zidour M, Benrahou KH, Semmah A, Naceri M, Belhadj HA, Bakhti K and Tounsi A. The thermal effect on vibration of zigzag single walled carbon nanotubes using nonlocal Timoshenko beam theory. Computational Materials Science 2012; 51: 252-260.
[16] Benzair A, Tounsi A, Besseghier A, Heireche H, Moulay N and Boumia L. The thermal effect on vibration of single-walled carbon nanotubes using nonlocal Timoshenko beam theory. J. Phys. D 2008; 41: 225404.
[17] Naceri M, Zidour M, Semmah A, Houari SA, Benzair A and Tounsi A. Sound wave propagation in armchair single walled carbon nanotubes under thermal environment. Journal of applied physics 2011; 110: 124322.
[18] Maachou M, Zidour M, Baghdadi H, Ziane N and Tounsi A, A nonlocal Levinson beam model for free vibration analysis of zigzag single-walled carbon nanotubes including thermal effects. Solid State Communications 2011; 151: 1467-1471.
[19] Adda Bedia W, Benzair A, Semmah A, Tounsi A, Mahmoud SR. On the Thermal Buckling Characteristics of Armchair Single-Walled Carbon Nanotube Embedded in an Elastic Medium Based on Nonlocal Continuum Elasticity . Brazilian Journal of Physics, , 2015; 45: 225-233.
[20] Murmu T and Pradhan SC, Thermal effects on the stability of embedded carbon nanotubes. Comput. Mater. Sci. 2010; 47: 721-726.
[21] Fu YM, Hong JW and Wang XQ, Analysis of nonlinear vibration for embedded carbon nanotubes. J. Sound Vib 2006; 296: 746-756.
[22] Wu Y, Zhang X, Leung AYT and Zhong W. An energy-equivalent model on studying the mechanical properties of single-walled carbon nanotubes. Thin-Walled Struct. 2006; 44: 667.
[23] Eringen AC. Nonlocal polar elastic continua. Int. J. Eng. Sci. 1972; 101-6.
[24] Eringen AC. On differential equations of nonlocal elasticity and solutions of screw dislocation and surface waves. J. Appl. Phys. 1983; 54: 4703.
[25] Tounsi A, Semmah A and Bousahla AA. Thermal buckling behavior of nanobeam using an efficient higher-order nonlocal beam theory. Journal of Nanomechanics and Micromechanics (ASCE) 2013; 3: 37-42.
[26] Boumia L, Zidour M, Benzair A and Tounsi A. Timoshenko beam model for vibration analysis of chiral single-walled carbon nanotubes. Physica E 2014; 59: 186-191.
[27] Heireche H, Tounsi A, Benzair A, Maachou M and Adda Bedia E. Sound wave propagation in single-walled carbon nanotubes using nonlocal elasticity. Physica E. 2008; 40: 2791.
[28] Zidour M, Daouadji TH, Benrahou KH, Tounsi A, Adda Bedia E and Hadji L, Buckling analysis of chiral single-walled carbon nanotubes by using the nonlocal timoshenko beam theory. Mechanics of Composite Materials, 2014; 50 (1): 95-104.
[29] Natsuki T, Hayashi T and Endo M, Wave propagation of carbon nanotubes embedded in an elastic medium. J. Appl. Phys. 2005; 97: 044307.
[30] Benzair A, Tounsi A, Besseghier A, Heireche H, Moulay N and Boumia L. Thethermal effect on vibration of single-walled carbon nanotubes using nonlocal Timoshenko beam theory. Journal of Physics D 2008; 41: 225404.
[31] Tokio Y. Recent development of carbon nanotube. Synth Met. 1995; 70: 1511-8.
[32] Eringen AC. Nonlocal Polar Field Models. Academic Press, New York,. 1976;
[33] Bourada M, Kaci A, Houari M S A and Tounsi A. A new simple shear and normal deformations theory for functionally graded beams. Steel and Composite Structures, 2015;18(2): 409-423.
[34] Timoshenko SP. On the Correction for Shear of the Differential Equation for Transverse Vibrations of Prismatic Bars. Philosophical Magazine. 1921; 41: 744-746.
[35] Avsec J and Oblak M. Thermal vibrational analysis for simply supported beam and clamped beam. J. Sound Vib. 2007; 308: 514-525.
[36] Zhang YC and Wang X.Thermal effects on interfacial stress transfer characteristics of carbon nanotubes/polymer composites. Int. J. Solids Struct. 2005; 42: 5399-5412.

INTERNATIONAL CONFERENCE ON ADVANCES IN SCIENCE AND ARTS ISTANBUL 2017

29 – 31 MARCH 2017, Istanbul, Turkey

SEMISYNTHETIC DERIVATIVES OF CURCUMINOIDS ISOLATED FROM *CURCUMA LONGA* L BY ESTERIFICATION REACTION

Nouara Ziani[a]*, Maroua Nasri [a], Assia Sid [b]

a) Laboratoire de Chimie-Ingénierie des Matériaux et Nanostructures, Département de Chimie, Université de Sétif-1,19000, Algérie

b) Laboratoire des sciences analytiques, matériaux et environnement (LSAME). Université Oum El Bouaghi.

Abstract

A curcuminoid is a linear diarylheptanoid, with molecules such as curcumin or derivatives of curcumin with different chemical groups that have been formed to increase solubility of curcumins and make them suitable for drug formulation. These compounds are natural phenols and produce a pronounced yellow color[1].
Many curcumin characters are unsuitable for use as drugs by them selves. They have poor solubility in water at acidic and physiological pH, and also hydrolyze rapidly in alkaline solutions. Therefore, curcumin derivatives are synthezised to increase their solubility and hence bioavailability.[2]
Three derivatives of curcumin were isoleted starting from the rhizomes of *Curcuma longa* L, trough extraction assisted by microwive using alternative and green solvants such as glysérol. Purification of curcuminoids was achieved by column chromatography. The products this way obtained it was subjected to an esterification reaction which allowed to obtain the semisynthetic derivatives which shown higher lipophility than curcumin.

Keywords: Curcuminoids, *Curcuma longa* L, esterification reaction, lipophility.

Reference

1. Tomren MA, Másson M, Loftsson T, Tonnesen HH (June 2007). "Studies on curcumin and curcuminoids XXXI. Symmetric and asymmetric curcuminoids: stability, activity and complexation with cyclodextrin". Int J Pharm. **338** (1–2): 27–34.
2. Tiyaboonchai W, Tungpradit W, Plianbangchang P (June 2007). "Formulation and characterization of curcuminoids loaded solid lipid nanoparticles". Int J Pharm. **337** (1–2): 299–306.

INVESTIGATION OF COMPATIBILIZER LOADING LEVEL ON THE PROPERTIES OF RECYCLED LOW DENSITY POLYETHYLENE/TPS BLENDS

Barış Öner[1], Tolga Gökkurt[2], Ayşe Aytaç [1,3]
[1] *Kocaeli University, Polymer Science and Technology Master Program, 41380 Kocaeli*
[2] *Polipro Plastic SAN, 41400, Gebze/Kocaeli*
[3] *Kocaeli Üniversitesi, Chemical Engineering Department, 41380 Kocaeli*
baris_oner@windowslive.com

In recent years, the growing environmental awareness has encouraged the development of biodegradable polymers to replace synthetic polymers in many applications. As is known, great amount of synthetic polymers has been thrown away from the domestic wastes and this waste creates important environmental problems. One of the solutions of this problem is blended biodegradable materials with synthetic polymers to reduce the amount of synthetic polymers. Another solution is recycling, which is also a good process to reduce the pollution. The aim of this study is using both of these methods and produces a material will be used an environmentally friendly bio-recycled garbage bags. Polyethylene, one of the most vastly used polymer on packaging industry and its wastes are obtained easily. Thermoplastic starch (TPS), being an inexpensive and renewable product and it has good potential as biodegradable filler for synthetic polymers. However, these materials are not compatible due to the difference in their chemical nature, polarity and their blends results in poor mechanical properties. In order to increase compatibility, it is necessary to use a compatibilizer. In this study, the effect of compatibilizers on the properties of recycled polyethylene (r-LDPE) and thermoplastic starch (TPS) blends were investigated. Polyethylene-grafted-Maleic anhydride (LDPE-g-MA) was selected as compatibilizer and it was used two different loading level as 5wt% and 10wt%. r-LDPE/TPS blends were prepared by using a twin screw extruder and characterized by means of mechanical, thermal tests and morphological analyses. It was found that the tensile strength values of the compatibilized blend were slightly changed. In addition to this the elongation at break values greatly increased as at 2000%.

Key Words: *Recycled LDPE / TPS Blends, Recycled LDPE, Compatibilizer*

INTERNATIONAL CONFERENCE ON ADVANCES IN SCIENCE AND ARTS ISTANBUL 2017

29 – 31 MARCH 2017, Istanbul, Turkey

NOVEL NİCKEL(II) AND MANGANESE(III) COMPLEXES WİTH BİDENTATE SCHİFF-BASE LİGAND: SYNTHESİS, SPECTRAL, THERMOGRAVİMETRY, ELECTROCHEMİCAL AND ELECTROCATALYTİCAL PROPERTİES

OUENNOUGHİ YASMİNA , BOUZERAFA BRAHIM

Département de Génie des Procédés Faculté de Technologie Université Ferhat ABBAS Sétif-1,Algérie

ABSTRACT

An unsymmetrical bidentate Schiff base ligand, ethane 2-(4-methoxyphenyl)-1-iminosalicylidene, and its novel two mononuclear complexes, Nickel(II)[Ni(II)-2L] and Manganese(III) [Mn(III)Cl-2L] where L represents the ligand, have been synthesized and characterized by various physicochemical methods. The Ni(II) ion is coordinated by two nitrogen and two oxygen atoms with both the bidentate Schiff base ligands in an approximately square planar coordination geometry, while the manganese complex, the Mn(III) ion, is involved in an additional contact with one chloride anion for which the coordination sphere appears as a square pyramidal arrangement. The thermogravimetric analyses of the synthesized compounds revealed three different stages of decomposition for NONO bis-bidentate manganese and nickel complexes. The cyclic voltammetry studies of these complexes in N,N-dimethylformamide showed a redox couple for each one of them, such as Ni(II)/Ni(I) and Mn(III)/Mn(II), which are quasi-reversible. Their catalytic behaviors were tested showing that the nickel complex is an effective electrocatalyst in the reduction of bromocyclopentane. Regarding the manganese complex, it was revealed that it is an efficient catalyst in the activation of molecular dioxygen, currently applied in oxidation reactions of hydrocarbons according to the monooxygenase enzymes as those of cytochrome P450 model.**Key words:** fungal disease, chytridiomycosis, amphibian, *Batrachochytrium*, Turkey

INTERNATIONAL CONFERENCE ON ADVANCES IN SCIENCE AND ARTS ISTANBUL 2017
29 – 31 MARCH 2017, Istanbul, Turkey

FREE VIBRATION ANALYSIS OF ARMCHAIR DOUBLE-WALLED CARBON NANOTUBES EMBEDDED IN AN ELASTIC MEDIUM USING NONLOCAL THEORY.

*** Mohamed ZIDOUR**
Université Ibn Khaldoun, BP 78
Zaaroura, 14000 Tiaret, Algeria

Tayeb BENSATTALAH
Université Ibn Khaldoun, BP 78
Zaaroura, 14000 Tiaret, Algeria

Hamidi AHMED
Université Tahri Mohammed
Béchar Rue de l'indépendance.
Béchar BP 417 Algeria

Belkacem ADIM
Université Ibn Khaldoun, BP 78
Zaaroura, 14000 Tiaret, Algeria

Keywords: nanotube, Vibration; armchair, Winkler, nonlocal
** Corresponding author:, Phone:213664701813*
E-mail address: zidour.mohamed@yahoo.fr

ABSTRACT

In the present work, nonlocal Euler-Bernoulli beam theory is used to investigate the free vibration response of armchair double-walled carbon nanotube (DWCNT) embedded in an elastic medium. Winkler-type foundation model is employed to simulate the interaction of the DWCNT with the surrounding elastic medium. It is noticed in the present study that the equivalent Young's modulus for armchair DWCNT is derived using an energy-equivalent model. The results indicate the dependence of nonlocal effects, the mode number and Winkler modulus parameter on the frequency of DWCNT.

INTRODUCTION

Since the single-walled carbon nanotube (SWCNT) and multi-walled carbon nanotube (MWCNT) are found by Iijima [1], there have been extensive researches on these nanomaterials. It has been found that carbon nanotubes possess many interesting and exceptional mechanical and electronic properties.

Experiments at the nanoscale are extremely difficult and atomistic modelling remains prohibitively expensive for large-sized atomic system. Consequently continuum models continue to play an essential role in the study of carbon nanotubes. Thereby size-dependent continuum based methods [2-3] are becoming popular in modelling small sized structures as it offers much faster solutions than molecular dynamics simulations for various engineering problems.

The nonlocal elasticity theory initiated by Eringen [4, 5] are captured by assuming that the stress at a point as a function not only of the strain at that point but also a function of the strains at all other points of the domain. Various works related to nonlocal elasticity theory are found in several references [6-7-8].

Recently, considerable attention has been turned to the mechanical behavior of single and multi-walled carbon nanotubes embedded in polymer or metal matrix [9-10]. Vibration and buckling analyses [11-12] of CNTs have shown the employment of Winkler-type elastic foundation for modelling continuous surrounding elastic medium.

In this paper, nonlocal Euler-Bernoulli beam theory has been implemented to investigate the vibration response of armchair double-walled carbon nanotubes (DWCNTs) embedded in an elastic medium. Winkler-type model is employed to simulate the interaction of the DWCNTs with a surrounding elastic medium. The influence of the scale parameter, the van der Waals forces, Winkler modulus parameter and the effect of the chirality of armchair DWCNT is taken into consideration in this study. It is hoped that the present analysis will be useful to researchers and engineers working on carbon nanotubes and CNT based composites.

GEOMETRY OF SINGLE WALLED NANOTUBE (SWNT)

Carbon nanotubes are considered to be tubes formed by rolling a graphene sheet a bout the chiral vector denoted by ($\vec{C}_h$). The

chiral vector ($\vec{C}_h$) can be expressed with respect to two base vectors ($\vec{a}_1$) and ($\vec{a}_2$) as under

$$\vec{C}_h = n\vec{a}_1 + m\vec{a}_2 \tag{1}$$

Where n and m are the indices of translation. If the indices of translation are such that (m = 0) and (n = m) then the corresponding (CNTs) are categorized as zigzag and armchair, respectively.

The radius of the armchair nanotube in terms of the chiral vector components can be obtained from the relation [13]

$$R = \frac{3n}{2\pi}a \tag{2}$$

where (a) is the length of the carbon–carbon bond which is ($1.42\ A°$).

Based on the link between molecular mechanics and solid mechanics, Wu et al. [14] developed an energy-equivalent model for studying the mechanical properties of (SWCNTs). Using the same method, the equivalent Young's modulus of armchair SWCNT are expressed as

$$E_{SWNT} = \frac{4\sqrt{3}}{3}\frac{KC}{3Ct + 4Ka^2t(\lambda_{a1}^2 + 2\lambda_{a2}^2)} \tag{3}$$

where (K) and (C) are the force constants. (t) is the thickness of the nanotube and the parameters (λ_{a1}) and (λ_{a2}) are given by.

$$\lambda_{a1} = \frac{4 - \cos^2(\pi/2n)}{16 + 2\cos^2(\pi/2n)} \tag{4}$$

and

$$\lambda_{a2} = \frac{-\sqrt{12 - 3\cos^2(\pi/2n)}\cos(\pi/2n)}{32 + 4\cos^2(\pi/2n)}$$

Tu and Ou-Yang [15] indicated that the relation between Young's modulus of multi-walled carbon nanotubes (MWCNTs) and the layer number (N) can be expressed as

$$E_{MWNT} = \frac{N}{N - 1 + t/h}\frac{t}{h}E_{SWNT} \tag{5}$$

where E_{MWNT} , E_{SWNT} , t , N and h are Young's modulus of multi-walled nanotubes, Young's modulus of single-walled nanotubes, effective wall thickness of single-walled nanotubes, number of layers and layer distance.

NONLOCAL DOUBLE – ELASTIC BEAM MODEL

The equations of motion for transversely vibrating Euler beam can be obtained as [16 – 17]

$$\frac{\partial Q}{\partial x} + f(x) + p(x) = \rho A\frac{\partial^2 w}{\partial t^2} \tag{6}$$

where $p(x)$ is the distributed transverse force along axis x , $w(x,t)$ is the transverse deflection, ρ is the density, A is the area of the cross section of the beam, $f(x)$ is the interaction pressure per unit axial length between the nanotube and the surrounding elastic medium, and Q is the resultant shear force on the cross section,

The one–dimensional nonlocal constitutive relation for the beam can be written as [5, 6, 7, 18]

$$\left[1 - (e_0a)^2\frac{\partial^2}{\partial x^2}\right]\sigma = E\varepsilon \tag{7}$$

where a is an internal characteristic length and e_0 is a constant for adjusting the model in matching some reliable results by experiments or other models. E is the Young's modulus of CNT, σ is the nonlocal axial stress of the nonlocal continuum theory.

By Eqs. (6) and (7), the nonlocal bending moment M and shear force Q can be obtained as

$$M = -EI\frac{\partial^2 w}{\partial x^2} + (e_0a)^2\left[\rho A\frac{\partial^2 w}{\partial t^2} - f(x) - p(x)\right] \tag{8}$$

and

$$Q = -EI\frac{\partial^3 w}{\partial x^3} + (e_0a)^2\left[\rho A\frac{\partial^3 w}{\partial x\partial t^2} - \frac{\partial f(x)}{\partial x} - \frac{\partial p(x)}{\partial x}\right] \tag{9}$$

The equation of motion (6) thus can be expressed by the transverse deflection as

$$f(x) + p(x) = EI\frac{\partial^4 w}{\partial x^4} + \rho A\frac{\partial^2 w}{\partial t^2} - (e_0a)^2\left(\rho A\frac{\partial^4 w}{\partial x^2\partial t^2} - \frac{\partial^2 f(x)}{\partial x^2} - \frac{\partial^2 p}{\partial x^2}\right) \tag{10}$$

This is the general equation for transverse vibrations of an elastic beam under distributed transverse pressure with the surrounding elastic medium on the basis of nonlocal elasticity.

It is known that double – walled carbon nanotubes are distinguished from traditional elastic beam by their hollow two – layer structures and associated intertube van der Waals forces. The equation (10) can be used to each of the inner and outer tubes of the double – walled carbon nanotubes. Assuming that the inner and outer tubes have the same thickness and effective material constants, we have

$$c(w_2 - w_1) = EI_1 \frac{\partial^4 w_1}{\partial x^4} + \rho A_1 \frac{\partial^2 w_1}{\partial t^2} - (e_0 a)^2 \left(\rho A_1 \frac{\partial^4 w_1}{\partial x^2 \partial t^2} - c \frac{\partial^2}{\partial x^2}(w_2 - w_1) \right) \quad (11a)$$

$$-k_W w_2 - c(w_2 - w_1) = EI_2 \frac{\partial^4 w_2}{\partial x^4} + \rho A_2 \frac{\partial^2 w_2}{\partial t^2} - (e_0 a)^2 \left(\rho A_2 \frac{\partial^4 w_2}{\partial x^2 \partial t^2} + k_W \frac{\partial^2 w_2}{\partial x^2} + c \frac{\partial^2}{\partial x^2}(w_2 - w_1) \right) \quad (11b)$$

Where subscripts 1 and 2 are used to denote the quantities associated with the inner and outer tubes, respectively.

Where k_W is spring constant of the surrounding elastic medium and c is the intertube interaction coefficient per unit length between two tubes, which can be estimated by [19]

$$c = \frac{320\,(2R_1)\,erg/cm^2}{0.16\,d^2} \quad (d = 0.142\,nm) \quad (12)$$

Where R_1 is the radius of the inner tube. In addition the pressure per unit axial length, acting on

Let us consider a double – walled carbon nanotube of length L in which the two ends are simply supported, so vibrational modes of the DWCNT are of the form [18]

$$w_1 = a_1 e^{i\omega t} \sin \lambda_k x, \quad w_2 = a_2 e^{i\omega t} \sin \lambda_k x, \quad \text{and} \quad \lambda_k = \frac{k\pi}{L} \quad (k = 1,2,.....) \quad (13)$$

where a_1 and a_2 are the amplitudes of deflections of the inner and outer tubes.

Thus, the two – k – order resonant frequencies of the DWCNT with thermal effect can be obtained via nonlocal model by substituting Eq. (13) into Eqs. (11a) and (11b), which yields

$$\omega_{kI}^2 = \frac{1}{2}\left(\alpha_k - \sqrt{\alpha_k^2 - 4\beta_k}\right),$$

$$\omega_{kII}^2 = \frac{1}{2}\left(\alpha_k + \sqrt{\alpha_k^2 - 4\beta_k}\right) \quad (14)$$

with

$$\alpha_k = \frac{c\,(A_1 + A_2)}{\rho\, A_1 A_2} + \frac{k_W}{\rho\, A_2} + \frac{E\,\lambda_k^4 (A_1 I_2 + A_2 I_1)}{\rho\, A_1 A_2 \left(1 + (e_0 a)^2 \lambda_k^2\right)} \quad (15)$$

$$\beta_k = c\lambda_k^4 \frac{EI_1 + EI_2}{\rho^2 A_1 A_2 \left(1 + (e_0 a)^2 \lambda_k^2\right)} + \lambda_k^8 \frac{EI_1 EI_2}{\rho^2 A_1 A_2 \left(1 + (e_0 a)^2 \lambda_k^2\right)^2} + \left(\frac{EI_1 \lambda_k^4}{\rho^2 A_1 A_2 \left(1 + (e_0 a)^2 \lambda_k^2\right)} + \frac{c}{\rho^2 A_1 A_2} \right) k_W \quad (16)$$

where ω_{kI} is the lower natural frequency, ω_{kII} is the higher natural frequency.

RESULTS AND DISCUSSIONS

Based on the formulations obtained above with the nonlocal Euler-Bernoulli beam theory, the effect of both chirality and Winkler modulus parameter on vibration properties of armchair double-walled nanotubes are discussed here. The parameters used in calculations for the armchair DWCNTs are given as follows: the effective thickness of CNTs taken to be 0.258 nm [14], the force constants K/2= 46900 kcal/mol/nm2 and C/2= 63 kcal/mol/rad2 [20], the mass density ρ = 2.3 g/cm3 [21] and layer distance h=0.34 nm [15].

To investigate the effect of scale parameter on vibrations of armchair DWCNTs embedded in an elastic medium, the results including and excluding the nonlocal parameter are compared. In addition, the vibration characteristics of different armchair DWCNTs are compared in order to explore the effect of chirality. It follows that the ratios of the results with the nonlocal parameter to those without nonlocal parameter are respectively given by:

$$\chi = \frac{(\omega)_N}{(\omega)_L} \quad (17)$$

where $(\omega)_L$ and $(\omega)_N$ are the local and the nonlocal higher natural frequency, based on the local and nonlocal Euler-Bernoulli beam model, respectively.

Figure 1 show the effect of small scale parameter on the higher vibration response of embedded armchair DWCNT with elastic medium modeled as Winkler-type foundation. For the present study, the nonlocal parameter ($e_0 a$) values of DWCNT were taken in the range of 0 – 2 nm as described in Ref [22]. The aspect ratio L/d is taken as 40. The Winkler modulus ratio parameter (k_W / c) values were taken in the range of 0 – 60. From figure 1, it is observed that there is significant influence of small scale parameter on the vibration response of embedded armchair DWCNT. The higher frequency ratios (χ) considering nonlocal model are always smaller than the local

(classical) model. This implies that the employment of the local Euler-Bernoulli beam model for DWCNT analysis would lead to an overprediction of the frequency if the small length scale effects between the individual carbon atoms are neglected. Further, with increase in $e_0 a$ values, the frequencies obtained by nonlocal Euler-Bernoulli theory become smaller compared to local model. Furthermore, it is seen that as the Winkler modulus ratio parameter increases the frequency ratio increases. This increasing trend is attributed to the stiffness of the elastic medium. With higher values of Winkler modulus ratio parameter, the rate of increase of frequency ratio reduces. This implies that nonlocal or small-scale effect in vibration response of armchair DWCNT looses its significance as the Winkler modulus ratio values increase. This is interpreted as follows: Although the small-scale effect makes the CNTs more flexible as CNT being assumed as atoms linked by springs, the external elastic medium "grips" the CNTs and forces it to be stiffer. Hence the nonlocal effect is found to be more significant without the presence of elastic medium.

Fig. 2 show the variation of frequency ratio with Winkler modulus ratio parameter for various modes of vibration. In the present study computation until four modes (k) of vibration are considered. It is observed that the nonlocal effects on vibration response are more significant for higher modes of vibration. This is interpreted from the fact that frequency ratio values for higher modes ($k = 3, 4$) are quite less than $k = 1$. This significance of nonlocal effects in higher modes is attributed to the influence of small wavelength for higher modes. For smaller wavelengths, interactions between atoms are increasing and this leads to an increase in the nonlocal effects. Furthermore, as the Winkler modulus parameter increases, the frequency ratios increase for higher modes except for first mode of vibration. This implies that there is comparatively less effect of elastic medium on higher mode frequency of armchair DWCNT.

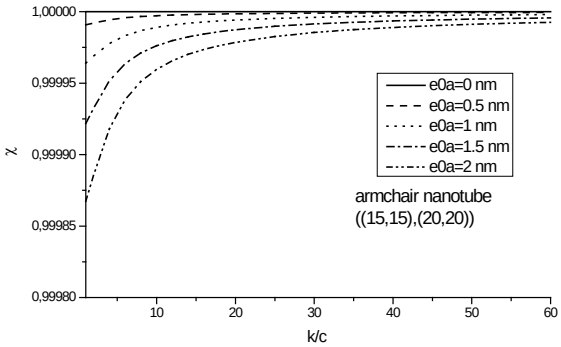

Fig. 1: Effect of Winkler modulus ratio parameter on the higher frequency ratio of armchair DWCNT for various small-scale coefficients with ($L/d = 40$ and $k = 6$).

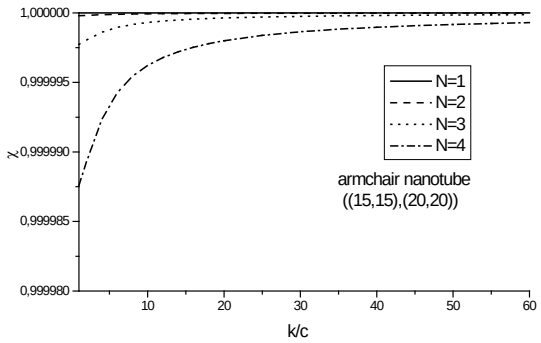

Fig. 2: Effect of Winkler modulus ratio parameter on the higher frequency ratio of armchair DWCNT for various mode numbers with ($e_0 a = 2$ nm and $L/d = 40$).

The variation of higher frequency ratio with shear modulus parameter for various aspect ratios (L/d). For different aspect ratios are taken, viz. L/d=3, 5, 10, and 20 are shown in figure 3 with the vibrational mode k=1 in this present computation the nonlocal parameter e0a= 2 nm is employed for the NL-EB model. It can be seen from the figure that as the Winkler modulus ratio parameter increases, the frequency ratio increases for all the different aspect ratios of DWCNT considered. Therefore, it is clear that the small scale effect is significant for short CNTs.

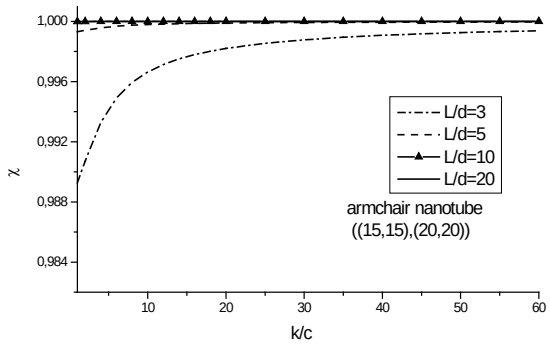

Fig. 3: Effect of Winkler modulus ratio parameter on the higher frequency ratio of DWCNT χ for various aspect ratios with, ($e_0 a = 2$ nm, $k = 1$).

CONCLUSION

This paper studies the vibration of armchair DWCNTs embedded in elastic medium based on Eringen's nonlocal elasticity theory and the Euler-Bernoulli beam theory. Influence of the stiffness of the surrounding elastic medium on the higher frequency of the armchair DCNTs is shown. According to the study, the results showed the dependence of the vibration characteristics on the nonlocal parameter, the mode number, Winkler modulus parameter and aspect ratios of armchair DWCNTs. With the results, the dynamic properties of the DWCNT beam have been discussed in detail; they are shown to be very different from those predicted by classic elasticity when

nonlocal effects become considerable. This means that as the length scales are reduced, the influences of long-range interatomic and intermolecular forces on the dynamic properties tend to be significant and cannot be neglected. The investigation presented may be helpful in the application of CNTs, such as ultrahigh-frequency resonators, electron emission devices, high-frequency oscillators and mechanical sensors.

REFERENCES

[1] S. Iijima, Nature 354 (1991) 56.
[2] Zhou S.J., Li Z.Q., J Shandong Univ of Tech 31 (5) (2001) 401.
[3] Yang, A.C.M. Chong, D.C.C. Lam, P. Tong, Int J Solids Struct 39 (10) (2002) 2731.
[4] Eringen A C, Int J Eng Sci 10 (1972) 1.
[5] Eringen A C, J Appl Phys, 54 (1983) 4703.
[6] Peddieson J, Buchanan G. G, McNitt R. P. Int J Engng Sci 41 (2003), 305.
[7] Zhang Y Q, Liu G R, Xie X Y, Phys Rev, 71 (2005) 195404-1-195404-7.
[8] M. Simsek, Steel Compos. Struct. 11 (2011) 59–76.
[9] C.Q. Ru, J Mech Phys Solids, 49 (2001) 1265.
[10] Qian, D., Dickey, E.C., Andrews, R., Rantell, T., Appl.Phys.Lett 76 (2000) 2868.
[11] Ranjbartoreh A.R, Ghorbanpour A and Soltani B, Physica E, 39 (2007) 230.
[12] Yoon J, Ru C.Q., Mioduchowski A. Int. J. Solids Struct. 43 (2006) 3337
[13] Y. Tokio, Synth Met 70 (1995) 1511–8.
[14] Y. Wu, X. Zhang, A.Y.T. Leung, W. Zhong, Thin-Walled Structures 44 (2006) 667 – 676.
[15] Z.C Tu, Z.C Ou-Yang, Phys. Rev. B 65, 233407 (2002).
[16] S.P. Timoshenko, Philos. Mag. 41, 744 (1921).
[17] J.F. Doyle, Wave Propagation in Structures, 2nd ed. (Springer, New York, 1997).
[18] H. Heireche, A. Tounsi, A. Benzair, Nanotechnology 19 (2008) 185703.
[19] Sudak L. J., J. Appl. Phys, 94 (2003) 7281.
[20] W.D. Cornell, P. Cieplak, C.I. Bayly, et al., J. Am. Chem. Soc. 117 (1995) 5179–5197.
[21] H. Heireche, A. Tounsi, A. Benzair, M. Maachou, E.A. Adda Bedia, Physica E 40 (2008). 27911-2799.
[22] Wang Q and Wang C M, Nanotechnology 18 (2007) 075702 (1-4).

INTERNATIONAL CONFERENCE ON ADVANCES IN SCIENCE AND ARTS ISTANBUL 2017

29 – 31 MARCH 2017, Istanbul, Turkey

THERMAL BEHAVIOR OF REVERSIBLE CROSSLINKED LOW DENSITY POLYETHYLENES

BOUZERAFA BRAHIM

Département de Génie des Procédés Faculté de Technologie Université Ferhat ABBAS Sétif-1,Algérie

ABSTRACT

The LDPE was modified by the RXR crosslinking method using three crosslinking agents. The first formulation contains unmodified LDPE, in the first case LDPE was crosslinked with peroxide (System I), in the second system, the LDPE was crosslinked by the Peroxide/Accelerator couple (System II) in the third case the LDPE was modified by peroxide, Accelerator and active sulfur (System III).
The thermal behavior of these three systems was elucidated using four numerical methods: Kissinger method, multiple heating rates, Ozawa and Coats-Redfern methods. The kinetic parameters, activation energy, order of reaction and pre-exponential factor were estimated and compared with those of unmodified LDPE.

INTERNATIONAL CONFERENCE ON ADVANCES IN SCIENCE AND ARTS ISTANBUL 2017

29 – 31 MARCH 2017, Istanbul, Turkey

SYNTHESİS, CHARACTERİZATİON AND ELECTROCHEMİCAL PROPERTİES OF SOME METALLİC COMPLEX DERİVATİVES OF DEHYDROACETİC ACİD

TABTİ SALİMA

UNİVERSTİTY OF BRORDJ BOU ARRERİDJ

ABSTRACT

In this study, the treatment of α,β-unsaturated carbonyl compounds, obtained by the reaction of dehydroacetic acid (DHA) and heteroaromatic aldehyde results in the formation of a heterocyclic compound, named 4-hydroxy-3-[(2*E*)-3-(4- (dimethylamino)phenyl)prop-2-enoyl]-6-methyl-2*H*-pyran-2-one (HL) in good yield that depending upon the reaction conditions. The ligand HL behaves as a monoanionic bidentate OO chelating agent. Its structure was characterized using the usual spectral characterization such as electronic absorption, by FT-IR, and ^{1}H NMR in addition to mass and elemental analyses. M(II) coordination compounds of Cu, Co and Ni with a this ligand (HL) derived from the condensation of DHA with aromatic amine were synthesized and characterized by several techniques, including elemental analysis , UV-Vis, FT-IR, EPR and ^{1}HNMR spectral studies. The analytical values indicated that the water and ammoniac fractions coordinate to the metal ions. Based on these studies, the general formulae $[M(L)_2(H_2O)]$ (M(II) = Cu) and $[M(L)_2(NH_3)_4]$ for (M(II) =Ni) are proposed for the complexes. Electrochemical behavior of all these complexes has been investigated by cyclic voltametry on glassy carbon electrode in acetonitrile at 100 mV/s scan rate. This study indicate that the reduction process corresponding to Cu^{II}/Cu^{I} is electrochemically quasi-reversible in complex of copper, and irreversible reduction process for Ni^{II}/Ni^{I} in complexes of nickel .

INTERNATIONAL CONFERENCE ON ADVANCES IN SCIENCE AND ARTS ISTANBUL 2017
29 – 31 MARCH 2017, Istanbul, Turkey

CONTRIBUTION OF THE HYDROGEOCHEMISTRY TO THE IDENTIFICATION OF THE HYDROTHERMAL SYSTEMS OF SETIF WILAYA, (NORTH-EAST ALGERIA)

TABTI SALIMA
UNİVERSTİTY OF BRORDJ BOU ARRERİDJ

ABSTRACT:

The synthesis of α, β-unsaturated carbonyl compounds by the condensation of dehydroacetic acid DHA with carboxaldehyde RCHO derivatives [R = quinoleine-8; Indole-3-; pyrrole-2; and -4-(dimethylamino) phenyl] afforded four chalcone ligands (L1-L4). These compounds when carbonyl group is conjugated with an alkene, from which they derive special properties. The investigation of functional model complexes for metalloenzymes with oxidase or oxygenase activity is therefore of great promise for the development of new and efficient catalysts for oxidation reactions. The in situ generated copper (II) complexes of the four compounds L1, L2, L3 and L4 were examined for their catalytic activities and were found to catalyze the oxidation reaction of catechol to ***o***-quinone under atmospheric dioxygen. The rates of this oxidation depend on three parameters: ligands, ion salts and solvent nature and the combination L2 [Cu $(CH_3COO)_2$] leads to the faster catalytic process.

INTERNATIONAL CONFERENCE ON ADVANCES IN SCIENCE AND ARTS ISTANBUL 2017

29 – 31 MARCH 2017, Istanbul, Turkey

SYNTHESIS, ELECTROCHEMICAL BEHAVIOR AND DFT STUDİES OF A NEW IRON COMPLEX - NON-SYMMETRIC

DEKAR SOUAD ,OUARİ KAMEL

ABSTRACT

Metal complex of a new potentially tetradentate non symmetrical Schiff base ligand (H_2L_{CH3}) with Fe(II) metal ions have been synthesized and characterized based on their spectral (IR, UV–Vis and mass spectra), elemental analysis and molar conductance revealed that the metal complex was non-electrolyte. Proposed structures for free thiourea ligand and its iron complex were corroborated by applying geometry optimization and conformational analysis.

Cyclic voltammetry of H_2L_{CH3} and $FeClL_{CH3}$ was achieved in DMF solution at a carbon vitreous disk electrode (d = 3 mm), with different speed scan (10, 25, 75,100 and 150mV/s) under N_2 atmosphere. In the same experimental conditions, $Fe(III)ClL_{CH3}$ exhibited a reversible redox couple Fe(III)/Fe(II) observed at $E_{1/2}$ = -240 mV. the diffusion coefficient is determinedusing GC rotating disk electrode. The Levich plot, was used to calculate the diffusion-convection controlled currents.

INTERNATIONAL CONFERENCE ON ADVANCES IN SCIENCE AND ARTS ISTANBUL 2017

29 – 31 MARCH 2017, Istanbul, Turkey

SYNTHESIS, SPECTRAL CHARACTERIZATION, ELECTROCHEMICAL AND ELECTROCATALYTICAL PROPERTIES OF A NEW NICKEL^{II}- TETRADENTATE SCHIFF BASE COMPLEX

Djouhra. AGGOUN, Ali. OURARI.

Laboratoire d'Electrochimie, d'Ingénierie Moléculaire et de Catalyse Rédox (LEIMCR), Département Génie des Procédés, Faculté des Sciences de l'Ingénieur, Université Farhat ABBAS de Sétif-1

aggoun81@yahoo.fr

ABSTRACT:

In this study, we have initiated the synthesis of an original pyrrole-Ni(II)-Schiff base complex derived from 6-(3'-N-pyrrolpropoxy)-2-hydroxyacetophenone and 1,2-diaminoethane. This nickel complex was was isolated with acceptable yields 68 %. The characterization was carried out with usual spectroscopic methods such as UV–Vis, FT-IR, NMR^{1}H, and elemental analysis. Based on these studies, the general formulae $Ni^{II}(L)_2$ is proposed for this complex. The Electrochemical behavior of this complex in the acetonitrile medium was studied by a cyclic voltammetry via the use of the two different working electrodes: glassy carbon (**GC**) and platinum electrode (**Pt**). The cyclic voltammetry studies reveal that this complex shows successively the $\mathbf{Ni^{II}/Ni^{I}}$ redox system. We have also electropolymerized this compound onto glassy carbon (GC), platinum disk (Pt) and indium tin oxide (ITO) electrode surfaces. The efficiency of the electrochemical polymerization was investigated as a function of several parameters such as the nature of the electrode material, the number of voltammetric scans and the scan rate dependence. The electrodeposited poly(pyrrole) films onto ITO surface was characterized by X-ray diffraction (XRD) and atomic force microscopy (AFM). This poly(pyrrole) matrix, containing metallic centers, was found to have good catalytic properties towards the reduction of iodobenzene and carbon dioxide CO_2.

***Keywords*:** Nickel-tetradentate Schiff base, Spectral characterization, Cyclic voltametry, Reduction of iodobenzene.

INTERNATIONAL CONFERENCE ON ADVANCES IN SCIENCE AND ARTS ISTANBUL 2017

29 – 31 MARCH 2017, Istanbul, Turkey

SYNTHESIS AND CHARACTERISATION OF NOVEL COPPER(II) COMPLEX OF 2-BENZIMIDAZOLYLUREA

MEHMET POYRAZ

AFYON KOCATEPE ÜNİVERSİTESİ

ABSTRACT:

2-Benzimidazolylurea in ethanol treated with $Cu(NO_3)_2$ 5 H_2O. The green coloured suspension refluxed for 2 hours then cooled and filtrated. The clear green solution was left slow evaporation and green crystals were collected in 10 days. The complex is represented by the chemical formula $[Cu(2\text{-Benzimidazolylurea})_2](NO_3)_2$. The complex was characterised by elemental analysis, spectroscopic techniques (FT-IR and 1H-NMR), molar conductivity, magnetic susceptibility. Single crystal X-ray diffraction analysis of the complex has been carried out at 293 K.

Research into the potential use of anticancer agent is still ongoing. The counterpart of the complex; mixed ligand silver(I) complex of 2-Benzimidazolyl-urea and triphenylphosphine mediates a strong cytotoxic response to the tested normal (MRC-5) and cancer cell lines (MCF-7). It is also exhibits four time stronger activity against cancer cells (MCF-7) than cisplatin while it is less toxic aginst normalcells (MRC-5) than cisplatin.

Acknowledgement

This work is supported by Afyon Kocatepe University, Scientific Research Project Commission, Project number: 13.FENED.07, Prof. Musa Sari for the structure determination and Prof. S.K. Hadjikakou's group for anticancer activities research.

***Keywords*:** Copper(II) Complex, 2-Benzimidazolylurea, Crystal Structure

INTERNATIONAL CONFERENCE ON ADVANCES IN SCIENCE AND ARTS ISTANBUL 2017

29 – 31 MARCH 2017, Istanbul, Turkey

SYNTHESİS AND CHARACTERİSATİON OF ZİNC(II) COMPLEX OF 2-BENZİMİDAZOLYLUREA

MEHMET POYRAZ

AFYON KOCATEPE ÜNİVERSİTESİ

ABSTRACT:

2-Benzimidazolylurea in ethanol treated with $Zn(NO_3)_2$ 5 H_2O. Colourless solution refluxed was obtained which was refluxed for 2 hours. The clear solution was left slow evaporation at room temperature and white crystals were collected after few days. The complex is represented by the chemical formula $[Zn(2\text{-Benzimidazolylüre})_2(H_2O)](NO_3)_2$. The complex was characterised by elemental analysis, spectroscopic techniques (FT-IR and 1H-NMR), molar conductivity, magnetic susceptibility. Single crystal X-ray diffraction analysis of the complex has been carried out at 293 K.

Research into the potential use of anticancer agent is still ongoing. The counterpart of the complex; mixed ligand silver(I) complex of 2-Benzimidazolyl-urea and triphenylphosphine mediates a strong cytotoxic response to the tested normal (MRC-5) and cancer cell lines (MCF-7). It is also exhibits four time stronger activity against cancer cells (MCF-7) than cisplatin while it is less toxic aginst normalcells (MRC-5) than cisplatin.

Acknowledgement

This work is supported by Afyon Kocatepe University, Scientific Research Project Commission, Project number: 13.FENED.07, Prof. Musa Sari for the structure determination and Prof. S.K. Hadjikakou's group for anticancer activities research.

***Keywords*:** zinc(II) complex, 2-Benzimidazolylurea, Crystal Structure

INTERNATIONAL CONFERENCE ON ADVANCES IN SCIENCE AND ARTS ISTANBUL 2017

29 – 31 MARCH 2017, Istanbul, Turkey

SYNTHESİS AND CRYSTAL STRUCTURE OF ONE-DİOMENSİONAL COPPER(II) POLYMER CONSTRUCTED BY (4-(1H-İMİDAZOL-1-YL)-PHENOL) AND ACETATE

MEHMET POYRAZ

AFYON KOCATEPE ÜNİVERSİTESİ

ABSTRACT:

4-(1H-imidazol-1-yl)phenol in ethanol, a water of Na_2CO_3 was slowly added, then an ethanol solution of $Cu(NO_3)_2 \cdot$ 2.5H2O was slowly added with stirring. To the formed cloudy suspension an aqueous solution of acetic acid was added. After stirring the solution was allowed to evaporate at room temperature. A number of blue single crystals were obtained after a few days. It was characterised by single crystal X-ray diffraction analysis.

In the title compound, $[Cu(C_9H_8N_2O)_2(CH_3COO)_2]n$, the Cu(II) ion resides on a centre of inversion, displaying a tetragonally distorted octahedral coordination environment defined by two pairs of N and O atoms of symmetry-related 4-(1H-imidazol-1-yl)-phenol ligands and the O atoms of two symmetry-related acetate ligands.

Note: This work is accepted for publication in Acta Crystallographica Section E.

Acknowledgements

The author acknowledge Scientific and Technological Research Application and Research Center, Sinop University, Turkey, for the use of the Bruker D8 QUEST diffractometer and Prof. Musa Sari for the structure determination.

***Keywords*:** Copper(II) Polymer, -(1H-imidazol-1-yl)- phenol, Crystal Structure

INTERNATIONAL CONFERENCE ON ADVANCES IN SCIENCE AND ARTS ISTANBUL 2017

29 – 31 MARCH 2017, Istanbul, Turkey

MOLECULAR STRUCTURE, VİBRATİONAL ANALYSİS (FT-IR), MEP AND HOMO–LUMO ANALYSİS OF COPPRE (II) COMPLEX DERİVE OF 3- α- (PARA-TOLYL) AMİNO ETHYL-4-HYDROXY-6-METHYL-2-PYRONE. BASED ON DFT CALCULATİON

DEKAR SOUAD ,OUARİ KAMEL

ABSTRACT

This paper contains a combined experimental and theoretical study of vibrational and electronic properties of cuivre (II) complexe derive of 3- α- (para-tolyl) amino ethyl-4-hydroxy-6-methyl-2-pyrone molecule. The FT-IR spectra of the title molecule in solid phase were recorded in the region 4000–500 cm^{-1}. The vibrational spectra calculated at the B3LYP / 6-311G (d,p) level were compared with the experimental spectra and assignment to each vibrational frequency was assigned on the basis of potential energy distribution (PED). The calculated electronic and nonlinear optical properties of the title molecule were reported.

INTERNATIONAL CONFERENCE ON ADVANCES IN SCIENCE AND ARTS ISTANBUL 2017
29 – 31 MARCH 2017, Istanbul, Turkey

A GENERAL OVERVIEW ON ENZYMATIC SYNTHESIS OF GLUCONIC ACID

Zeynep Pekcan
Department of Chemical Engineering, Kocaeli University, 41380 Kocaeli, Turkey

***Togayhan Kutluk**
Department of Chemical Engineering, Kocaeli University, 41380 Kocaeli, Turkey

Nurcan Kapucu
Department of Chemical Engineering, Kocaeli University, 41380 Kocaeli, Turkey

Keywords: Glucose, glucose oxidation, gluconic acid, glucose oxidase

** Corresponding author:, Phone:,+902623033526 Fax: +902623591262*
E-mail address: togayhan.kutluk@kocaeli.edu.tr

ABSTRACT

Gluconic acid is a non-toxic, non-corrosive, odorless and easily biodegradable weak organic acid. Gluconic acid and its derivatives, which have been commercially available since the 1930's, have found many uses since it is a multifunctional organic acid in the chemical, food and beverage, pharmaceutical, construction and other industries. Although a variety of chemical and biochemical methods of producing gluconic acid have been tried for production, gluconic acid is commercially produced by fermentation. Many researchers have been examined to produce gluconic acid due to the low cost, environmentally sensitive, high conversion of glucose oxidation cause of the multiple stepwise product separation and the cost of these processes. In the presence of immobilized enzymes in gluconic acid synthesis have the advantages which they can be used repeatedly, without the need for multi-step purification processes when compared with fermentation.

1. INTRODUCTION

The chemical substances that can take the place of the chemicals produced in the petroleum produced in the bioresafin are organic acids derived from sugars. Organic acids account for 50% of biologically produced platform chemistry [1, 2]. Aldonic acid, a type of sugar acid, is formed by oxidizing aldehyde group of an aldose to carboxylic acid. Gluconic acid or polyhydroxy caproic acid is an important example of aldonic acid, whose chemical formula is $C_6H_{12}O_7$. Gluconic acid occurs in plants, fruits, wine (up to 0.25%), honey (up to 1%), rice, meat, vinegar and other natural sources [1, 3, 4]. Gluconic acid, the oxidation product of glucose by glucose oxidase enzyme, is noncorrosive, nontoxic, nonvolatile, odourless and easily biodegradable a weak organic acid that is soluble in water and insoluble in non-polar solvents [2, 3, 5]. Gluconic acid and its derivatives of bulk chemicals are known as multifunctional carbonic acids, have been a great interest for many applications depending their features. Gluconic acid (Fig. 1) with reactive hydroxyl and carboxyl group, its salts and gluconolactone form have a multiple usage area in chemical, pharmaceutical (e.g. iron and calcium deficiency), food, beverage, textile, detergent, leather, photographic, construction and other industries. Because of that metal salts of gluconic acid have been found usage area in different industries, amount of gluconic acid demanded increased. Along with this demand there has been an increased interest in developing an efficient, economical and feasible gluconic acid process. The current estimated production of gluconic acid which is produced by using biotechnology is 100.000 tonnes/ year. [2, 3, 6].

Table 1. World wide consumption of gluconic acid based on major industrial applications[6]

Usage	Ouantity (in tonnes)
Pharmaceutical industries	8,000
Food industries	30,000
Construction industries	40,000
Other usage	9,000
Total	87,000

Commercially available 50% aqueous solutions are prepared which are in equilibrium with lactone derivatives (Fig. 1) since gluconic acid is difficult to prepare in solid crystalline form. The γ-lactone forms relatively slow compared to the δ-lactone [2, 7].

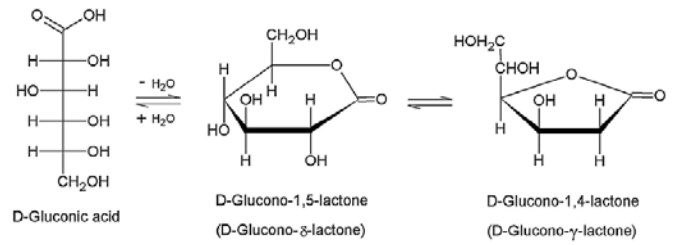

Figure 1. Chemical equilibrium of gluconic acid and its lactones in aqueous solution [2].

2. APPLICATION OF GLUCONIC ACID

Gluconic acid and its derivatives (except glucono-γ-lactone) are used as food, beverage, household and industrial cleaners, agrochemicals, construction chemicals, water treatment, textile auxiliaries and many other areas [2, 3]. The most significant feature of gluconic acid is a fine chelator substance more than others like ethylenediaminetetraacetic acid (EDTA), nitrilotriacetic acid (NTA) especially in alkaline and concentrated alkaline solutions [3, 5]. Sodim gluconate, as an additive, is used in construction field the aim of improving the cement resistance and stability under extreme climatic conditions [3, 4, 6]. Gluconolactone and sodium gluconate are approved as Generally Recognized As Safe (GRAS) by the US-FDA (United States-Food and Drug Administration) in 1986. Moreover gluconic acid is known generally permitted food additive(E574) in the European Parliament and the Council Directive No. 95/2/EC. Gluconic acid and its derivatives are used as food additives such as acidity regulators (E574-E580), preventing clouding, improving the sensory properties of food, food preservative and also can be used as cleaning agents for the industrial facilities [2, 4, 5].

3. GLUCONIC ACID PRODUCTION

Many different routes for gluconic acid production exist in literature. Chemical catalysis, enzymatic catalysis, and fermentation systems are known. Production using fermantation system is the most common one for gluconic acid production in the world. Cause these systems are economic, feasible, the easiest one and more efficient than other systems. With fermentation, renewable sources can be used as raw material in production. In addition to advantages of fermentation, there are some disadvantages such as difficulties in separating microorganisms and products, control of by-product formation and waste water disposal [3, 4, 7]. Gluconic acid production by fermentation can be carried out using various fungal species, bacterial species and yeast. Gluconic acid synthesis is carried out by glucose oxidase in fungi and glucose dehydrogenase in bacteria. Fungi such as Aspergillus and *Penicillium* species, bacteria such as *Gluconobacter, Pseudomonas*, *Phytomonas*, *Achromobacter,* Kiebsiella, *Zymomonas mobilis* ve *Acetobacter methanolicus* are used, among these the most widely used a sort of fungi is *Aspergillus niger* [3, 5, 7].

Although many different chemical catalysts have been tried for the production of gluconic acid and chemical methods are not preferred in spite of obtaining a pure chemical conversion by one step reaction. Chemical catalysis methods are also used and searched but they are not so feasible as fermentation system. Actually using catalyst for oxidizing of glucose can be done easily, not only the catalysts used can be deactivated, but also they are so expensive. Beside these, downstream processes have some problems [2, 3, 4, 5].

In enzymatic methods, using free enzymes for oxidizing glucose is only suitable for once batch use, not for large scale. Because of enzymes are unstable, expensive and easily inhibited, these kind of systems have high costs. Beside these problem glucose oxidase can be easily inactivated cause of by product hydrogen peroxide (H_2O_2) even in presence of catalase enzyme (for decomposition of H_2O_2) [3, 7, 8]. Contrary to fermentation, enzymatic gluconic acid production can be easily obtained by centrifugation, filtration etc., if the process carries out with immobilized enzymes. Besides immobilized enzymes can be reused. In a study conducted by Ozyilmaz, co-immobilized glucose oxidase and catalase system maintained 85 % of initial activity after 50 times used, 72.5 % of activity after 75 times used (Fig. 2) [9]. In enzymatic production, oxidation of glucose requires less time than fermentation processes [3]. Moreover, since enzymes are unique to a single substance, they are not confused with unexpected by-products. This makes enzymatic production with immobilized enzymes superior to fermentation [3, 7].

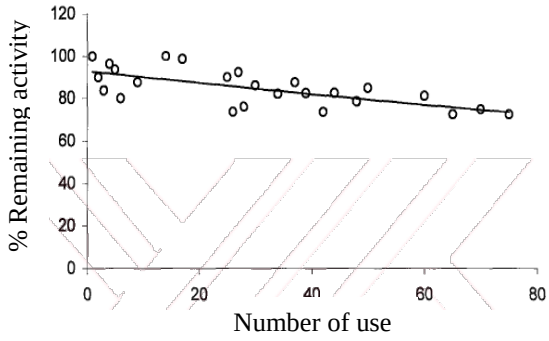

Figure 2. Re-use stability of glucose oxidase enzyme in co-immobilized glucose oxidase-catalase system [9]

3.1. REACTION MECHANISM

Gluconic acid is formed by the oxidation of glucose by glucose oxidase enzyme in the presence of oxygen. Glucose oxidase is specific to β-Glucose and converts only β-D-Glucose to gluconic acid. The enzyme do not work over α-Glucose. A flavoprotein, glucose oxidase has two flavin adenine dinucleotide (FAD) cofactor molecules which are tightly bound but noncovalently (Fig. 3) [10, 11]. Reactions occurring during production are shown below (Fig. 4). During the oxidation process, the glucose first turns into D-gluconolactone. This product is converted into gluconic acid by itself or by the lactonase enzyme. H_2O_2, the byproduct formed, can cause competitive inhibition by forming an inactive complex with the reduced FAD cofactor, so it must be splitted [11]. Catalase

enzyme is used for decomposition of H_2O_2 to moleculer oxygen and water [9], but it is unstable and also expensive [3, 4, 6]. Therefore, it has been tried to use different substances (Palladium (Pd) particles, manganese dioxide (MnO_2)) together with glucose oxidase enzyme in the literature. Studies have shown that MnO_2 has a positive effect on glucose oxidase activity along with splitting H_2O_2 [7, 8].

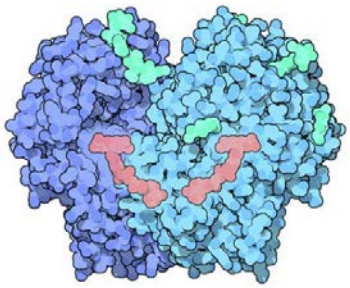

Figure 3. The pink parts represent the FAD coenzyme, and the dark and light blue parts represent glucose oxidase and its two subunits [10]

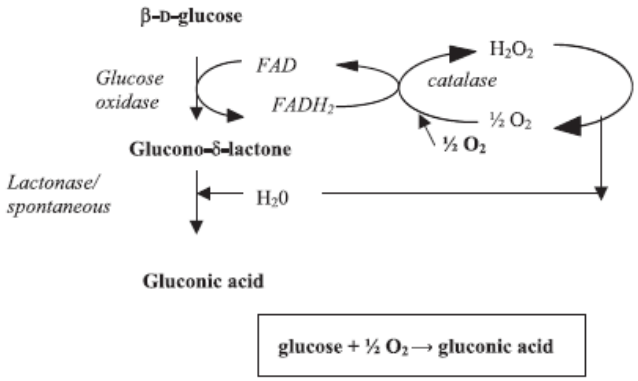

Figure 4. Reaction mechanism of gluconic acid synthesis [5]

3.2. LITERATURE OVERVIEW

Nakao et al. [12] immobilized fine palladium particle, instead of catalase, used with glucose oxidase to produce gluconic acid in diffent kinds of bubble reactor. This work's aim was to study kinetic parameters of gluconic acid reactions, optimal reactor design parameter and operating conditions.

Bao et al. [8] used free glucose oxidase and immobilized glucose oxidase and/ or MnO_2 instead of palladium (used in previous study) to make kinetic study while producing calcium gluconate crystals. Bao et al. [13] this time tried to find out inhibition effect of by product H_2O_2 over oxidation of glucose by free glucose oxidase. Beltrame et al. [14] examined selective oxidation of glucose by Hyderase (commercial mixture of glucose oxidase and catalase) at atmospheric pressure, controlled pH value, and constant oxygen concentration, in the temperature range from 273.2 to 303.2 K to be found out the kinetic parameters of the reaction between glucose and oxidized enzyme.

Odenbunmi and Owalude [15] studied on kinetic and thermodynamic properties of oxidation of glucose by glucose oxidase enzyme over different reaction medium conditions. As a result, the large negative value of entropy of activation $\Delta S^{\neq} = -148.8$ J K^{-1} mol^{-1} and positive value of the enthalpy of activation $\Delta H^{\neq} = 26.3$ kJ mol^{-1} have been found out.

Içli [7] searched in the presence of silicone and soy oil to improve features of the immobilized glucose oxidase on sodium alginate and enhance enzyme activity. Consequently When 4% (v/ v) silicon oil and soybean oil were used, the activity of immobilized glucose oxidase was increased respectively 1.69 and 1.33 times, by comparison with non-use of these oils.

Ramezani et al. [16] examined how oxygen velocity's effects are on the apparent velocity of the oxidation reaction. When oxygen transfer becomes higher, apparent reaction rate increases, but at two gas velocities of 0.0028 and 0.0056 m s^{-1}, the apparent reaction rates are very close to each other due to the similarity of the gas hold-ups, specific gas-liquid interfacial areas and the volumetric oxygen transfer coefficients.

Ozyılmaz [9] carried out both immobilization and characterisation of glucose oxidase, catalase and glucose oxidase-catalase enzymes over florisil activated with glutaraldehyde through in two different ways (together and sequentially) Catalase prevented the inhibition effect of hydrogen peroxide when co-immobilized glucose oxidase plus catalase used. It has been observed that the best system using the packed bed column reactors in different operating types is the co-immobilized glucose oxidase plus catalase system in the feedback packed bed column reactor.

4. CONCLUSION

In this study, we mentioned briefly glunonic acid and its production. Although commercial and preferable production type is fermentation, enzymatic production has been searched by many researchers. Cause enzymatic production has advantages to fermentation processes. Especially, in the case of production with immobilized enzymes, downstream processes become easier. Beside that there is no unexpected byproduct. Therefore we want to study gluconic acid production by enzymatic methods. Our study is still going on in our research laboratuary about both enhance production efficiency and produce.

REFERENCES

[1] Mehtiö T., Toivari M., Wiebe M. G., Harlin A., Penttilä M., Koivula A., Production and applications of carbohydrate-derived sugar acids as generic biobased chemicals, Critical Reviews in Biotechnology, 36(5), 904-916, 2016.

[2] Rodriguez A., Duenas I., Hornero J., Ehrenreich A., Liebl W.,Garcia I., Gluconic acid: Properties, production methods and applications—Anexcellent opportunity for agro-industrial by-products and wastebio-valorization, Process Biochem, 2016.

[3] Anastassiadis S., Morgunov I., Gluconic Acid Production, Recent Patents on Biotechnology, 1(2), 167-80, 2007.

[4] Pal P., Kumar R., Banerjee S., Manufacture of gluconic acid: a review towards process intensification for green production. Chemical Engineering and Processing: Process Intensification, 104, 160-171, 2016.

[5] Ramachandran, S., Fontanille, P., Pandey, A., Larroche, C., "Gluconic Acid: Properties, Applications and Microbial Production", Food Technology Biotechnology, 44(2), 185-195, 2006.

[6] Singh O. V., Kumar R., Biotechnological production of gluconic acid: future implications, Applied microbiology and biotechnology, 75(4), 713-722, 2007.

[7] İçli N., "İmmobilize Glukoz Oksidaz Enziminin Özellikleri Ve Enzim Aktifliğinin Arttırılması", Yüksek Lisans Tezi, Gazi Üniversitesi, Fen Bilimleri Ensitüsü, Ankara, 2008.

[8] Bao J., Furumoto K., Fukunaga K., Nakao K., A kinetic study on air oxidation of glucose catalyzed by immobilized glucose oxidase for production of calcium gluconate. Biochemical Engineering Journal, 8(2), 91-102, 2001.

[9] Ozyılmaz G., "Glukoz Oksidaz Ve Katalazın Ayrı Ayrı Ve Birlikte İmmobilizasyonu ve Karakterizasyonu", Doctoral Thesis, Çukurova University, Institute of Science , Adana, 2005

[10] Wong C. M., Wong K. H., Chen X. D., Glucose oxidase: natural occurrence, function, properties and industrial applications, Applied Microbiology and Biotechnology, 78(6), 927-938, 2008.

[11] Yoshimoto M., Sato M., Wang S., Fukunaga K., Nakao K., Structural stability of glucose oxidase encapsulated in liposomes to inhibition by hydrogen peroxide produced during glucose oxidation, Biochemical engineering journal, 30(2), 158-163, 2006.

[12] Nakao K., Kiefner A., Furumoto K., Harada T., Production of gluconic acid with immobilized glucose oxidase in airlift reactors. Chemical Engineering Science, 52(21-22), 4127-4133, 1997.

[13] Bao J., Furumoto K., Yoshimoto M., Fukunaga K., Nakao K., Competitive inhibition by hydrogen peroxide produced in glucose oxidation catalyzed by glucose oxidase. Biochemical engineering journal, 13(1), 69-72, 2003.

[14] Beltrame, P., Comotti, M., Della Pina, C., & Rossi, M., Aerobic oxidation of glucose I. Enzymatic catalysis. Journal of Catalysis, 228(2), 282-287, 2004.

[15] Odebunmi E., Owalude S., Kinetic and thermodynamic studies of glucose oxidasecatalysed oxidation reaction of glucose. Journal of Applied Sciences and Environmental Management, 11(4) 95 – 100, 2009.

[16] Ramezani, M., Mostoufi, N., & Mehrnia, R. M., Effect of hydrodynamics on kinetics of gluconic acid enzymatic production in bubble column reactor. Chemical Industry and Chemical Engineering Quarterly, 19(3), 411-422, 2013.

INTERNATIONAL CONFERENCE ON ADVANCES IN SCIENCE AND ARTS ISTANBUL 2017 – ICASA 2017
29- 31 MARCH 2017, Istanbul, Turkey

OPTİMAL SİZİNG AND SİTİNG OF RENEWABLE DİSTRİBUTED GENERATİON İN DİSTRİBUTİON SYSTEMS

Ahmed Isam ABDULSAHIB
Yildiz Technical University
Istanbul, Turkey

Asst. Prof. Dr. Ozan ERDİNÇ
Yildiz Technical University
Istanbul, Turkey

Keywords: Distribution Generation (DG), minimize total power , size optimal ,location optimal , Bus System, Reduce loss

Ahmed Isam ABDULSAHIB:,00905373767927
E-mail address:AL_MOHNDS2006@YAHOO.COM

A B S T R A C T :

The power of transmission lines is becoming the main bottleneck of the existing transmission network. power are being conveyed over the interconnections to important load centers, the faraway of the demand load to source energy and the ratio of R/X. In this study, the optimum size and siting of distributed The load ability of transmission lines is increased due to the surge in loads. Larger amounts of generation will be defined so as to minimize total power losses by an analytical method based on 12 bus test system technique. The main goal of this paper is to solve the optimal sizing and siting problem in distribution networks. This problem is treated objective optimization problem by Capturing the effects that the variability of both demand and (renewable) generation.

Introduction :

Many power companies with the Distributed Generation (DG) are investing in small scale renewable energy resources like photo-voltaic cells, wind, micro-turbines, small hydro turbines , CHP or hybrid. Today this figure has increased substantially and reached up to over 12 GW [1]. It is also expected with the KYOTO protocol commitment by various countries to reduce CO2 emission, the market for DGs as a ‘‘Clean Power’’ resource is promising. According to Energy Network Association (ENA) report [2], the UK government is targeting to achieve 15% of electricity from renewable exporter by 2015, implying rapid growth in DG and investment in the power infrastructure. However there are several issues concerning the integration of DGs with existing energy system grid ; that needs to be addressed [3–5]. The integration of DG changes the system from passive to active networks, which affects the reliability and operation of a power system network [4]. Further , the non-optimal placement of DG can result in an increase of the system losses and thus making the voltage profile lower than the allowable limit [6]. Since utilities are non-technical issues and already facing technical , they cannot tolerate such additional issues. Hence an optimum placement of DG is needed in order to minimize overall system losses and therefore improve voltage profiles.

Last time ,different methodologies have been developed to determine the location and size optimum of the DG. These methodologies are either based on analytical tools or on optimal programming methods. Analytical approaches have been suggest by several authors. In [7], the authors presented analytical approach to determine the optimal location for the Distribution generator (DG) with an objective of loss minimization for distribution and transmission grid . In [8], the author used the loss sensitivity equation to determine the optimization sizing of DG and the exact loss power to determine the optimum location of DG based on minimum losses. In [9], the author presented the loss sensitivity factor based on equivalent current injection using two type Bus-Injection in Branch-Current (BIBC) and Branch-Current in Bus-Voltage (BCBV) matrix. A simple search algorithm is proposed in [10] for optimal placement and sizing of DG for a network system, based on losses and function as an objective function. The method is simple but time consuming for searching both the best location and optimum size. In [11],

the author considered the minimum loss and generation as a parameter in addition to DG power limits to determine the optimal size and location of the DG. The author developed two programs named ‘‘Bloss’’ and ‘‘dpslack’’ for optimum sizing of Distribution Generator, considering DG min–max limits also. Later-on, site is decided by considering the minimum total power losses considering DG on each bus. The method is exact but very boring and mathematical computation need much computation time. In [12] authors have estimated the effect of DG placement on grid reliability, power losses reduction and power quality using the simple analytical approach and has shown the optimum DG allocation affects the system accuracy and system losses.

(Ant Colony Search Algorithm) is used here to find the optimal placement of DG and reclosers based on system reliability. Particle Swarm Optimization algorithm is used in [13,14]. In [15], authors have presented the dynamic based programming approach to find the best location for DG with maximum profit as an objective function. Genetic Algorithm (GA) based methods are proposed in [16–18] for optimal sizing and placement of DG, considering different objective functions. GA-Fuzzy based optimal placement of DG is discussed in [19], considering multi-objective functions including system losses, system loading as well as the profit for DISCOs (Distribution Companies). In [20], the author has presented the combine GA and PSO based approach for optimal location and capacity of DG, considering multi- objective constraints like voltage stability, losses and improved voltage regulations. GAs based methods are slow in computation and convergence [11], particularly useful when multi-objective conditions are considered.

This paper proposes a new method for DG placement and sizing based on the line voltage stability . So this method determine the most voltage-sensitive bus in the distribution system which could results in voltage instability in the system. DG is placed on the identified sensitive bus and the size of DG on that bus is increased gradually till the objective function (voltage constraints) is achieved. The proposed algorithm is also working on the same objective function for DG allocation. The developed index is used to identify the most critical bus in the system that can lead to system voltage instability when load increase above certain limit. The DG is placed at the identified bus. The search algorithm is used for estimating the size of DG considering minimum network losses. Overall, this proposed method is simpler and requires less computational time for determining the optimum placement and size of DG as compared to classical search algorithms.

A new analytical approach :

To gain the large benefit from the placement of DG, So needful to consider the impact of DG on a power system. Must we now the factors that represented sizing and siting .

1. Reduction in line losses.
2. Improvement in voltage profile and stability.

The simple two bus network shown in Fig. 1.a and its corresponding phasor diagram in Fig. 1.b

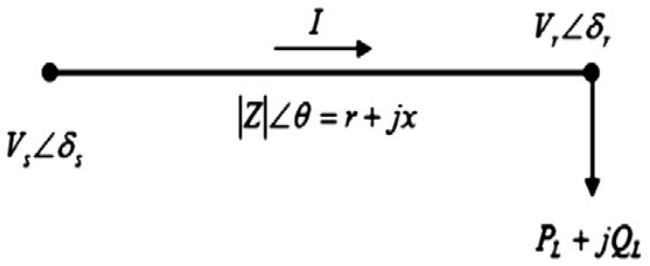

Fig .1.a two bus network.

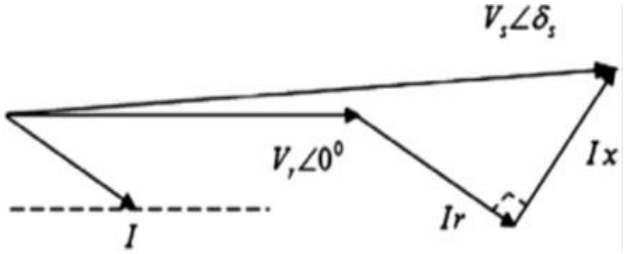

Fig .1.b Phasor diagram of a simple two bus network.

Consider a simple two bus network shown in Fig. 1 and its corresponding phasor diagram in Fig. 1.
From the phasor diagram, we can write:

$$\overrightarrow{Vr} = \overrightarrow{Vs} + \overrightarrow{IZ} \qquad (1)$$

where Z is the r + jx is the impedance of the line.

If we reduce the IZ component in the Eq. (1), the receiving end voltage can be improved. There are three ways to reduce the IZ components.

1. Provide active power support to the system locally using renewable energy or distributed resources or FACTS (in the present case we are considering the impact of DG only).
2. Provide reactive power support to the system locally using static condensers or FACTS.
3. Use of Anti Z element, which is only possible through series capacitance.

The Fig.2.a shows when we provide active power support (-PG) to the system locally. The phasor diagram is shown in Fig.2.b , which shows that the introduction of DG will reduce the active line component of the current from I to $I^{=}$to $I^{\equiv}$($I > I^{=} > I^{\equiv}$) as the DG size will increase. This will result in lesser Ir and Ix drop (for simplicity $I^{=}$and $I^{\equiv}$drops are not shown in the phasor diagram).

DG is mostly used for providing active power support to the system. However results could be seen for partially injecting reactive power support at that bus. Fig. 3a shows the scenario when we provide reactive power to the system. This will reduce the reactive current component

from I to $I^{=}$to $I^{\equiv}$ ($I^{\equiv}$< $I^{=}$< I) shown in phasor diagram Fig. 3b, which will results in lesser Ir and Ix drop.

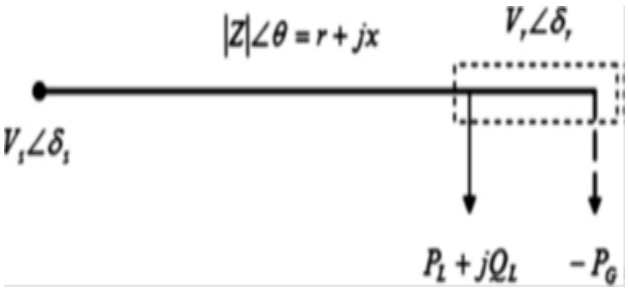

Fig.2.a Active power support

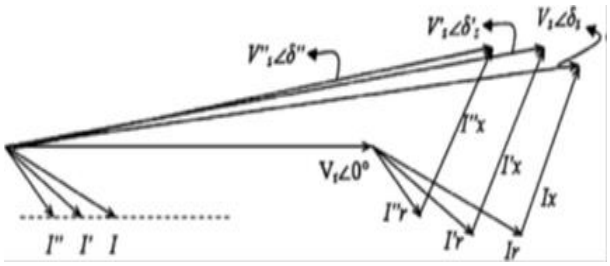

Fig.2.b Phasor diagram for active power support.

DG is mostly used for providing active power support to the system. However results could be seen for partially injecting reactive power support at that bus. Fig. 5 shows when we provide reactive power to the system. This will reduce the reactive current component from I to $I^{-}$to $I^{=}$ ($I^{=}$< I^{-} < I) shown in phasor diagram Fig. 6, which will results in lesser Ir and Ix drop**.**

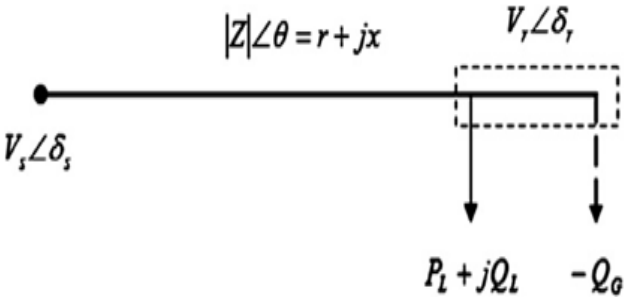

Fig.3.a Reactive power support.

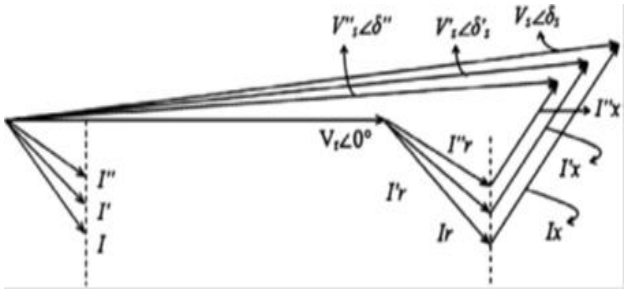

Fig.3.b Phasor diagram for reactive power support.

To find a simple two bus network, the losses that occurs in the line is given by,

$$P_e + jQ_e = I^2(r + jx) \quad \textbf{(2)}$$

Represented $\boldsymbol{P_e}$ is the active power loss; $\boldsymbol{Q_e}$ the reactive power loss; and **I** is the line current, given by:

$$I = \frac{Vs\angle\delta + Vr\angle\delta}{r + Jx} \quad \textbf{(3)}$$

Where

$Vs\angle\delta s$ = Vs (cos δs+jsin δs)

$Vr\angle\delta r$ =Vr (cos δr + jsin δr)

From (3) and (2) results in

$$[\![Vs\angle\delta s - Vr\angle\delta r]\!]^2 = (P_e + jQ_e)(r + jx) \quad \textbf{(4)}$$

From Eq. (2) and Eq. (3), we can conclude that

1. The line resistance and reactance play a very crucial role for voltage stability.

2. The line losses (or current) should be reduced for stable and improved voltages, which is only possible by providing active and reactive power support to the system. Economically it is not possible to provide support on each bus. Therefore the most suitable site and size of **DG** should be selected from where the maximum benefits could be achieved.

In [21], the author used the following mathematical formulation which needs to be considered in **DG** placement. Minimize total active power losses $\boldsymbol{P_l}$**,**

$Min\{P_l = \sum_{i=1}^{n} \backslash I_i \backslash \hat{} 2R_i\}$ **(5)**

Subject to the following generation and voltage constraints:

$$0 \leq P_{dg} \leq \sum P_{load} \quad \textbf{(6)}$$

$$|V_{i\ min}| \leq |V_i| \leq |V_{i\ max}| \quad i = 1, 2, \ldots..m \quad \textbf{(7a)}$$

$$|V_i| \leq 1 \pm 0.05_{pu} \quad i = 1, 2, \ldots\ldots m \quad \textbf{(7b)}$$

where ***n*** is the no. of lines; m the no. of buses ; i no. of repetition ; $\boldsymbol{P_{dg}}$the distributed generation power; and $\boldsymbol{P_{load}}$ is the total connected load .

The main constraints as defined in Eqs. (6–7) are to restrain the voltages at each bus along the radial system within the acceptable range and the total active power support should not exceed the system load.

Proposed method :

The important factor in maintaining the voltage between two nodes is the drop in the line connecting the two nodes, commonly known as voltage regulation. Ideally voltage regulation should be zero, but there are drops due to resistance and reactance of a line.

In transmission lines, resistance is much less than the reactance of the transmission line (r ≪ x); while in overhead distribution system, reactance is much less than the resistance of the line (x ≪ r). There is no anti-resistance element which could improve the voltage regulation. The series capacitor is commonly connected in long transmission lines having high reactance than a distribution network, in order to improve the voltage profile and increasing the system efficiency. However by supporting the active and reactive power demands locally could significantly reduced the voltage drop in the line by reduction in line current and losses and thus improves the system efficiency.

Development of an index for DG placement

An index is derived for finding the most optimum site of **DG** based on the most critical bus in the system that can lead to system voltage instability when the load increases above certain limit.

Consider a simple two bus network without and with **DG** shown in Figs. **1a** and **2a**, with their phasor diagram also presented in Figs. **1b** and **2b**.

From Fig. 1 we can write**,**

$$S_l = P_l + jQ_l = V_r\, I_r^{\star} \quad \textbf{(8)}$$

$$\overrightarrow{Vr} = \overrightarrow{Vs} - \overrightarrow{I_r Z} \quad \textbf{(9)}$$

Where

$$I_r = \frac{(P_l) + j(Q_l)}{V_r^*} \quad \textbf{(10)}$$

From Figs. 2a and 3a we can write:

$$I_r = \frac{(P_l - Pg) - j(Q_l - Qg)}{V_r^*} \quad \textbf{(11)}$$

Substitute Ir from Eq. (11) into Eq. (9) and separate into real and imaginary parts will give:

$$P_L - P_G = \frac{|Vr||Vs|}{V_r^*} \cos(\theta - \delta_s + \delta_r) - \frac{|V_r|^2}{Z} \cos\theta \quad \textbf{(12)}$$

$$Q_G - Q_G = \frac{|Vr||Vs|}{V_r^*} sin(\theta - \delta_s + \delta_r) - \frac{|V_r|^2}{Z} \sin\theta \quad \textbf{(13)}$$

Rearranging Eq. (12) will give:

$$|V_r|^2 - \frac{|Vr||Vs| \cos(\theta - \delta)}{\cos(\theta)} + \frac{Z(P_L - P_G)}{\cos(\theta)} = 0 \quad \textbf{(14)}$$

Where

$$\delta = \delta_s - \delta_r$$

The Eq. (14) is a quadratic equation. For stable node voltages, Eq. (14) should have real roots, i.e. discriminant $\boldsymbol{B^2\_\ 4AC} > 0$,which results in the proposed index referred as Power Stability Index (PSI) given by Eq. (15):

$$PSI = \frac{4r_{ji}(P_L - P_G)}{[|V_i| \cos(\theta - \delta)]^2} \leq 1$$

Under stable operation, this value should be less than unity; closer the value of PSI to zero, more stable will be the system. The above index is used to find the optimum placement of **DG**. The PSI value is calculated for each line in the given network and sorted from the highest to the lowest value. For the **i** - **j** line having the highest value of PSI .

Optimum sizing of DG :

Once the optimum location of **DG** is identified, the amount of active power from DG changes from 0% to 100% of the total active load, with generation and voltage constraint given in Eqs. (6 –7). The main objective in selecting **DG** size is to minimize total system power losses ($\boldsymbol{P_{loss}}$) by injecting active power ($\boldsymbol{P_{dg}}$), given in Eq. **(5)**. The relation between **DG** size and losses follow the parabolic curve, first decreases and then start increases, thus the accuracy of the **DG** size estimated will depend on the step size selected. In the present case, the step size is maintained 1% of total load. However much smaller size could also be used, but the computation will take much longer time.

Proposed algorithm :

For a radial distribution network, load flow analysis is carried out and PSI value is computed for each line using Eq. (15). For i _ j line having the highest value of PSI, the DG will be placed at jth bus. The search algorithm is used for finding the optimum size of DG at optimum location based on a minimum total power loss, with constraints given in Eqs. (6–7). The complete flow chart for DG allocation and sizing is represented in Fig. **4**.

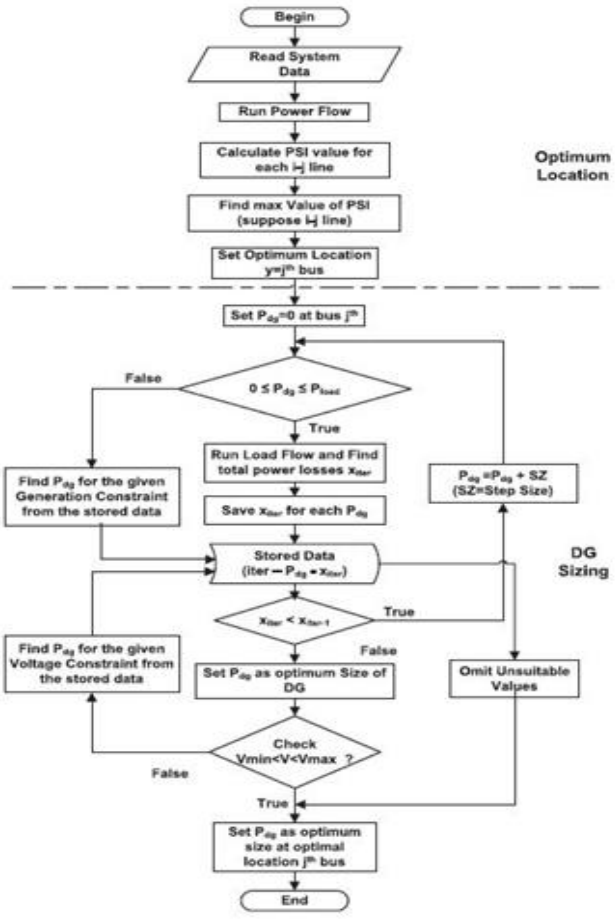

Fig .4 Flow chart of proposed algorithm

Simulations and results :

In Section 3, the proposed algorithm for DG placement and sizing is presented. For verification, the proposed algorithm is applied on 12-bus , modified 12-bus . A computer program has been written in MATLAB 7.12 and run on Cor 2 Duo 3.07 GHz processor. Shirmohammadi theorem [22] is used to carry out the load flow analysis. As conventional load flows are not suitable for radial distribution systems because they got diverges, due to high X/R ratio which results in singularity of Jacobian matrix .

1. Test systems :

The test system of 12-bus [23] and radial distribution test systems are shown in Figs. **5** respectively. In modified 12-bus system, the active load on each bus is multipliedby 5 for better visualization of results, as the actual value of load is very small.

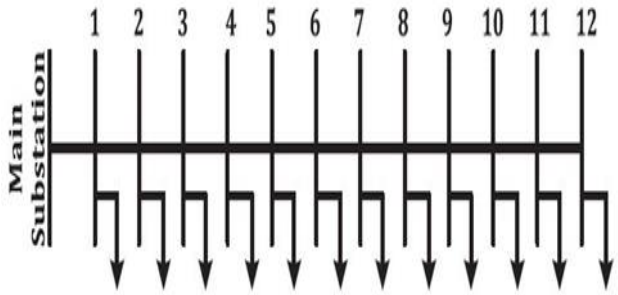

Fig. 5. Single line diagram of 12-bus radial network.

2. DG placement based on PSI :

The load flow analysis is carried out on 12-bus system and the PSI value is computed for each line using Eq. (15) considering initially no DG. The PSI value for each line is shown in Fig. 6a. It could be observed that the 8th line connecting bus 8 and bus 9 have the highest value than the others. So the installation of DG at bus 9 will be the optimum place. The same approach is carried out for modified 12-bus test system; PSI graph for system is shown Fig. 6b respectively. From Fig. 6b, it could be observed that the 8th line in modified 12-bus test system has the highest value of PSI respectively. Hence, the optimum location of DG is at bus 9 for 12-bus and test systems .

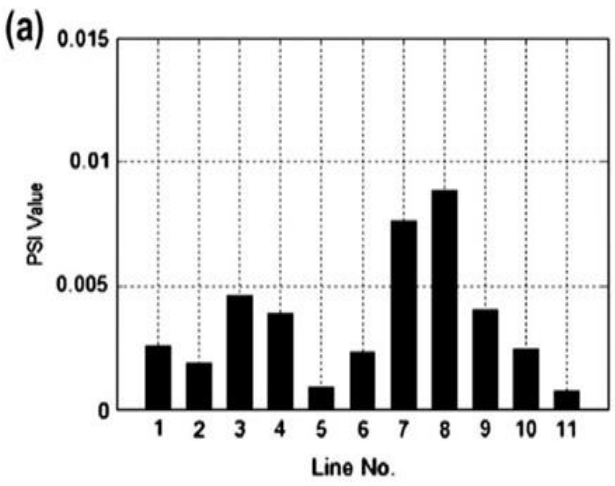

Fig. 6. PSI value for each line in (a) 12-bus system

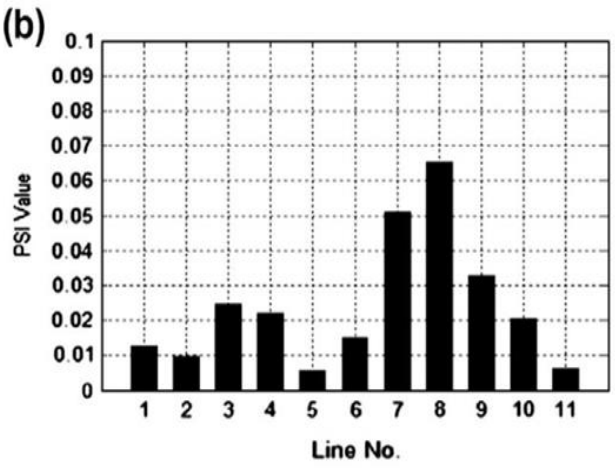

Fig. 6. PSI value for each line in (b) 12-bus system

3. Effect of DG on voltage stability :

In order to see the effects of DG on voltage stability on any bus, the load at that bus is increases gradually to find out the maximum load that cause instability. For example, in the modified 12-bus system when there is no DG, bus 7 reaches its maximum value
of load at 1.2909 MW, after that voltage collapse could be observed as shown in Table 1. The PSI value calculated using Eq. (15) is also shown in Table 1.

From Table 1, it could be seen that:

(1) More the value of PSI approach to the unity, more the link will be weak and additional load could result in voltage collapse .
(2) Adding DG on bus 7th will result in stable voltage operation.
(3) The system capacity has increased, more load could be added.

4. Effect of DG on reactive power :

Although DGs are mostly used for active power support, reactive power could also be injected to supply reactive load in the system. To see the effect of reactive power support (-QG) to the system, the modified 12-bus system is used as an example. The summary of the test result is shown in Figs. 7 .

S no.	load at bus7 P2 (MW)	V7	DG at bus7 P7 (MW)	losses		PSI
				Pe	Qe	
1	0.04	0.9553	0	0.0207	0.0381	0.00885
2	0.5	0.8896	0	0.1167	0.0426	0.127
3	1	0.7879	0	0.4574	0.163	0.32151
4	1.1909	0.7224	0	0.7951	0.2817	0.45323
5	1.2909	0.6307	0	1.4153	0.4996	0.63961
6	13	NC	0	NC	NC	NC
7	13	0.8349	0.5	0.2715	0.974	0.22982
8	13	0.8896	0.8	0.1167	0.426	0.127
9	13	0.9476	1.2	0.0268	0.0103	0.02247

Table 1. Effect of load on PSL

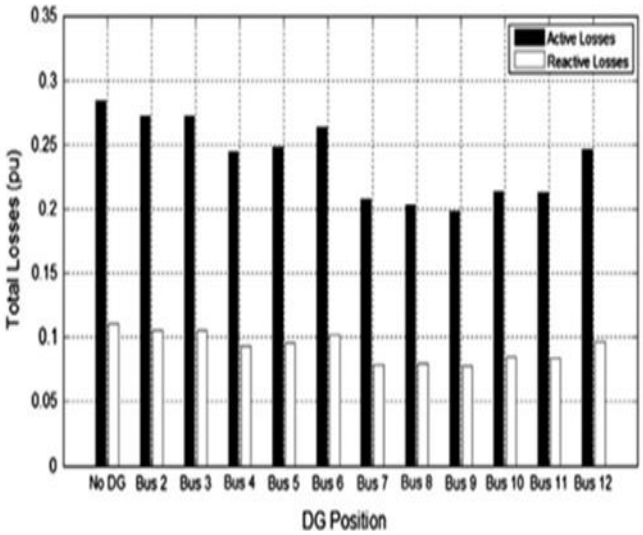

Fig.7. Effect of QG on system losses of modified 12-bus system.

Fig.7 shows the results when a reactive power equal to the reactive load on each bus is injected by the DG. It could be seen the active and reactive power losses have reduced as compared to without reactive power support on ith bus.

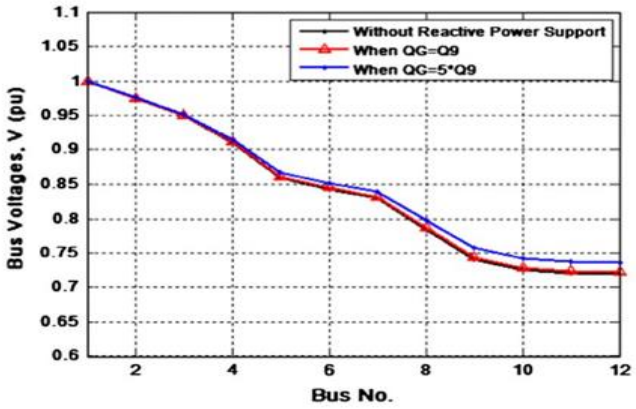

Fig.8. Effect of QG on system voltage profile of modified 12-bus system.

Fig. 8 shows the effect of reactive power support on system voltage profile. When a reactive power is supplied on bus 9 from the DG, the overall voltage profile has improved.

5. Optimum DG size :

To determine the optimum size of DG, the proposed algorithm is applied on all test systems and the results are tabulated in Table 2. The proposed algorithm is also compared with the GSS Algorithm, implemented using VS&OP power tool [24]. The results are :

shown in Table 2, from where it could be seen the close agreement of the propose method with the existing one. From Table 2, it could be observed that:

a) The proposed method results are in close agreement with GSS algorithm .
b) The computation time has been decreased considerably for three test systems (53.6%, 52.39% respectively with the 12-bus, modified 12-bus).

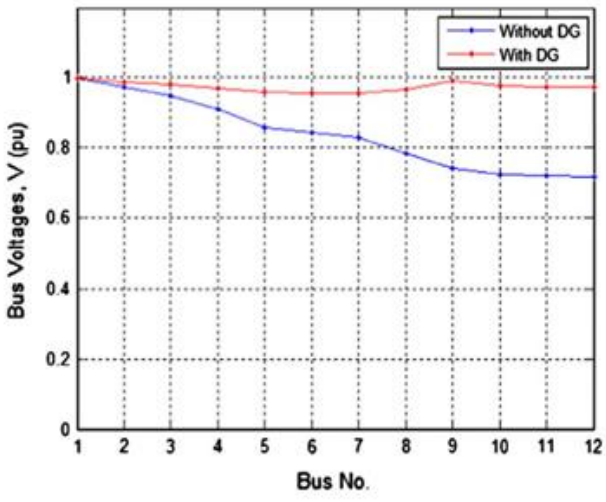

Fig. 9.Effect of DG on system voltage profile of modified 12-bus system

We note in the Fig. 11. Effect of DG on system voltage profile of modified 12-bus system, (a) 12 bus network (DG size = 0.2349MW @ Bus 9th). (b) Modified 12 bus network (DG size = 1.2MW @ Bus 9th).

Bus system	Proposed Algorithm				Golden Section Search algorithm		
	Max PSI values	Bus no.	Optimum size (MW)	CPU time (s)	Bus no.	Optimum size (MW)	CPU time (s)
12	0.008845	9th	0.2349	0.414	9th	0.235 45	0.892
Modified 12 Bus	0.065252	9th	1.2	0.427	9th	1.191 19	0.897

Table .2 Applcaion of algorithm on radial distribution network

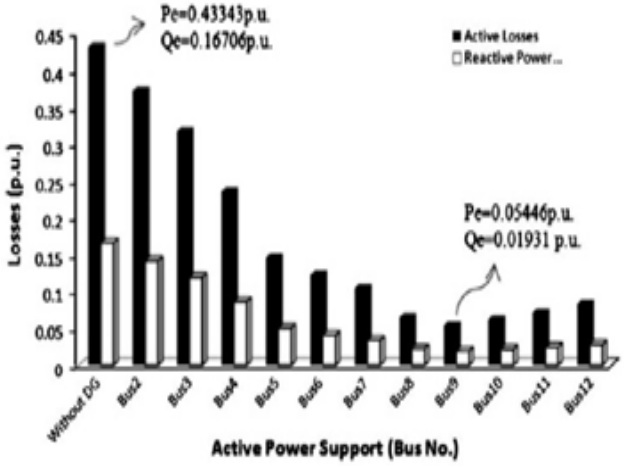

Fig. 10. System losses profile of modified 12-bus with optimum DG size = 1.2 MW at bus-9.

The DG size vs. loss-curves follow a parabolic curve, first decreases and then increases. Thus the size of DG should be carefully selected, above optimum size of DG the system losses increases which results in poor efficiency and voltage regulation.

6. Effect of DG on system losses and voltage profile :

In Section 2, we have seen the impact of DG on system losses based on analytical analysis. To verify the derived analytical equations, the effect of DG on modified 12-bus system studied by injecting optimum active power of 1.2MW on each bus. The total active and reactive losses occurring due to different DG location is shown in Fig. 9. It

can be observed that the most suitable location of DG in terms of losses is at bus 9, which is in agreement with the result in Fig. 9.

In Section 2, it has also been shown that the reduction in active and reactive losses improve the voltage profile. From Fig. 10, this could be visualized whereby the optimum placement of DG at 9th bus has improved the overall voltage profile.

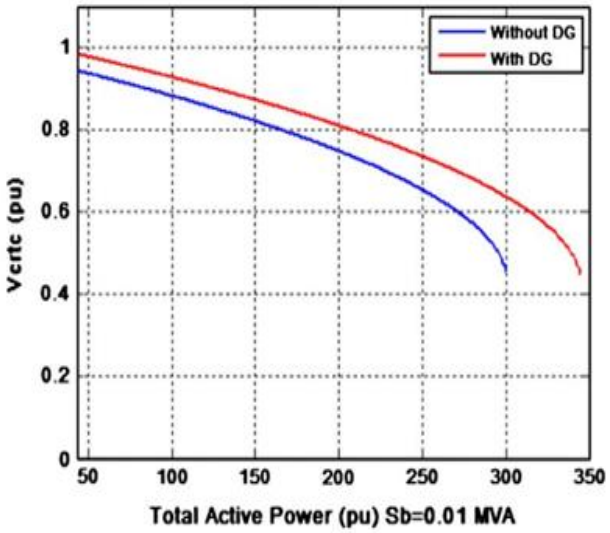

Fig.11. a) 12 bus Network (DG Size = 0.2349 MW @ Bus 9th).

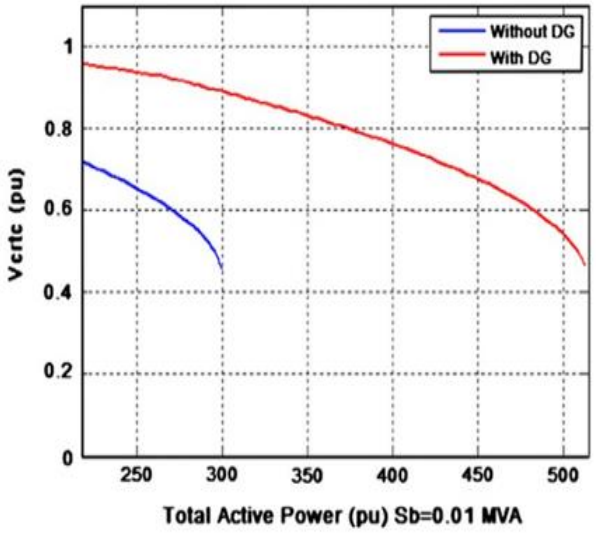

Fig. 11. b) Modified 12 bus Network (DG Size = 1.2 MW @ Bus 9th)

7. Overall findings :

From the analysis of the simulation results presented in Section 4, we can conclude the following due to DG placement.

1. The voltage profile has improved and the system voltage stability has increased.
2. Line losses have reduced.
3. The overall system capacity has increased.

Fig. 11 demonstrates that the system capacity has increased due to the installation of DG at the best location and of optimum size.

Conclusion :

In this paper, a new analytical approach is presented on the impact of DG in power system. A new algorithm is also proposed for DG location and sizing. The DG allocation and sizing is based on a novel Power Stability Index (PSI) index to determine the most voltage sensitive bus and minimum total power losses. Using the proposed algorithm optimum DG allocation and correct sizing results in an improved voltage profile and minimizes the burden of system losses.

The proposed algorithm has also been tested using three different radial distribution test systems and the results are verified using GSS Algorithm. It has been found that overall the proposed algorithm takes less computation time by 50–60% as compared to Golden Section Search (GSS) algorithm.

References :

[1] Jenkins N, Ekanayake J, Strbac G. Distributed generation – IET Factfiles; 2010. <http://www.theiet.org/factfiles/energy/distributed-generation.cfm>[accessed 10.08.11].

[2] Energy Networks Association (UK). <http://2010.energynetworks.org/ distributed-generation> [accessed 10.08.11].

[3] Koeppel. G. Distributed generation-literature review and outline of the Swiss station: Internal Report, ETH Zurich; November 2003.

[4] Hadjsaid N, Canard JF, Dumas F. Dispersed generation impact on distribution networks. IEEE Comput Appl Power 1999;12:22–8.

[5] Tuitemwong K, Premrudeepreechacharn S. Expert system for protection coordination of distribution system with distributed generators. Int J Electr Power 2011;33:466–71.

[6] Griffin T, Tomosovic K, Secrest D, Law A. Placement of dispersed generations systems for reduced losses. In: 33rd International conference on sciences. Hawaii; 2000.

[7] Caisheng W, Nehrir MH. Analytical approaches for optimal placement of distributed generation sources in power systems. IEEE Trans Power Syst 2004;19(4):2068–76.

[8] Acharya N, Mahat P, Mithulananthan N. An analytical approach for DG allocation in primary distribution network. Int J Electr Power. 2006;28(10):669–78.

[9] Gozel T, Hocaoglu MH. An analytical method for the sizing and siting of distributed generators in radial systems. Electr Power Syst Res 2009;79(6):912–8.
[10] Ghosh S, Ghoshal SP, Ghosh SA. Optimal sizing and placement of distributed generation in a network system. Int J Electr Power 2010;32(8):849–56.
[11] Kamel RM, Kermanshahi B. Optimal size and location of distributed generations for minimizing power losses in a primary distribution network. Scientia Iranica, Comput Sci Eng Electr Eng Trans D 2009;16(6):137–44.
[12] Hamedi H, Gandomkar M. A straightforward approach to minimizing unsupplied energy and power loss through DG placement and evaluating power quality in relation to load variations over time. Int J Elec Power 2012;35:93–6.
[13] Lingfeng W, Singh C. Reliability-constrained optimum placement of reclosers and distributed generators in distribution networks using an ant colony system algorithm. IEEE Trans Syst, Man Cyber, Part C: Appl Rev 2008;38:757–64.
[14] Kuersuk W, Ongsakul W. Optimal placement of distributed generation using particle swarm optimization. In: Australian universities power engineering conference (AUPEC' 06); 2006.
[15] Khalesi N, Rezaei N, Haghifam MR. DG allocation with application of dynamic programming for loss reduction and reliability improvement. Int J Electr Power 2011;33:288–95.
[16] Borges CLT, Falc˜o DM. Optimal distributed generation allocation for reliability, losses, and voltage improvement. Int J Electr Power 2006;28(6):413–20.
[17] Abou El-Ela AA, Allam SM, Shatla MM. Maximal optimal benefits of distributed generation using genetic algorithms. Electr Power Syst Res 2010;80:869–77.
[18] Kim K-H, Lee Y-J, Rhee S-B, Lee S-K, You S-K. Dispersed generator placement using fuzzy-GA in distribution systems. In: Proceeding of IEEE power engineering society summer meeting. Chicago; July 2002. p. 1148–53.
[19] Akorede MF, Hizam H, Aris I, Ab Kadir MZA. Effective method for optimal allocation of distributed generation units in meshed electric power systems. IET Gene Trans Dist 2011;5(2):276–87.
[20] Moradi MH, Abedini M. A combination of genetic algorithm and particle swarm optimization for optimal DG location and sizing in distribution systems. Int J Electr Power Energy Syst 2012;34:66–74.
[21] Lalitha MP, Reddy VCV, Usha V. Optimal DG placement for minimum real power loss in radial distribution systems using PSO. J Theor Appl Inform Technol 2010;13:107–16.
[22] Shirmohammadi D, Hong HW, Semlyen A, Luo GX.A compensation-based power flow method for weakly meshed distribution and transmission networks. IEEE Trans Power Syst 1988;3(2):753–62.
[23] Das D, Nagi HS, Kothari DP. Novel method for solving radial distribute networks. IEE Proc – Gene Trans Distrib 1994;141(4):291–8.
[24] Gozel T, Eminoglu U, Hocaoglu MH. A tool for voltage stability and optimization (VS&OP) in radial distribution systems using matlab graphical user interface (GUI). Simul Model Pract Theory 2008;16(5):505–18.

INTERNATIONAL CONFERENCE ON ADVANCES IN SCIENCE AND ARTS ISTANBUL 2017
29 – 31 MARCH 2017, Istanbul, Turkey

SYNTHESIS, CHARACTERIZATION, X-RAY CRYSTAL STRUCTURES AND BIOLOGICAL ACTIVITY OF ZN(II) COMPLEX OF BIDENTATE SCHIFF BASES OF SALICYLALDEHYDES AND AMINOALCOHOL

Hana amira GUADOURI*, Kamel OUARI and Sabrina BENDIA

Laboratoire d'Electrochimie, d'Ingénierie Moléculaire et de Catalyse Rédox (LEIMCR), Faculté de Technologie, Université Sétif-1, DZ-19000 Sétif, Algeria

Keywords: Zinc; Schiff base; Synthesis; NMR, Crystallography; Biologic activity

** Corresponding author : 00213555502673 hanaamiraguadouri@yahoo.fr*

Abstract

Schiff bases play an important role in inorganic chemistry as they easily form stable complexes with most transition metal ions [1-3]. The high stability potential of Schiff base complexes with different oxidation states extended the application of these compounds in a wide range.

The catalytic activity of Schiff base metal complexes has been analyzed critically in various reactions such as polymerization, oxidation, epoxidation, reduction of ketones, allylic alkylation and Michael addition reactions [4-6].

Apart from the catalytic applications of Schiff base compounds, they are important class of compounds in medicinal and pharmaceutical fields. They show potential applications and properties such as anticancer, anticonvulsant, antitumor, antifungal, antibacterial, antitubercular, antioxidant, antimalarial, antiinflammatory and anti-HIV activities [7-8].

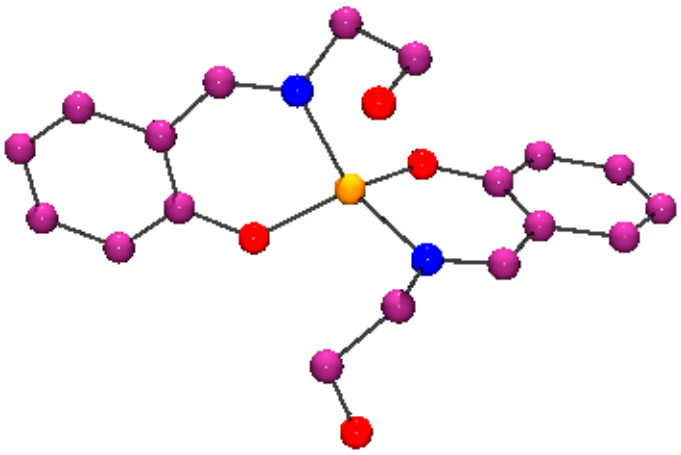

Mononuclear zinc(II) complex, [Zn(II)L], has been synthesized and characterized by IR and NMR [1H, 13C, DEPT] spectroscopic techniques. Structural analysis of the complex by single crystal X-ray crystallography shows the presence of a distorted square planar coordination geometry (NNOO) of the metal center.

Electrochemical behavior of the Zn(II)L complex has been investigated by cyclic voltammetryon glassy carbon electrode in ACN at 100 mV/s scan rate. The Zn (II) L compound was tested for their in vitro antimicrobial activity against Staphylococcus aureus and Escherichia coli as examples of Gram-positive and Gram-negative bacterial strains, respectively, by disc diffusion method.

References

[1] S. Chakraborty, C.R. Bhattacharjee, P. Mondal, S.K. Prasad, D.S. Rao, Dalton Trans. 44 (2015) 7477-7488.
[2] H. Amiri Rudbari, M.R. Farsani, S. Lanza, G. Bruno, B. Yadollahi, Comptes Rendus Chim. 18 (2015) 391-398.
[3] M. Khorshidifard, H. Amiri Rudbari, B. Askari, M. Sahihi, M.R. Farsani, F. Jalilian, G. Bruno, Polyhedron 95 (2015) 1-13.
[4] A. Ghaffari, M. Behzad, M. Pooyan, H. Amiri Rudbari, G. Bruno, J. Mol. Struct. 1063 (2014) 1-7.
[5] S. Menati, H. Amiri Rudbari, B. Askari, M.R. Farsani, F. Jalilian, G. Dini, Comptes Rendus Chim. 19 (2016) 347-356.
[6] S. Rayati, E. Bohloulbandi, S. Zakavi, Inorg. Chem. Commun. 54 (2015) 38e40. [17] M.R. Maurya, S. Dhaka, F. Avecilla, New J. Chem. 39 (2015) 2130-2139.
[7] A. Terenzi, R. Bonsignore, A. Spinello, C. Gentile, A. Martorana, C. Ducani, B. Hogberg, A.M. Almerico, A. Lauria, G. Barone, RSC Adv. 4 (2014) 33245-33256.
[8] M. Niu, Z. Li, H. Li, X. Li, J. Dou, S. Wang, RSC Adv. 5 (2015) 37085-37095.

REMOVAL OF ARSENATE IONS FROM WATER USING CALIX[4]ARENE BASED THIOUREA DERIVATIVES

Selahattin BOZKURT[1,2], Mustafa Burak Türkmen[1], Erkan HALAY[1*]

[1]*Uşak University, Scientific Analysis Technological Application and Research Center (UBATAM), 64200, Uşak, Turkey*

[2]*Uşak University, Vocational School of Health Services, 64200, Uşak, Turkey*

** Presenting author: erkan.halay@usak.edu.tr ; Phone: +90 276 221 21 21/4852*

Various problems concerning soil and water, especially drinking/well water pollution caused by toxic oxyanions have been an important topic in the recent years. In particular, the enlargement of the polluted area by diffusion of these toxic materials such as arsenate ions has been a serious problem in many countries [1].

Due to the above reasons, the purification of contaminated water and soil is a critical problem that must be considered and these toxic oxyanions need to be determined in the environmental samples for ensuring human health. In this regard, toxic metal oxyanions and cations, or their species have been the subject of a considerable number of papers which are based on their toxicity and methodological analysis including the processes of determination and extraction [2]. For this purpose, ligands which contains calixarene skeleton are ideal and frequently used macrocyclic structures due to their unique compositions involving the presence of phenols and promoting the complexation of metal atoms [3].

From this point of view, in this work, removal process of arsenate ($H_2AsO_4^-$) ions in aqueous solution using calix[4]arene scaffold as host molecules which is a technically easy-to-use method was investigated. The structures of synthesized three novel calix[4]arene-based thiourea derivatives were established on the basis of spectroscopic methods such as FTIR, ^1H and ^{13}C NMR. The complexing properties of these three calix[4]arene scaffold have been explored towards As(V). As a result, compound shown below was found to be an effective extractant, in other words, better receptors for $H_2AsO_4^-$ anions.

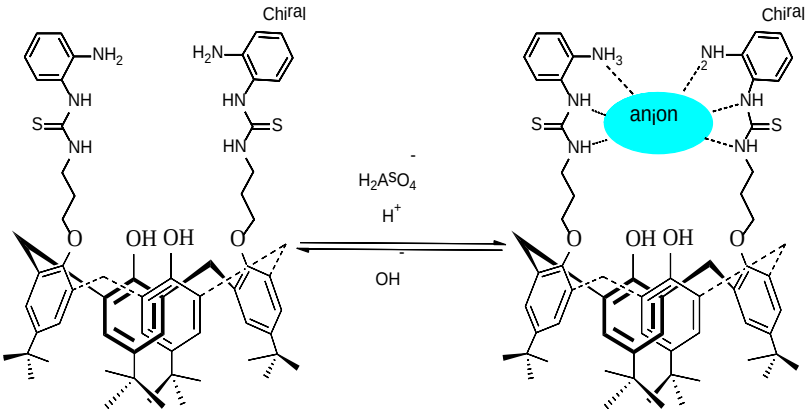

This work was supported by the Research Foundation of Uşak University (2014/SB002).

Keywords: Calixarene, Thiourea, Arsenate, Extraction, Toxic oxyanion

References

1. H. Sango, M. Hirano, *Key. Eng. Mater.* **617**, 40-45 (2014).
2. T.M. Abdel-Fattah, M.E. Mahmoud, *Chem. Eng. J.* **172**, 177-183 (2011).
3. T. Tuntulani, P. Thavornyutikarn, S. Poompradub, N. Jaiboon, V. Ruangpornvisuti, N. Chaichit, Z. Asfari, J. Vicens, *Tetrahedron*, **58**, 10277-85 (2002).